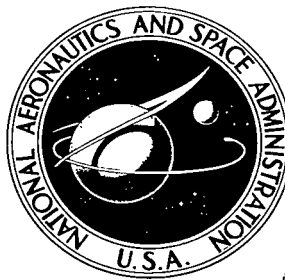


NASA TECHNICAL NOTE



NASA TN D-4042

c.1

LOAN COPY: RETURN
AFWL OFFICE
KIRTLAND AFB, NM

0130779



TECH LIBRARY KAFB, NM

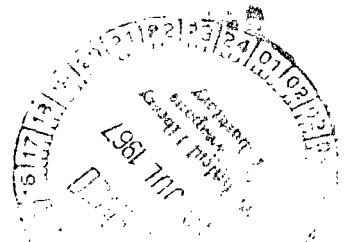
NASA TN D-4042

**NUMERICAL CALCULATIONS FOR THE
CHARACTERISTICS OF A GAS FLOWING
AXIALLY THROUGH A CONSTRICTED ARC**

by Velvin R. Watson and Eva B. Pegot

*Ames Research Center
Moffett Field, Calif.*

NATIONAL AERONAUTICS AND SPACE ADMINISTRATION • WASHINGTON, D. C. • JUNE 1967





NUMERICAL CALCULATIONS FOR THE CHARACTERISTICS OF A GAS
FLOWING AXIALLY THROUGH A CONSTRICTED ARC

By Velvin R. Watson and Eva B. Pegot

Ames Research Center
Moffett Field, Calif.

NATIONAL AERONAUTICS AND SPACE ADMINISTRATION

For sale by the Clearinghouse for Federal Scientific and Technical Information
Springfield, Virginia 22151 - CFSTI price \$3.00

NUMERICAL CALCULATIONS FOR THE CHARACTERISTICS OF A GAS FLOWING AXIALLY THROUGH A CONSTRICTED ARC

By Velvin R. Watson and Eva B. Pegot

Ames Research Center

SUMMARY

Numerical programs to obtain solutions for the characteristics of a gas flowing axially through a constricted arc are presented. The numerical programs use real equilibrium gas properties and solve simultaneously the energy, momentum, and continuity equations. Axial conduction, radial pressure gradients, and radial voltage gradients are neglected. The solutions give the arc characteristics in sufficient detail to evaluate the many approximate solutions, and the computing time (approximately 2 min) is sufficiently short that the programs may be used directly to obtain design criteria for plasma generators.

Numerical solutions for arcs within 0.635 and 1.27-cm-diameter constrictors are presented and the design optimization of constricted-arc plasma generators is discussed. The numerical solutions indicate that with nitrogen, total enthalpies in excess of 5×10^8 J/kg and velocities in excess of 18,000 m/s may be obtainable at the exit of a constricted-arc plasma generator.

INTRODUCTION

The constricted arc has recently been employed (as in the device shown in fig. 1) to generate hot, dense plasma flows for production of the very high heat fluxes required in materials testing, and to produce thrust. Approximate solutions for the characteristics of the flow through this constricted arc (refs. 1-6) predict the arc-column characteristics with varying degrees of accuracy. The discrepancies between actual and predicted characteristics are a result of the simplifying approximations incorporated into each model to permit an analytical or semianalytical solution; the extent to which these various approximations influence the behavior of the solutions, however, is not readily apparent.

The purpose of this paper is to present numerical methods for solving a more complete model with fewer and, presumably, more realistic assumptions. These solutions are sufficiently detailed to evaluate the simplified models and to gain further insight into the behavior of the constricted arc.

An evaluation of the approximations for the theoretical model presented in reference 1 has already been made and was presented in reference 7. The numerical solutions used for this evaluation are presented in appendix A.

Several arc characteristics were studied with these numerical methods and the results of these studies are presented. The results indicate methods for optimizing the design of a plasma generator for particular arc characteristics, and these methods are discussed.

In a previous work by Masser (ref. 8) a similarly complete method was presented for solving the constricted-arc problem. However, it will be shown that to obtain the same accuracy Masser's method may require a longer computing time than the method presented herein.

NOMENCLATURE

A	cross-sectional area of the constrictor, m^2
A_g	parameter of the linear approximation $\sigma = A_g \phi$, mho/W
a	zero frequency speed of sound, m/s
c_p	specific heat at constant pressure, J/kg $^{\circ}K$
d	diameter
E	voltage gradient, V/m
E_{∞}	$2.4/RA_g^{1/2}$
H_m	mass-average enthalpy, J/kg ($H_m = 0$ at $0^{\circ} K$)
H_s	enthalpy averaged over space, J/kg ($H_s = 0$ at $0^{\circ} K$)
H_{∞}	theoretical mass average enthalpy in the asymptotic region of the arc (ref. 1), $0.133 c_p I/kRA_g^{1/2}$, J/kg
h	enthalpy, J/kg ($h = 0$ at $0^{\circ} K$)
h_E	center-line enthalpy, J/kg
h_t	total enthalpy, J/kg
h_{∞}	theoretical center-line enthalpy in the asymptotic region of the arc (ref. 1), $0.307 c_p I/kRA_g^{1/2}$, J/kg
I	current, A
k	thermal conductivity, W/m $^{\circ}K$
\dot{m}	mass-flow rate, kg/s
p	pressure, N/m 2

p_0	constrictor inlet pressure, N/m^2
q	local heat transfer rate from the surface of the arc column to the constrictor wall, W/m^2
q_r	radiative component of the heat transfer rate to the constrictor wall, W/m^2
q_t	total heat transfer rate to the constrictor wall, W/m^2
q_∞	theoretical heat transfer rate from the surface of the arc column in the asymptotic region of the arc (ref. 1), $0.383 I/R^2 A_g^{1/2}$, W/m^2
R	constrictor radius, m; also gas constant
r	radial distance from the axis of the arc column, m
T	temperature, $^{\circ}K$
u	axial velocity, m/s
v	radial velocity, m/s
Z	compressibility
z	axial distance along the column, m
z_0	characteristic length for the arc (ref. 1), $\dot{m}c_p/\pi k$, m
θ	azimuthal coordinate of the arc column, radians
μ	viscosity, Ns/m^2
μ_0	magnetic permeability, N/A^2
ρ	density, kg/m^3
σ	electric conductivity, mho/m
ϕ	thermal conductivity function, $\int k dT$, W/m ($\phi = 0$ at $0^{\circ} K$)

DEVELOPMENT OF NUMERICAL ANALYSIS

Theoretical Models for the Numerical Calculations

The theoretical models for this work are assumed to be governed by one of the following two sets of equations. Equation (1) is applicable to the case of axial symmetry; equation (2) allows for asymmetric flow without swirl.

$$\left. \begin{aligned}
\frac{\rho u}{\partial z} \frac{\partial h_t}{\partial z} + \frac{\rho v}{\partial r} \frac{\partial h_t}{\partial r} &= \frac{I^2 \sigma}{\left(\int_A \sigma \, dA \right)^2} + \frac{1}{r} \frac{\partial \varphi}{\partial r} + \frac{\partial^2 \varphi}{\partial r^2} - \text{radiation} \\
\frac{\rho u}{\partial z} \frac{\partial u}{\partial z} + \frac{\rho v}{\partial r} \frac{\partial u}{\partial r} &= -\frac{dp}{dz} + \frac{1}{r} \frac{\partial}{\partial r} \left(r \mu \frac{\partial u}{\partial r} \right) \\
\int_A \rho u \, dA &= \dot{m}
\end{aligned} \right\} \quad (1)$$

$$\left. \begin{aligned}
\frac{\rho u}{\partial z} \frac{\partial h_t}{\partial z} &= \frac{I^2 \sigma}{\left(\int_A \sigma \, dA \right)^2} + \frac{1}{r} \frac{\partial \varphi}{\partial r} + \frac{\partial^2 \varphi}{\partial r^2} + \frac{1}{r^2} \frac{\partial^2 \varphi}{\partial \theta^2} - \text{radiation} \\
\frac{\rho u}{\partial z} \frac{\partial h_t}{\partial z} &= -\frac{dp}{dz} + \frac{1}{r} \frac{\partial}{\partial r} \left(r \mu \frac{\partial u}{\partial r} \right) + \frac{1}{r^2} \frac{\partial}{\partial \theta} \left(\mu \frac{\partial u}{\partial \theta} \right) \\
\int_A \rho u \, dA &= \dot{m}
\end{aligned} \right\} \quad (2)$$

In presenting the equations in the above form it is assumed that:

1. The gas flow is steady and laminar.
2. The electric discharge is stationary and the electric potential is constant on planes perpendicular to the axis.
3. Axial heat conduction is negligible compared to radial heat conduction.
4. Lorentz forces are negligible compared to dynamic and static pressure forces.
5. The radial pressure gradient is negligible compared to the static pressure.

A detailed discussion of these assumptions is presented in reference 1.

In comparison, the model of reference 1 contains all of the above assumptions and approximations in addition to the following simplifying approximations:

1. The mass flux is assumed constant throughout the constrictor.
2. The enthalpy profile at the constrictor inlet is assumed to be a Bessel function.
3. The more important gas properties - enthalpy, thermal conductivity potential, and electrical conductivity - are assumed to be linearly related and the radiance and viscosity are neglected.

The gas properties used in the numerical solutions for this report are theoretical estimates of real, equilibrium properties for nitrogen and hydrogen and are shown in figures 2 and 3. (In some of the numerical calculations the radiance of air was used in place of the radiance of nitrogen; so the radiance of air is also shown in figs. 2 and 3.) Table I lists the source for each of these gas properties (refs. 9-11).

Numerical Procedures

The numerical procedure for solving equations (1) and (2) is to satisfy finite-difference representations of the equations by forward marching from assumed upstream and constrictor wall boundary conditions. The step-by-step procedure for obtaining solutions to equation (2) is presented below. Figure 4 illustrates the arrangement of the finite-difference network.

1. Establish the following initial and boundary conditions:
 - (a) Enthalpy distribution at station 1
 - (b) Velocity distribution at station 1
 - (c) Enthalpy of the gas adjacent to the constrictor wall, that is, the enthalpy of the gas at the wall temperature
 - (d) The pressure at station 1
 - (e) The total current through the constrictor
2. Evaluate the distribution of the following gas properties at station 1 from the known values of enthalpy and pressure:
 - (a) Thermal conductivity potential
 - (b) Electrical conductivity
 - (c) Radiance
 - (d) Viscosity
 - (e) Density

3. Evaluate the electrical conductance at station 1 by integrating the electrical conductivity over the area at station 1. Evaluate the electrical voltage gradient at station 1 from the total current and electrical conductance.
4. Evaluate the total flow rate by integrating the local mass flow, ρu , over the area at station 1.
5. Compute the enthalpy at all mesh points at station 2 from the energy equation.
6. Estimate a trial pressure drop between stations 1 and 2; calculate the velocity at station 2 from the momentum equation.
7. Evaluate the density for all mesh points at station 2 from the known values of enthalpy and pressure.
8. Evaluate the total flow rate at station 2 by the same method as described in step 4.
9. If the total flow rate at station 2 agrees with the specified flow rate to within the specified accuracy, continue by repeating steps 2 through 9 for each new station; otherwise, change the trial pressure drop between stations 1 and 2 and repeat steps 6, 7, and 8. (To increase the flow rate at station 2, the trial pressure drop must be increased for subsonic flow values and decreased for supersonic flow values.)

If a repeated change of the trial pressure drop does not produce a calculated flow rate sufficiently near the specified flow rate, then either the calculations have become unstable or the flow has been aerodynamically choked in the tube. If the flow has become choked, the calculations can be continued into the supersonic region by causing the diameter to increase and by reversing the conditions on the trial pressure at the station of choking; that is, if the flow rate is too large at the station, then the trial pressure drop should be increased.

The procedure for solving equation (1) is similar except that the radial convection term is present in the momentum and energy equations. The radial mass flux required for the radial convection terms is determined by means of a local mass flux balance in each volume element, starting with the center element; that is, for the center volume element between stations n and $n + 1$, the radial mass flux into this volume is equal to the axial mass flux out at station $n + 1$ minus the axial mass flux in at station n . For computing convenience the radial momentum and energy fluxes between stations n and $n + 1$ are added downstream between stations $n + 1$ and $n + 2$.

Fortran Programs

The programs that solve equations (1) and (2) are written in Fortran II and are presented in appendixes B and C. Included in the appendixes are descriptions of the required subroutines and definitions of the variables used within the programs.

The programs that calculate the gas properties from known values of enthalpy and pressure are given in appendix D.

The program that prepares the magnetic tape required for the program given in appendix D from a table of gas properties is given in appendix E.

Display of Solutions

The above Fortran programs solve for the local state properties and velocity of the gas throughout the constricted arc. For the symmetric arc, the distribution of these local properties can easily be visualized with an oblique projection as shown in figure 5. Figure 5(a) represents a constant area constrictor whereas figure 5(b) represents a constrictor with a contoured inlet section. The horizontal scale represents the radial distance from the axis of symmetry, the oblique scale represents the axial distance within the constrictor, and the vertical scale represents the magnitude of the local property - in this illustration, enthalpy. The local values of enthalpy, mass flow, energy flow, velocity, and momentum flow are illustrated with these oblique projections in parts (a) through (e) of figures 6 through 34.

All arc-column characteristics of interest can be calculated from the local properties obtained from the numerical solutions. Local properties that have been calculated and plotted as functions of axial distance are center-line enthalpy, average enthalpy (averaged over both space coordinates or mass flux coordinates) voltage, constrictor wall heat transfer rate, and static pressure. These are shown in parts (f) through (k), respectively, of figures 6 to 34. The predictions from the analytical model of reference 1 for the constricted arc with negligible radiation losses are also shown in parts (f) through (j) for comparison. The program that plots these graphs from the results of the numerical program given in appendix B, is given in appendix F.

The results for the asymmetric arc cannot be shown completely by the oblique projections used to display the results for the symmetric arc. Nevertheless, the tabular output of the above programs can be visualized if the results are arranged as shown in figure 35, wherein the magnitudes of the enthalpy and the mass flux are shown as functions of radius and azimuthal position at each axial station.

Although the arc is not symmetric, the hot section of the arc does not rotate with axial distance, and the values of the gas properties on a plane of constant azimuthal position that passes through the hot spot is of interest. The values of the gas properties on this plane can be shown by the oblique projection as illustrated in figure 36.

Computational Accuracy

Mesh size. - The calculations for the symmetric arc were made with 13 radial mesh points between the constrictor axis and the constrictor wall and with sufficient axial stations to yield a stable solution (usually between

200 and 1000 stations). A comparison was made for a case in which only the mesh size was changed. The number of radial mesh points was changed from 13 to 26 and the number of axial stations was changed from 263 to 847. The heat flux to the constrictor wall, which is obtained from the derivatives of the local enthalpy profile, changed the most (nearly 10 percent) whereas the mass-averaged enthalpy which is obtained from the integral of the local enthalpy profile, changed by less than 3 percent. The heat transfer rate is the only property that is obtained from a derivative, and most of the arc properties changed less than 5 percent as a result of the change in mesh size.

Stability.- A rigorous stability criterion for the finite difference solutions of these nonlinear equations is not known. However, a stability criterion for the finite difference solution of linear parabolic equations is that

$$\frac{\Delta z}{\Delta r^2} < \frac{u\alpha}{2}$$

where

u gas velocity

α thermal diffusivity

Furthermore, whenever the local values of $\Delta z/\Delta r^2$ exceeded this limit in the numerical calculations of the nonlinear equations, instabilities were encountered. Therefore, the above criterion for stability appears to apply locally for the nonlinear equations, and a step was added to the above numerical procedure to keep the local value of $\Delta z/\Delta r^2$ less than this limit.

Instabilities were encountered in the program for the numerical calculations for equation (1) when the pressures were high. These instabilities were eliminated by changing the method of handling the radial convection. The instabilities were encountered when the momentum and energy that were convected radially between stations n and $n + 1$ were added at station $n + 2$ as described under numerical procedures. Adding one-fourth of this radially convected momentum and energy to each of the stations $n + 2$, $n + 3$, $n + 4$, and $n + 5$ eliminated the instability.

Computation time.- The programs presented herein are written in Fortran II and were executed by an IBM 7094. The computation time required for the calculation of the solutions is approximately 2 minutes. The time for each case shown in figures is given in table II.

The computing time is proportional to the dimensionless length of the constrictor and is approximately proportional to the cube of the number of radial mesh points.

Discussion

It will be shown in the sections that follow that the numerical solutions display the qualitative features of the constricted arc in sufficient detail to gain an understanding of the arc column and to evaluate the various approximate analyses of the constricted arc.

The computation times for the programs for the first set of equations (approximately 2 min) are sufficiently short that it appears feasible to use these programs directly to obtain design criteria for plasma generators.

Several physical phenomena that were neglected in these calculations can be included without greatly increasing the complexity or calculation times of the program. For example, if the operating conditions are changed so that the magnetic pressure term will not be negligible, this term can easily be included in the calculations. (The current distribution is known and because of symmetry, the magnetic field is easily calculated.) Also, the effects of radiation absorption could be approximated if the frequency of the radiation were divided into intervals and the radiation and absorption path length were specified for each frequency interval. The radiation at all frequencies for which the path length is much greater than the constrictor radius could be specified with one term and the gas considered to be transparent to this radiation, and the radiation at all frequencies for which the path length is much less than the radial mesh increment could be included as a single term similar to the thermal conduction term. Since the variation of radiation with axial distance is small compared to the variation of radiation with radial distance, the radiation absorbed at each axial station can be calculated approximately from the temperature and density profiles of the previous axial station. For the higher flow rates, turbulence may become significant and the convective transfer of energy and momentum could be approximated with the Prandtl mixing length theory.

The starting conditions (i.e., the enthalpy and velocity at the first axial station) are usually unknown and must be assumed. Figures 6 through 9 compare solutions in which only these assumed starting conditions were changed. Here one can see that the effect of the starting conditions on the solutions at very short characteristic lengths (i.e., very small z/z_0) is severe. Nevertheless, this effect diminishes rapidly downstream, and even at moderately small characteristic lengths the effect of the starting conditions is small.

A procedure for the numerical solution of equation (1) is given by Masser (ref. 8). Comparing Masser's work with the present procedure, the two differ in their respective location of the radial mesh points; Masser's are fixed on streamlines whereas in the present program they are fixed in space. Since the dominant heat-transfer mechanisms (i.e., thermal conduction, radiation, and ohmic heating) are dependent upon space coordinates rather than mass flux coordinates, the accuracy with which these terms can be calculated depends upon the mesh distances in space coordinates. From part (b) of the figures illustrating the solutions, it can be seen that the mesh distances in

space would vary radically if the mesh points were fixed on streamlines. Masser's procedure, therefore, would probably require more mesh points for the same degree of accuracy.

EVALUATION OF THE NUMERICAL SOLUTIONS

The numerical solutions were compared with an exact analytical solution to determine whether the numerical procedures yield the proper solutions to the equations for the theoretical models. Then the numerical solutions were compared with experimental measurements to determine whether the theoretical model yields the correct arc column features.

Comparison of the Numerical Solution With an Exact Solution

An exact analytical solution for a theoretical model of the arc column with one set of boundary conditions is given in reference 1. The theoretical model of reference 1 is the same as the theoretical model used for the numerical calculations for this paper except that the model of reference 1 contains additional simplifying approximations. (The list of additional simplifying approximations is given in a previous section "Theoretical Models for the Numerical Calculations.") In order to compare the numerical solutions with the exact solution, the additional approximations of reference 1 were incorporated into the model used for the numerical calculations (e.g., linearized gas properties were used for the numerical calculations). The number of radial mesh points for the numerical calculation was 13 and the number of axial mesh points was 195. The difference between the numerical solution and the exact solution was less than 1 percent (nearly indistinguishable on a graphical illustration) indicating that the numerical procedures give the proper solution to the equations for the theoretical model.

Comparison of the Numerical Solutions With Experimental Results

The numerical calculations are compared with the experimental measurements of the mass average enthalpy, voltage gradient, and wall heat transfer rate in a 1.27-cm-diameter constricted-arc plasma generator (figs. 10-14), and in a 0.635-cm-diameter constricted-arc plasma generator (figs. 15-20). (Figs. 10-20 display 10 arc column features even though there are experimental measurements for only three of these features. The three features for which the numerical solutions are compared with experimental measurements are shown in parts (h), (i), and (j) of these figures.)

The mass average enthalpy was measured experimentally by subtracting the heat losses from the electrical power input. The 1.27-cm-diameter constrictor was made in two modules and only the average heat transfer rate to each module was measured. Therefore, the mass average enthalpy could be determined only at the end of each module. The electrical voltage gradient was not measured for all runs.

The starting conditions for the numerical calculations are not known a priori; the distribution of enthalpy and velocity at the inlet must be assumed. For the 1.27-cm-diameter constrictor, an arbitrary and fairly low

value of enthalpy was selected at the start. When the average enthalpy in the numerical calculations became equal to the average enthalpy of the gas entering the constant area constrictor of the plasma generator, the axial distance of the numerical calculations was made to coincide with the start of the constrictor in the plasma generator. This is shown graphically in part (h) of the figures wherein the curve for the numerical calculations is forced to pass through the first data point representing the average enthalpy of the gas entering the constant area constrictor of the plasma generator, and the axial distance is set equal to zero at this point. (A dashed line in parts (f) through (j) of the figures represents the analytical theory of reference 1. In figures 10 through 14, the average enthalpy of the analytical theory was also made to match the average enthalpy of the gas entering the constant area constrictor in the plasma generator, as shown in part (h).)

For the comparison with the experimental measurements within the 0.635-cm-diameter plasma generator (figs. 15-20), the numerical calculations were started in the stagnation region a short distance downstream from the tip of the cathode. It has been shown that a change in the starting conditions strongly affects the solutions only within a short distance downstream from the starting location. (See discussion under "Development of the Numerical Analysis.") Therefore, since the numerical solutions were started in the stagnation chamber, the solutions throughout the narrow constricted section were affected very little by the assumed starting conditions; so it was not necessary to match the average enthalpies at the inlet of the constant area constrictor when the numerical calculations were started in the stagnation chamber.

The enthalpy at the start of the narrow constricted section was arbitrarily assumed to be zero for the analytical model of reference 1 in figures 15 through 20. This theoretical model applies only to the constant area section, and for predictions from this theory when the inlet enthalpy is unknown, an arbitrary assumption of negligible enthalpy at the inlet has usually been employed.

Values of gas radiance for the numerical calculations shown in figures 15 through 20 were taken from reference 12 rather than reference 10 and are higher than the values given in reference 10. However, the radiation transport for these calculations is small compared to the thermal conduction; consequently, the solutions would be nearly the same if values of gas radiance from reference 10 had been used.

The numerical calculations agree with the experimental measurements within a factor of 2 and illustrate the qualitative trends of the measurements. This agreement is within the agreement between the theoretical and the measured transport properties at high temperatures.

The deviation between the numerical calculations and the experimental data for the 0.635-cm constrictor is larger than for the 1.27-cm constrictor. In the present numerical calculations the variation of the gas properties with pressure was extrapolated below 1 atmosphere. The large extrapolation to the low pressures for the comparison with the experimental results in the 0.635-cm constrictor may be the cause of this larger discrepancy between the numerical solutions and the experimental data for the 0.635-cm constrictor.

Arc-column characteristics were predicted within the accuracy with which the transport properties are known. The accuracy with which the theoretical model used in the numerical calculations represents the physical arc column cannot be determined from the above comparisons because of the uncertainties in the theoretical transport properties.

STUDY OF ARC CHARACTERISTICS WITH THE NUMERICAL PROGRAM

The qualitative picture of the arc given by the numerical calculations (e.g., see fig. 10) shows that most of the gas is forced to the constrictor wall near the constrictor entrance; as the gas proceeds downstream, it is slowly ingested into the hot core of the arc (fig. 10(b)). The hottest region is near the constrictor entrance (fig. 10(a)). The energy flux densities (fig. 10(c)) are highest at the constrictor exit rather than in the hot region near the entrance because near the entrance, most of the gas flows close to the cold wall rather than through the hot region. The radial velocity profiles (fig. 10(d)) are approximately parabolic, similar to Poiseuille flow. (The velocity gradients are caused mainly by large density gradients rather than by viscous forces for this case. The effects of viscosity are illustrated later in this section.) The distribution of momentum flux (fig. 10(e)) illustrates that near the constrictor inlet, momentum is convected to the constrictor walls causing the "ears" on the momentum flux profiles near the constrictor inlet. Farther downstream, as the gas is ingested into the arc core, the momentum is convected radially inward, causing high momentum flux in the center of the arc. (The ears downstream appear to be caused by large variations in gas viscosity since they disappear when the viscosity is set equal to zero.)

A comparison of the analytical model of reference 1 with the numerical solutions indicates that many of the important qualitative trends to the constricted arc are predicted by the analytical model of reference 1 whenever the conduction heat losses are dominant. For example, figures 11(f)-(h) illustrate that the analytical theory gives a fair estimate of the enthalpy at the constrictor exit (i.e., at $z/z_0 = 0.1$) and figures 11(i) and (j) illustrate that the theory gives the approximate values for the voltage gradient and wall heat transfer rate throughout the constrictor.

For pressures over 1 atm within the 1.27-cm-diameter constrictor or for larger constrictors at atmospheric pressure, the radiation losses are dominant and the more complete numerical calculations are required for reasonable predictions of the constricted arc behavior. Figures 10(h) and 10(j) illustrate that the theory of reference 1 predicts a higher mass average enthalpy and lower wall heat transfer rate than obtained from experimental measurements or from the numerical calculations for a case wherein radiation losses are large compared to conduction losses.

The effects of various approximations in the theoretical model are illustrated in appendix A. A more complete discussion of these approximations and a comparison of the numerical solutions with several other theoretical models that contain different approximations are given in reference 7.

The following additional arc characteristics were investigated with the numerical program:

1. The effect of asymmetries at the inlet of the constrictor.
2. The effect of radiation heat losses on the characteristics of the constricted thermal arc.
3. The importance of viscous forces on the constricted thermal arc.
4. The effect of radial convection within the constricted-arc column, including effects of transpiration-cooled constrictors.
5. Behavior of the constricted arc at large dimensionless length.

The numerical solutions obtained for these studies are illustrated in figures 21 through 36. Since the reader may wish to make many comparisons between the solutions in addition to those specifically mentioned herein, the solutions are presented completely and uniformly rather than for specific comparisons only. The solution of the simplified model in reference 1 is also included in parts (f) through (j) of these figures.

Results of these studies are as follows:

1. Any asymmetry that may be imposed on the arc at the constrictor inlet decays to a negligible value within a constrictor length equal to one-tenth the characteristic length, z_0 , as shown in figure 36.

2. The major effect of large radiation losses is to lower and flatten the enthalpy distribution (cf. figures 21-23 that are cases with negligible, moderate, and large ratios of radiation losses to conduction losses).

Note that the radiation does not appear to change the characteristic length greatly for the arc to approach an asymptotic state wherein the mass average enthalpy does not change with axial distance. The theory of reference 1 predicts that the mass average enthalpy will approach 80 percent of the asymptotic value at $z/z_0 = 0.1$. The solution in figure 23 indicates that the same may be true for arcs with high radiation. This result illustrates that the spreading of the arc to the constrictor wall is due to thermal conduction; therefore, the theoretical characteristic length given in reference 2 that has been modified to reflect a large dependence on radiation losses (modified length = z_0 times fraction of heat losses due to thermal conduction) may underestimate the characteristic length considerably. From this modified characteristic length one would have predicted that the mass average enthalpy would have approached 80 percent of the final value at z/z_0 less than 0.03 for the case shown in figure 23.

3. The viscous forces are negligible compared to inertia forces in plasma generators of the size and with the gas flows normally used in wind tunnels (constrictor diameters over 1 cm and mass flows over 1/2 g/s). A comparison of figures 24 and 25 shows that neglecting the viscous forces in the numerical calculations does not change the solution appreciably. Furthermore, when the viscous forces are negligible, the pressure drop through an aerodynamically choked constrictor is approximately half the inlet pressure.

For smaller diameter constrictors at lower flow rates, viscous forces tend to flatten the velocity profiles. Figures 26 and 27 illustrate the effect of viscosity in a 0.635-cm-diameter constrictor with a mass flow of only 0.227 g/s.

4. The radial heat conduction is large compared to radial heat convection within constricted arcs longer than $0.1z_0$ (cf. figs. 28 and 29 that show the numerical calculations with and without the radial heat convection). The solutions of the constricted arcs with part of the gas transpired through the constrictor wall do not differ appreciably from the solutions for the arcs where all of the gas enters at the constrictor inlet (provided the total gas flow rate is the same for both cases), even at flow rates sufficiently large that radial convection is appreciable. Anderson (ref. 13) showed that radial convection can be made equal to radial conduction for gas flow rates greater than $20\pi k/c_p$ times the constrictor length (or equivalently, with flow rates such that the constrictor length is less than $0.05z_0$). Figures 30 through 33 show that the enthalpy and energy flux at the constrictor exit are nearly the same in hydrogen or nitrogen arcs whether the gas is transpired through the walls or put in at the constrictor inlet. When all the gas enters at the constrictor inlet, it rapidly spreads to the wall and then gradually returns toward the axis with a radial flow similar to the radial flow within the transpiration cooled constrictor.

5. The enthalpy, mass flow, and energy flux distributions approach asymptotic values at large dimensionless lengths, but the velocity and momentum distributions continually increase in magnitude with length as shown in figure 34.

PREDICTIONS OF CONSTRICTED-ARC PLASMA GENERATOR PERFORMANCE

The numerical calculations indicate that the constricted arc may be used to produce gas flows with high energy flux density, with high enthalpy, and with high velocity. Figure 37 illustrates that an energy flux density of 2600 kW/cm² may be obtained with hydrogen with a 0.635-cm-diameter constrictor that experiences a maximum wall heat transfer rate of only 2.4 kW/cm², and figure 38 illustrates that an energy flux density of 1400 kW/cm² may be obtained with nitrogen in a 0.635-cm-diameter constrictor that experiences a maximum wall heat transfer rate of 8 kW/cm². Figure 39 illustrates that with nitrogen, enthalpies over 5×10^8 J/kg and velocities in excess of 9000 m/s may be obtainable at the constrictor exit. (Note that the velocity at the exit is approximately sonic. A simple estimate of the exit velocity can be made from the enthalpy by noting that for nitrogen the sonic velocity is approximately equal to $(0.14 \text{ times enthalpy})^{1/2}$ for enthalpies over 2×10^7 J/kg as shown in fig. 40.) The velocity at the exit of the divergent section of a plasma generator such as shown in figure 1 should be more than twice as high as the velocity at the constrictor exit. Even if the gas were frozen and monatomic, the velocity at the nozzle exit would be nearly twice the velocity at the throat; and if the gas were not frozen or not monatomic, the velocity would be greater. Therefore, velocities in excess of 18,000 m/s may be obtainable at the nozzle exit.

The energy flux density, enthalpy, and velocity given above cannot be obtained simultaneously; the conditions were chosen to optimize either the energy flux density or the enthalpy and velocity. (The methods to optimize the constrictor design to obtain the specific arc features are discussed in the next section.) Theoretical estimates of a more complete list of plasma properties that may be obtained simultaneously with a constricted-arc plasma generator similar to the one shown in figure 1 are given in table III for a single set of operating conditions. The theoretical estimates were based on a numerical solution for the constricted arc in the constant area portion of the constrictor; this numerical solution is shown in figure 41.

This table illustrates that the constricted arc should be capable of producing plasmas that interact appreciably with magnetic fields as required for experiments in magnetoplasma dynamics.

Some interesting arc-column properties for a variety of operating conditions are shown in table II.

DESIGN OPTIMIZATION OF CONSTRICTED-ARC PLASMA GENERATORS

There is no constrictor size that is simultaneously optimum for all of the desirable performance characteristics of the constricted-arc plasma generators, but the constrictor size, operating pressure, and current can be chosen to optimize any single performance characteristics.

The features most often desired for these plasma generators are:

- (a) High enthalpy
- (b) High velocity
- (c) Broad uniform plasma stream for testing
- (d) High energy flux density
- (e) High electron density
- (f) High efficiency

The limitations for obtaining the above features are the current that can be carried by the electrodes, the heat transfer rate that can be accommodated by the constrictor walls, and the voltage gradient that can be supported by the constrictor insulation.

Any single characteristic above can be improved, and simultaneously some of the other performance characteristics reduced, if the constrictor size, the operating pressure, and the current are modified as follows:

- (a) High enthalpy

Maximum enthalpy can be achieved by operating with the maximum current that the electrodes can carry at a pressure sufficiently low that the radiation losses are negligible. The constrictor diameter should be just small enough that the heat transfer rate to the constrictor wall is the maximum that the wall can accommodate. (In the conduction dominant regime, the enthalpy is approximately proportional to I/R , as shown in ref. 1.) Furthermore, the maximum local enthalpy occurs on the center line near the cathode, so for maximum enthalpy, the constrictor length should be short.

(b) High velocity

The highest velocities at the constrictor exit can be obtained with aerodynamically choked constrictors that produce the highest enthalpies; so the optimization given above for high enthalpy also applies to high velocity.

(c) Broad, uniform plasma stream for testing

The uniform portion of the test stream can be increased by increasing the pressure until the radiation losses flatten the profile (cf. figs. 41(a) and 42(a)) and by lengthening the constrictor until the enthalpy profile becomes asymptotic. The diameter of the constrictor should be just large enough that the heat transfer rate to the wall is the maximum that the constrictor wall can accommodate. (In the regime wherein radiation losses are dominant the wall heat transfer rate increases with increasing diameter.) The current should be sufficiently great to heat the gas to a temperature that will produce high radiation; that is, to approximately $15,000^{\circ}\text{K}$ (see figs. 2(q) and 2(w)). Too high a current heats the gas in the center of the arc to a temperature sufficiently high that the radiation losses decrease with increasing temperature, and, despite high pressures, causes peaking in the enthalpy profile as shown in figure 43.

(d) High energy flux density

The energy flux density can be increased by decreasing the constrictor diameter, increasing the constrictor length until an asymptotic profile is obtained, and increasing the pressure. The current should be just high enough that the heat transfer rate to the constrictor wall is the maximum that the wall can accommodate. Higher energy fluxes can be obtained with the lighter gases because they radiate the least. (Compare the two cases shown in figs. 37 and 38 wherein the energy flux density with hydrogen is approximately twice that with nitrogen, even though the heat transfer rate to the constrictor wall for the nitrogen is greater than that with the hydrogen.)

(e) High electron densities

The number density of electrons can be increased by decreasing the diameter and increasing the length until the profile becomes asymptotic. The current should be just high enough that the enthalpy of the gas is that for which the maximum electron density occurs at constant pressure, and the pressure should be just high enough that the wall heat transfer rate is the maximum that the wall can accommodate.

(f) Efficiency

The efficiency can be increased by operating at low pressure with short constrictors. At low pressure, the efficiency is not strongly influenced by either the constrictor diameter or by the current. If high pressure operation is mandatory, then for some cases, contrary to all of the simplified theories, the efficiency may be improved while maintaining the same mass average enthalpy at the exit by lengthening the constrictor and reducing the current. (Compare figs. 42 and 44 that illustrate that the efficiency was increased from 35 to 37 percent by increasing the length and decreasing the current while maintaining the same mass average enthalpy at the exit.)

CONCLUSIONS

The equations that govern the energy and mass transport in the constricted arc have been solved numerically. The numerical program uses real equilibrium gas properties and solves simultaneously the energy, momentum, and continuity equations. Axial conduction, radial pressure gradients, and radial voltage gradients are neglected. From given initial and boundary conditions the numerical program solves for the local state properties and velocity of the gas within the constricted thermal arc. From these properties all other characteristics of interest (i.e., voltage gradient and wall heat transfer rates) can be obtained. These solutions give sufficient detail to evaluate other approximate solutions, and the computing time (approximately 2 min) is sufficiently short that the programs may be used directly to obtain design criteria for plasma generators.

Ames Research Center

National Aeronautics and Space Administration

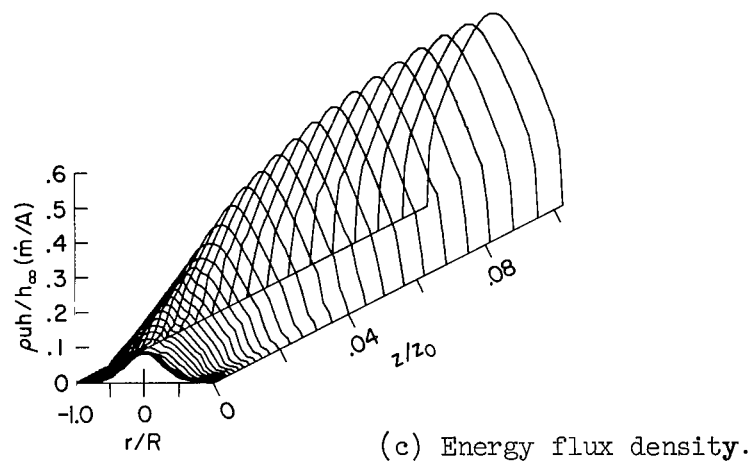
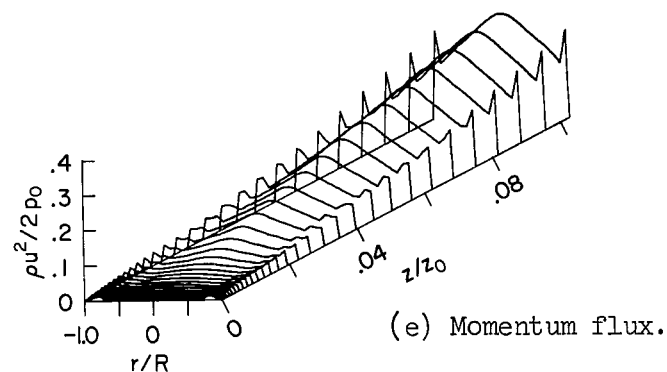
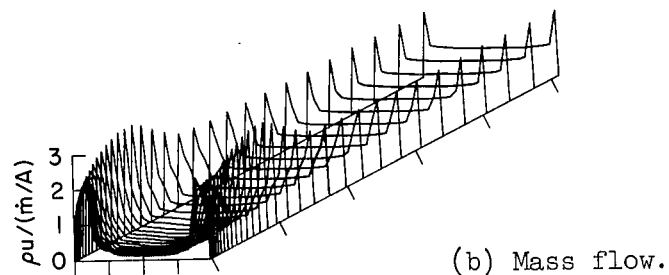
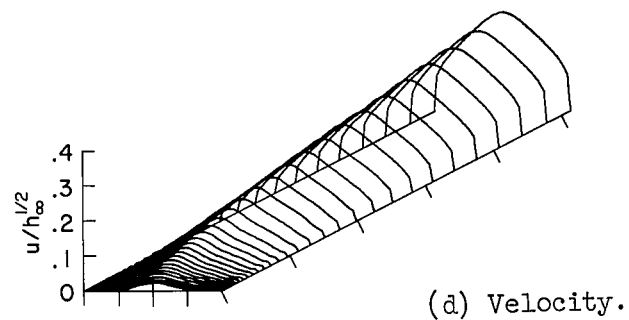
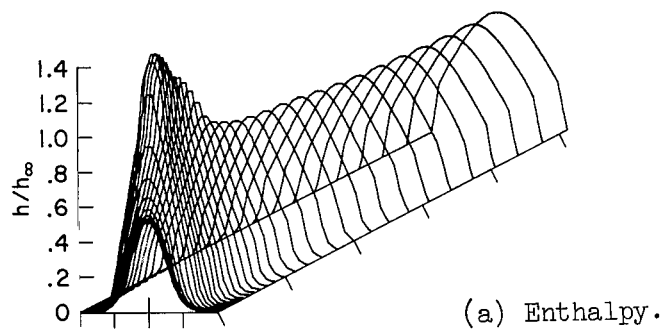
Moffett Field, Calif., 94035, Oct. 13, 1966

129-01-02-01-00-21



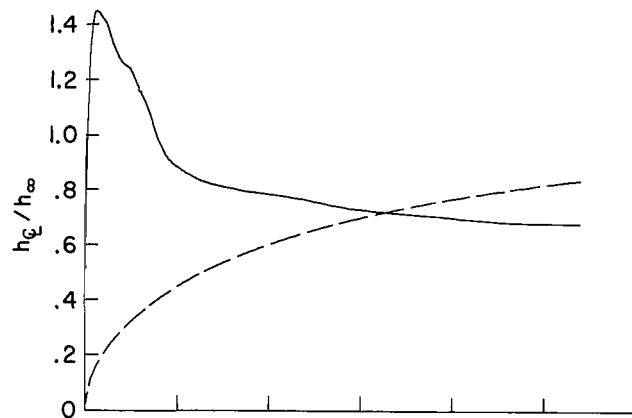
APPENDIX A

NUMERICAL SOLUTIONS FOR EVALUATING APPROXIMATIONS OF THE
SIMPLIFIED THEORETICAL MODELS OF THE CONSTRICTED ARC

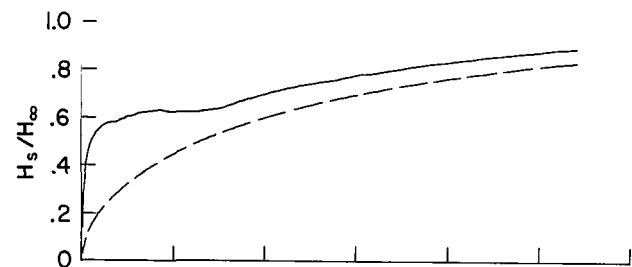


$I = 693$	A	$h_\infty = 2.25 \times 10^8$	J/kg
$\dot{m} = .00216$	kg/s	$\dot{m}/A = 17.1$	kg/sm ²
$R = .00635$	m	$h_\infty \dot{m}/A = 3.85 \times 10^9$	W/m ²
$z_0 = 2.14$	m	$\sqrt{h_\infty} = 1.50 \times 10^4$	m/s
		$p_0 = 9.65 \times 10^4$	N/m ² (.952 atm)
		$H_\infty = 9.76 \times 10^7$	J/kg
		$E_\infty = 819$	V/m
		$q_\infty = 1.42 \times 10^7$	W/m ²

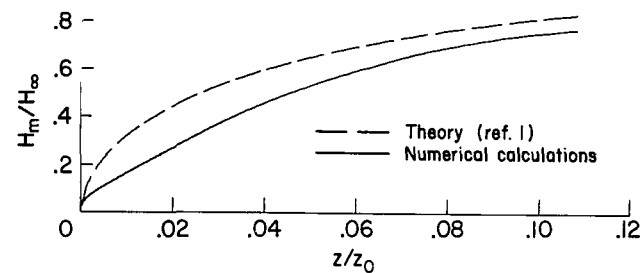
Figure A1.- The complete numerical solution without the simplifying approximations.



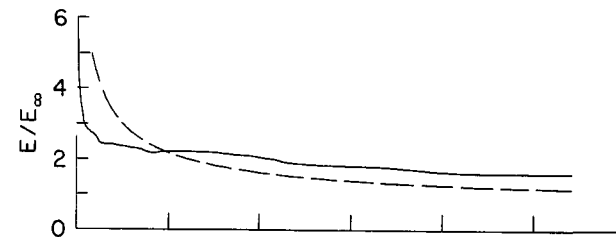
(f) Center-line enthalpy.



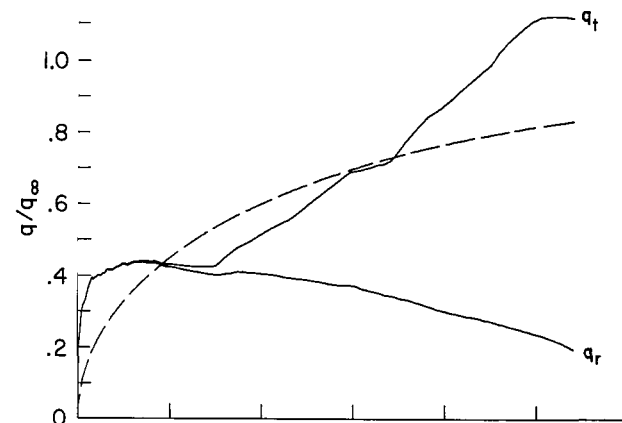
(g) Space-average enthalpy.



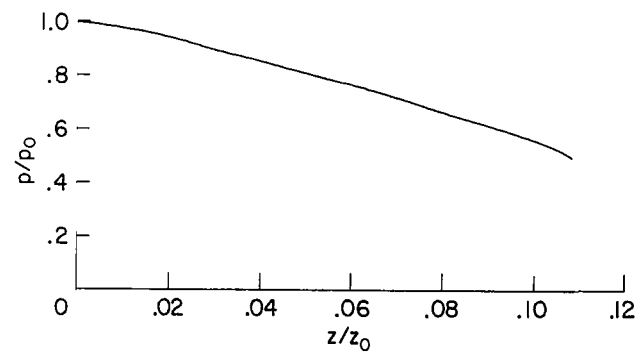
(h) Mass-average enthalpy.



(i) Voltage gradient.

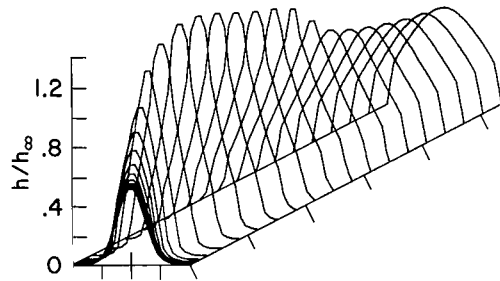


(j) Local heat transfer rate.

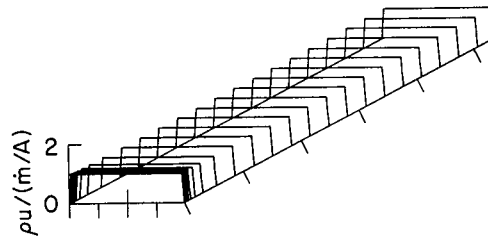


(k) Pressure.

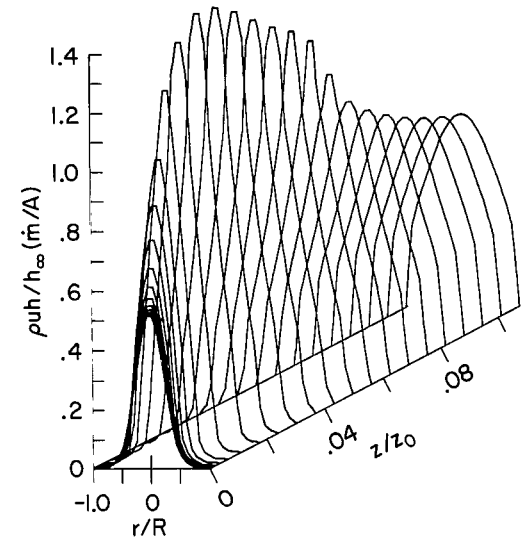
Figure A1.- Concluded.



(a) Enthalpy.



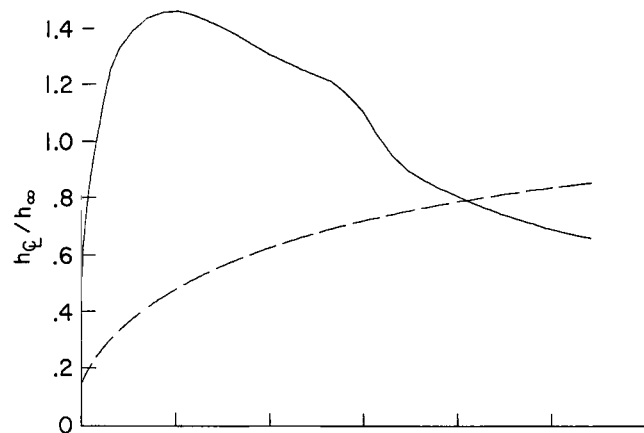
(b) Mass flow.



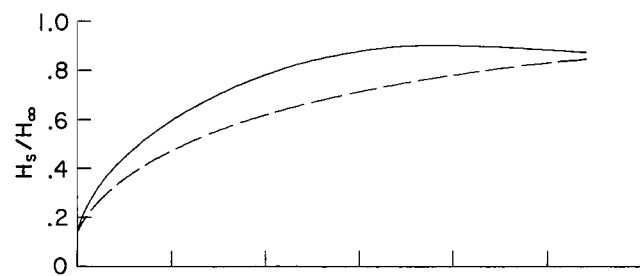
(c) Energy flux density.

		$h_{\infty} =$	2.25×10^8	J/kg
		$\dot{m}/A =$	17.1	kg/sm ²
		$h_{\infty} \dot{m}/A =$	3.85×10^9	W/m ²
		$\sqrt{h_{\infty}} =$	1.50×10^4	m/s
		$p_0 =$	9.65×10^4	N/m ² (.952 atm)
$I =$	693	A		
$\dot{m} =$.00216	kg/s		
$R =$.00635	m		
$z_0 =$	2.14	m		
		$H_{\infty} =$	9.76×10^7	J/kg
		$E_{\infty} =$	819	V/m
		$q_{\infty} =$	1.42×10^7	W/m ²

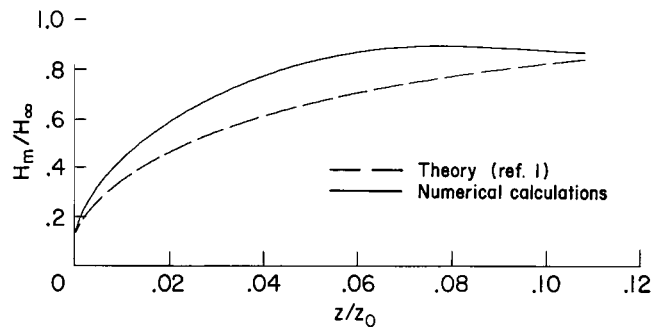
Figure A2.- Numerical solution with the approximation that mass flux density is constant.



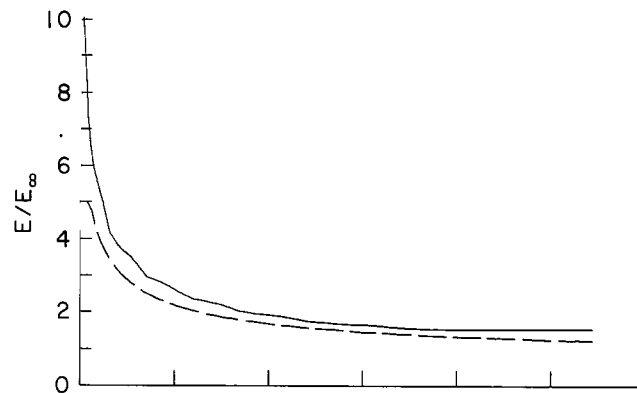
(d) Center-line enthalpy.



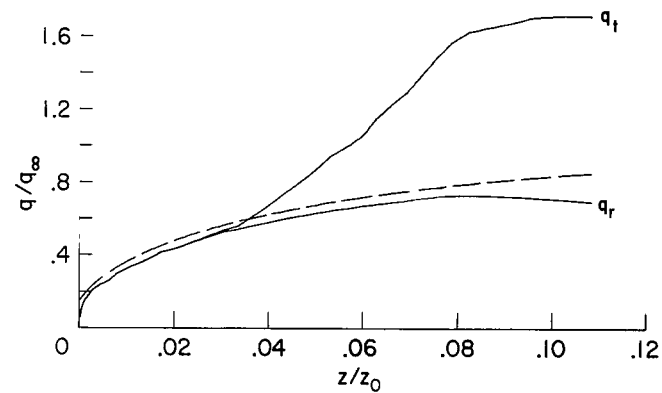
(e) Space-average enthalpy.



(f) Mass-average enthalpy.

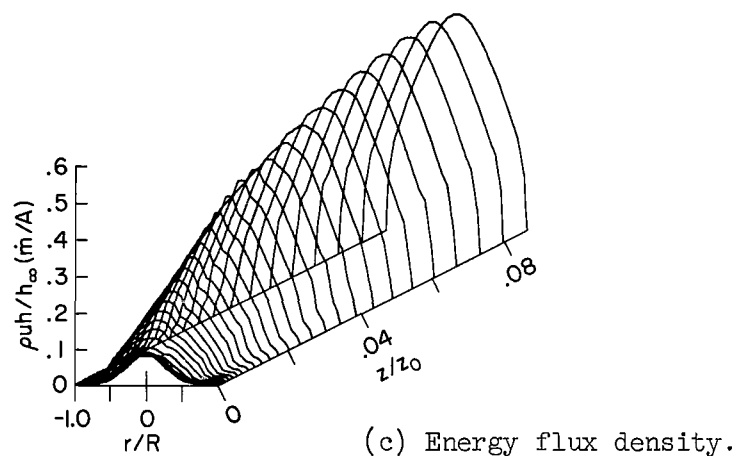
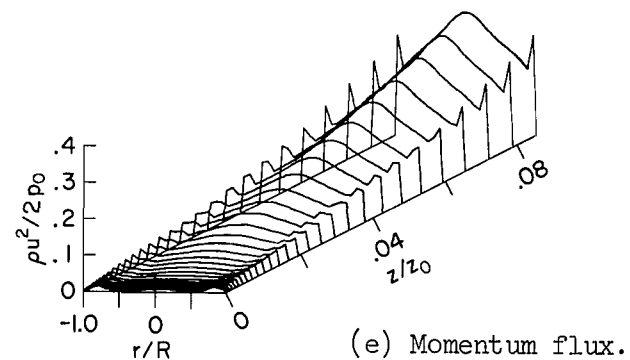
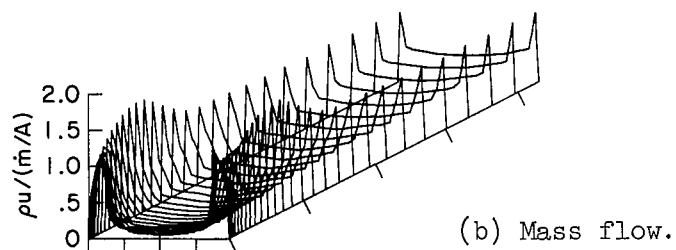
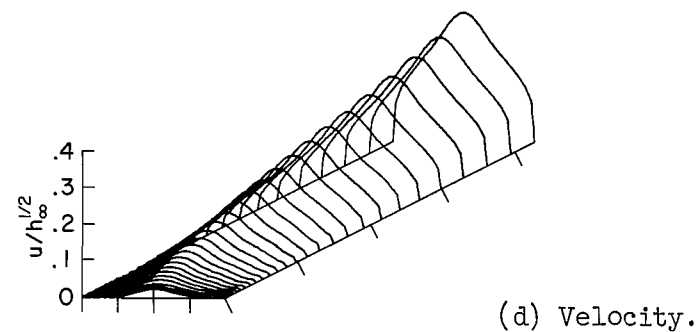
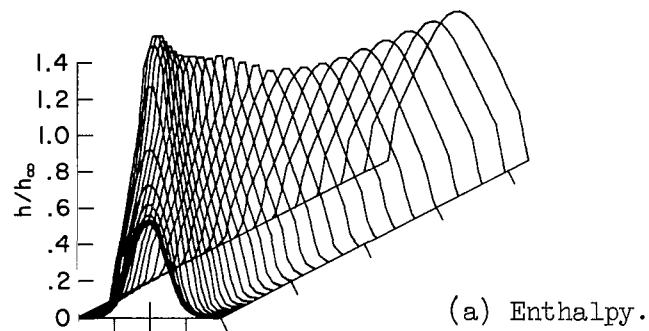


(g) Voltage gradient.



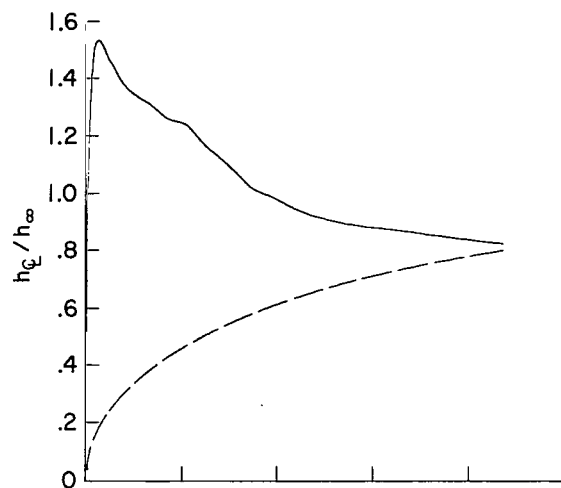
(h) Local heat transfer rate.

Figure A2.- Concluded.

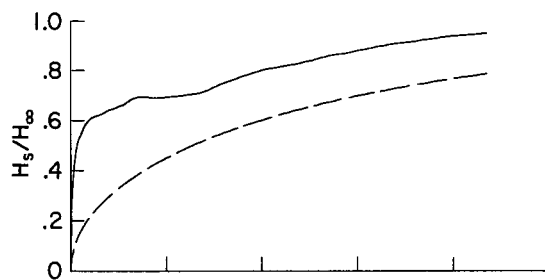


$I = 693$	A	$h_\infty = 2.25 \times 10^8$	J/kg
$\dot{m} = .00216$	kg/s	$\dot{m}/A = 17.1$	kg/sm ²
$R = .00635$	m	$h_\infty \dot{m}/A = 3.85 \times 10^9$	W/m ²
$z_0 = 2.14$	m	$\sqrt{h_\infty} = 1.50 \times 10^4$	m/s
		$p_0 = 9.65 \times 10^4$	N/m ² (.952 atm)
		$H_\infty = 9.76 \times 10^7$	J/kg
		$E_\infty = 819$	V/m
		$q_\infty = 1.42 \times 10^7$	W/m ²

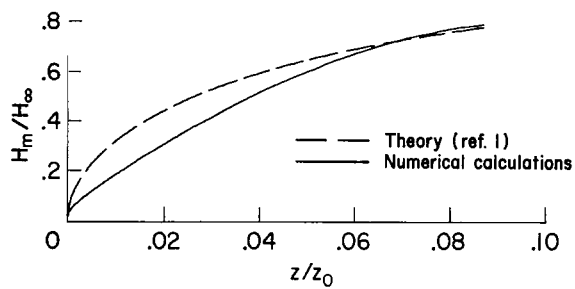
Figure A3.- Numerical solution with the approximation that the radiance is zero.



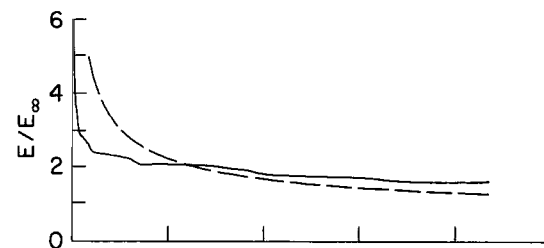
(f) Center-line enthalpy.



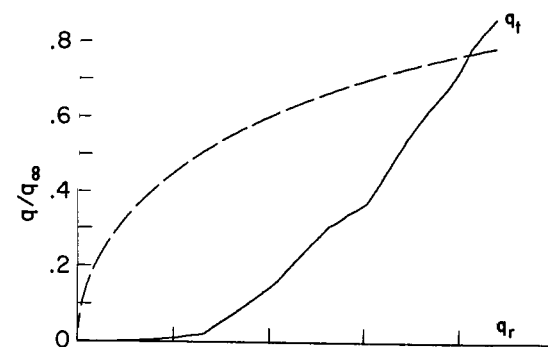
(g) Space-average enthalpy.



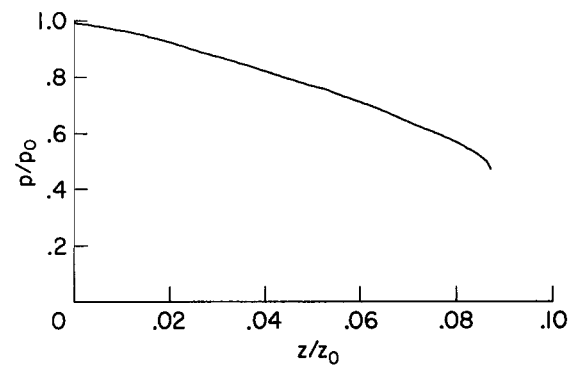
(h) Mass-average enthalpy.



(i) Voltage gradient.

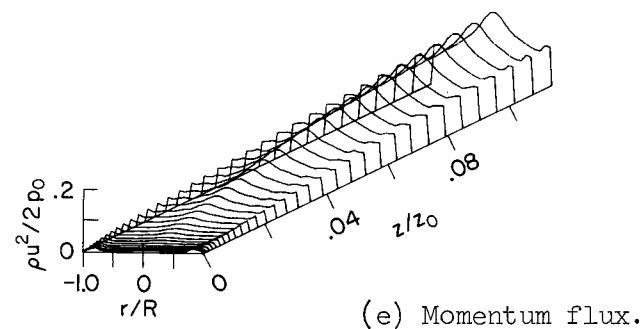
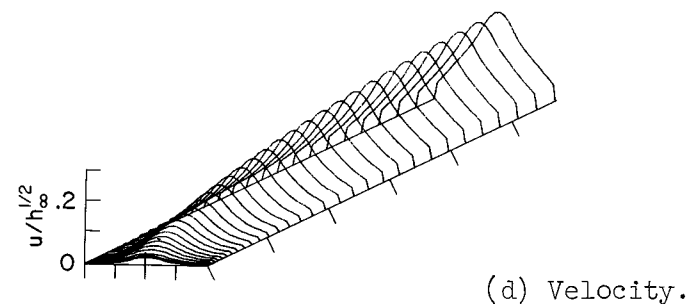
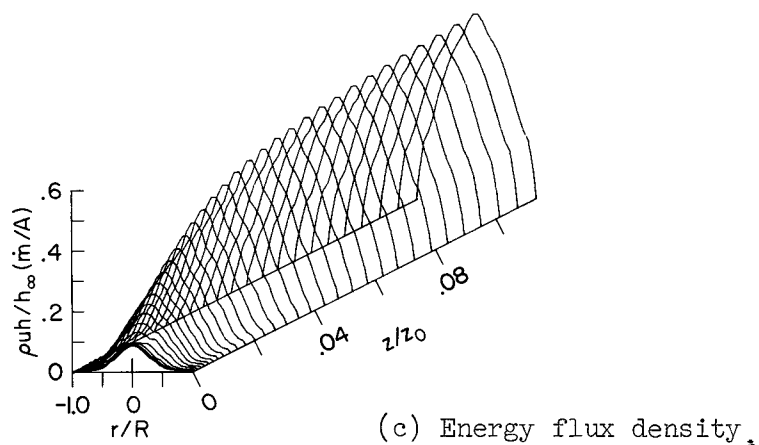
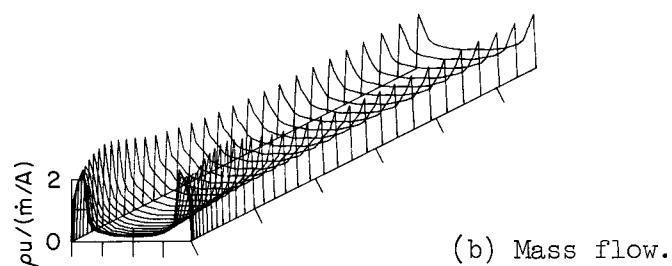
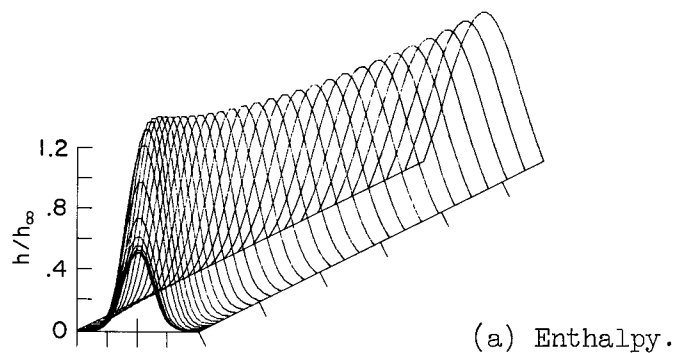


(j) Local heat transfer rate.



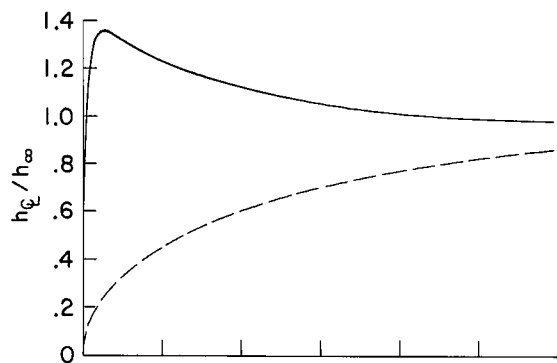
(k) Pressure.

Figure A3.- Concluded.

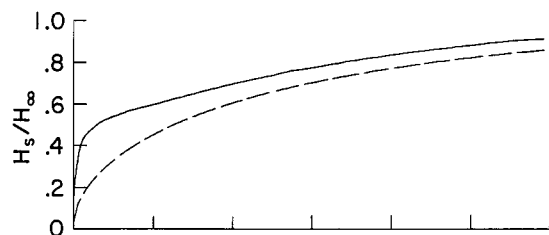


$I = 693$	A	$h_\infty = 2.25 \times 10^8$	J/kg
$\dot{m} = .00216$	kg/s	$\dot{m}/A = 17.1$	kg/sm ²
$R = .00635$	m	$h_\infty \dot{m}/A = 3.85 \times 10^9$	W/m ²
$z_0 = 2.14$	m	$\sqrt{h_\infty} = 1.50 \times 10^4$	m/s
		$p_0 = 9.65 \times 10^4$	N/m ² (.952 atm)
		$H_\infty = 9.76 \times 10^7$	J/kg
		$E_\infty = 819$	V/m
		$q_\infty = 1.42 \times 10^7$	W/m ²

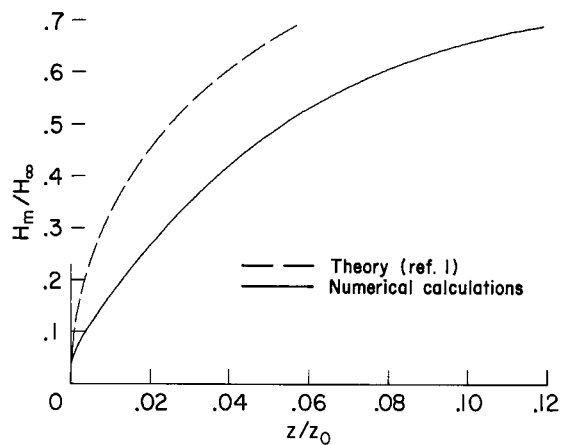
Figure A4.- Numerical solution with the idealized gas of reference 1.



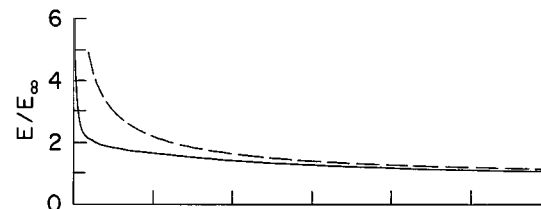
(f) Center-line enthalpy.



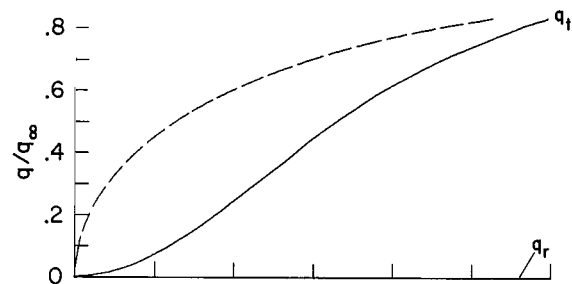
(g) Space-average enthalpy.



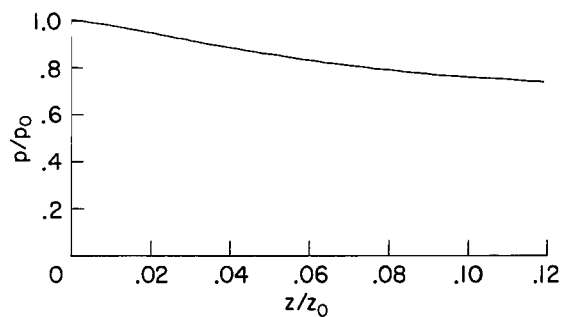
(h) Mass-average enthalpy.



(i) Voltage gradient.

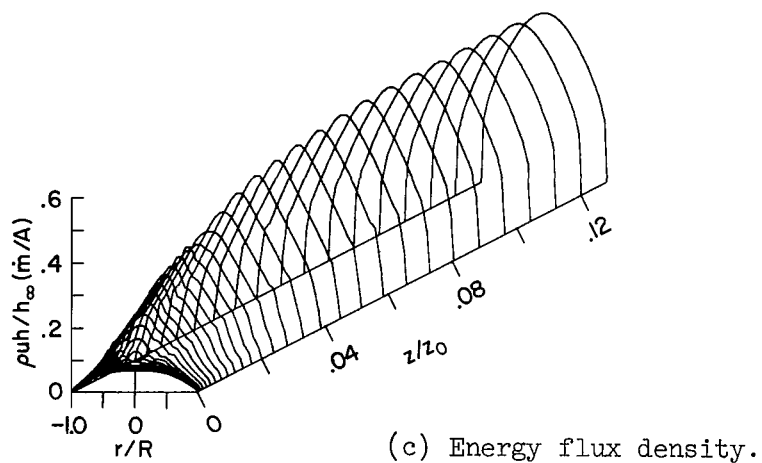
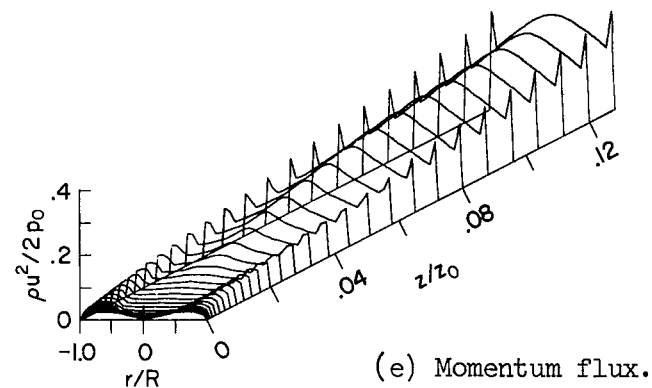
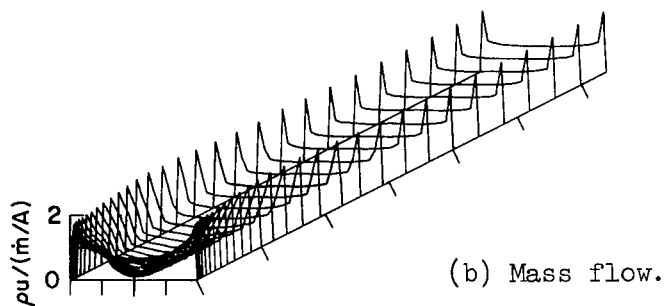
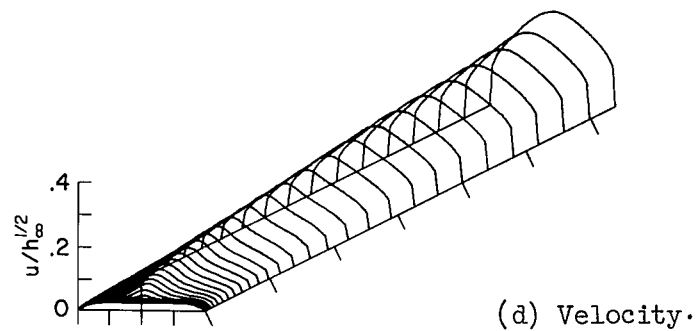
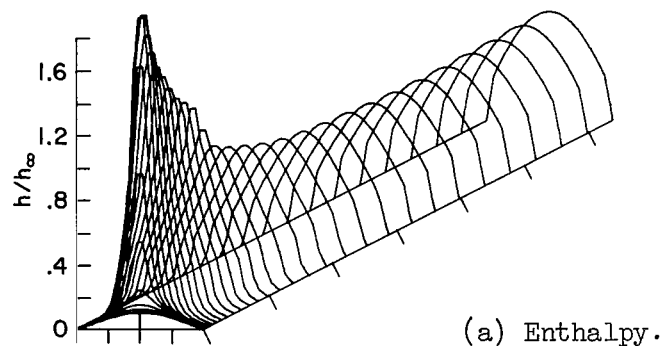


(j) Local heat transfer rate.



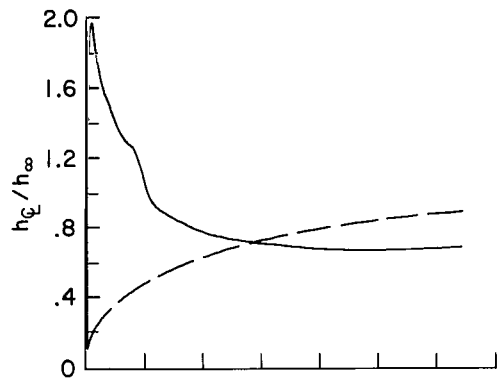
(k) Pressure.

Figure A4.- Concluded.

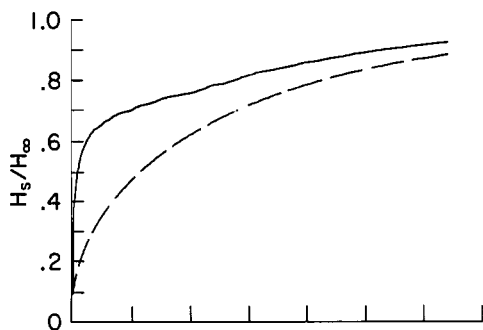


$I = 693$	A	$h_\infty = 2.25 \times 10^8$	J/kg
$\dot{m} = .00216$	kg/s	$\dot{m}/A = 17.1$	kg/sm ²
$R = .00635$	m	$h_\infty \dot{m}/A = 3.85 \times 10^9$	W/m ²
$z_0 = 2.14$	m	$\sqrt{h_\infty} = 1.50 \times 10^4$	m/s
		$p_0 = 9.65 \times 10^4$	N/m ² (.952 atm)
		$H_\infty = 9.76 \times 10^7$	J/kg
		$E_\infty = 819$	V/m
		$q_\infty = 1.42 \times 10^7$	W/m ²

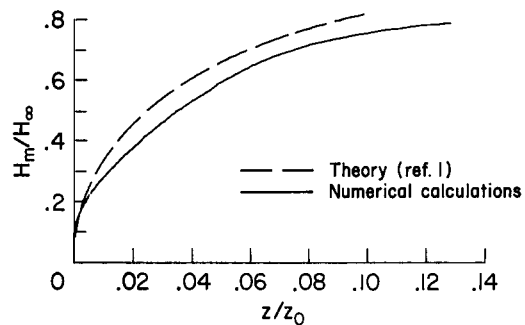
Figure A5.- Numerical solution with the assumption that the initial enthalpy distribution is a Bessel function.



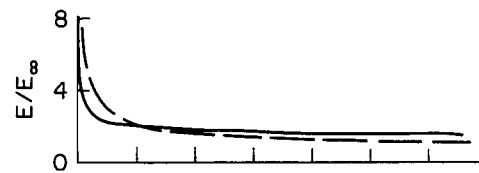
(f) Center-line enthalpy.



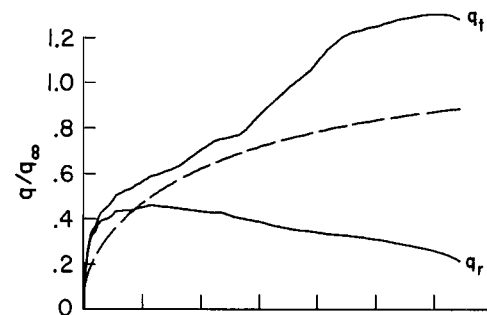
(g) Space-average enthalpy.



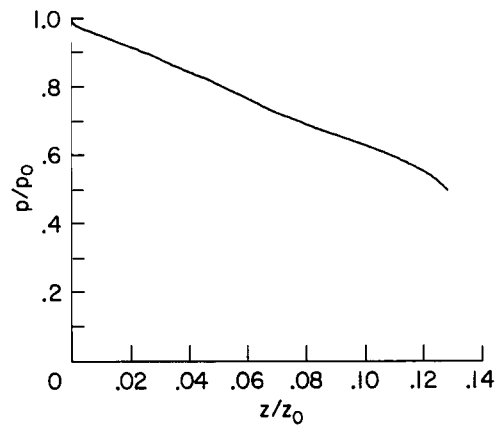
(h) Mass-average enthalpy.



(i) Voltage gradient.

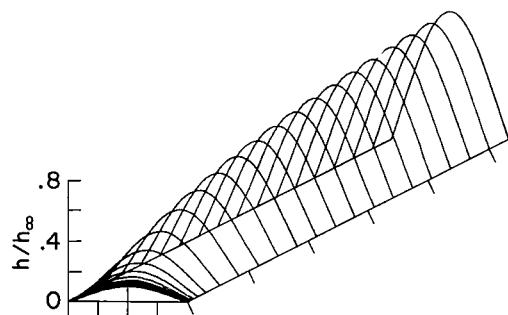


(j) Local heat transfer rate.

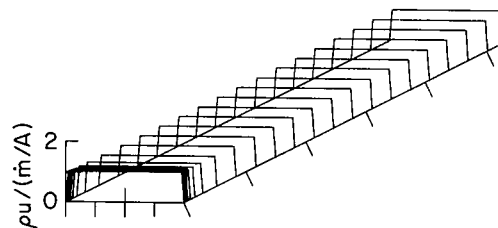


(k) Pressure.

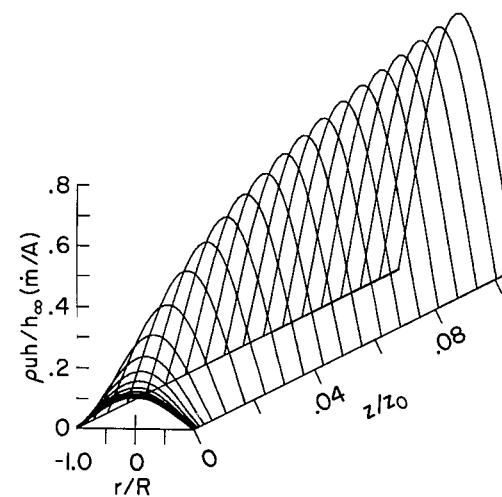
Figure A5.- Concluded.



(a) Enthalpy.



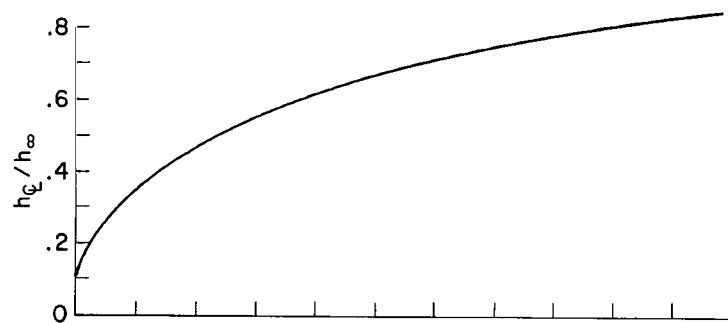
(b) Mass flow.



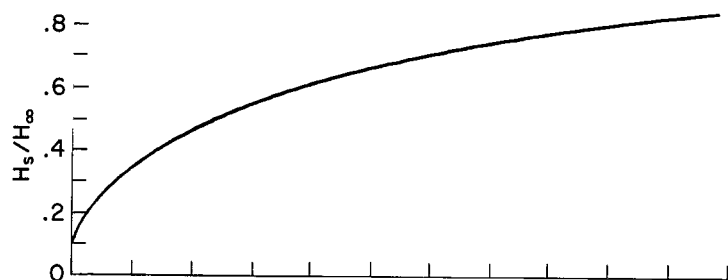
(c) Energy flux density.

$I = 693$	A	$h_{\infty} = 2.25 \times 10^8$	J/kg
$\dot{m} = .00216$	kg/s	$\dot{m}/A = 17.1$	kg/sm ²
$R = .00635$	m	$h_{\infty} \dot{m}/A = 3.85 \times 10^9$	W/m ²
$z_0 = 2.14$	m	$\sqrt{h_{\infty}} = 1.50 \times 10^4$	m/s
		$p_0 = 9.65 \times 10^4$	N/m ² (.952 atm)
		$H_{\infty} = 9.76 \times 10^7$	J/kg
		$E_{\infty} = 819$	V/m
		$q_{\infty} = 1.42 \times 10^7$	W/m ²

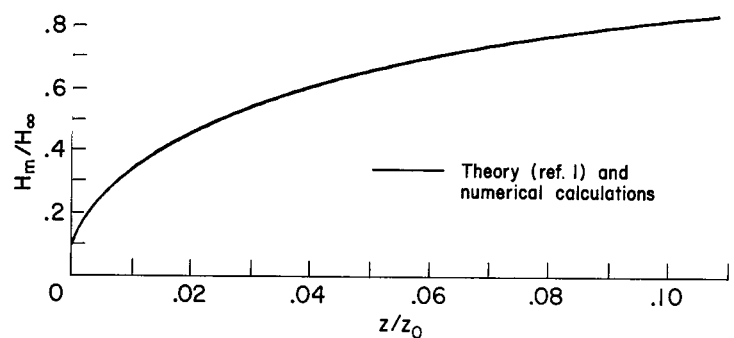
Figure A6.- The simplified theoretical model of reference 1. (This model contains all of the approximations in figures A2 through A5.)



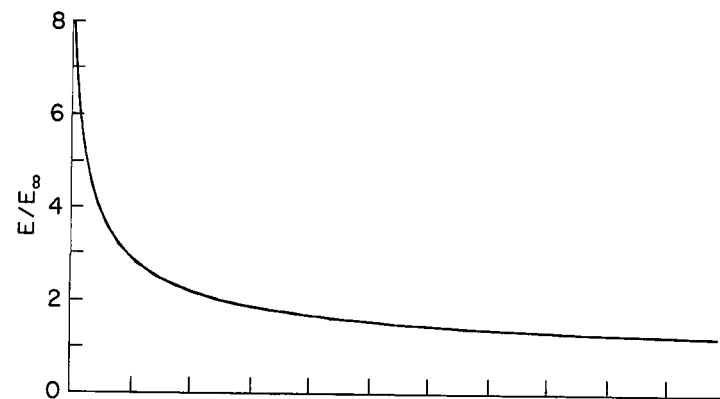
(d) Center-line enthalpy.



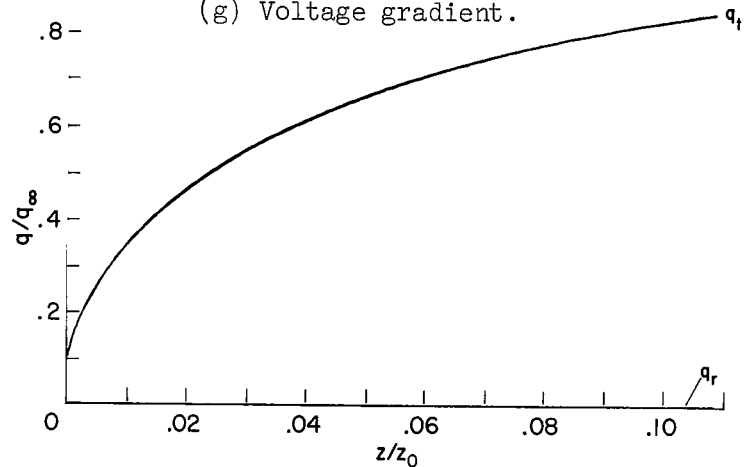
(e) Space-average enthalpy.



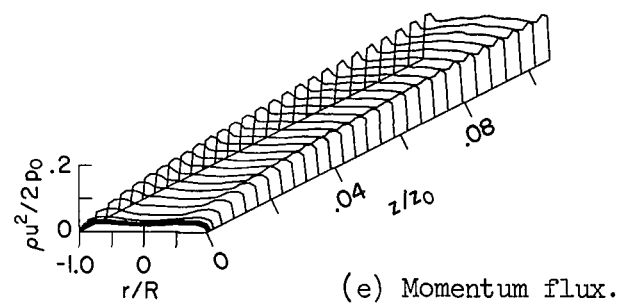
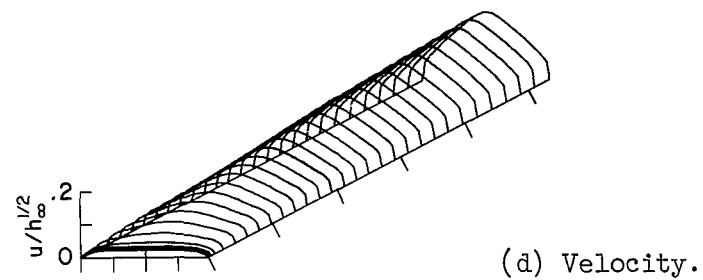
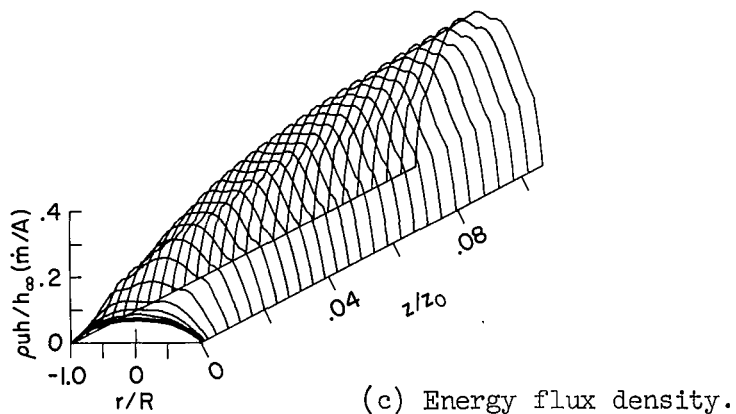
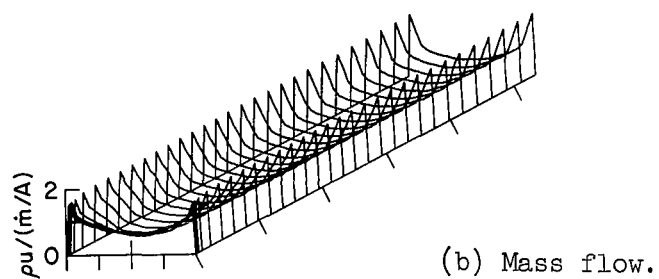
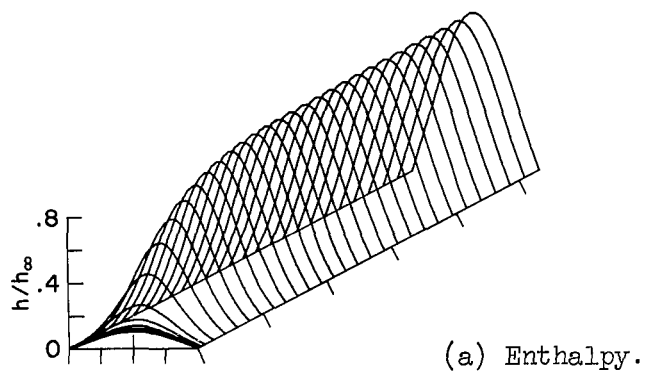
(f) Mass-average enthalpy.



(g) Voltage gradient.

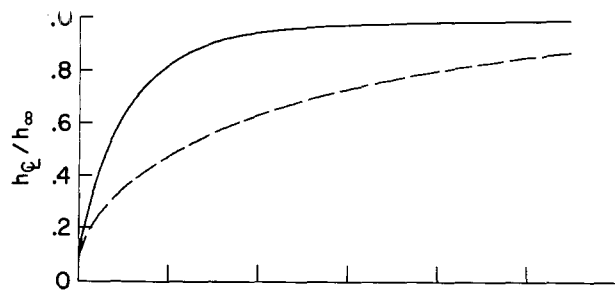


(h) Local heat transfer rate.

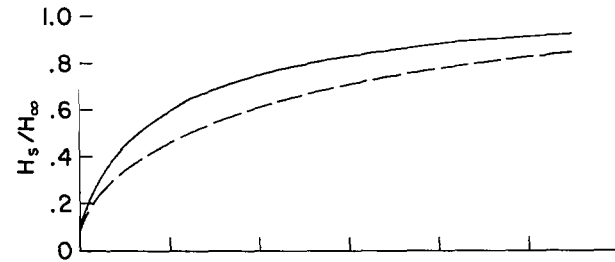


$I = 693$	A	$h_\infty = 2.25 \times 10^8$	J/kg
$\dot{m} = .00216$	kg/s	$\dot{m}/A = 17.1$	kg/sm ²
$R = .00635$	m	$h_\infty \dot{m}/A = 3.85 \times 10^9$	W/m ²
$z_0 = 2.14$	m	$\sqrt{h_\infty} = 1.50 \times 10^4$	m/s
		$p_0 = 9.65 \times 10^4$	N/m ² (.952 atm)
		$H_\infty = 9.76 \times 10^7$	J/kg
		$E_\infty = 819$	V/m
		$q_\infty = 1.42 \times 10^7$	W/m ²

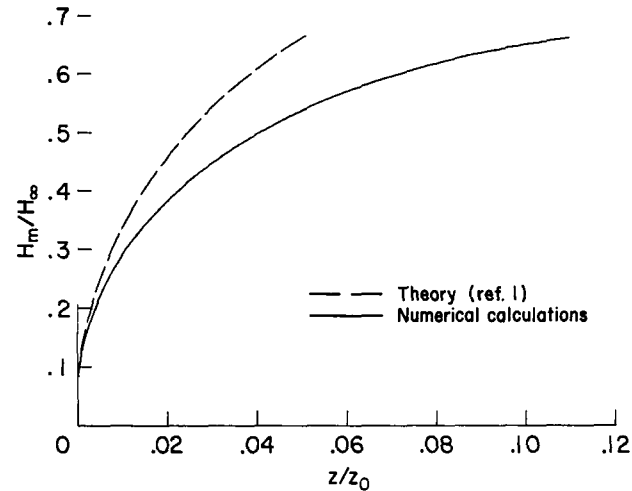
Figure A7.- The model of reference 1 without the approximation that the mass-flow density is constant.



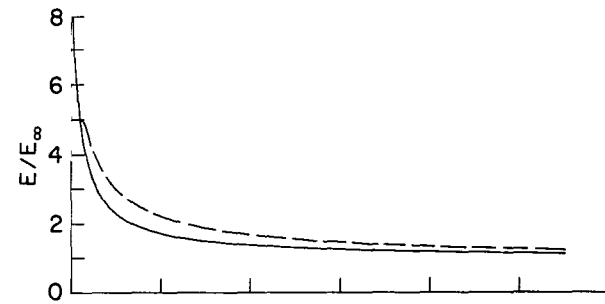
(f) Center-line enthalpy.



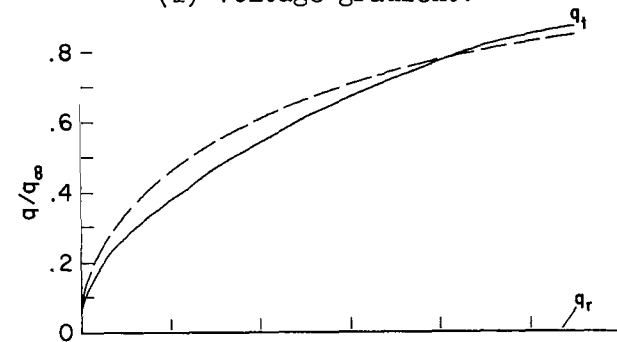
(g) Space-average enthalpy.



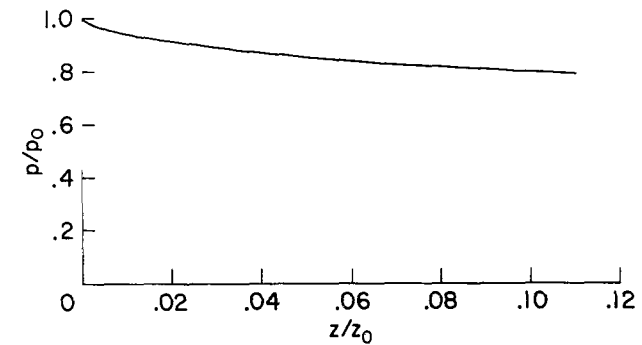
(h) Mass-average enthalpy.



(i) Voltage gradient.

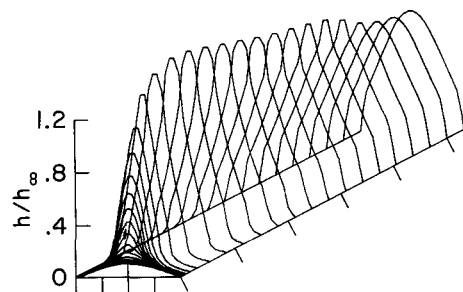


(j) Local heat transfer rate.

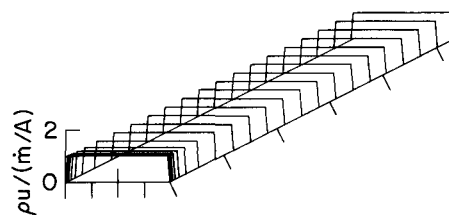


(k) Pressure.

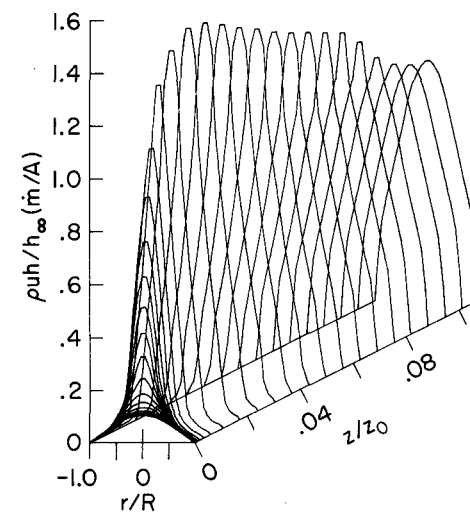
Figure A7.- Concluded.



(a) Enthalpy.



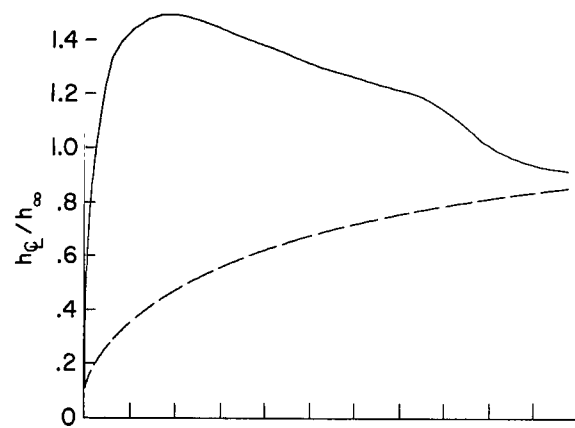
(b) Mass flow.



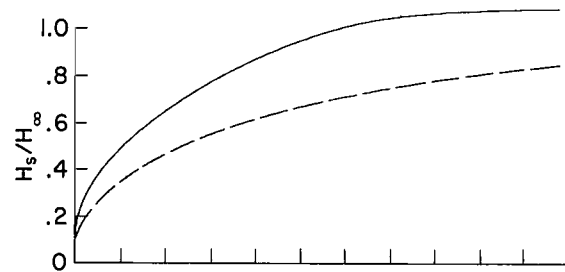
(c) Energy flux density.

$I = 693$	A	$h_{\infty} = 2.25 \times 10^8$	J/kg
$\dot{m} = .00216$	kg/s	$\dot{m}/A = 17.1$	kg/sm ²
$R = .00635$	m	$h_{\infty} \dot{m}/A = 3.85 \times 10^9$	W/m ²
$z_0 = 2.14$	m	$\sqrt{h_{\infty}} = 1.50 \times 10^4$	m/s
		$p_0 = 9.65 \times 10^4$	N/m ² (.952 atm)
		$H_{\infty} = 9.76 \times 10^7$	J/kg
		$E_{\infty} = 819$	V/m
		$q_{\infty} = 1.42 \times 10^7$	W/m ²

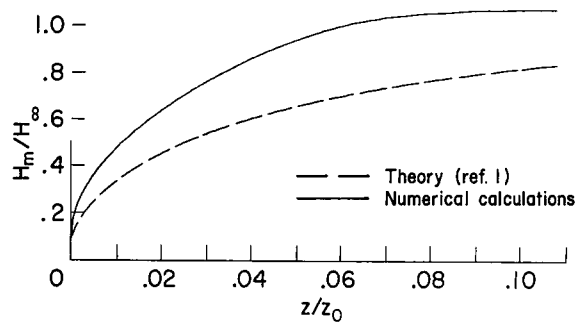
Figure A8.- The model of reference 1 without linearization of the gas properties.



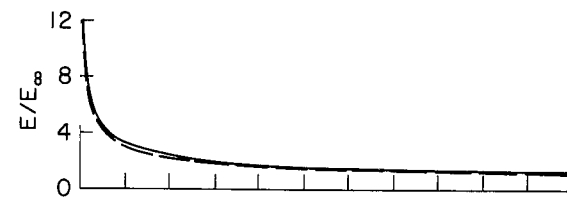
(d) Center-line enthalpy.



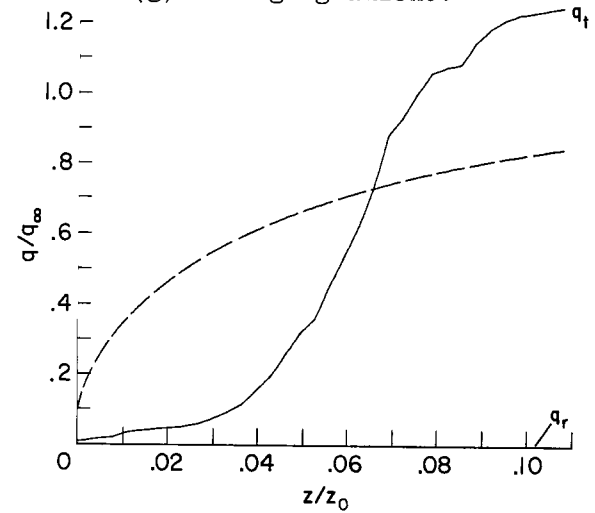
(e) Space-average enthalpy.



(f) Mass-average enthalpy.

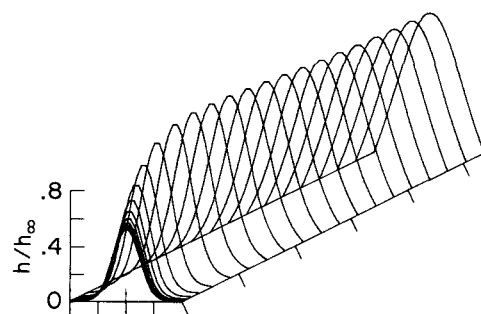


(g) Voltage gradient.

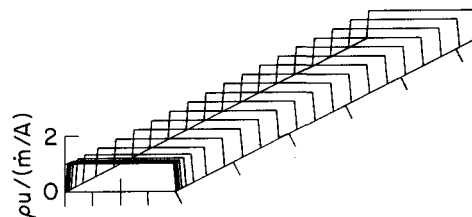


(h) Local heat transfer rate.

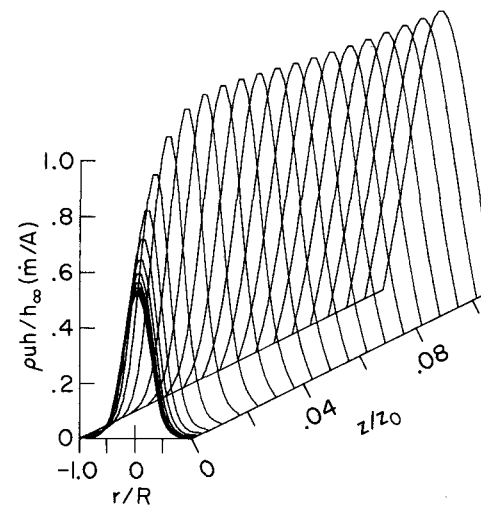
Figure A8.- Concluded.



(a) Enthalpy.



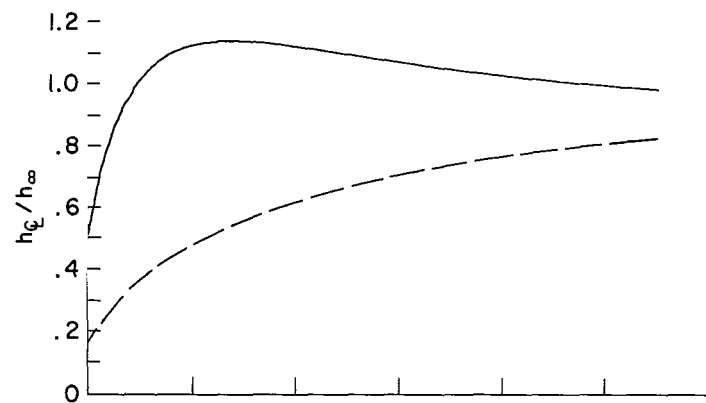
(b) Mass flow.



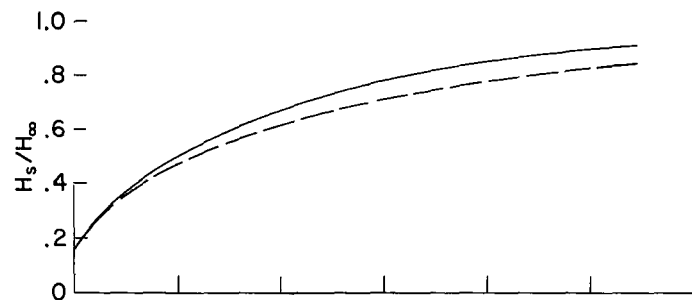
(c) Energy flux density.

$I = 693$	A	$h_\infty = 2.25 \times 10^8$	J/kg
$\dot{m} = .00216$	kg/s	$\dot{m}/A = 17.1$	kg/sm ²
$R = .00635$	m	$h_\infty \dot{m}/A = 3.85 \times 10^9$	W/m ²
$z_0 = 2.14$	m	$\sqrt{h_\infty} = 1.50 \times 10^4$	m/s
		$P_0 = 9.65 \times 10^4$	N/m ² (.952 atm)
		$H_\infty = 9.76 \times 10^7$	J/kg
		$E_\infty = 819$	V/m
		$q_\infty = 1.42 \times 10^7$	W/m ²

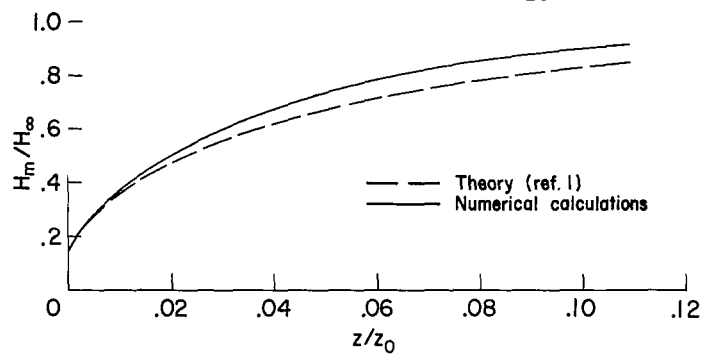
Figure A9.- The model of reference 1 without the assumption that the initial enthalpy distribution is a Bessel function.



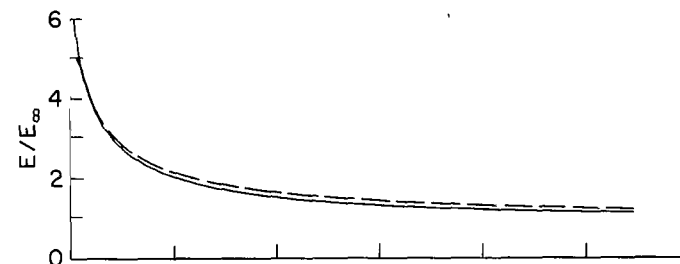
(d) Center-line enthalpy.



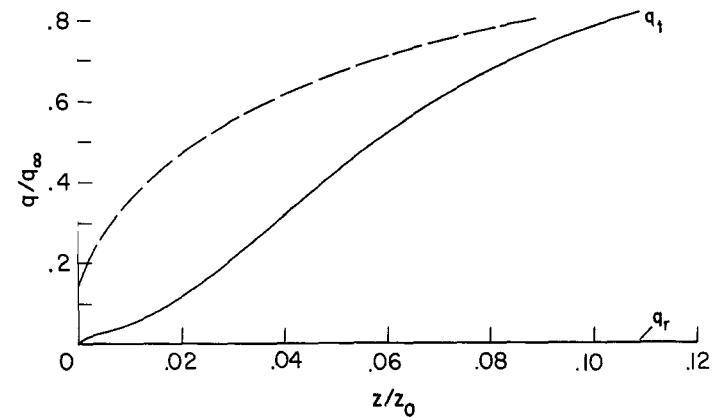
(e) Space-average enthalpy.



(f) Mass-average enthalpy.



(g) Voltage gradient.



(h) Local heat transfer rate.

Figure A9.- Concluded.

APPENDIX B

FORTRAN PROGRAM FOR THE SOLUTION OF THE AXISYMMETRIC CONSTRICTED ARC WITH AN AXIAL FLOW OF GAS

This appendix contains the Fortran II programs for the numerical solution of the axisymmetric constricted arc with an axial flow of gas. The data required for input into these programs and a legend for the Fortran variables is also included.

The function of each subroutine is described below.

BOUNDC	provides for the specification of the boundary conditions for the main program
STATEP	evaluates the state properties (except density) for all of the mesh points at each axial station
WDOT	evaluates the density for all of the mesh points at each axial station and calculates the mass flow rate by integration of the mass flux over the constrictor cross-sectional area
ITER	provides the iteration of pressure to obtain the correct mass flow in the subsonic portion of the nozzle
ITERS	provides the iteration of pressure to obtain the correct mass flow in the supersonic portion of the nozzle
MOM	calculates the velocity for all mesh points at the next axial station from the momentum equation
ENERGY	calculates the enthalpy for all mesh points at the next axial station from the energy equation
OUTPT	prints and writes on magnetic tape the results of the main program

INPUT DATA REQUIRED

Card number	Data or Fortran variable	Format
1	NFILE	14
2	NTAPE	14
3	KMAX	14
4	KINC	14
5	AMPS	E10.3
6	WS	E10.3
7	TRCL	E10.3
8	P(1)	E10.3
9	DIAM(1)	E10.3
10	THETA	E10.3
11	HWALL(1)	E10.3
12	NMESH	14
13	FZO	E10.3
14	EX	E10.3
15	EXX	E10.3
16	EPS	E10.3
17 through 17 + N	H(1) through H(NMESH)	5E10.3
18 + N through 18 + 2N	U(1) through U(NMESH)	5E10.3

where

$$N = \text{MOD}[(\text{NMESH} - 1)/5]$$

These Fortran variables are described in the following legend under the variables common to all of the programs or under the variables for program number HT0702.

VARIABLES USED IN THE PROGRAMS FOR THE NUMERICAL SOLUTIONS OF THE SYMMETRIC CONSTRICTED THERMAL ARC WITH AN AXIAL FLOW OF GAS

Variables Common to All Programs

Variable Name	Description
AMPS	total current carried by the constrictor, A
DIAM	diameter of the constrictor (an array), m
DIA	diameter of the constrictor, m
DP	pressure drop between axial stations, N/m ²
DRDR	square of the incremental radial distance, DR, m ²
DR	incremental radial distance, m
DW	discrepancy between the mass flow rate at this axial station and the initial mass flow rate, kg/s

<u>Variable name</u>	<u>Description</u>
DZ	incremental axial distance, m
EPS	maximum allowable relative discrepancy of the mass flow rate
E	axial voltage gradient, V/m
EX	factor by which the axial incremental distance is increased for the next axial station
EXX	stability factor that limits maximum size of DZ in order to maintain stability
FZO	length of the first axial increment divided by the characteristic arc length, z_0
HAVE	space average of the enthalpy, $\frac{1}{A} \int_A h \, dA$, J/kg
HRAVE	average energy density, $\frac{1}{A} \int_A \rho h \, dA$, J/m ³
H	local enthalpy, J/kg
HWALL	enthalpy of the gas at the constrictor wall, J/kg
KINC	number of axial stations between printout of results
KMAX	maximum number of axial stations to be calculated
K	axial station number
LOC	number of iterations required to satisfy the continuity equation (i.e., the number of iterations required such that the flow rate at this axial station is sufficiently near the initial flow rate)
L	relative axial station number
M	second relative axial station number
NCHOK	flag indicating that the flow is choked
NERR	error flag for the gas property subroutines
NFILE	file number on the magnetic tape used to store the solutions
NK	extra variable not used

<u>Variable name</u>	<u>Description</u>
NMESH	number of radial increments from the center line to the constrictor wall
NNN	flag indicating this is the first iteration on pressure drop (zero indicates first iteration, 1 indicates all iterations thereafter)
NTAPE	magnetic tape on which the solution is stored
PHI	local thermal conductivity potential, W/m
PHIW	thermal conductivity potential of the gas at the constrictor wall, W/m
P	static pressure at this axial station, N/m ²
QR	heat transfer rate to the constrictor wall that is due to radiation, W/m ²
Q	heat transfer rate to the constrictor wall that is due to thermal conduction, W/m ²
RCAP	local radiation, W/m ³
RHOAV	space average density, kg/m ³
RHO	local density, kg/m ³
RHOU	local product of density and velocity at this station, kg/sm ²
RROU	local product of density times velocity at the previous axial station, kg/sm ²
R	local radius, m
RUH	total energy flux at this axial station, W/m ²
SIGMA	local electrical conductivity, 1/Ω-m
THETA	half-angle of divergence of the supersonic nozzle, deg
TRCL	mass flux density of constrictor transpiration cooling, kg/sm ²
U	local velocity, m/s
VISC	local viscosity, Ns/m ²
W	mass flow rate at the initial axial station, kg/s

<u>Variable name</u>	<u>Description</u>
WW	mass flow rate at this axial station, kg/s
Z	axial distance of this axial station from the initial axial station, m
Variables Local to Program HT-0701	
DZMAX	upper limit of the axial increment distance (the incremental axial distance is never allowed to exceed this value in order to keep the solution stable), m
FNMESH	number of radial increments from the center line to the constrictor wall (floating number)
KC	axial station number at which aerodynamic choking occurs
KI	index for the main loop within the program
NMESH	radial index for the constrictor wall
NN	index to indicate the axial stations for which the results should be printed and stored
NSS	flag to indicate that the flow is supersonic
PRAD	percentage of the heat flux to the constrictor wall at this axial station that is due to radiation
PRES	local static pressure, atm
QT	total heat transfer rate to the constrictor wall at this axial station, W/m ²
RUHA	mass average energy at this axial station, $\frac{1}{\dot{m}} \int_A \rho u h \, dA$, J/kg
THETAR	half-angle of divergence of the supersonic nozzle, radians
ZC	axial distance from station 1 for which the flow chokes, m

Variables for Program HT-0702

CWF	scaling factor that changes the magnitude of the velocity profile to obtain the desired initial flow rate
RHOA	space average of the density at this axial station, kg/m ³

<u>Variable name</u>	<u>Description</u>
THETAR	half-angle of divergence of the supersonic nozzle, radians
WS	mass flow rate through the constrictor
ZO	characteristic arc length, z_0 , m

Variables for Program HT-0703

DA	incremental cross-sectional area, m^2
DHA	product of the local enthalpy and the incremental area, Jm^2/kg
DHRA	product of the local enthalpy, the local density, and the incremental area, J/m
DQR	product of the local radiation and the incremental area, W/m
DSS	product of the local electrical conductivity and the incremental area, m/Ω
FJ	floating index for the radial position
HA	running total of the product of the enthalpy and the area, Jm^2/kg
HRA	running total of the product of enthalpy, density, and the area, J/m
J	index for the radial position
NMESH	radial index for the constrictor wall
PRES	local static pressure, atm
RDR	product of the local radius and incremental radial distance, m^2
RW	dummy variable not used
SS	running total of the product of electrical conductivity and area, m/Ω
SW	electrical conductivity at the constrictor wall, $1/\Omega\text{-m}$
VW	viscosity at the constrictor wall, Ns/m^2

Variables Local to Program HT-0704

<u>Variable name</u>	<u>Description</u>
DA	incremental cross-sectional area, m^2
DRA	product of the incremental cross-sectional area and the local mass flux, kg/s
DRUH	product of the incremental cross-sectional area and the local energy flux, W
J	index for the radial incremental distance
PRES	local static pressure, atm
RA	running sum of the mass flux, kg/s
RDR	product of the radius and the incremental radial distance, m^2

Variables Local to Programs HT-0705 and 0706

DDP	amount that the pressure drop is changed for each iteration at this axial station, N/m^2
IND	flag used in adjusting the pressure drop during the iterations at this station
N	index for the iterations

Variables Local to Program HT-0707

AR	cross-sectional area of the previous station divided by the cross-sectional area of this station
DA	incremental cross-sectional area, m^2
DRUTP	radial mass flux from this volume increment toward the center of the column, kg/sm^2
DRUT	radial mass flux toward the center of the column into this volume increment, kg/sm^2
GA	velocity of the gas associated with the radial mass flux, DRUTP, m/s
GB	velocity of the gas associated with the radial mass flux, DRUT, m/s

<u>Variable name</u>	<u>Description</u>
NMESHPI	index for the radial incremental distance that designates the constrictor wall
RADCON	momentum convected radially into this volume increment, kg/ms^2
RCP1	momentum convected radially into the volume element at the previous axial station, kg/ms^2
RCP2	momentum convected radially into the volume increment two axial stations ahead of this one, kg/ms^2
RCP3	momentum convected radially into the volume increment three axial stations ahead of this one, kg/ms^2
RCP4	momentum convected radially into the volume increment four axial stations ahead of this one, kg/ms^2
RDR	product of the radius and the radial incremental distance, m^2
RUPREV	local mass flux at the previous axial station, kg/sm^2
VL	viscous losses for this volume increment, N/m^2

Variables Local to Program HT-0708

AR	cross-sectional area of the previous station divided by the cross-sectional area of this station
CL	conduction losses from this incremental volume, W/m^3
DA	incremental cross-sectional area, m^2
DRUTP	radial mass flux from this volume increment toward the center of the column, kg/sm^2
DRUT	radial mass flux toward the center of the column into this volume increment, kg/sm^2
FJ	index for the radial incremental distance (floating)
GA	energy of the gas associated with the radial mass flow, DRUT, J/kg
GB	energy of the gas associated with the radial mass flow, DRUTP, J/kg
J	index for the radial incremental distance

<u>Variable name</u>	<u>Description</u>
OH	ohmic heating within this volume element, W/m^3
RADCON	energy convected radially into this volume increment, kg/ms^2
RCP1	energy convected radially into the volume element at the previous axial station, kg/ms^2
RCP2	energy convected radially into the volume increment two axial stations previous to this one, kg/ms^2
RCP3	energy convected radially into the volume increment three axial stations previous to this one, kg/ms^2
RCP4	energy convected radially into the volume increment four axial stations previous to this one, kg/ms^2
RDR	product of the radius and the radial incremental distance, m^2
RL	local radiation, W/m^3
TE	local kinetic energy (an array), J/kg
TEP	local kinetic energy, J/kg

Variables Local to Program HT-0709

PRAD	percentage of the constrictor wall heat flux that is due to radiation
PRES	local static pressure, atm
QT	total heat transfer rate to the constrictor wall, W/m^2
RUHA	mass average energy at this axial station, $\frac{1}{\dot{m}} \int_A \rho u h \, dA$, J/kg

```

CHT0701 VAL WATSON  DC ARC - AXIAL FLOW - REAL GAS - 2D
      COMMON AMPS, DIAM, DIA, DP, DRDR, DR, DW, DZ, EPS, E
1      , EX, EXX, FZO, HAVE, HRAVE, H, HWALL, K, KINC, KMAX, LOC, L
1      , M, NCHOKE, NERR, NFILE, NK, NMESH, NNN, NTAPE, PHI, PHIW
1      , P, QR, Q, RCAP, RHOAV, RHO, RHOV, RROU, R, RUH
1      , SIGMA, THETA, TRCL, U, VISC, W, WW, Z
      DIMENSION DIAM(2000), P(2000), E(2000), HWALL(2000)
1      , PHI(100), SIGMA(100), RCAP(100), VISC(100), RHO(100)
1      , R(100), RHOV(100), RROU(100)
1      , H(2,100), U(2,100)
      CALL CRISIS(ZZ,AA,AMPS,Z)
98  CONTINUE
      NSS = 0

C
C SET INITIAL CONDITIONS AND COMPUTE FIRST AXIAL STEP
      CALL BOUNDC
      FNMESH = NMESH

C
      REWIND 8
C MAIN LOOP FOR COMPUTING EACH AXIAL STEP
      DO 6 KI= 3 ,KMAX
        K = K +1
        NN = NN - 1

C
C MAINTAIN AXIAL STEP SIZE LESS THAN STEP SIZE FOR INSTABILITY
        DZMAX = ((DIA*DIA/4.0)*RHOV(2)*H(M,2)/(PHI(2)*FNMESH*FNMESH))*EXX
        IF(DZ-DZMAX) 40,42,42
40         DZ = EX*DZ
42         CONTINUE
        Z = Z + DZ

C
C START DIVERGENCE OF NOZZLE AFTER CHOKING
        IF(NSS) 58,58,52
52        IF(Z-ZC) 58,56,56
56         DIAM(K) = DIAM(KC) +2.0*(Z-ZC)*TANF(THETAR)
58        CONTINUE
        DIA = DIAM(K)
        DR = DIA/(2.0*FLOATF(NMESH-1))
        DRDR = DR*DR

C
C INCREASE IN FLOW RATE FROM TRANSPIRATION COOLING
        W = W + DZ*3.1416*DIA*TRCL

C
C ALTERNATING STORAGE LOCATION FOR AXIAL STATIONS
        M = 1
        L = L + 1
        IF(3-L) 1,1,2

```

```

1          M = 2
          L = 1
2          CONTINUE
C
C EVALUATION OF THE ENTHALPY AT NEXT AXIAL STATION FROM ENERGY EQUATION
          CALL ENERGY
C
C CHECK FOR SUPERSONIC OR SUBSONIC FLOW
          IF(NSS) 60,60,62
C
C CALCULATION OF VELOCITY AT NEXT STA THRU ITERATION - SUBSONIC FLOW
60 CALL ITER
   GO TO 68
62 IF(Z-ZC) 64,66,66
64 CALL ITER
   GO TO 68
C
C CALCULATION OF VELOCITY AT NEXT STA THRU ITERATION - SUPERSONIC FLOW
66 CALL ITERRS
68 CONTINUE
C
C CHECK FOR CHOKED FLOW
C IF CHOKED AND SUBSONIC, START DIVERGING NOZZLE
C IF CHOKED AND SUPERSONIC, GIVE ERROR READING AND EXIT
          IF(NCHOKE) 4,4,70
70          IF(NSS) 72,72,3
72          NSS = 1
          KC = K - 1
          ZC = Z - DZ/2.0
          CALL SKIP(-1,NTAPE)
          READ TAPE NTAPE, K, DIAM(K), Z, AMPS, E(K), W,QT,HWall(K)
1          ,PRAD, NMESH, PRES,FZO,LOC,EPS,DW, DP, DZ
2          , HAVE, RUHA,HRAVE
          P(K) = PRES*1.013E5
          READ TAPE NTAPE, (R(J), H(M,J), U(M,J), RHOU(J), J=1,NMESH)
          NMESHP = NMESH + 1
          U(M,NMESHP) = 0.0 - U(M,NMESH)
          DO 73 J=1,NMESH
73 RROU(J)=RHOU(J)
          NN=KC-K
          CALL SKIP(1, NTAPE)
          CALL STATEP
          CALL WDOT
          GO TO 6
3          WRITE OUTPUT TAPE 6, 202, K, DW, U(M,2)
          GO TO 8
4          CONTINUE

```

```

      CALL STATEP
C
C IF PRESSURE TOO LOW FOR GAS TABLES, EXIT
      IF(P(K) - 0.1E5) 74,74,76
      74      CALL OUTPT
              GO TO 8
      76 CONTINUE
C
C WRITE OUT VALUES FOR EVERY (KINC)TH AXIAL STATION
      IF(NN) 5,5,6
      5      NN = KINC
              CALL OUTPT
      6 CONTINUE
      8 CONTINUE
      REWIND NTAPE
202 FORMAT(1H0, 18HFLOW CHOKED AT K = , I4, 10X,
1      20HFLOW RATE ERROR IS      , 2PF12.7, 10H PERCENT ,
2 14 HCL VELOCITY = ,0PF10.1, 8H M/SEC      )
      GO TO 98
      END

```



CHT0702 VAL WATSON SUBROUTINE BOUNDC FOR HT0720

SUBROUTINE BOUNDC

COMMON AMPS, DIAM, DIA, DP, DRDR, DR, DW, DZ, EPS, E

1 , EX, EXX, FZO, HAVE, HRAVE, H, HWALL, K, KINC, KMAX, LOC, L

1 , M, NCHOKE, NERR, NFILE, NK, NMESH, NNN, NTAPE, PHI, PHIW

1 , P, QR, Q, RCAP, RHOAV, RHO, RHOU, RROU, R, RUH

1 , SIGMA, THETA, TRCL, U, VISC, W, WW, Z

DIMENSION DIAM(2000), P(2000), E(2000), HWALL(2000)

1 , PHI(100), SIGMA(100), RCAP(100), VISC(100), RHO(100)

1 , R(100), RHOU(100), RROU(100)

1 , H(2,100), U(2,100)

CALL CRISIS (ZZ,AA)

C

C SET UP MAGNETIC TAPES

READ INPUT TAPE 5, 100, NFILE , NTAPE

CALL LOCATE(NFILE,NTAPE)

C

C SET MAX ALLOWABLE AXIAL STATIONS AND INTERVAL BETWEEN PRINTOUT

READ INPUT TAPE 5, 100, KMAX, KINC

C

C SET INITIAL VALUES OF CURRENT, FLOW RATES, AND PRESSURE

READ INPUT TAPE 5, 101, AMPS, WS, TRCL, P(1)

P(1) = P(1)*1.013E5

C

C SET UP THE DIA AS A FUNCTION OF AXIAL DIST

C DIAMETER IS CONSTANT IN THIS CASE

C (THETA IS THE HALF ANGLE OF DIVERGENCE AFTER CHOKING OCCURS)

READ INPUT TAPE 5, 101, DIAM(1)

DO 300 ID = 2,KMAX

300 DIAM(ID) = DIAM(1)

READ INPUT TAPE 5, 101, THETA

THETAR = THETA*2.0*3.1416/360.0

C

C SET THE WALL TEMP EQUAL TO A FUNCTION OF AXIAL DISTANCE

C WALL TEMP IS CONSTANT IN THIS CASE

READ INPUT TAPE 5, 101, HWALL(1)

DO 400 IW = 2,KMAX

400 HWALL(IW) = HWALL(1)

C

C SET THE RADIAL MESH SIZE, THE RELATIVE AXIAL INCREMENT SIZES,

C THE STABILITY FACTOR(RATIO OF MESH SIZES), AND THE FLOW RATE ACCURACY

READ INPUT TAPE 5,100, NMESH

READ INPUT TAPE 5, 101, FZO, EX, EXX, EPS

C

C SET THE INITIAL ENTHALPY AND VELOCITY RADIAL PROFILES AT FIRST STATION

READ INPUT TAPE 5,102, (H(1,J), J=1,NMESH)

READ INPUT TAPE 5,102, (U(1,J), J=1,NMESH)

```

C
C EVALUATE THE REMAINING PROPERTIES AT THE FIRST AXIAL STATION
  K = 1
  DIA = DIAM(K)
  DR = DIA/(2.0*FLOAT(NMESH-1))
  DRDR = DR*DR
  L = 1
  M = 1
  Z = 0.0
  CALL STATEP
  CALL WDOT
C
C ADJUSTMENT FOR PROPER FLOW RATE
  CWF = WS/WW
  DO 2 J=1,NMESH
    U(1,J) = CWF*U(1,J)
    U(2,J) = U(1,J)
  2   CALL WDOT
  W = WW
C
C SET THE INITIAL AXIAL INCREMENTAL DISTANCE EQUAL TO FZO*CHARACT. LENGTH
  ZO = W*H(1,2)/(PHI(2)*3.1416)
  DZ = FZO*ZO
  CALL OUTPT
C
C CALCULATE THE PROPERTIES FOR THE SECOND AXIAL STATION
  M = 2
  K = 2
  DIA = DIAM(K)
  DR = DIA/(2.0*FLOAT(NMESH-1))
  DRDR = DR*DR
  DP = 0.0
  P(K) = P(K-1) + DP
  CALL ENERGY
  RHOA = RHOAV
  CALL WDOT
  DP = W*W*(RHOAV-RHOA)/(((RHOA*3.1416*DIA*DIA)/4.0)**2)
  CALL ITER
  Z = Z + DZ
  CALL STATEP
  CALL OUTPT
100 FORMAT(I4)
101 FORMAT(E10.3)
102 FORMAT(5E10.3)
  RETURN
  END

```

```

CHT0703 VAL WATSON  SUBROUTINE STATEP FOR HT0720
  SUBROUTINE STATEP
    COMMON AMPS, DIAM, DIA, DP, DRDR, DR, DW, DZ, EPS, E
1      , EX, EXX, FZO, HAVE, HRAVE, H, HWALL, K, KINC, KMAX, LOC, L
1      , M, NCHOKE, NERR, NFILE, NK, NMESH, NNN, NTAPE, PHI, PHIW
1      , P, QR, Q, RCAP, RHOAV, RHO, RHOV, RROU, R, RUH
1      , SIGMA, THETA, TRCL, U, VISC, W, WW, Z
    DIMENSION DIAM(2000), P(2000), E(2000), HWALL(2000)
1      , PHI(100), SIGMA(100), RCAP(100), VISC(100), RHO(100)
1      , R(100), RHOV(100), RROU(100)
1      , H(2,100), U(2,100)
    CALL CRISIS (ZZ,AA )

C
C EVALUATION OF THE GAS PROPERTIES AT THE WALL TEMPERATURE
  PRES = P(K)/1.013E5
  CALL NTAB(PRES,HWALL(K), PHIW, SW, RW, VW, 8, NERR)
  NERR = NERR
  HA = 0.0
  SS = 0.0
  HRA = 0.0
  QR = 0.0
  DO 30 J=1,NMESH

C
C EVALUATION OF THE GAS PROPERTIES AT EACH RADIAL STATION
  CALL NTAB(PRES,H(M,J),PHI(J),SIGMA(J),RCAP(J),VISC(J), 8, NERR)
  NERR = NERR
  IF (NERR) 10,10,40
10 CONTINUE
    IF (J-1) 20,30,20
    CONTINUE
    FJ = J
    R(J) = (FJ-1.5)*DR
    RDR = R(J)*DR
    DA = 6.2832*RDR
    DHA = DA*H(M,J)
    DSS = DA*SIGMA(J)
    DHRA = DHA*RHO(J)
    DQR = DA*RCAP(J)
    HA = HA + DHA
    SS = SS + DSS
    HRA = HRA + DHRA
    QR = QR + DQR
30 CONTINUE
    NMESHP = NMESH + 1
    PHI(NMESHP) = 2.0*PHIW - PHI(NMESH)
    R(NMESHP) = DIA/2.0
    H(M,NMESHP) = HWALL(K)

```



```

      VISC(NMESH) = 2.0*VW - VISC(NMESH)
C
C CALCULATION OF THE VOLTAGE GRADIENT, AVE ENTHALPY, AND HEAT FLUXES
      E(K) = AMPS/SS
      HAVE = HA/(3.1416*DIA*DIA/4.0)
      HRAVE= HRA/(3.1416*DIA*DIA/4.0)
      QR = QR/(3.1416*DIA)
      Q = 2.0*(PHI(NMESH) - PHIW)/DR
40 CONTINUE
      RETURN
      END

```

CHT0704 VAL WATSON SUBROUTINE WDOT FOR HT0720

SUBROUTINE WDOT

```
COMMON AMPS, DIAM, DIA, DP, DRDR, DR, DW, DZ, EPS, E
1      , EX, EXX, FZO, HAVE, HRAVE, H, HWALL, K, KINC, KMAX, LOC, L
1      , M, NCHOKE, NERR, NFILE, NK, NMESH, NNN, NTAP, PHI, PHIW
1      , P, QR, Q, RCAP, RHOAV, RHO, RHOU, RROU, R, RUH
1      , SIGMA, THETA, TRCL, U, VISC, W, WW, Z
DIMENSION DIAM(2000), P(2000), E(2000), HWALL(2000)
1      , PHI(100), SIGMA(100), RCAP(100), VISC(100), RHO(100)
1      , R(100), RHOU(100), RROU(100)
1      , H(2,100), U(2,100)
CALL CRISIS (ZZ,AA)
```

C

C EVALUATION OF THE FLOW RATE, AVERAGE DENSITY, AND ENERGY FLUX

```
WW = 0.0
RA = 0.0
RUH = 0.0
PRES = P(K)/1.013E5
DO 30 J=1,NMESH
    CALL NRHO(PRES, H(M,J), RHO(J), 8, NERR)
    NERR = NERR
    RHOU(J) = RHO(J)*U(M,J)
    IF(J-1) 20,30,20
20    CONTINUE
    RDR = R(J)*DR
    DA = 6.2832*RDR
    WW = WW + RHOU(J)*DA
    DRA = DA*RHO(J)
    RA = RA + DRA
    DRUH = DA*H(M,J)*RHOU(J)
    RUH = RUH + DRUH
30 CONTINUE
    RHOAV = RA/(3.1416*DIA*DIA/4.0)
RETURN
END
```

```

CHT0705 VAL WATSON  SUBROUTINE ITER FOR HT0720
      SUBROUTINE ITER
      COMMON AMPS, DIAM, DIA, DP, DRDR, DR, DW, DZ, EPS, E
1      , EX, EXX, FZO, HAVE, HRAVE, H, HWALL, K, KINC, KMAX, LOC, L
1      , M, NCHOKE, NERR, NFILE, NK, NMESH, NNN, NTAPE, PHI, PHIW
1      , P, QR, Q, RCAP, RHOAV, RHO, RHOU, RROU, R, RUH
1      , SIGMA, THETA, TRCL, U, VISC, W, WW, Z
      DIMENSION DIAM(2000), P(2000), E(2000), HWALL(2000)
1      , PHI(100), SIGMA(100), RCAP(100), VISC(100), RHO(100)
1      , R(100), RHOU(100), RROU(100)
1      , H(2,100), U(2,100)
      CALL CRISIS (ZZ,AA )

C
C  ITERATION TO CALCULATE THE VELOCITY AT THE NEXT AXIAL STATION  - SUBSONIC
C  VELOCITY IS FROM MOMENTUM  EQUATION
C  ITERATE UNTIL THE MASS FLOW IS CONSERVED
      IND = 0
      NCHOKE = 0
      DDP = DP
      P(K) = P(K-1) + DP
      LOC = 0
      NNN = 0
      DO 15 N=1,50
        LOC = N
        CALL MOM
        NNN = 1
        CALL WDOT
        DW = (WW - W)/W
        IF(ABSF(DW) - EPS) 20,1,1
1        IF(DW) 3,20,9
3        IF(IND) 7,7,5
5        DDP = DDP/2.0
7        DP = DP + DDP
        P(K) = P(K-1) + DP
        GO TO 15
9        DDP = DDP/2.0
        DP = DP - DDP
        P(K) = P(K-1) + DP
      IND = 1
15 CONTINUE
      NCHOKE = 1
20 CONTINUE
      RETURN
      END

```

CHT0706 VAL WATSON SUBROUTINE ITES FOR HT0720

SUBROUTINE ITES

COMMON AMPS, DIAM, DIA, DP, DRDR, DR, DW, DZ, EPS, E

1 , EX, EXX, FZO, HAVE, HRAVE, H, HWALL, K, KINC, KMAX, LOC, L

1 , M, NCHOKE, NERR, NFILE, NK, NMESH, NNN, NTAPE, PHI, PHIW

1 , P, QR, Q, RCAP, RHOAV, RHO, RHOU, RROU, R, RUH

1 , SIGMA, THETA, TRCL, U, VISC, W, WW, Z

DIMENSION DIAM(2000), P(2000), E(2000), HWALL(2000)

1 , PHI(100), SIGMA(100), RCAP(100), VISC(100), RHO(100)

1 , R(100), RHOU(100), RROU(100)

1 , H(2,100), U(2,100)

CALL CRISIS(ZZ,AAA)

C

C ITERATION TO CALCULATE THE VELOCITY AT THE NEXT AXIAL STATION - SUPERSONIC

C VELOCITY IS FROM MOMENTUM EQUATION

C ITERATE UNTIL THE MASS FLOW IS CONSERVED

IND = 0

NCHOKE = 0

DDP = DP

P(K) = P(K-1) + DP

LOC = 0

NNN = 0

DO 15 N=1,30

LOC = N

CALL MOM

NNN = 1

CALL WDOT

DW = (WW - W)/W

IF(ABS(DW) - EPS) 20,1,1

1 IF(DW) 9,20,3

3 IF(IND) 7,7,5

5 DDP = DDP/2.0

7 DP = DP + DDP

P(K) = P(K-1) + DP

GO TO 15

9 DDP = DDP/2.0

DP = DP - DDP

P(K) = P(K-1) + DP

IND = 1

15 CONTINUE

NCHOKE = 1

20 CONTINUE

RETURN

END



```

CHT0707 VAL WATSON SUBROUTINE MOM FOR HT0720
SUBROUTINE MOM
COMMON AMPS, DIAM, DIA, DP, DRDR, DR, DW, DZ, EPS, E
1    , EX, EXX, FZO, HAVE, HRAVE, H, HWALL, K, KINC, KMAX, LOC, L
1    , M, NCHOKE, NERR, NFILE, NK, NMESH, NNN, NTAPE, PHI, PHIW
1    , P, QR, Q, RCAP, RHOAV, RHO, RHOU, RROU, R, RUH
1    , SIGMA, THETA, TRCL, U, VISC, W, WW, Z
DIMENSION DIAM(2000), P(2000), E(2000), HWALL(2000)
1    , PHI(100), SIGMA(100), RCAP(100), VISC(100), RHO(100)
1    , R(100), RHOU(100), RROU(100)
1    , H(2,100), U(2,100)
1    , RUPREV(100), RCP1(100), RCP2(100), RCP3(100), RCP4(100)
CALL CRISIS (ZZ,RUPREV)

C
C CALCULATE THE VELOCITY AT THE NEXT AXIAL STATION
NMESHP = NMESH + 1
IF(NNN) 10,10,20
10 CONTINUE
DRUT = 0.0
U(L,NMESHP) = 0.0
AR = DIAM(K-1)*DIAM(K-1)/(DIAM(K)*DIAM(K))
DO 30 J=2,NMESH
RUPREV(J) = RROU(J)
RROU(J) = RHOU(J)

C
C CORRECTION FOR RADIAL CONVECTION
DRUTP = DRUT*R(J-1)/R(J)
DRUT = RROU(J) - RUPREV(J)*AR + DRUTP
62    IF(DRUT) 64,68,66
64    GB = U(L,J)
GO TO 68
66    GB = U(L,J+1)
68    IF(DRUTP) 70,74,72
70    GA = U(L,J-1)
GO TO 74
72    GA = U(L,J)
74    CONTINUE
RADCON = DRUT*GB - DRUTP*GA
1    + 1.0*U(L,J)*(RUPREV(J)*AR - RROU(J))

C
C SMOOTHING THE RADIAL CONVECTION
RCP4(J) = RCP3(J)
RCP3(J) = RCP2(J)
RCP2(J) = RCP1(J)
RCP1(J) = RADCON
40    IF(K - 4) 42,42,30
42    CONTINUE

```

```

        RCP1(J) = 0.0
        RCP2(J) = 0.0
        RCP3(J) = 0.0
        RCP4(J) = 0.0
        RUPREV(J) = RROU(J)
30 CONTINUE
    U(L,NMESH) = 0.0 - U(L,NMESH)
    U(M,NMESH) = 0.0
20 CONTINUE
    DO 50 J=2,NMESH
        RDR = R(J)*DR
        DA = 6.2832*RDR
        VL = 0.0 - (1.0/RDR)*
1          ((R(J+1) + R(J))/2.0)*((VISC(J+1) + VISC(J))/2.0)*
2          ((U(L,J+1) - U(L,J))/DR)
3          -((R(J) + R(J-1))/2.0)*((VISC(J) + VISC(J-1))/2.0)*
4          ((U(L,J) - U(L,J-1))/DR)
        RADCON = 0.25(RCP1(J) + RCP2(J) + RCP3(J) + RCP4(J))
        U(M,J) = U(L,J) - (DP + DZ*VL - RADCON)*(RUPREV(J)/
2          (RROU(J)*RROU(J)))
50 CONTINUE
    U(M,1) = U(M,2)
    RETURN
    END

```

```

CHT0708 VAL WATSON  SUBROUTINE ENERGY FOR HT0720
SUBROUTINE ENERGY
COMMON AMPS, DIAM, DIA, DP, DRDR, DR, DW, DZ, EPS, E
1   , EX, EXX, FZO, HAVE, HRAVE, H, HWALL, K, KINC, KMAX, LOC, L
1   , M, NCHOKE, NERR, NFILE, NK, NMESH, NNN, NTAPE, PHI, PHIW
1   , P, QR, Q, RCAP, RHOAV, RHO, RHOV, RROU, R, RUH
1   , SIGMA, THETA, TRCL, U, VISC, W, WW, Z
DIMENSION DIAM(2000), P(2000), E(2000), HWALL(2000)
1   , PHI(100), SIGMA(100), RCAP(100), VISC(100), RHO(100)
1   , R(100), RHOV(100), RROU(100)
1   , H(2,100), U(2,100)
1   , RCP1(100), RCP2(100), RCP3(100), RCP4(100)
1   , TE(100)
      CALL CRISIS (ZZ,RCP1)

C
C CALCULATE THE ENTHALPY AT THE NEXT AXIAL STATION
      DRUT = 0.0
      TE(2) = U(M,2)*U(M,2)/2.0
      AR = DIAM(K-1)*DIAM(K-1)/(DIAM(K)*DIAM(K))
      DO 40 J=2,NMESH
        FJ = J
        R(J) = (FJ-1.5)*DR
        RDR = R(J)*DR
        DA = 6.2832*RDR
        CL = 0.0 - ((PHI(J+1) - 2.0*PHI(J) + PHI(J-1))/DRDR
1       + (PHI(J+1) - PHI(J-1))/(2.0*RDR) )
        RL = RCAP(J)
        OH = (E(K-1)*E(K-1)*SIGMA(J))
        TE(J+1) = U(M,J+1)*U(M,J+1)/2.0
        TEP = U(L,J )*U(L,J )/2.0

C
C CORRECTION FOR RADIAL CONVECTION
      DRUTP = DRUT*R(J-1)/R(J)
      DRUT = RHOV(J) - RROU(J)*AR + DRUTP
62     IF(DRUT) 64,68,66
64       GB = H(L,J) + TE(J)
        GO TO 68
66       GB = H(L,J+1) + TE(J+1)
68     IF(DRUTP) 70,74,72
70       GA = H(L,J-1) + TE(J-1)
        GO TO 74
72       GA = H(L,J) + TE(J)
74     CONTINUE
      RADCON = DRUT*GB - DRUTP*GA
2     + 1.0*H(L,J)*(RROU(J)*AR - RHOV(J))

C
C SMOOTHING THE RADIAL CONVECTION

```



```

        RCP4(J) = RCP3(J)
        RCP3(J) = RCP2(J)
        RCP2(J) = RCP1(J)
        RCP1(J) = RADCON
20      IF(K-4) 20,20,22
        CONTINUE
        RCP1(J) = 0.0
        RCP2(J) = 0.0
        RCP3(J) = 0.0
        RCP4(J) = 0.0
        RROU(J) = RHOU(J)
22      CONTINUE
        RADCON = 0.25(RCP1(J) + RCP2(J) + RCP3(J) + RCP4(J))
        H(M,J) = H(L,J) + (DZ*(OH-CL-RL) + RADCON)*(RROU(J)/
1      (RHOU(J)*RHOU(J))) + TEP - TE(J)
40 CONTINUE
        H(M,1) = H(M,2)
        RETURN
        END

```

CHT0709 VAL WATSON SUBROUTINE OUTPT FOR HT0720

```

SUBROUTINE OUTPT
COMMON AMPS, DIAM, DIA, DP, DRDR, DR, DW, DZ, EPS, E
1      , EX, EXX, FZO, HAVE, HRAVE, H, HWALL, K, KINC, KMAX, LOC, L
1      , M, NCHOKE, NERR, NFILE, NK, NMESH, NNN, NTAPE, PHI, PHIW
1      , P, QR, Q, RCAP, RHOAV, RHO, RHOU, RROU, R, RUH
1      , SIGMA, THETA, TRCL, U, VISC, W, WW, Z
DIMENSION DIAM(2000), P(2000), E(2000), HWALL(2000)
1      , PHI(100), SIGMA(100), RCAP(100), VISC(100), RHO(100)
1      , R(100), RHOU(100), RROU(100)
1      , H(2,100), U(2,100)
CALL CRISIS (ZZ,AA )
QT = Q+QR
RUHA = RUH/W
PRAD = QR/QT *100.0
PRES = P(K)/1.013E5
WRITE TAPE NTAPE, K, DIAM(K), Z, AMPS, E(K), W,QT,HWALL(K)
1      ,PRAD, NMESH, PRES,FZO,LOC,EPS,DW, DP, DZ
2      , HAVE, RUHA,HRAVE
WRITE TAPE NTAPE, (R(J), H(M,J), U(M,J), RHOU(J), J=1,NMESH)
END FILE NTAPE
WRITE OUTPUT TAPE 6,300,K, DIAM(K),Z,AMPS,E(K),W,QT,TRCL
WRITE OUTPUT TAPE 6,299,PRAD,HWALL(K),PRES, NMESH,LOC,FZO,DW,EPS,
1      NFILE, EX
WRITE OUTPUT TAPE 6, 298, HAVE, RUHA, HRAVE
WRITE OUTPUT TAPE 6,301,(R(J), H(M,J), U(M,J), RHOU(J),
1      R(J+25), H(M,J+25), U(M,J+25), RHOU(J+25), J=1,25 )
300 FORMAT(1H1,
1      15HAXIAL STATION = , I4 , 16X,
3 50H DC THERMAL ARC WITH AXIAL GAS FLOW ,
2      15HDIAMETER = , E10.3, 10H METERS /
1      1X, 15HAXIAL DIST = , E10.3, 10H METERS ,
2      50X, 15HCURRENT = , E10.3, 10H AMPS /
1      1X, 15HVOLTAGE GRAD = , E10.3, 10H VOLTS/M ,
2      50X, 15HFLOW RATE = , E10.3, 10H KG/SEC /
2      1X, 15HWALL HEAT FLUX= , E10.3, 22H WATTS/M**2 ,
2      38X, 15HTRANS COOLING = , E10.3, 12H KG/SEC-M**2 )
299 FORMAT(1H ,
2      15HRADIATION LOSS= , F10.4, 10H PERCENT ,
2      50X, 15HWALL ENTHALPY = , E10.3, 10H JOULES/KG /
2      1X, 15HPPRESSURE = , F10.4, 10H ATMOS ,
2      50X, 15HNMESH = , I4 /
2      1X, 15HLOC = , I4, 16X,
2      50X, 15HFZO = , E10.3 /
2      1X, 15HDW = , E10.3,10X
2      50X, 15HEPS = , E10.3 /
2      1X, 15HFILE = , I4,66X,15HEX = ,E10.3)

```

```

298 FORMAT(1H0,
1      25HSPACE AVERAGE ENTHALPY =      , E15.5, 10H JOULES/KG      /
2      1X, 25HMASS AVERAGE ENTHALPY =      , E15.5, 10H JOULES/KG      /
3      1X, 25HAVERAGE ENERGY DENSITY =      , E15.5, 12H JOULES/M**3 )
301 FORMAT(1H0, 3X, 10H RADIUS      , 5X, 10H ENTHALPY      ,
1  5X, 10H VELOCITY      , 5X, 10H MASS FLUX      ,
2      5X, 10H RADIUS      , 5X, 10H ENTHALPY      ,
3  5X, 10H VELOCITY      , 5X, 10H MASS FLUX      /
4      1X, 3X, 10H METERS      , 5X, 10H JOULES/KG      ,
5  5X, 10H      M/S      , 5X, 10H KG/S M**2      ,
4      5X, 10H METERS      , 5X, 10H JOULES/KG      ,
5  5X, 10H      M/S      , 5X, 10H KG/S M**2      //
9  (8(E15.5)))
  NFILE = NFILE + 1
  RETURN
  END

```



APPENDIX C

FORTRAN PROGRAM FOR THE SOLUTION OF THE ASYMMETRIC CONSTRICTED ARC WITH AN AXIAL FLOW OF GAS

This appendix contains the Fortran II programs for the numerical solution of the asymmetric constricted arc with an axial flow of gas. The data required for input into these programs and a legend for the Fortran variables are also included.

The function of each subroutine is described below.

BOUNDC	provides for the specification of the boundary conditions for the main program
STATEP	evaluates the state properties (except density) for all of the mesh points at each axial station
WDOT	evaluates the density for all mesh points at each axial station and calculates the mass flow rate by integration of the mass flux over the constrictor cross-sectional area
ENERGY	calculates the enthalpy for all mesh points at the next axial station from the energy equation
MOM	calculates the velocity for all mesh points at the next axial station from the momentum equation
ITER	provides the iteration of pressure to obtain the correct mass flow in the subsonic portion of the nozzle
OUTPT	prints and writes on magnetic tape the results of the main program

A second main program entitled herein "Supersonic Continuation" uses the same subroutines to continue into the supersonic region of the nozzle with the exception that the following subroutine replaces ITER.

ITERS	provides the iteration of pressure to obtain the correct mass flow in the supersonic portion of the nozzle
-------	--

INPUT DATA REQUIRED

<u>Card number</u>	<u>Fortran variables</u>	<u>Format</u>
1	NMESH, NFILE, NTAPE, NK	4I4
2	CDIA	E10.3
3	AMPS	↓
4	P(1)	
5	EXX	
6	CHWALL	
7	FZO	
8	EPS	
9	EX	
10	NCD	I4
11 through 11 + NCD	J, I, H(1, J, I)	2I4, E10.3

These Fortran variables are described in the following legend under the variables common to all programs or under the variables for program HT 0751.

INPUT DATA REQUIRED FOR SUPERSONIC CONTINUATION

<u>Card number</u>	<u>Fortran variables</u>	<u>Format</u>
1	NFILE(1), NTAPE(1)	2I4
2	NFILE, NTAPE, KMAX, KINC	4I4
3	EX	E10.3
4	ZC	E10.3
5	THETA	E10.3

VARIABLES USED IN THE PROGRAMS FOR THE NUMERICAL SOLUTIONS OF THE ASYMMETRIC CONSTRICTED THERMAL ARC WITH AN AXIAL FLOW OF GAS

Variables Common to all Programs

<u>Variable name</u>	<u>Description</u>
AMPS	total current carried by the constrictor, A
DIAM	diameter of the constrictor (an array), m
DIA	diameter of the constrictor, m
DP	pressure drop between axial stations, N/m ²
DW	discrepancy between the mass flow rate at this axial station and the initial mass flow rate, kg/s
DZ	incremental axial distance, m
EPS	maximum allowable relative discrepancy of the mass flow rate
E	axial voltage gradient, V/m
EX	factor by which the axial incremental distance is increased for the next axial station
EXX	mass flow rate at the initial axial station, kg/s
FZO	length of the first axial increment divided by the characteristic arc length, z ₀
H	local enthalpy, J/kg
HWALL	enthalpy of the gas at the constrictor wall, J/kg
K	axial station number

<u>Variable name</u>	<u>Description</u>
LOC	number of iterations required to satisfy the continuity equation (i.e., the number of iterations required such that the flow rate at this axial station is sufficiently near the initial flow rate)
L	relative axial station number
M	second relative axial station number
NCHOKE	flag indicating that the flow is choked
NFILE	file number on the magnetic tape used to store the solutions
NK	maximum number of axial stations to be calculated
NMESH	number of radial increments from the center line to the constrictor wall
NNN	flag indicating that this is the first iteration on pressure drop (zero indicates first iteration, 1 indicates all iterations thereafter)
NTAPE	magnetic tape on which the solution is stored
PHI	local thermal conductivity potential, W/m
PHIW	thermal conductivity potential of the gas at the constrictor wall, W/m
P	static pressure at this axial station, N/m ²
QR	heat transfer rate to the constrictor wall that is due to radiation, W/m ²
Q	heat transfer rate to the constrictor wall that is due to thermal conduction, W/m ²
RCAP	local radiation, W/m ³
RHOAV	space average density, kg/m ³
RHO	local density, kg/m ³
RHOU	local product of density and velocity at this station, kg/sm ²
SIGMA	local electrical conductivity, 1/Ω-m
U	local velocity, m/s

<u>Variable name</u>	<u>Description</u>
VISC	local viscosity, Ns/m^2
W	mass flow rate at the initial axial station, kg/s
WW	mass flow rate at this axial station, kg/s
Z	axial distance of this axial station from the initial axial station, m

Variables Local to Program HT-0750

CWF	scaling factor that changes the magnitude of the velocity profile to obtain the desired initial flow rate
DZMAX	upper limit of the axial incremental distance (the incremental axial distance is never allowed to exceed this value in order to keep the solution stable), m
RHOA	space average of the density at this axial station, kg/m^3
ZO	characteristic arc length, z_0

Variables Local to Program HT-0751

CDIA	constrictor wall diameter, m
CHWALL	enthalpy of the gas at the constrictor wall, J/kg
FJ	floating index for the radial position
FNI	number of increments in the azimuthal direction (floating)
I	index for the azimuthal position
J	index for the radial position
NCD	number of data cards used to specify the initial enthalpy distribution
NI	number of azimuthal increments

Variables Local to Program HT-0752

DA	incremental cross-sectional area, m^2
DRDR	square of the incremental radial distance, DR , m^2

<u>Variable name</u>	<u>Description</u>
DR	incremental radial distance, m
DTH	incremental azimuthal distance, radians
FJ	floating index for the radial position
FNI	number of increments in the azimuthal direction (floating)
I	index for the azimuthal position
J	index for the radial position
NERR	error flag for the gas property subroutines
NI	number of azimuthal increments
QRR	running total of the product of radiation and area, W/m
R	radial position, m
RW	dummy variable not used
SS	running total of the product of the electrical conductivity and area, m/ Ω
SW	dummy variable not used

Variables Local to Programs HT-0753 and 0754

DA	incremental cross-sectional area, m ²
DRDR	square of the incremental radial distance, DR, m ²
DR	incremental radial distance, m
DTH	incremental azimuthal distance, radians
FJ	floating index for the radial position
FNI	number of increments in the azimuthal direction (floating)
I	index for the azimuthal position
J	index for the radial position
NERR	error flag for the gas property subroutines
NI	number of azimuthal increments
R	radial position, m

Variables Local to Program HT-0755

<u>Variable name</u>	<u>Description</u>
CL	conduction losses from this incremental volume, W/m^3
DA	incremental cross-sectional area, m^2
DRDR	square of the incremental radial distance, DR , m^2
DR	incremental radial distance, m
DPH	incremental azimuthal distance, radians
DZRU	local DZ divided by the local $RHOU$, m^3s/kg
FJ	index for the radial incremental distance (floating)
FNI	number of azimuthal increments
ICC	index for changing the number of azimuthal increments
IC	second index for changing the number of azimuthal increments
IMM	index for the previous azimuthal position
IM	index for the azimuthal position at the previous radial position
IPP	index for the next azimuthal position
IP	index for the azimuthal position at the next radial position
I	index for the azimuthal position
J	index for the radial position
NI	number of azimuthal increments
OH	ohmic heating within this volume element, W/m^3
PHIMM	thermal conductivity potential at the previous radial position, W/m
PHIM	thermal conductivity potential at the previous azimuthal position, W/m
PHIO	thermal conductivity potential at this radial and azimuthal position, W/m

<u>Variable name</u>	<u>Description</u>
PHIPP	thermal conductivity potential at the next azimuthal position, W/m
PHIP	thermal conductivity potential at the next radial position, W/m
RDR	product of the local radius and incremental radial distance, m^2
RDTH2	square of the product of radius and incremental azimuthal distance, m^2
RL	radiation losses from this incremental volume, W/m^3
R	radial position, m
SLOPE	gradient of the thermal conductivity potential at the wall, W/m^2

Variables Local to Program HT-0756

DA	incremental cross-sectional area, m^2
DRDR	square of the incremental radial distance, DR, m^2
DR	incremental radial distance, m
DTH	incremental azimuthal distance, radians
DZRU	local DZ divided by the local RHOU, m^3s/kg
FJ	index for the radial incremental distance (floating)
FNI	number of azimuthal increments
ICC	index for changing the number of azimuthal increments
IC	second index for changing the number of azimuthal increments
IMM	index for the previous azimuthal position
IM	index for the azimuthal position at the previous radial position
IPP	index for the next azimuthal position
IP	index for the azimuthal position at the next radial position

<u>Variable name</u>	<u>Description</u>
I	index for the azimuthal position
J	index for the radial position
NI	number of azimuthal increments
RDR	product of the local radius and incremental radial distance, m^2
RDTH2	square of the product of radius and incremental azimuthal distance, m^2
R	radial position, m
UMM	velocity at the previous azimuthal position, m/s
UM	velocity at the previous radial position, m/s
UO	velocity at this radial and azimuthal position, m/s
UPP	velocity at the next azimuthal position, m/s
UP	velocity at the next radial position, m/s
VL	viscous losses from this volume increment, N/m^3
VMM	viscosity at the previous azimuthal position, Ns/m^2
VM	viscosity at the previous radial position, Ns/m^2
VO	viscosity at this radial and azimuthal position, Ns/m^2
VPP	viscosity at the next azimuthal position, Ns/m^2
VP	viscosity at the next radial position, Ns/m^2

Variables Local to Program HT-0757

DDP	amount that the pressure drop has changed for each iteration at this axial station, N/m^2
IND	flag used in adjusting the pressure drop during the iterations at this station
N	index for the iterations

Variables Local to Program HT-0758

<u>Variable name</u>	<u>Description</u>
FJ	index for the radial position (floating)
FNI	number of azimuthal increments (floating)
J	index for the radial position
NI	number of azimuthal increments
PRAD	percentage of the constrictor wall heat flux that is due to radiation
QT	total heat transfer rate to the constrictor wall, W/m^2

Variables Local to Program HT-0780

KINC	number of axial stations between printout of results
KMAX	maximum number of axial stations to be calculated
NFILE1	magnetic tape file number indicating the last file of the subsonic results
NI	number of azimuthal increments
NN	index for printing results
NTAPE1	magnetic tape on which the subsonic results are stored
PX	pressure at the last axial station of the subsonic flow regime, N/m^2
QX	heat flux to the constrictor wall at the last axial station of the subsonic regime, W/m^2
THETAR	half-angle of divergence of the supersonic nozzle, radians
THETA	half-angle of divergence of the supersonic nozzle, deg
ZC	axial position at choking, m

Variables Local to Program HT-0781

DDP	amount that pressure drop has changed for each iteration at this axial station, N/m^2
-----	---

<u>Variable name</u>	<u>Description</u>
IND	flag used in adjusting the pressure drop during the iterations at this station
N	index for the iterations

```

CHT0750 VAL WATSON   DC ARC  =  AXIAL FLOW  =  REAL GAS
COMMON AMPS, W, WW, DP, DZ, EPS, FZO, Z, Q, QR, DW, DIA, EX, EXX,
1      H, PHI, SIGMA, RCAP, RHO, VISC, HWALL, RHOAV, RHOV, PHIW,
1      P, E, DIAM, U,
1      NMESH, K, L, M, LOC, NFILE, NTAPE, NCHOKE, NK, NNN
DIMENSION DIAM(1000), P(1000), E(1000), HWALL(1000)
DIMENSION H(2,12,48), U(2,12,48), PHI(12,48), SIGMA(12,48),
1      RCAP(12,48), VISC(12,48), RHO(12,48), RHOV(12,48)
CALL CRISIS (ZZ,AAA,AMPS, NNN)
CALL BOUNDC
K = 1
DIA = DIAM(K)
L = 1
M = 1
Z = 0.0
CALL STATEP
CALL WDOT
      CWF = EXX/WW
      DO 20 J=1,NMESH
          DO 18 I=1,48
18      U(1,J,I) = CWF*U(1,J,I)
20      CONTINUE
      CALL WDOT
W = WW
ZO = (W*3111.0)/3.1416
DZ = FZO*ZO
CALL RHOAVE
RHOA = RHOAV
      CALL LOCATE (NFILE,NTAPE)
CALL OUTPT
M = 2
K = 2
DIA = DIAM(K)
DP = 0.0
      P(K) = P(K-1) + DP
CALL ENERGY
CALL RHOAVE
DP = W*W*(RHOAV-RHOA)/(((RHOA*3.1416*DIA*DIA)/4.0)**2)
CALL ITER
Z = Z + DZ
CALL STATEP
CALL OUTPT
DO 6 K = 3,NK
DIA = DIAM(K)
DZMAX = 0.2*DIA*DIA*RHOV(3,1)*200.0/(FLOAT(NMESH)*FLOAT(NMESH))
IF(DZ-DZMAX) 40,42,42
40 DZ = DZ*EX

```



```

42 CONTINUE
      M = 1
      L = L + 1
      IF(3-L) 1,1,2
1      M = 2
      L = 1
2      CONTINUE
      CALL ENERGY
      CALL ITER
      IF(NCHOK) 4,4,3
3      WRITE OUTPUT TAPE 6, 202, K, DW,U(M,1,1)
      GO TO 8
4      CONTINUE
      CALL STATEP
      Z = Z + DZ
      CALL OUTPT
6 CONTINUE
8 CONTINUE
  REWIND NTAPE
  REWIND 8
202 FORMAT(1H0, 18HFLOW CHOKED AT K = , I4, 10X,
1      20HFLOW RATE ERROR IS      , 2PF12.7, 10H PERCENT      ,
2 14 HCL VELOCITY = ,0PF10.1, 8H M/SEC      )
  CALL EXIT
  END

```

```

CHT0751 VAL WATSON SUBROUTINE BOUNDC FOR HT0750
SUBROUTINE BOUNDC
COMMON AMPS, W, WW, DP, DZ, EPS, FZO, Z, Q, QR, DW, DIA, EX, EXX,
1      H, PHI, SIGMA, RCAP, RHO, VISC, HWALL, RHOAV, RHOV, PHIW,
1      P, E, DIAM, U,
1      NMESH, K, L, M, LOC, NFILE, NTAPE, NCHOK, NK, NNN
DIMENSION DIAM(1000), P(1000), E(1000), HWALL(1000)
DIMENSION H(2,12,48), U(2,12,48), PHI(12,48), SIGMA(12,48),
1      RCAP(12,48), VISC(12,48), RHO(12,48), RHOV(12,48)
CALL CRISIS(ZZ,AAA)
READ INPUT TAPE 5, 99, NMESH, NFILE, NTAPE, NK
99 FORMAT(4I4)
READ INPUT TAPE 5, 100, CDIA, AMPS, P(1), EXX, CHWALL, FZO, EPS, EX
100 FORMAT(E10.3)
P(1) = P(1)*1.013EK
DO 5 K = 1, NK
    DIAM(K) = CDIA
    HWALL(K) = CHWALL
5 CONTINUE
NI = 6
DO 10 J = 1, NMESH
    DO 6 I = 1, NI
        H(1,J,I) = HWALL(1)
        U(1,J,I) = 100.0
6      FJ = J
        FNI = NI
        IF ((FNI/FJ)-4.0) 8,8,10
8      NI = NI*2
10 CONTINUE
READ INPUT TAPE 5, 102, NCD, (J, I, H(1,J,I), K=1,NCD)
102 FORMAT(I4/(2I4,E10.3))
RETURN
END

```



```

CHT0752 VAL WATSON  SUBROUTINE STATEP FOR HT0750
  SUBROUTINE STATEP
  COMMON AMPS, W, WW, DP, DZ, EPS, FZO, Z, Q, QR, DW, DIA, EX, EXX,
1    H, PHI, SIGMA, RCAP, RHO, VISC, HWALL, RHOAV, RHOU, PHIW,
1    P, E, DIAM, U,
1    NMESH, K, L, M, LOC, NFILE, NTAPE, NCHOKE, NK, NNN
  DIMENSION DIAM(1000), P(1000), E(1000), HWALL(1000)
  DIMENSION H(2,12,48), U(2,12,48), PHI(12,48), SIGMA(12,48),
1    RCAP(12,48), VISC(12,48), RHO(12,48), RHOU(12,48)
  CALL CRISIS(ZZ,AAA)
  QR = QRR
  PRES=P(K)/1.013E5
  CALL NTAB(PRES, HWALL(K), PHIW, SW, RW, VISC(NMESH+1,1), 8, NERR)
  DR = DIA/(2.0*FLOATF(NMESH)-1.0)
  DRDR = DR*DR
  R = 0.0
  J = 1
  I = 1
      CALL NTAB(PRES, H(M,J,I), PHI(J,I), SIGMA(J,I),
1    RCAP(J,I), VISC(J,I), 8, NERR)
  PHI(1,2) = PHI(1,1)
  PHI(1,3) = PHI(1,1)
  VISC(1,2) = VISC(1,1)
  VISC(1,3) = VISC(1,1)
  SS = SIGMA(J,I)*3.1416*DRDR*0.25
  QRR= RCAP(J,I)*3.1416*DRDR*0.25
  NI = 6
  DO 14 J = 2,NMESH
    R = R + DR
    DTH = 6.2832/FLOATF(NI)
    DA = R*DR*DTH
    DO 10 I = 1,NI
      CALL NTAB(P(K), H(M,J,I), PHI(J,I), SIGMA(J,I),
1    RCAP(J,I), VISC(J,I), 8, NERR)
      SS = SS + SIGMA(J,I)*DA
      QRR= QRR+ RCAP(J,I)*DA
10    CONTINUE
    FJ = J
    FNI = NI
    IF ((FNI/FJ) - 4.0) 12,12,14
12    NI = NI*2
14  CONTINUE
    E(K) = AMPS/SS
    QRR=QRR/(3.1416*DIA)
    IF(NERR) 22,22,20
20  WRITE OUTPUT TAPE 6, 110, K
22  CONTINUE

```

```
110 FORMAT(1H0, 24HEXCEEDED TABLES AT K = , I4)  
RETURN  
END
```

```

CHT0753 VAL WATSON SUBROUTINE WDOT FOR HT0750
SUBROUTINE WDOT
COMMON AMPS, W, WW, DP, DZ, EPS, FZO, Z, Q, QR, DW, DIA, EX, EXX,
1 H, PHI, SIGMA, RCAP, RHO, VISC, HWALL, RHOAV, RHOU, PHIW,
1 P, E, DIAM, U,
1 NMESH, K, L, M, LOC, NFILE, NTAPE, NCHOKE, NK, NNN
DIMENSION DIAM(1000), P(1000), E(1000), HWALL(1000)
1 DIMENSION H(2,12,48), U(2,12,48), PHI(12,48), SIGMA(12,48),
1 RCAP(12,48), VISC(12,48), RHO(12,48), RHOU(12,48)
CALL CRISIS(ZZ,AAA)
DR = DIA/(2.0*FLOAT(NMESH)-1.0)
DRDR = DR*DR
R = 0.0
J = 1
I = 1
PRES=P(K)/1.013E5
CALL NRHO(PRES, H(M,J,I), RHO(J,I), 8, NERR)
RHOU(J,I) = RHO(J,I)*U(M,J,I)
WW = RHOU(J,I)*3.1416*DRDR*0.25
NI = 6
DO 14 J = 2,NMESH
R = R + DR
DTH = 6.2832/FLOAT(NI)
DA = R*DR*DTH
DO 10 I = 1,NI
CALL NRHO(PRES, H(M,J,I), RHO(J,I), 8, NERR)
RHOU(J,I) = RHO(J,I)*U(M,J,I)
WW = WW + RHOU(J,I)*DA
10 CONTINUE
FJ = J
FNI = NI
IF ((FNI/FJ) - 4.0) 12,12,14
12 NI = NI*2
14 CONTINUE
IF(NERR) 22,22,20
20 WRITE OUTPUT TAPE 6, 110, K
22 CONTINUE
110 FORMAT(1H0, 24HEXCEEDED TABLES AT K = , I4)
RETURN
END

```

```

CHT0754 VAL WATSON  SUBROUTINE RHOAVE FOR HT0750
  SUBROUTINE RHOAVE
  COMMON AMPS, W, WW, DP, DZ, EPS, FZO, Z, Q, QR, DW, DIA, EX, EXX,
1      H, PHI, SIGMA, RCAP, RHO, VISC, HWALL, RHOAV, RHOU, PHIW,
1      P, E, DIAM, U,
1      NMESH, K, L, M, LOC, NFILE, NTAPE, NCHOKE, NK, NNN
  DIMENSION DIAM(1000), P(1000), E(1000), HWALL(1000)
  DIMENSION H(2,12,48), U(2,12,48), PHI(12,48), SIGMA(12,48),
1      RCAP(12,48), VISC(12,48), RHO(12,48), RHOU(12,48)
  CALL CRISIS(ZZ,AAA)
  DR = DIA/(2.0*FLOATF(NMESH)-1.0)
  DRDR = DR*DR
  R = 0.0
  J = 1
  I = 1
  PRES=P(K)/1.013E5
      CALL NRHO(PRES, H(M,J,I), RHO(J,I), 8, NERR)
  RHOAV = 3.1416*DRDR*0.25*RHO(J,I)
  NI = 6
  DO 14 J = 2,NMESH
    R = R + DR
    DTH = 6.2832/FLOATF(NI)
    DA = R*DR*DTH
    DO 10 I = 1,NI
      CALL NRHO(PRES, H(M,J,I), RHO(J,I), 8, NERR)
      RHOAV = RHOAV +DA*RHO(J,I)
10    CONTINUE
    FJ = J
    FNI = NI
    IF ((FNI/FJ) - 4.0) 12,12,14
12    NI = NI*2
14  CONTINUE
    RHOAV = RHOAV/(3.1416*DIA*DIA*0.25)
    IF(NERR) 22,22,20
20  WRITE OUTPUT TAPE 6, 110, K
22  CONTINUE
110 FORMAT(1H0, 24HEXCEEDED TABLES AT K = , I4)
    RETURN
  END

```

```

CHT0755 VAL WATSON  SUBROUTINE ENERGY FOR HT0750
  SUBROUTINE ENERGY
  COMMON AMPS, W, WW, DP, DZ, EPS, FZO, Z, Q, QR, DW, DIA, EX, EXX,
1      H, PHI, SIGMA, RCAP, RHO, VISC, HWALL, RHOAV, RHOU, PHIW,
1      P, E, DIAM, U,
1      NMESH, K, L, M, LOC, NFILE, NTAPE, NCHOKE, NK, NNN
  DIMENSION DIAM(1000), P(1000), E(1000), HWALL(1000)
  DIMENSION H(2,12,48), U(2,12,48), PHI(12,48), SIGMA(12,48),
1      RCAP(12,48), VISC(12,48), RHO(12,48), RHOU(12,48)
  CALL CRISIS(ZZ,AAA)
  O = 0.0
  I = 1
  J = 1
  DR = DIA/(2.0*FLOAT(NMESH)-1.0)
  DRDR = DR*DR
  R = 0.0
  DZRU = DZ/RHOU(J,I)
  CL = (6.0*PHI(1,1) - PHI(2,1) - PHI(2,2) - PHI(2,3) - PHI(2,4)
1      - PHI(2,5) - PHI(2,6))/(6.0*0.25 *DRDR)
  RL = RCAP(1,1)
  OH = (E(K-1)*E(K-1)*SIGMA(J,I))
  H(M,J,I) = H(L,J,I) + (DP/RHO(J,I))
1      +DZRU*(OH -CL -RL)
  ICC = 1
  NI = 6
  DO 40 J = 2,NMESH
    FJ = J
    FNI = NI
    IF ((FNI/FJ)-4.0) 1,1,3
1      IC = 1
3      CONTINUE
    R = R + DR
    RDR = R*DR
    DTH = 6.2832/FLOAT(NI)
    DA = R*DR*DTH
    RDTH2 = R*R*DTH*DTH
    DO 30 I = 1,NI
      IP = I
      IM = I
      IPP = I + 1
      IMM = I - 1
      IF(I-1) 2,2,4
2      IMM = NI
4      IF(NI - I) 6,6,8
6      IPP = 1
8      IF(IC) 12,12,10
10     IP = 2*I

```



```

12      IF(ICC) 16,16,14
14          IM = (I+1)/2
16      CONTINUE
      DZRU = DZ/RHOU(J,I)
      PHIO = PHI(J,I)
      PHIP = PHI(J+1,IP )
      PHIM = PHI(J-1,IM )
      PHIPP = PHI(J,IPP)
      PHIMM = PHI(J,IMM)
      IF(NMESH-J) 20,20,22
20          PHIP = 2.0*PHIW      - PHI(J,I)
      SLOPE = (PHIW -PHIP)*2.0/DR
      IF (Q-SLOPE) 21,22,22
21  Q = SLOPE
22      CONTINUE
      CL = 0.0 - ((PHIP-PHIM)/(2.0*RDR)
1          + (PHIP-2.0*PHIO+PHIM)/DRDR
1          + (PHIPP-2.0*PHIO+PHIMM)/RDTH2)
      RL = RCAP(J,I)
      OH = (E(K-1)*E(K-1)*SIGMA(J,I))
      H(M,J,I) = H(L,J,I) + (DP/RHO(J,I))
1          + DZRU*(OH - CL - RL)
30      CONTINUE
      ICC = 0
      IF(IC) 40,40,32
32          ICC = 1
          IC = 0
          NI = 2*NI
40 CONTINUE
      RETURN
      END

```

```

CHT0756 VAL WATSON  SUBROUTINE MOM FOR HT0750
      SUBROUTINE MOM
      COMMON AMPS, W, WW, DP, DZ, EPS, FZO, Z, Q, QR, DW, DIA, EX, EXX,
1      H, PHI, SIGMA, RCAP, RHO, VISC, HWALL, RHOAV, RHOU, PHIW,
1      P, E, DIAM, U,
1      NMESH, K, L, M, LOC, NFILE, NTAPE, NCHOKE, NK, NNN
      DIMENSION DIAM(1000), P(1000), E(1000), HWALL(1000)
      DIMENSION H(2,12,48), U(2,12,48), PHI(12,48), SIGMA(12,48),
1      RCAP(12,48), VISC(12,48), RHO(12,48), RHOU(12,48), RROU(12,48)
      CALL CRISIS (ZZ,AAA)
      IF (NNN) 99,99,102
99  IF (NMESH - 7) 200,201,201
200 NI = 24
      GO TO 202
201 NI = 48
202 CONTINUE
      DO 101 J=1,NMESH
          DO 100 I=1,NI
              RROU(J,I) = RHOU(J,I)
100 CONTINUE
101 CONTINUE
102 CONTINUE
      I = 1
      J = 1
      DR = DIA/(2.0*FLOAT(NMESH)-1.0)
      DRDR = DR*DR
      R = 0.0
      DZRU = DZ/ RROU(J,I)
      VL = VISC(J,I)*(6.0*U(L,1,1) - U(L,2,1) - U(L,2,2) - U(L,2,3) -
1      U(L,2,4) - U(L,2,5) -U(L,2,6))/(6.0*3.1416*DRDR)
      U(M,J,I) = U(L,J,I) - (DP/RROU(J,I)) - DZRU*VL
      U(M,1,2) = U(M,1,1)
      U(M,1,3) = U(M,1,1)
      ICC = 1
      NI = 6
      DO 40 J = 2,NMESH
          FJ = J
          FNI = NI
              IF((FNI/FJ) -4.0) 1,1,3
1          IC = 1
3          CONTINUE
          R = R + DR
          RDR = R*DR
          DTH = 6.2832/FLOAT(NI)
          DA = R*DR*DTH
          RDTH2 = R*R*DTH*DTH
          DO 30 I = 1,NI

```

```

        IP = I
        IM = I
        IPP = I + 1
        IMM = I - 1
        IF(I-1) 2,2,4
2         IMM = NI
4         IF(NI - I) 6,6,8
6         IPP = 1
8         IF(IC) 12,12,10
10        IP = 2*I
12        IF(ICC) 16,16,14
14        IM = (I+1)/2
16        CONTINUE
        DZRU = DZ/RRU(J,I)
        UO = U(L,J,I)
        UP = U(L,J+1,IP)
        UM = U(L,J-1,IM)
        UPP = U(L,J,IPP)
        UMM = U(L,J,IMM)
        VO = VISC(J,I)
        VP = VISC(J+1,IP)
        VM = VISC(J-1,IM)
        VPP = VISC(J,IPP)
        VMM = VISC(J,IMM)
        IF(NMESH-J) 20,20,22
20        UP = 0.0 - U(L,J,I)
        VP = VISC(NMESH+1,1)*2.0 - VISC(J,I)
22        CONTINUE
        VL = (((R+DR/2.0)*((VP+VO)/2.0)*(UO-UP) +
1          (R-DR/2.0)*((VO+VM)/2.0)*(UO-UM)) / (RDR*DR)
2          + (((VPP+VO)/2.0)*(UO-UP) + ((VO+VMM)/2.0)*(UO-UM))
3          / (RDTH2))
        U(M,J,I) = U(L,J,I) - (DP/RRU(J,I)) - DZRU*VL
30        CONTINUE
        ICC = 0
        IF(IC) 40,40,32
32        ICC = 1
        IC = 0
        NI = 2*NI
40 CONTINUE
        RETURN
        END

```

CHT0757 VAL WATSON SUBROUTINE ITER FOR HT0750

```

SUBROUTINE ITER
COMMON AMPS, W, WW, DP, DZ, EPS, FZO, Z, Q, QR, DW, DIA, EX, EXX,
1      H, PHI, SIGMA, RCAP, RHO, VISC, HWALL, RHOAV, RHOU, PHIW,
1      P, E, DIAM, U,
1      NMESH, K, L, M, LOC, NFILE, NTAPE, NCHOK, NK, NNN
DIMENSION DIAM(1000), P(1000), E(1000), HWALL(1000)
      DIMENSION H(2,12,48), U(2,12,48), PHI(12,48), SIGMA(12,48),
1      RCAP(12,48), VISC(12,48), RHO(12,48), RHOU(12,48)
CALL CRISIS(ZZ,AAA)
IND = 0
NCHOK = 0
DDP = DP
P(K) = P(K-1) + DP
LOC = 0
NNN = 0
DO 4 N = 1,30
      LOC = N
      CALL MOM
      NNN = 1
      CALL WDOT
      DW = (WW - W)/W
      IF(ABSF(DW) - EPS) 10,20,20
20      IF(IND) 22,22,1
1      DDP = DDP/2.0
22      IF(DW) 2,10,3
2      DP = DP + DDP
      P(K) = P(K-1) + DP
      GO TO 4
3      DP = DP - DDP
      P(K) = P(K-1) + DP
      IND = 1
4 CONTINUE
      NCHOK = 1
10 CONTINUE
      RETURN
      END

```



1-

```

CHT0758 VAL WATSON  SUBROUTINE OUTPT FOR HT0750
SUBROUTINE OUTPT
COMMON AMPS, W, WW, DP, DZ, EPS, FZO, Z, Q, QR, DW, DIA, EX, EXX,
1      H, PHI, SIGMA, RCAP, RHO, VISC, HWALL, RHOAV, RHOU, PHIW,
1      P, E, DIAM, U,
1      NMESH, K, L, M, LOC, NFILE, NTAPE, NCHOKE, NK, NNN
DIMENSION DIAM(1000), P(1000), E(1000), HWALL(1000)
DIMENSION H(2,12,48), U(2,12,48), PHI(12,48), SIGMA(12,48),
1      RCAP(12,48), VISC(12,48), RHO(12,48), RHOU(12,48)
CALL CRISIS (ZZ,AAA)
QT = Q+QR
PRAD = QR/QT *100.0
WRITE TAPE NTAPE,          K, DIAM(K), Z, AMPS, E(K), W,QT,HWALL(K)
1      ,PRAD, NMESH, P(K),FZO,LOC,EPS,DW, DP, DZ
IF (NMESH - 7) 11,12,12
11      NI = 24
        GO TO 13
12      NI = 48
13 CONTINUE
WRITE TAPE NTAPE, NI, ((H(M,J,I), U(M,J,I), RHOU( J,I), I=1,NI),
1      J=1,NMESH)
END FILE NTAPE
WRITE OUTPUT TAPE 6,300,K, DIAM(K),Z,AMPS,E(K),W,QT,HWALL(K)
P(K) = P(K)/1.013E5
WRITE OUTPUT TAPE 6,299,PRAD,NMESH,P(K),FZO,LOC,EPS,DW,EX,NFILE
P(K) = P(K)*1.013E5
WRITE OUTPUT TAPE 6,301,H(M,1,1)
NI = 6
DO 2 J = 2,NMESH
WRITE OUTPUT TAPE 6,302,(H(M,J,I) ,I =1,NI)
FJ = J
FNI = NI
IF ((FNI/FJ) -4.0) 1,1,2
1      NI = 2*NI
2 CONTINUE
WRITE OUTPUT TAPE 6,301, RHOU(1,1)
NI = 6
DO 4 J = 2,NMESH
WRITE OUTPUT TAPE 6,302, (RHOU(J,I), I=1,NI)
FJ = J
FNI = NI
IF((FNI/FJ) -4.0) 3,3,4
3      NI = 2*NI
4 CONTINUE
300 FORMAT(1H1,
1      15HK          =      , 14      ,      16X,
3 50H      DC THERMAL ARC WITH AXIAL GAS FLOW

```

```

2      15HDIAMETER      =      , E10.3,    10H METERS      /
1      1X, 15HAXIAL DIST =      , E10.3,    10H METERS      ,
2      50X, 15HCURRENT  =      , E10.3,    10H AMPS       /
1      1X, 15HVOLTAGE GRAD =      , E10.3,    10H VOLTS/M    ,
2      50X, 15HFLOW RATE =      , E10.3,    10H KG/SEC     /
2      1X, 15HWALL HEAT FLUX=      , E10.3, 22H W/M**2     PREV STA
2      38X, 15HWALL ENTHALPY =      , E10.3,    10H J/KG      )
299  FORMAT(1H ,
2      15HRADIATION LOSS=      , F10.3,    10H PERCENT    ,
2      50X, 15HNMESH    =      , I4 /
2      1X, 15HPRESSURE  =      , E10.3,    10H ATMOS      ,
2      50X, 15HFZO      =      , E10.3 /
2      1X, 15HLOC       =      , I4, 16X,
2      50X, 15HEPS      =      , E10.3 /
2      1X, 15HDW        =      , E10.3, 10X
2      50X, 15HEX       =      , E10.3 /
2      1X, 15HFILE      =      , I4)
301  FORMAT(1H0, E12.3)
302  FORMAT(1H0, (6E12.3/))
      NFILE = NFILE +1
      RETURN
      END

```

```

CHT0780 VAL WATSON   DC ARC - SUPERSONIC CONTINUATION - REAL GAS
COMMON AMPS, W, WW, DP, DZ, EPS, FZO, Z, Q, QR, DW, DIA, EX, EXX,
1      H, PHI, SIGMA, RCAP, RHO, VISC, HWALL, RHOAV, RHOU, PHIW,
1      P, E, DIAM, U,
1      NMESH, K, L, M, LOC, NFILE, NTAPE, NCHOKE, NK, NNN
DIMENSION DIAM(1000), P(1000), E(1000), HWALL(1000)
DIMENSION H(2,12,48), U(2,12,48), PHI(12,48), SIGMA(12,48),
1      RCAP(12,48), VISC(12,48), RHO(12,48), RHOU(12,48)
CALL CRISIS (ZZ,AAA,AMPS, NNN)
M = 1
L = 2
READ INPUT TAPE 5,100,NFILE1, NTAPE1, NFILE, NTAPE, KMAX, KINC
100 FORMAT (2I4/4I4)
READ INPUT TAPE 5,101, EX, ZC, THETA
101 FORMAT ( E10.3)
THETAR = THETA*2.0*3.1416/360.0
CALL LOCATE(NFILE1, NTAPE1)
READ TAPE NTAPE1,      K, DIAM(2), Z, AMPS, E(2), W,QX,HWALL(2)
1      ,PX , NMESH, P(2),EZO,LOC,EPS,DW, DP, DZ
READ TAPE NTAPE1,NI, ((H(M,J,I), U(M,J,I), RHOU( J,I), I=1,NI),
1      J=1,NMESH)
P(1) = P(2) - DP
DO 11 K = 3 ,KMAX
11      HWALL (K) = HWALL(2)
      K = 2
      DIA = DIAM(2)
      CALL RHOAVE
      CALL STATEP
      QR = QX*PX/100.0
      Q = QX - QR
      CALL LOCATE (NFILE,NTAPE)
      CALL OUTPT
      DO 6 K = 3 ,KMAX
        DZ = EX *DZ
        Z = Z +      DZ
      IF(Z-ZC) 50,50,51
50 DIAM(K) = DIAM(2)
   GO TO 52
51 DIAM(K) = DIAM(2) + 2.0*(Z-ZC)*TANF(THETAR)
52 CONTINUE
   DIA = DIAM(K)
   M = 1
   L = L + 1
   IF(3-L) 1,1,2
1     M = 2
     L = 1
2     CONTINUE

```



```

      CALL ENERGY
      IF(2-2C) 60,60,61
60  CALL ITER
      GO TO 62
61  CALL ITERS
62  CONTINUE
      IF(NCHOKE) 4,4,3
      3      WRITE OUTPUT TAPE 6, 202, K, DW, U(M,2,2)
            GO TO 8
      4      CONTINUE
            CALL STATEP
            NN = NN - 1
            IF(NN) 5,5,6
      5      NN = KINC
            CALL OUTPT
      6  CONTINUE
      8  CONTINUE
      REWIND NTAPE1
      REWIND NTAPE
      REWIND 8
202  FORMAT(1H0, 18HFLOW CHOKED AT K = , I4, 10X,
1      20HFLOW RATE ERROR IS      , 2PF12.7, 10H PERCENT
2 14 HCL VELOCITY = ,0PF10.1, 8H FT/SEC      )
      CALL EXIT
      END

```

CHT0781 VAL WATSON SUBROUTINE ITES FOR HT0780

```

SUBROUTINE ITES
COMMON AMPS, W, WW, DP, DZ, EPS, FZO, Z, Q, QR, DW, DIA, EX, EXX,
1      H, PHI, SIGMA, RCAP, RHO, VISC, HWALL, RHOAV, RHOU, PHIW,
1      P, E, DIAM, U,
1      NMESH, K, L, M, LOC, NFILE, NTAPE, NCHOKE, NK, NNN
DIMENSION DIAM(100), P(100), E(100), HWALL(100)
DIMENSION H(2,12,48), U(2,12,48), PHI(12,48), SIGMA(12,48),
1      RCAP(12,48), VISC(12,48), RHO(12,48), RHOU(12,48)
IND = 0
CALL CRISIS(ZZ,AAA)
NCHOKE = 0
DDP = DP
P(K) = P(K-1) + DP
LOC = 0
NNN = 0
DO 4 N = 1,30
    LOC = N
    CALL MOM
    NNN = 1
    CALL WDOT
    DW = (WW - W)/W
    IF(ABSF(DW) - EPS) 10,20,20
20    IF(IND) 22,22,1
1      DDP = DDP/2.0
22    IF(DW) 3,10,2
2      DP = DP + DDP
      P(K) = P(K-1) + DP
      GO TO 4
3      DP = DP - DDP
      P(K) = P(K-1) + DP
      IND = 1
4 CONTINUE
    NCHOKE = 1
10 CONTINUE
    RETURN
END

```

APPENDIX D

FORTTRAN PROGRAM TO EVALUATE GAS PROPERTIES USING PREPARED TABLES STORED ON A MAGNETIC TAPE

These programs move prepared gas tables from a magnetic tape to the core storage and make interpolations (either logarithmic or linear) from the tables to obtain the gas density, thermal conductivity potential, electrical conductivity, radiance, and viscosity from known values of enthalpy and pressure.

The input for these programs is the magnetic tape prepared by the program in appendix E.

```

CHT0767 VAL WATSON SUBROUTINE FOR AIR TABLES - INPUT ENTHALPY AND P
SUBROUTINE NTAB (P, H, PHI, SIGMA, RCAP, VISC, NTAPE, NERR)
  DIMENSION PHIT(2,300), SIGMAT(2,300), RCAPT(2,300), VISCT(2,300)
  CALL CRISIS (ZZ,PHIT)
  IF (IN) 1,1,2
1 CALL LOCATE ( 2,NTAPE)
  READ TAPE NTAPE, ((SIGMAT(I,J), J=1,281), I=1,2),
1 (( PHIT(I,J), J=1,281), I=1,2) ,
1 (( RCAPT(I,J), J=1,281), I=1,2) ,
1 (( VISCT(I,J), J=1,281), I=1,2)
  REWIND NTAPE
  IN = 1
2 NERR = 0
  IF (2.0E9-H ) 3,4,4
3 NERR = 1
  GO TO 10
4 IF (H - 2.0E7) 5,5,60
5 I = XINTF(H/2.0E+5) + 1
  HH = (H/2.0E+5) - FLOATF(I-1)
  GO TO 7
60 IF (H-2.0E8) 61,61,62
61 I = XINTF(H/2.0E+6) +91
  HH = (H/2.0E+6) - FLOATF(I- 91)
  GO TO 7
62 I = XINTF(H/2.0E+7) +181
  HH = (H/2.0E+7) - FLOATF(I-181)
7 P1 = PHIT(1,I) + ( PHIT(1,I+1) - PHIT(1,I))*HH
  P2 = PHIT(2,I) + ( PHIT(2,I+1) - PHIT(2,I))*HH
  S1 = SIGMAT(1,I) + (SIGMAT(1,I+1) - SIGMAT(1,I))*HH
  S2 = SIGMAT(2,I) + (SIGMAT(2,I+1) - SIGMAT(2,I))*HH
  R1 = RCAPT(1,I) + ( RCAPT(1,I+1) - RCAPT(1,I))*HH
  R2 = RCAPT(2,I) + ( RCAPT(2,I+1) - RCAPT(2,I))*HH
  V1 = VISCT(1,I) + ( VISCT(1,I+1) - VISCT(1,I))*HH
  V2 = VISCT(2,I) + ( VISCT(2,I+1) - VISCT(2,I))*HH
  PP = LOGF(P)/2.3026
  PHI = P1 + (P2 - P1)*PP
  SIGMA = EXPF(S1 + (S2 - S1)*PP)
  RCAP = EXPF(R1 + (R2 - R1)*PP)
  VISC = V1 + (V2 - V1)*PP
10 RETURN
END

```

```

CHT0768 VAL WATSON SUBROUTINE FOR AIR DENSITY TABLE
      SUBROUTINE NRHO (P, H, RHO, NTAPE, NERR)
      DIMENSION RHOT(2,300)
      CALL CRISIS (ZZ,RHOT)
      IF (IN) 1,1,2
1     CALL LOCATE (1 ,NTAPE)
      READ TAPE NTAPE, (( RHOT(I,J), J=1,281), I=1,2)
      REWIND NTAPE
      IN = 1
2     NERR = 0
      IF (2.0E9-H ) 3,4,4
3     NERR = 1
      GO TO 10
4     IF (H - 2.0E7) 5,5,60
5     I = XINTF(H/2.0E+5) + 1
      HH = (H/2.0E+5) - FLOATF(I-1)
      GO TO 7
60    IF (H-2.0E8) 61,61,62
61    I = XINTF(H/2.0E+6) +91
      HH = (H/2.0E+6) - FLOATF(I- 91)
      GO TO 7
62    I = XINTF(H/2.0E+7) +181
      HH = (H/2.0E+7) - FLOATF(I-181)
7     RH1 = RHOT(1,I) + ( RHOT(1,I+1) - RHOT(1,I))*HH
      RH2 = RHOT(2,I) + ( RHOT(2,I+1) - RHOT(2,I))*HH
      PP = LOGF(P)/2.3026
      RHO = P/(RH1 + (RH2 - RH1)*PP)
10    RETURN
      END

```

```

CHT0769 VAL WATSON SUBROUTINE FOR AIR TABLES - INPUT ENTHALPY AND P
      SUBROUTINE NTEMP(P,H,SIGMA,NTAPE,NERR)
      DIMENSION SIGMAT(2,300)
      CALL CRISIS (ZZ,SIGMAT)
      IF (IN) 1,1,2
1     CALL LOCATE( 3,NTAPE)
      READ TAPE NTAPE, ((SIGMAT(I,J), J=1,281), I=1,2)
      REWIND NTAPE
      IN = 1
2     NERR = 0
      IF (2.0E9-H ) 3,4,4
3     NERR = 1
      GO TO 10
4     IF (H - 2.0E7) 5,5,60
5     I = XINTF(H/2.0E+5) + 1
      HH = (H/2.0E+5) - FLOATF(I-1)
      GO TO 7
60    IF (H-2.0E8) 61,61,62
61    I = XINTF(H/2.0E+6) +91
      HH = (H/2.0E+6) - FLOATF(I- 91)
      GO TO 7
62    I = XINTF(H/2.0E+7) +181
      HH = (H/2.0E+7) - FLOATF(I-181)
7     S1 = SIGMAT(1,I) + (SIGMAT(1,I+1) - SIGMAT(1,I))*HH
      S2 = SIGMAT(2,I) + (SIGMAT(2,I+1) - SIGMAT(2,I))*HH
      PP=LOGF (P) / 2.3026
      SIGMA = (S1 + (S2 - S1)*PP)
10    RETURN
      END

```

APPENDIX E

FORTTRAN PROGRAM FOR PREPARING GAS TABLES FOR USE IN THE PROGRAM

IN APPENDIX D

This program prepares the magnetic tape required for the program in Appendix D from any gas tables wherein the gas properties are given in terms of any two state properties. The program fits a third-order polynomial curve between the middle two points of each set of four adjacent points of the input tables. The gas properties are taken from this curve in equal increments of enthalpy to form the table that is put on magnetic tape for use with the programs of appendix D. To check the fitted curves, the program plots the input data (shown as circles) and the fitted curves on the same graph, as shown in figure 2. (When the curve did not go through the symbols, the automatic plotter was out of adjustment; within the program the curve was forced through each point.)

```

CHT0766 PEGOT GENERATES TABLES AND PREPARES TAPE AND PLOTS 2401
  DIMENSION H1(100),P(10),PHI1(100),SIGMA1(100),RCAP1(100),VISC1(100)HT0766
  1),RHO1(100),HTEMP1(100) HT0766
  DIMENSION HA(300),PHIA(300),SIGMAA(300),RCAPA(300),VISCA(300),RHOAHT0766
  1(300),TEMPA(300),YY(300),RCAPLA(300),RRHOA(300) HT0766
  DIMENSION H2(100),PHI2(100),SIGMA2(100),RCAP2(100),VISC2(100),RHO2HT0766
  1(100),HTEMP2(100),PTEMP1(100),PTEMP2(100),STEMP1(100),STEMP2(100),HT0766
  2RTEMP1(100),RTEMP2(100),VTEMP1(100),VTEMP2(100),OTEMP1(100),OTEMP2HT0766
  3(100) HT0766
  DIMENSION RHOT(2,300), TEMPT(2,300), HT(2,300)
  DIMENSION PHIT(2,300), SIGMAT(2,300), RCAPT(2,300), VISCT(2,300)
  CALL CRISIS (ZZ,H1)
    CALL LOCATE (1,8)
    P(1)=1.0
    P(2)=10.0
    P(3) = 0.5
    P(4) = 5.0
    P(5) = 50.0
    P(6) = 1.0 .
C
  WRITE OUTPUT TAPE 6,299
299 FORMAT (1H1,5X, 10H PAGE 1 )
  I=1 HT0766
  CALL GENTAB(H1,HTEMP1,NXY1H,HA,TEMPA,DXX,N,0,2,PHIA,TEMPA,P,I) HT0766
  CALL GENTAB(STEMP1,SIGMA1,NXY1S,TEMPA,SIGMAA,DXX,N,0,3,PHIA,TEMPA,HT0766
  1 P,I)
  CALL GENTAB(RTEMP1,RCAP1,NXY1R,TEMPA,RCAPA,DXX,N,0,3,PHIA,TEMPA,P,HT0766
  1I) HT0766
  CALL GENTAB(VTEMP1,VISC1,NXY1V,TEMPA,VISCA,DXX,N,0,2,PHIA,TEMPA,P,HT0766
  1I) HT0766
  CALL GENTAB(PTEMP1,PHI1,NXY1P,TEMPA,YY,DXX,N,1,2,PHIA,TEMPA,P,I) HT0766
  CALL GENTAB(OTEMP1,RHO1,NXY1O,TEMPA,RHOA,DXX,N,0,4,PHIA,TEMPA,P,I)HT0766
  END FILE 7
  GO TO 300 HT0766
301 WRITE OUTPUT TAPE 6,298
298 FORMAT (1H1,5X, 10H PAGE 2 )
  CALL GENTAB(H2,HTEMP2,NXY2H,HA,TEMPA,DXX,N,0,2,PHIA,TEMPA,P,I) HT0766
  CALL GENTAB(STEMP2,SIGMA2,NXY2S,TEMPA,SIGMAA,DXX,N,0,3,PHIA,TEMPA,HT0766
  1P,I) HT0766
  CALL GENTAB(RTEMP2,RCAP2,NXY2R,TEMPA,RCAPA,DXX,N,0,3,PHIA,TEMPA,P,HT0766
  1I) HT0766
  CALL GENTAB(VTEMP2,VISC2,NXY2V,TEMPA,VISCA,DXX,N,0,2,PHIA,TEMPA,P,HT0766
  1I) HT0766
  CALL GENTAB(PTEMP2,PHI2,NXY2P,TEMPA,YY,DXX,N,1,2,PHIA,TEMPA,P,I) HT0766
  CALL GENTAB(OTEMP2,RHO2,NXY2O,TEMPA,RHOA,DXX,N,0,4,PHIA,TEMPA,P,I)HT0766
  END FILE 7
300 DO 320 J=1,N HT0766

```



```

      HT(I,J)      =HA(J)
      TEMPT(I,J)   =TEMPA(J)
      RHOT(I,J)    =RHOA(J)
      SIGMAT(I,J)  =SIGMAA(J)
      RCAPT(I,J)   =RCAPA(J)
      VISCT(I,J)   =VISCA(J)
320  PHIT(I,J)     =PHIA(J)
C
C PREPARING VALUES FOR TAPE
      I=I+1
      IF(I-2) 301,301,302
302  WRITE TAPE 8,((RHOT(I,J),J=1,N),I=1,2)
      END FILE 8
      WRITE TAPE 8,      ((SIGMAT(I,J), J=1, N ), I=1,2)      ,
1      (( PHIT(I,J), J=1, N ), I=1,2)      ,
1      (( RCAPT(I,J), J=1, N ), I=1,2)      ,
1      (( VISCT(I,J), J=1, N ), I=1,2)
      END FILE 8
      WRITE TAPE 8,      ((TEMPT(I,J),J=1, N ),I=1,2)
      END FILE 8
      REWIND 8
100  FORMAT (5E12.5/(5E12.5))
C
C PRINTOUT AND PLOTS
C
C CHECK FOR ERROR IF OVERRUN TABLES
      NERR=NERR
      IF (NERR) 60,60,61
61  WRITE OUTPUT TAPE 6,102
      GO TO 62
60  WRITE OUTPUT TAPE 6, 103
62  NERR = 0
      HOM = 2.5E6
      POM = 1.0
      CALL NRHO(POM,HOM,RHOA,8,NERR)
      IF (NERR) 70,70,71
70  WRITE OUTPUT TAPE 6,102
      GO TO 72
71  WRITE OUTPUT TAPE 6,103
72  NERR = 0
      CALL NTAB(POM,HOM,PHIA,SIGMAA,RCAPA,VISCA,8,NERR)
      IF (NERR) 80,80,81
80  WRITE OUTPUT TAPE 6,102
      GO. TO 90
81  WRITE OUTPUT TAPE 6,103
90  CONTINUE
C

```

HT0766
HT0766
HT0766

HT0766

HT0766

```

102 FORMAT (1H0, 30H ERROR SIGNAL INOP
103 FORMAT (1H0, 30H ERROR SIGNAL OKAY
405 READ INPUT TAPE 5,400,JAM
404 READ INPUT TAPE 5,400,NOC
      READ INPUT TAPE 5,2,XRANGE
      2 FORMAT (2E10.3)
400 FORMAT (I4)
      KATH = 1
403 IN =0
      NPLOT = 0
      DO 401 K=2,6
      CALL NPLOTS(XNAME,YNAME,XRANGE,P(K),CONVX,CONVY,SCALEX,SCALEY,
1 NPLOT,IN,ORIGX,ORIGY,CONVL)
      IN=1
401 NPLOT=1
407 KATH=KATH+1
      NOC=NOC+1
      IF (NOC)402,402,403
402 END FILE 7
      JAM=JAM+1
      REWIND 8
      IF(JAM) 405,405,404

```

HT0766

HT0766


```

CHT0785  PEGOT SUBROUTINE TO GENERATE TABLE VALUES . 401
SUBROUTINE GENTAB(X,Y,NXY,XX,YY,DXX,N,NUMB,JUMB,PHIA,TEMPA,P,I)
DIMENSION X(300),Y(300),XX(300),YY(300),PHIA(300),TEMPA(300),P(10)
1,HA(300)
CALL CRISIS (ZZZ,X)
READ INPUT TAPE 5,199,NAX,NAY
199  FORMAT(2A6)
READ INPUT TAPE 5,200,NXY
READ INPUT TAPE 5,201,CX,CY
READ INPUT TAPE 5,201,OX,OY
301 READ INPUT TAPE 5,201, (X( JJ),Y( JJ),JJ=1,NXY)
200 FORMAT(I4)
201 FORMAT(2E10.3)
WRITE OUTPUT TAPE 6,198,NAX,NAY,CX,CY,(X(JJ),Y(JJ),JJ=1,NXY)
198  FORMAT(1H1,25X,A6,15X,A6//24X,10HCONVERSION,10X,10HCONVERSION/
1 17X,2E20.8//((17X,2E20.8))
C NAX,NAY,=NAME OF X AND Y ARRAYS
C CX,CY,=CONVERSION FACTORS
C OX,OY,=ORIGINS FOR X,Y PLOTS
C X=X ARRAY OF INPUT TABLES
C Y=Y ARRAY OF INPUT TABLES
C NXY=NUMBER OF ARRAY VALUES IN EACH X AND Y
C XX=ABSCISSA TABLE VALUES (IN OUR CASE HT)
C YY=ORDINATE TABLE VALUES (TEMPT,PHIT,SIGMAT,ETC.)
C DXX=DELTA HT VALUE
C N=NUMBER OF VALUES IN FINAL TABLE (191)
C JUMB FOR UNITS NEED CORRECTED FOR TAPE
C NUMB=1 FOR PHIT TO USE SIMP SUBROUTINE,=0 FOR ALL OTHERS
DMON=0.0
GO TO(304,302,310,312),JUMB
310 DO 331 JJ=1,NXY
Y(JJ)=Y(JJ)*CY
331 X(JJ)=X(JJ)*CX
CALL SPLOTS( X, Y,NXY,7.0,10.0,OX,OY,SX,SY,17)
AY=LOGF(CY)
DO 313 JJ=1,NXY
X(JJ)=X(JJ)/CX
313 Y( JJ )=LOGF(Y( JJ)/CY) +AY
GO TO 304
312 DO 314 JJ=1,NXY
314 Y( JJ )=P(I)/(Y(JJ) *CY)
GO TO 304
302 DO 303 JJ=1,NXY
Y( JJ )=Y( JJ )*CY
303 X( JJ )=X( JJ )*CX
304 YY( 1)=Y( 1)
DXX=2.0E5

```

```

      N=281
      XX(1)=0.0
      DO 305 J=2,N
      IF (KITE ) 350,349,350
349 IF (XX(J-1) - 1.99E7 ) 315,316,316
316 DXX=2.0E6
      IF (XX(J-1) - 1.99E8 ) 315,317,317
317 DXX=2.0E7
315 XX(J)=XX(J-1)+DXX
350 CALL TAIN(X,Y,XX( J),YY( J),NXY,3,NERR,DMON)
      NERR=NERR
      GO TO (305,306,306),NERR
306 WRITE OUTPUT TAPE 6,307,XX( J),YY( J)
307 FORMAT(1H1,28X,25HERROR IN TAIN SUBROUTINE //30X,2HXX,12X,2HYY/24
1X,2E15.8)
      CALL EXIT
305 CONTINUE
      KITE = 1
      IF(NUMB) 308,351,308
308 PHIA( 1)=YY( 1)
      DO 311 J=2,N
      CALL SIMP(PHIA( J),TFMPA ,YY ,J,II)
      GO TO (311,309,309,309),II
309 WRITE OUTPUT TAPE 6,300,II,J
300 FORMAT(1H1,28X,25HERROR IN SIMP SUBROUTINE //30X,2HI ,12X,2HJ /24
1X,2I10)
      CALL EXIT
311 CONTINUE
351 GO TO (321,321,332,321),JUMB
332 DO 333 K=1,N
333 Y(K) = EXPF(YY(K))
      CALL PLOTWS(OX,OY,SX,SY,XX, Y,N,7,-17,NERR )
      GO TO 322
321 CALL SLOTS ( X,Y,NXY,7.0,10.0,OX,OY,SX,SY,17)
      CALL PLOTWS ( OX,OY,SX,SY,XX,YY,N,7,-17,NERR )
322 WRITE OUTPUT TAPE 6,253,NAX,NAY,SX,SY,OX,OY
253 FORMAT ( 1H1, 5X,A6, 5X,A6,5X,10HSCALE X = ,E10.3,5X,10HSCALE Y =
1 ,E10.3,5X,10H ORIG X = ,E10.3,5X,10H ORIG Y = ,E10.3 )
      RETURN

```

```

CHT2136 EVA PEGOT SET UP SCALES AND PLOT
SUBROUTINE SLOTS(X,Y,NUM,RANGEX,RANGEY,ORIGX,ORIGY,SCALEX,SCALEY,
1  NBYM)
  DIMENSION X(500), Y(500)
  CALL CRISIS (ZZZ, A11)
  XM=X(1)
  DO 11 J=1,NUM
    IF (XM-X(J)) 10,10,11
10  XM=X(J)
11  CONTINUE
  YM=Y(1)
  DO 13 J=1,NUM
    IF (YM-Y(J)) 12,12,13
12  YM=Y(J)
13  CONTINUE
    QY = YM/RANGEY - 1.0E-30
    EXPQY = (LOGF (QY)/2.30258 )
    IF (EXPQY ) 1,1,2
1  EXPQY = EXPQY -1.0
2  EXPQY = INTF ( EXPQY )
    AQY = EXPF (LOGF (QY) - EXPQY * 2.30258 )
    IF (AQY -2.0 ) 32,34,34
32  SCALEY =2.0*10.0**EXPQY
    GO TO 41
34  IF (AQY - 4.0 ) 36,36,38
36  SCALEY = 4.0*10.0**EXPQY
    GO TO 41
38  SCALEY = 10.0*10.0**EXPQY
41  QX = XM/RANGEX -1.0E-30
    EXPQX = (LOGF (QX )/ 2.30258 )
    IF (EXPQX ) 3,3,4
3  EXPQX = EXPQX -1.0
4  EXPQX = INTF ( EXPQX )
    AQX = EXPF (LOGF (QX) - EXPQX * 2.30258 )
    IF (AQX - 2.0 ) 42,44,44
42  SCALEX = 2.0*10.0**EXPQX
    GO TO 51
44  IF ( AQX - 4.0 ) 46,46,48
46  SCALEX = 4.0*10.0**EXPQX
    GO TO 51
48  SCALEX = 10.0*10.0**EXPQX
51  CALL PLOTWS (ORIGX,ORIGY,SCALEX,SCALEY,X,Y,NUM,7,NBYM,NERR)
  RETURN
END

```

APPENDIX F

FORTRAN PROGRAM FOR PLOTTING IN PICTORIAL FORM THE RESULTS OF THE PROGRAM IN APPENDIX B

This program reads from magnetic tape the results of the program in appendix B and plots these results in pictorial form as shown in figures 41 through 44.

```

CHT073T VAL WATSON PLOTS OUTPUT FOR HT0720 PLOTS TEMP 401
  DIMENSION H(100), R(100), RHOU(100), U(100), RUH(100), RUU(100),
1    HH(1000), HR(1000), HAVE(1000), RUHA(1000), HRAVE(1000),
2    QR(1000), QT(1000), PRAD(1000), E(1000), P(1000), Z(1000)
  **TEMP(100)
  CALL CRISIS(ZZ,H)
2  READ INPUT TAPE 5, 104, KS, KL, KI, NTAPE
  READ INPUT TAPE 5, 100, CRA, CRB, CH, CRU, CRUH
  READ INPUT TAPE 5, 100, SR, SH, SRU, SRUH, SU, SRUU, EX
  READ INPUT TAPE 5,100,STEMP
  READ INPUT TAPE 5, 104, NOTHC
    IF(NOTHC) 400,400,402
400    READ INPUT TAPE 5, 100, A, CPOK
402    CONTINUE
100  FORMAT(E10.3)
104  FORMAT(I4)
    IF (NT -NTAPE ) 40,42,40
40  CALL LOCATE (1,NTAPE )
    KEND = 1
    NT = NTAPE
42  KSKIP = KS-KEND
    IF(KSKIP) 700,702,700
702  KSKIP = -0
700  CONTINUE
    CALL SKIP(KSKIP,NTAPE)
    KEND = KL
    NUMM = KL - KS + 1
    KR = KI
    DO 50 K = 1,NUMM
      READ TAPE NTAPE, M, DIAM, Z(K), AMPS, E(K), W, QT(K), HWALL,
1      PRAD(K), NMESH, P(K), FZO, LOC, EPS, DW, DP, DZ,
2      HAVE(K), RUHA(K), HRAVE(K)
      READ TAPE NTAPE, (R(J), H( J), U( J), RHOU(J), J=1,NMESH)
      U(NMESH) = 0.0
      RHOU(NMESH) = 0.0
      R(1) = 0.0
      NMESH = NMESH + 1
      R(NMESH) = DIAM/2.0
      H(NMESH) = HWALL
      HH(K) = H(2)
      HR(K) = HAVE(K)/HH(K)
      QR(K) = QT(K)*PRAD(K)/100.0
      KR = KR + 1
      IF(KI-KR) 10,10,12
10      KR = 0
      DO 8 J=1,NMESH
        RUU(J) = RHOU(J)*U(J)

```



```

      RUH(J) = RHOU(J)*H(J)
8      CONTINUE
      DOR = EX*Z(K)
      ORA = CRA + DOR
      ORB = CRB + DOR
      OH  = CH  + 0.5*DOR
      ORU = CRU + 0.5*DOR
      ORUH = CRUH + 0.5*DOR
      NUM = 2*NMESH+1
      NP = NUM
      DO 20 JP = 1,NMESH
      JJP      = (NMESH-JP+1)
      R(NP) = R(JJP)
      H(NP) = H(JJP)
      U(NP) = U(JJP)
      RHOU(NP) = RHOU(JJP)
      RUU(NP) = RUU(JJP)
      RUH(NP) = RUH(JJP)
      CALL NTEMP (P(K),H(NP),TEMP(NP), 8 ,NERR)
      NP = NP-1
20      CONTINUE
      DO 22 JP=2,NMESH
      JPN = (JP+NMESH)
      R(NP) = 0.0-R(JPN)
      H(NP) = H(JPN)
      U(NP) = U(JPN)
      RHOU(NP) = RHOU(JPN)
      RUU(NP) = RUU(JPN)
      RUH(NP) = RUH(JPN)
      TEMP(NP)=TEMP(JPN)
      NP = NP-1
22      CONTINUE
      CALL PLOTWS(ORA, OH , SR , SH , R, H ,NUM,7,-1,NERR)
      CALL PLOTWS(ORB, OH , SR , SU , R, U ,NUM,7,-1,NERR)
      CALL PLOTWS(ORA, ORU , SR , SRU , R, RHOU ,NUM,7,-1,NERR)
      CALL PLOTWS(ORB, ORU , SR , SRU , R, RUU ,NUM,7,-1,NERR)
      CALL PLOTWS(ORA, ORUH, SR , SRUH, R, RUH ,NUM,7,-1,NERR)
      CALL PLOTWS (ORB,ORUH,SR,STEMP,R,TEMP,NUM,7,-1,NERR)
12      CONTINUE
      IF(K-NUMM) 24,50,50
24      CALL SKIP(1,NTAPE)
50      CONTINUE
      END FILE 7
      CALL SPLOTS(Z,HH, NUMM, 10.0, 7.0, -14.0,-14.,SSX,SS1,-1)
      CALL SPLOTS(Z,HAVE, NUMM, 10.0, 7.0, -14.0,-5.0,SSX,SS2,-1)
      CALL SPLOTS(Z,RUHA, NUMM, 10.0, 7.0, -14.0,+4.,SSX,SS3,-1)
      CALL SPLOTS(Z,E, NUMM, 10.0, 7.0, 0.0,-14.,SSX,SS4,-1)

```

```

CALL SPLOTS(Z,QT,          NUMM, 10.0, 7.0,   0.0,- 5.,SSX,SS5,-1)
CALL PLOTWS(0.,-5.,SSX,SS5,Z,QR,NUMM,7,-1,NERR)
CALL SPLOTS(Z,HR,          NUMM, 10.0, 7.0,   0.0,  4.,SSX,SS6,-1)
CALL SPLOTS(Z,P,           NUMM, 10.0, 7.0,   0.0,  4.,SSX,SS7,-1)
IF(NOTHC) 500,500,502
500  ZO = W*CPOK/3.1416
      ZBAR = Z(NUMM)/(ZO)
      HINF = 0.307 *CPOK*AMPS/(SQRTF(A)*DIAM/2.0)
      HINFA = HINF*0.433
      QINF = 0.3831 *AMPS/(SQRTF(A)*DIAM*DIAM/4.0)
      EINF = 2.40/(SQRTF(A)*DIAM/2.0)
      HOBAR = HH(1)/HINF
      RUHAB = RUHA(1)/HINFA
      HAVEB = HAVE(1)/HINFA
      SCZ = SSX/(ZO)
      SC1 = SS1/HINF
      SC2 = SS2/HINFA
      SC3 = SS3/HINFA
      SC4 = SS4/EINF
      SC5 = SS5/QINF
      CALL TCURVE(ZBAR,RUHAB, -14.0, -14.0, SCZ, SC1, NERR)
      CALL TCURVE(ZBAR,RUHAB, -14.0, -5.0, SCZ, SC2, NERR)
      CALL TCURVE(ZBAR,RUHAB, -14.0,  4.0, SCZ, SC3, NERR)
      CALL ECURVE(ZBAR,RUHAB,  0.0, -14.0, SCZ, SC4, NERR)
      CALL TCURVE(ZBAR,RUHAB,  0.0, -5.0, SCZ, SC5, NERR)
502  CONTINUE
      END FILE 7
      CALL SIMP(VOLT,Z,E,NUMM,NERR)
      NERR=NERR
      GO TO (900,901,901,901),NERR
901  WRITE OUTPUT TAPE 6,902 ,NERR
902  FORMAT(1H1,25H ERROR IN SIMP NERR =          ,I2          )
      CALL EXIT
900  WRITE OUTPUT TAPE 6, 204
204  FORMAT(1H1, 30HPLOTS IN MKS UNITS
11X,  50H SHEET 1 - RADIAL PROFILES
4 5X,  50H      ENTHALPY          - LOWER LEFT
4 5X,  50H      MASS FLUX         - CENTER LEFT
4 5X,  50H      ENERGY FLUX     - UPPER LEFT
4 5X,  50H      VELOCITY         - LOWER RIGHT
4 5X,  50H      MOMENTUM FLUX    - CENTER RIGHT
4 5X,  50H      TEMPERATURE      - UPPER RIGHT
      SL = 1.0/EX
      SR = ABSF(SR)
      WRITE OUTPUT TAPE 6, 210, SR, SL, SH, SRU, SRUH, SU, SRUU,STEMP
210  FORMAT(1H0, 40H SCALES FOR RADIAL PROFILES ARE
1 20X, 30HRADIAL DISTANCE          , E10.3 /

```

```

1 20X, 30HAXIAL DISTANCE , E10.3 /
1 20X, 30HENTHALPY , E10.3 /
1 20X, 30HMASS FLUX , E10.3 /
1 20X, 30HENERGY FLUX , E10.3 /
1 20X, 30HVELOCITY , E10.3 /
1 20X, 30HMOMENTUM FLUX , E10.3 /
1 20X, 30HTEMPERATURE , E10.3 )
WRITE OUTPUT TAPE 6, 200
200 FORMAT(1H0,
1 50H SHEET 2 - AXIAL PROFILES /
2 5X, 50H CENTERLINE ENTHALPY - LOWER LEFT /
3 5X, 50H SPACE AVERAGE ENTH - CENTER LEFT /
4 5X, 50H MASS AVERAGE ENTH - UPPER LEFT /
4 5X, 50H VOLTAGE GRADIENT - LOWER RIGHT /
4 5X, 50H WALL HEAT FLUX - CENTER RIGHT /
4 5X, 50H PRESSURE GRADIENT - UPPER RIGHT /
4 5X, 50H RATIO OF AVE TO CL ENTHALPY - UR )
WRITE OUTPUT TAPE 6, 202, SSX, SS1, SS2, SS3, SS4, SS5, SS7, SS6
.,VOLT
202 FORMAT(1H0, 40H SCALES FOR AXIAL PROFILES ARE /
1 20X, 30HAXIAL DISTANCE , E10.3 /
1 20X, 30HCENTERLINE ENTHALPY , E10.3 /
1 20X, 30HSPACE AVERAGE ENTHALPY , E10.3 /
1 20X, 30HMASS AVERAGE ENTHALPY , E10.3 /
1 20X, 30HVOLTAGE GRADIENT , E10.3 /
1 20X, 30HWALL HEAT FLUXES , E10.3 /
1 20X, 30HPRESSURE GRADIENT , E10.3 /
1 20X, 30HRATIO OF AVE TO CL ENTHALPY , E10.3 /
1 20X, 30HCONSTRUCTOR VOLTAGE , E10.3 )
RADIUS=DIAM/2.0
WOVA=W/(3.14159*DIAM*DIAM/4.0)
HWOVA=HINF*WOVA
SHINF=SQRTF(HINF)
PMKS=1.013E5*P(1)
WRITE OUTPUT TAPE 6,300,ZO,RADIUS ,HINF,WOVA,HWOVA,SHINF,PMKS,
.P(1)
300 FORMAT(1H1,4X,20H(LC)Z(0) ,E12.5,15H M /
. 5X,20HR ,E12.5,15H M /
. 5X,20H(LC)H(INF) ,E12.5,15H J/KG /
. 5X,20H(LC)W/A ,E12.5,15H KG/SM**2 /
. 5X,20H(LC)H(INF)(LC)W/A ,E12.5,15H W/M**2 /
. 5X,20H(LC)H(INF)**1/2 ,E12.5,15H M/S /
. 5X,20H(LC)P(0) ,E12.5,15H NEWTONS/M**2 ,
.5X,E12.5,15H ATM //)
WRITE OUTPUT TAPE6,301,ZO,RADIUS ,HINF,HINF,A,EINF,QINF,PMKS,P(1)
301 FORMAT(1H0,4X,20H(LC)Z(0) ,E12.5,15H M /
. 5X,20HR ,E12.5,15H M /

```

```

      •      5X,20H(LC)H(INF)      ,E12.5,15H  J/KG      /
      •      5X,20HH(INF)          ,E12.5,15H  J/KG      /
      •      5X,20HE(INF)          ,E12.5,15H  V/M      /
      •      5X,20H(LC)Q(INF)      ,E12.5,15H  W/M**2     /
      •      5X,20H(LC)P(O)        ,E12.5,15H  NEWTONS/M**2 ,
      •5X,E12.5,15H  ATM          //)
      WRITE OUTPUT TAPE 6,302 ,CPOK,A
302 FORMAT(1H0,4X,29H(LC) SIGNIFIES LOWER CASE
      •/ 5X,29H( ) SIGNIFIES SUBSCRIPT      ///
      •5X,20HCP/K                      ,E12.5,15H  MS/KG      /
      •5X,20HA                          ,E12.5,15H  1/V**2     )
      GO TO 2
      END

```

```

CHT0738 VAL WATSON - PLOT OF 1/F(Z)
      SUBROUTINE ECURVE(ZBAR,HOBAR,OX,OY,SX,SY,NERR)
      DIMENSION F(110), Z(110), E(110)
      NERR=0
      IF (1.0-HOBAR) 1,1,2
1  NERR = 1
      GO TO 10
2  ZS=0.0- LOGF(1.0-HOBAR*HOBAR)/11.5
      DZ = ZBAR/100.0
      ZR = ZS
      DO 3 I=1,101
          F(I) = SQRTF(1.0 - EXPF(-11.5*ZR))
          E(I) = 1.0/F(I)
          IF(E(I)-5.0) 20,20,22
22      E(I) = 5.0
20  CONTINUE
          Z(I) = ZR - ZS
3  ZR = ZR + DZ
      CALL PLOTWS(OX,OY,SX,SY,Z,E,101,7,-17,NERR)
10  RETURN
      END

```

```

CHT0743 VAL WATSON - PLOT OF F(Z)
      SUBROUTINE TCURVE(ZBAR,HOBAR,OX,OY,SX,SY,NERR)
      DIMENSION F(110), Z(110)
      NERR=0
      IF (1.0-HOBAR) 1,1,2
1  NERR = 1
      GO TO 10
2  ZS=0.0- LOGF(1.0-HOBAR*HOBAR)/11.5
      DZ = ZBAR/100.0
      ZR = ZS
      DO 3 I=1,101
          F(I) = SQRTF(1.0 - EXPF(-11.5*ZR))
          Z(I) = ZR      -ZS
3  ZR = ZR + DZ
      CALL PLOTWS(OX,OY,SX,SY,Z,F,101,7,-17,NERR)
10  RETURN
      END

```

REFERENCES

1. Stine, Howard A.; and Watson, Velvin R.: The Theoretical Enthalpy Distribution of Air in Steady Flow Along the Axis of a Direct-Current Electric Arc. NASA TN D-1331, 1962.
2. Marlotte, G. L.; Harder, R. L.; and Prichard, R. W.: The Radiating Arc Column. AGARDograph 84, pt. 2, 1964, pp. 633-672.
3. John, R. R., et al.: Thirty-Kilowatt Plasmajet Rocket-Engine Development - Third-Year Development Program. Avco Rep. RAD-SR-64-80, March 1964.
4. Weber, H. E.: Growth of an Arc Column in Flow and Pressure Fields. AGARDograph 84, pt. 2, 1964, pp. 845-881.
5. John, R. R., et al.: Theoretical and Experimental Investigation of Arc Plasma-Generator Technology. Part I. Applied Research on Direct and Alternating Current Electric Arc Plasma Generators. Avco Rep. ASD-TDR-62-729, Sept. 1963.
6. Eckert, E. R. G.; and Anderson, J. E.: Performance Characteristics of a Fully-Developed Constricted Transpiration-Cooled Arc. AGARDograph 84, pt. 2, 1964, pp. 751-795.
7. Watson, Velvin R.: Comparison of Detailed Numerical Solutions With Simplified Theories for the Characteristics of the Constricted-Arc Plasma Generator. Proc. 1965 Heat Transfer and Fluid Mechanics Institute, Stanford Univ. Press, 1965, pp. 24-41.
8. Masser, P. S.: Arc Jet Design. ARS Paper 2352-62, March 1962.
9. Ahtye, Warren F.; and Peng, Tzy-Cheng: Approximations for the Thermodynamic and Transport Properties of High Temperature Nitrogen With Shock-Tube Applications. NASA TN D-1303, 1962.
10. Yos, Jerrold M.: Transport Properties of Nitrogen, Hydrogen, Oxygen, and Air up to 30,000° K. Research and Advanced Development Division, Avco Rep. RAD TM 63-7, March 1963.
11. Spitzer, L.: Physics of Fully Ionized Gases. Interscience Pub., Inc., N. Y., 1956.
12. Nardone, M. C.; Breene, R. G.; Zeldin, S. S.; and Riethof, T. R.: Radiance of Species in High Temperature Air. Space Sciences Laboratory, General Electric Co., R63SD3, June 1963.
13. Anderson, J. E.: Transpiration Cooling of a Constricted Electric-Arc Heater. Rep. AFARL 66-0157, Aerospace Res. Lab., Wright Patterson AFB, Ohio (Heat Transfer Lab., Univ. of Minnesota, AF contract no. AF 33(657)-7380), March 1966.

TABLE I.- SOURCES OF THERMODYNAMIC AND TRANSPORT PROPERTIES
FOR HYDROGEN AND NITROGEN

Property	Gas		
	Nitrogen		Hydrogen
$h(\text{J/kg})$	$0 - 7 \times 10^7$	$7 \times 10^7 - 23 \times 10^7$	$0 - 5.6 \times 10^9$
ρ	Ref. 9	Ref. 10	Ref. 10
k	Ref. 9	Ref. 10	↓
σ	Ref. 10	Ref. 10	
μ	Ref. 9	Ref. 11	
Radiation	Ref. 10	Ref. 10	

TABLE II. - SEVERAL INTERESTING PROPERTIES OF THE CONSTRICTED ARCS THAT ARE SHOWN PICTORIALY IN FIGURES

Figure	Gas	Constrictor diameter, cm	Current, amps	Flow rate at exit, g/s	Transpiration cooling mass flux, kg/sm ²	Inlet pressure, atm	Constrictor length, m	Percent radiation at exit	Mass average enthalpy at exit, J/kg, $\times 10^6$	Space average enthalpy at exit, J/kg, $\times 10^6$	Voltage gradient at exit, V/m	Wall heat transfer rate at exit, W/m ² , $\times 10^6$	Maximum wall heat transfer rate, W/m ² , $\times 10^6$	Length at maximum wall heat transfer rate, m	Computing time, min	Flow choked at exit
10	N ₂	1.270	896	4.804	0	1.700	0.209	75.51	0.546	0.773	1855	11.63	19.12	0.038	2.28	✓
11			693	2.159		.952	.231	17.66	.759	.880	1351	16.12	16.20	.224	2.71	✓
12			686	4.763		1.544	.233	70.93	.455	.648	1713	7.32	13.03	.039	2.89	✓
13			473	4.854		1.347	.254	67.27	.333	.501	1506	3.50	7.00	.013	---	✓
14			436	4.795		1.211	.219	79.93	.287	.460	1599	2.32	5.38	.013	3.12	✓
15		.635	240	.240		.504	.188	5.93	.677	.763	2260	26.10	26.10	.185	4.30	✓
16			210	.139		.337	.129	7.03	.604	.674	2090	21.80	21.80	.120	4.65	
17			210	.369		.565	.107	9.22	.561	.644	2230	17.40	17.40	.107	2.73	✓
18			183	.265		.470	.158	5.83	.546	.615	2020	18.10	18.10	.152	3.94	✓
19			180	.504		.710	.116	13.18	.468	.554	2140	11.60	11.60	.116	2.67	✓
20			150	.139		.278	.127	4.73	.486	.548	1910	14.20	14.20	.120	4.81	
28		1.270	1000	1.619		1.000	.223	13.29	1.195	1.268	1473	25.57	26.74	.204	2.92	✓
29		1.270	1000	1.619		1.000	.274	8.26	1.204	1.329	1492	25.62	31.69	.126	---	✓
30	H ₂	1.000	1000	.538	.15	1.000	.112	9.88	4.701	10.851	2370	11.00	12.50	.025	3.00	✓
31	H ₂	1.000	1000	.538	0	1.000	.106	7.00	5.320	12.407	2050	24.50	24.50	.106	1.82	✓
32	N ₂	1.270	580	3.760	.38	1.157	.222	65.59	.408	.575	1724	3.29	7.36	.067	1.86	✓
33	N ₂	1.270	580	3.529	0	1.157	.203	50.82	.462	.637	1505	5.30	7.17	.022	2.98	✓
34	N ₂	1.270	500	2.268		1.0	.683	14.10	.609	.718	1119	12.23	13.12	.467	2.34	✓
37	H ₂	.635	1000	2.270		4.0	.073	98.65	1.529	10.150	4760	12.40	24.50	.022	2.39	✓
38	N ₂	.635	1000	2.268		4.0	.058	80.71	.902	1.571	4408	40.89	80.65	.015	1.23	✓
39		1.270	1500	1.400		1.0	.243	12.51	1.833	2.439	1470	45.50	47.10	.190	2.65	✓
41		.635	500	2.270		4.0	.160	53.67	.721	.842	3140	45.10	48.80	.028	1.94	✓
42		.635	500	10.000		10.0	.284	99.19	.351	.766	6480	138.00	279.00	.012	1.89	✓
43		.635	1000	10.000		10.0	.144	99.82	.278	.480	4660	54.60	143.00	.006	1.74	✓
44		.635	250	10.000		11.0	.742	86.65	.279	.391	3260	21.50	110.00	.000	2.12	✓

LEGENDS FOR THE COLUMNS OF TABLE II

Figure number - figure in which the numerical solutions are shown pictorially at the end of this report.

Gas - type of gas used in the calculations (the gas properties used are shown in fig. 3).

Constrictor diameter - diameter of the constant area portion of the constrictor.

Current - the total arc current passed through the constrictor.

Flow rate at exit - the total gas flow passed through the constrictor (when no gas enters through the constrictor walls, this is equal to the gas flow rate at the inlet).

Transpiration cooling mass flux - the gas flow transpired through the constrictor walls.

Inlet pressure - pressure at the constrictor inlet.

Constrictor length - the length between the constrictor inlet and the constrictor exit.

Percent radiation at exit - the percentage of the wall heat flux at the constrictor exit that is due to the radiation heat losses.

Mass average enthalpy at exit - the energy flux at the constrictor exit divided by the flow rate (this is the average enthalpy obtained by subtracting the total heat losses from the total power input and dividing by the flow rate - normally called the first law enthalpy measurement).

Space average enthalpy at exit - $\frac{1}{A} \int_A h \, dA$ at the constrictor exit.

Voltage gradient at exit - the voltage gradient within the arc measured at the constrictor exit.

Wall heat transfer rate at exit - the heat transfer rate impinging on the constrictor wall at the exit.

Maximum wall heat transfer rate - the maximum heat transfer rate impingement on the constrictor wall.

Length at maximum wall heat transfer rate - the axial position at which the maximum wall heat transfer rate occurs.

Computing time - the computing time required on the IBM 7094 for this numerical calculation.

Flow choked at exit - a check in this column indicates that the flow is aerodynamically choked at the constrictor exit.

TABLE III.- THEORETICAL ESTIMATES OF THE PROPERTIES OF THE PLASMA PRODUCED BY A CONSTRICTED-ARC PLASMA GENERATOR FOR ONE SET OF OPERATING CONDITIONS

Plasma generator size	
Diameter of the constant area constrictor	0.00635 m
Length of the constant area constrictor	0.16 m
Diameter of the nozzle exit	0.0318 m
Operating conditions	
Current	500 A
Arc voltage	620 V
Mass flow rate (nitrogen)	0.00227 kg/s
Chamber pressure	4.05×10^5 N/m ² (4.0 atm)
Resulting maximum constrictor wall heat transfer rate . . .	4.8×10^7 W/m ²
Efficiency of constricted arc	53 percent
Plasma properties at the constrictor exit	
Center-line enthalpy	1.4×10^8 J/kg
Center-line energy flux density	8.7×10^9 W/m ²
Center-line velocity	4.2×10^3 m/s
Center-line temperature	16,000° K
Pressure	2.2×10^5 N/m ²
Center-line electron number density	3.5×10^{17} electrons/cm ³
Center-line degree of ionization	55 percent
Center-line electrical conductivity	7×10^3 1/Ω-m
Plasma properties at the nozzle exit	
Size of uniform stream (less than 10-percent variation)	0.01 m
Center-line total enthalpy	1.5×10^8 J/kg
Center-line energy flux density	3.5×10^8 W/m ²
Center-line velocity	9×10^3 m/s
Center-line density	1.2×10^{-4} kg/m ³
Center-line electrical conductivity (order of magnitude only)	4×10^3 1/Ω-m
Center-line Reynolds number per cm (order of magnitude only)	100
Center-line magnetic Reynolds number per cm (order of magnitude only)	0.5
Plasma properties in the stagnation region ahead of a blunt test body	
Enthalpy	1.5×10^8 J/kg
Temperature	14,500° K
Pressure	2×10^4 N/m ² (0.2 atm)
Electron number density	4×10^{16} electrons/cc
Degree of ionization	75 percent
Electrical conductivity	5×10^3 1/Ω-m

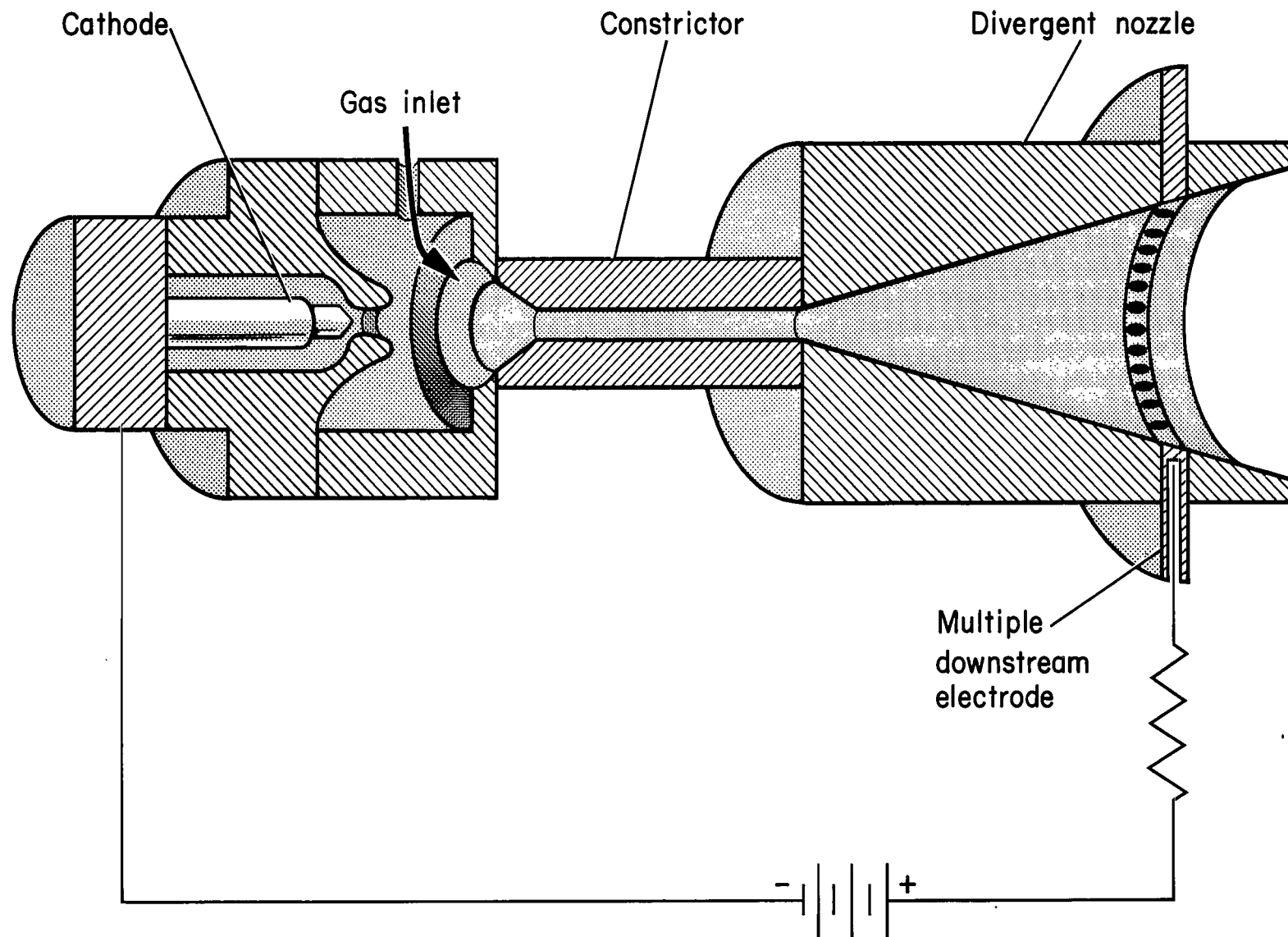
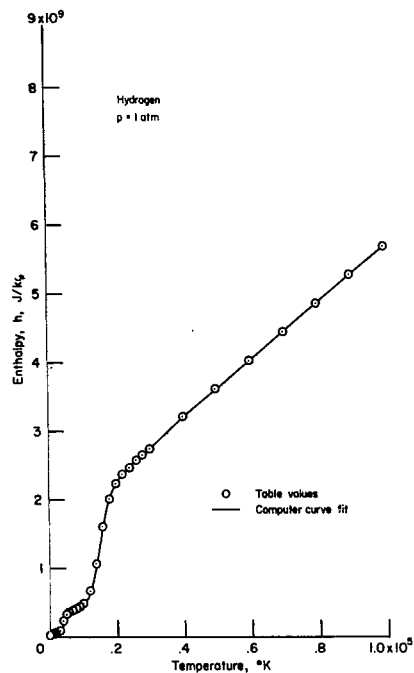
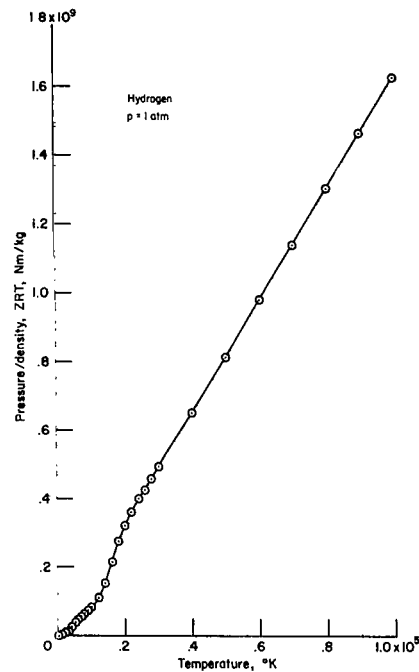


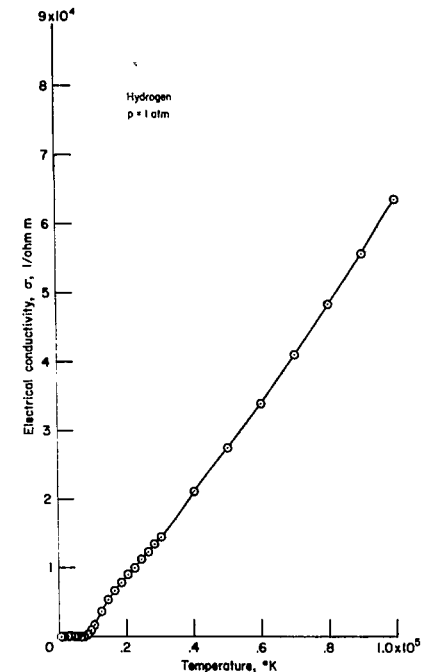
Figure 1.- The constricted-arc plasma generator.



(a) Hydrogen, $p = 1 \text{ atm}$,
enthalpy.

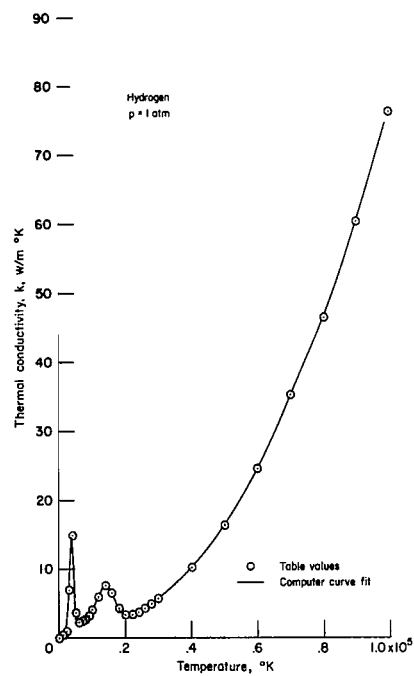


(b) Hydrogen, $p = 1 \text{ atm}$,
pressure/density.

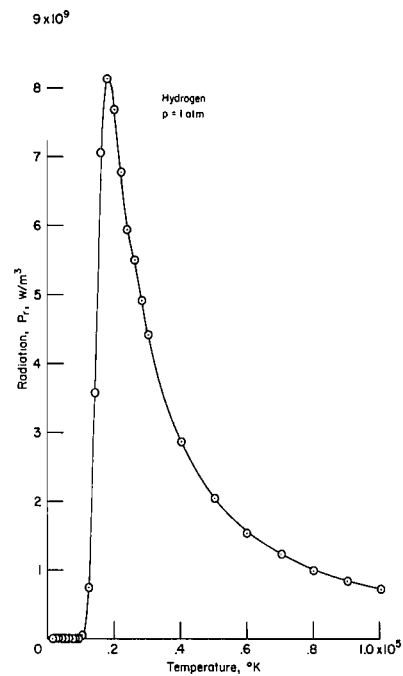


(c) Hydrogen, $p = 1 \text{ atm}$, elec-
trical conductivity.

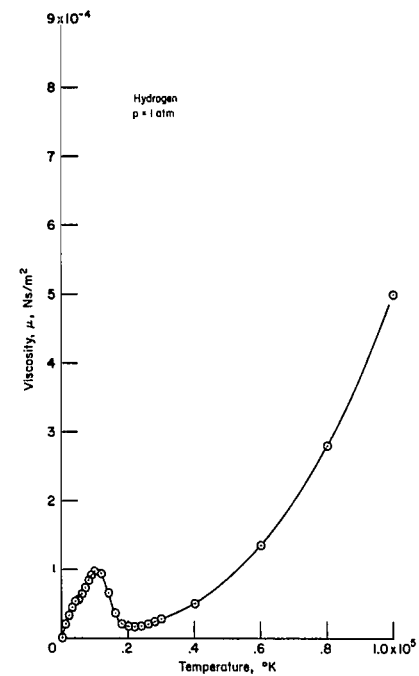
Figure 2.- Values of gas properties used to prepare tapes for the numerical calculations.



(d) Hydrogen, $p = 1 \text{ atm}$,
thermal conductivity.

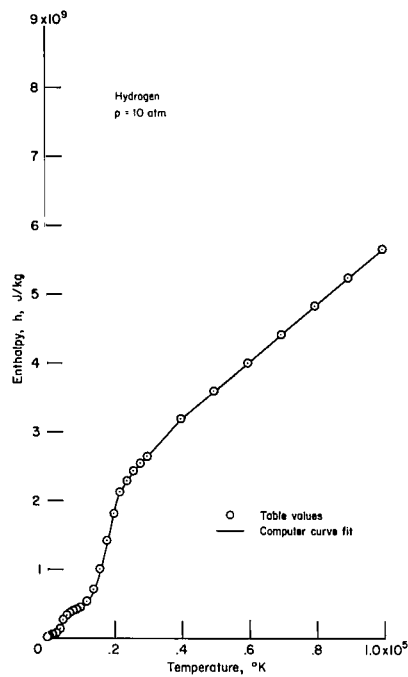


(e) Hydrogen, $p = 1 \text{ atm}$,
radiation.

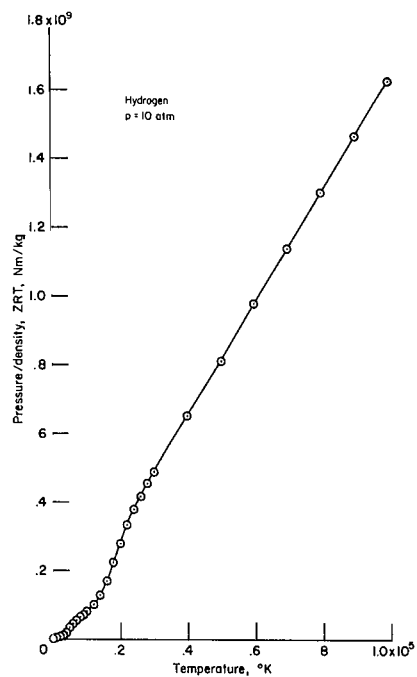


(f) Hydrogen, $p = 1 \text{ atm}$,
viscosity.

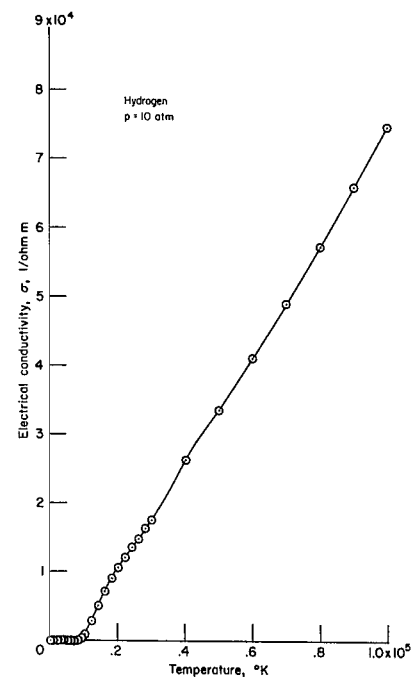
Figure 2.- Continued.



(g) Hydrogen, $p = 10 \text{ atm}$,
enthalpy.

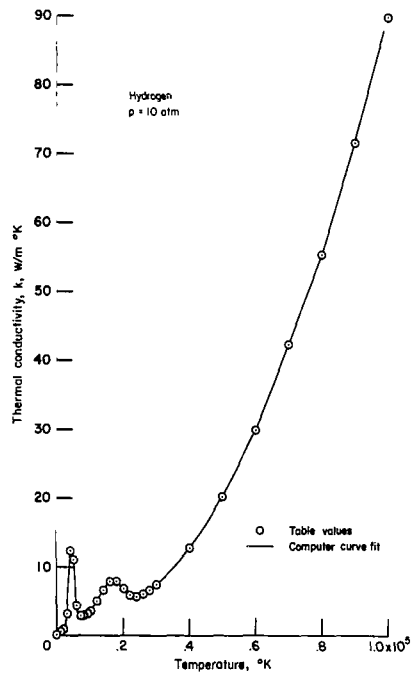


(h) Hydrogen, $p = 10 \text{ atm}$,
pressure/density.

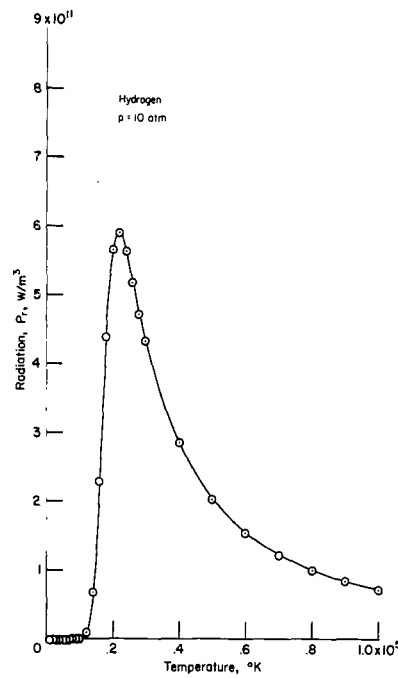


(i) Hydrogen, $p = 10 \text{ atm}$, elec-
trical conductivity.

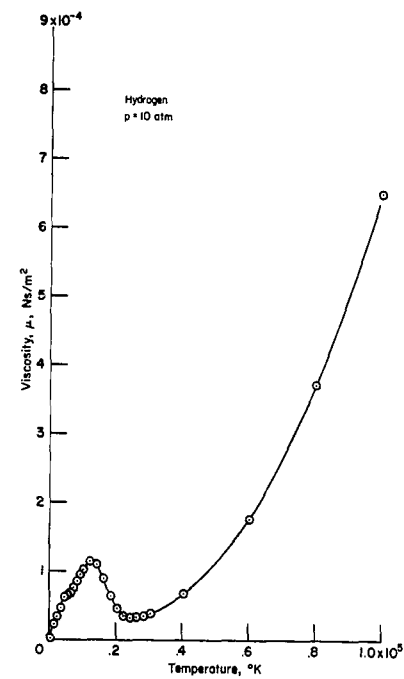
Figure 2.- Continued.



(j) Hydrogen, $p = 10 \text{ atm}$,
thermal conductivity.

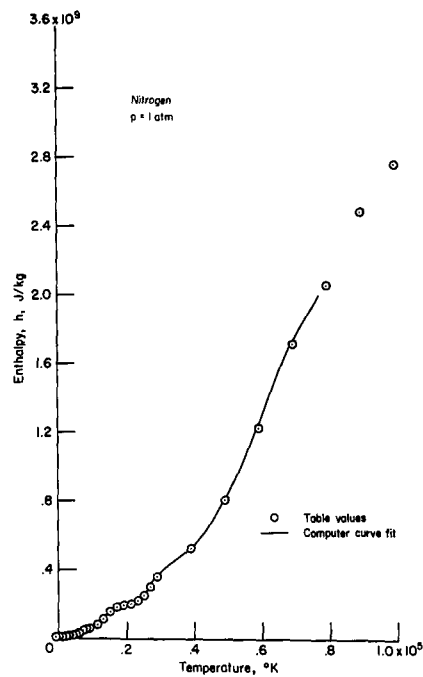


(k) Hydrogen, $p = 10 \text{ atm}$,
radiation.

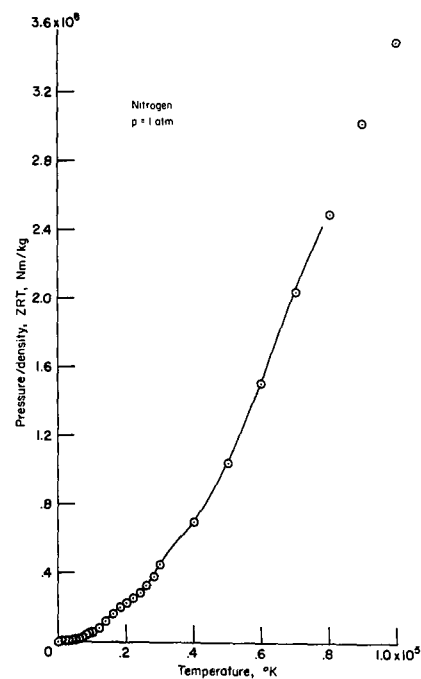


(l) Hydrogen, $p = 10 \text{ atm}$,
viscosity.

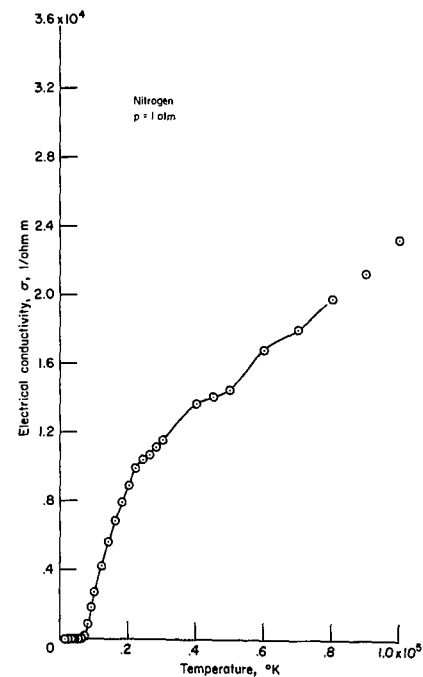
Figure 2.- Continued.



(m) Nitrogen, $p = 1$ atm, enthalpy.

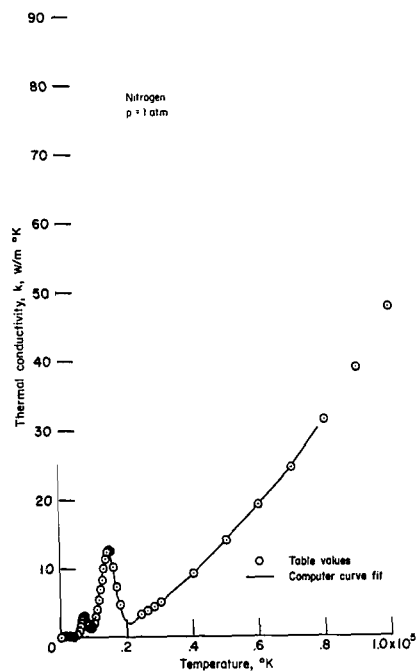


(n) Nitrogen, $p = 10$ atm, pressure/density.

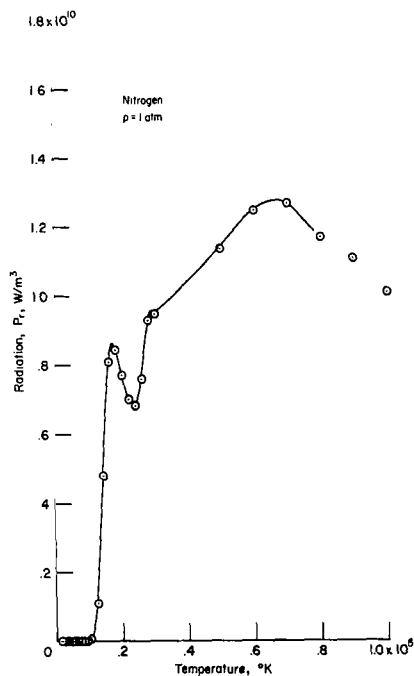


(o) Nitrogen, $p = 1$ atm, electrical conductivity.

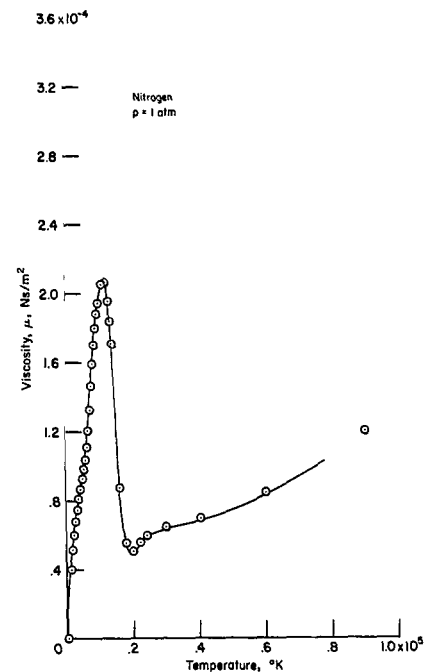
Figure 2.- Continued.



(p) Nitrogen, $p = 1$ atm,
thermal conductivity.

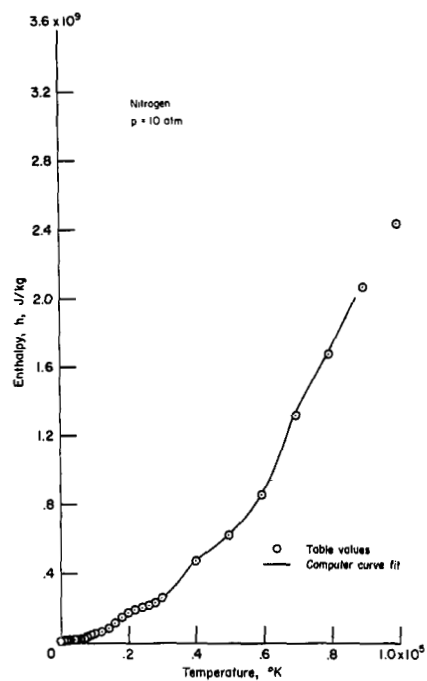


(q) Nitrogen, $p = 1$ atm,
radiation.

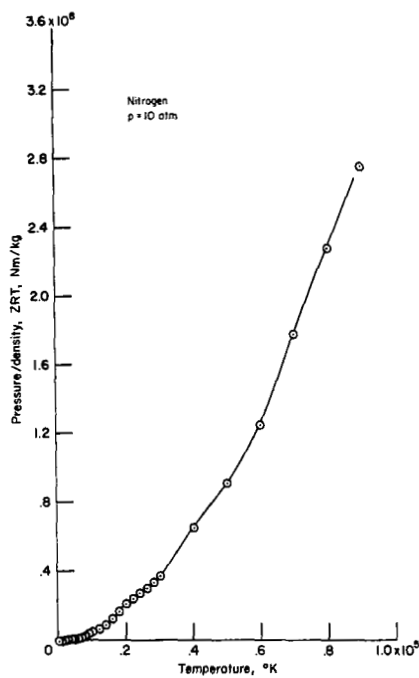


(r) Nitrogen, $p = 1$ atm,
viscosity.

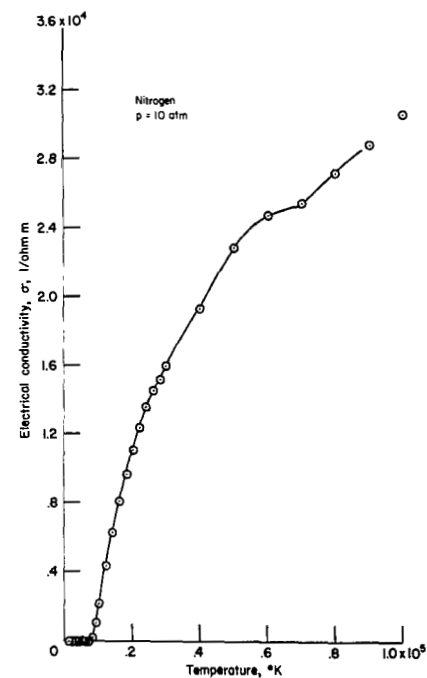
Figure 2.- Continued.



(s) Nitrogen, $p = 10 \text{ atm}$,
enthalpy.

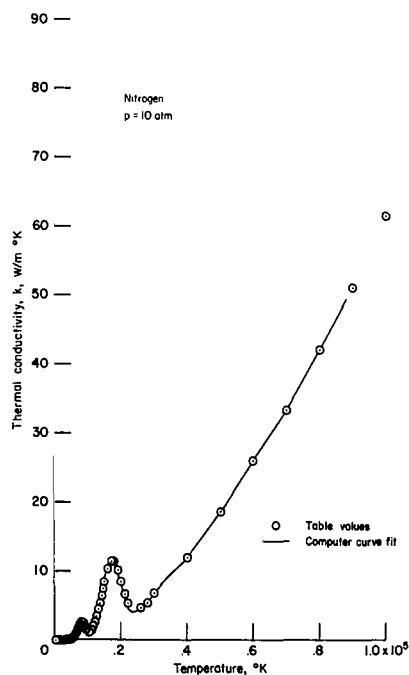


(t) Nitrogen, $p = 10 \text{ atm}$,
pressure/density.

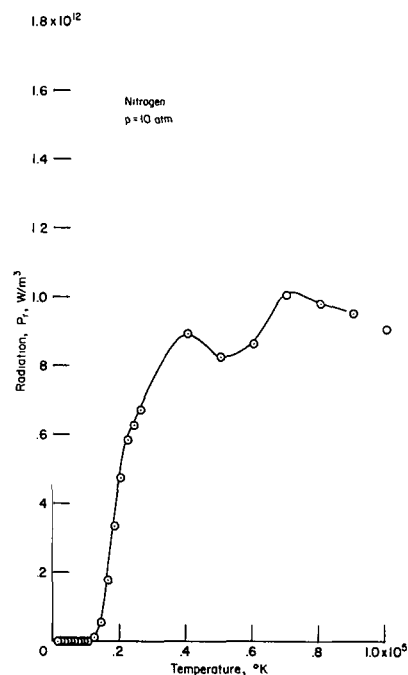


(u) Nitrogen, $p = 10 \text{ atm}$, elec-
trical conductivity.

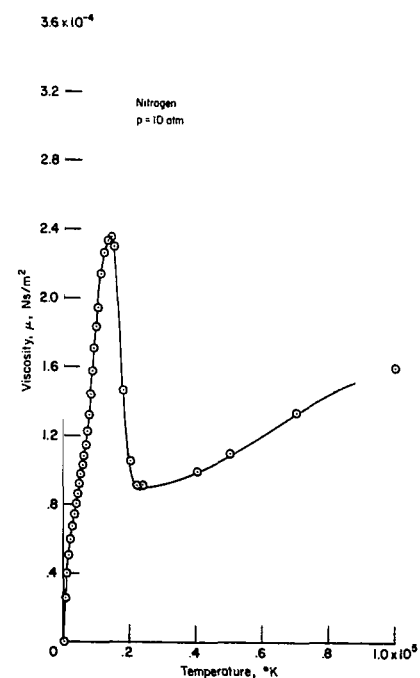
Figure 2.- Continued.



(v) Nitrogen, $p = 10$ atm, thermal conductivity.

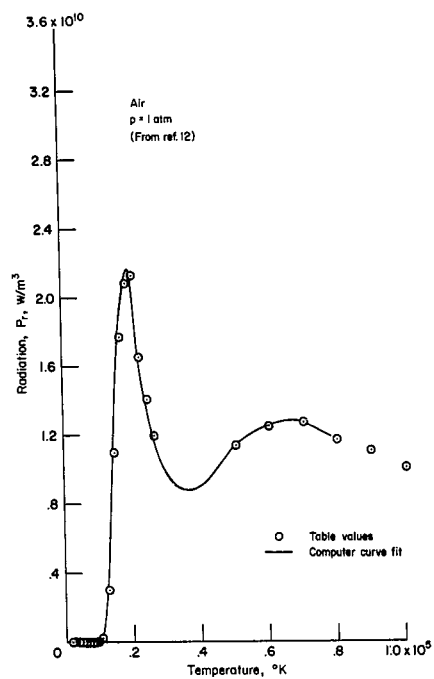


(w) Nitrogen, $p = 10$ atm, radiation.

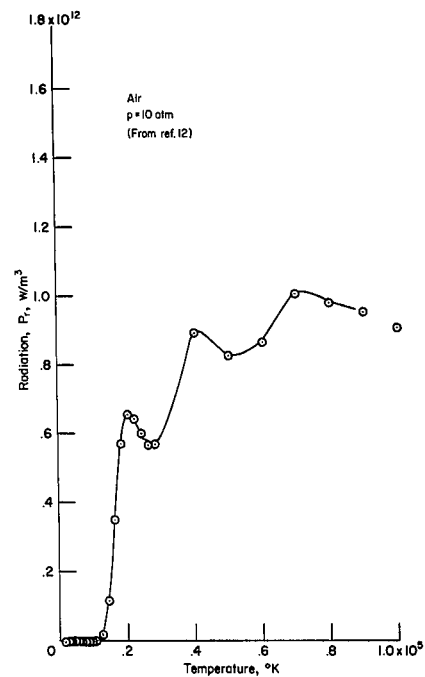


(x) Nitrogen, $p = 1$ atm, viscosity.

Figure 2.- Continued.



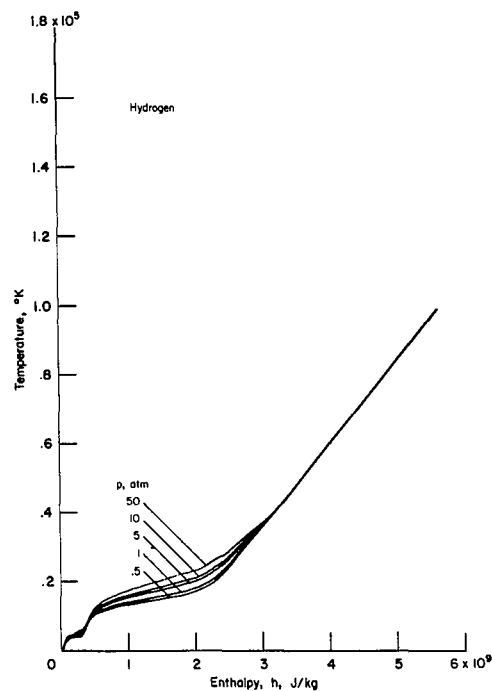
(y) Air, $p = 1 \text{ atm}$,
radiation.



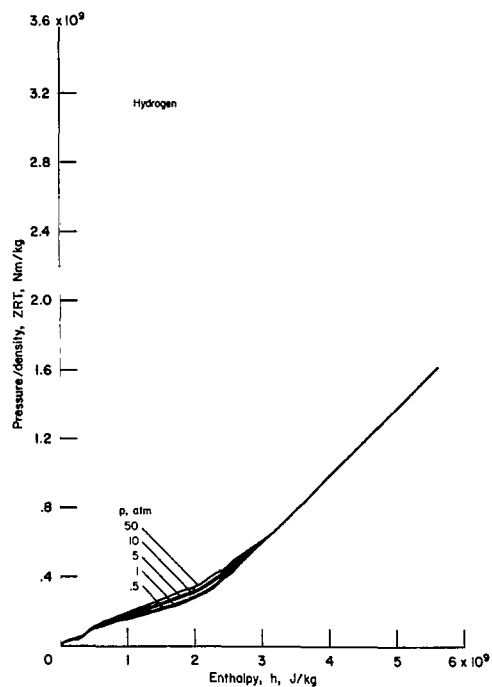
(z) Air, $p = 10 \text{ atm}$,
radiation.

Figure 2.- Concluded.

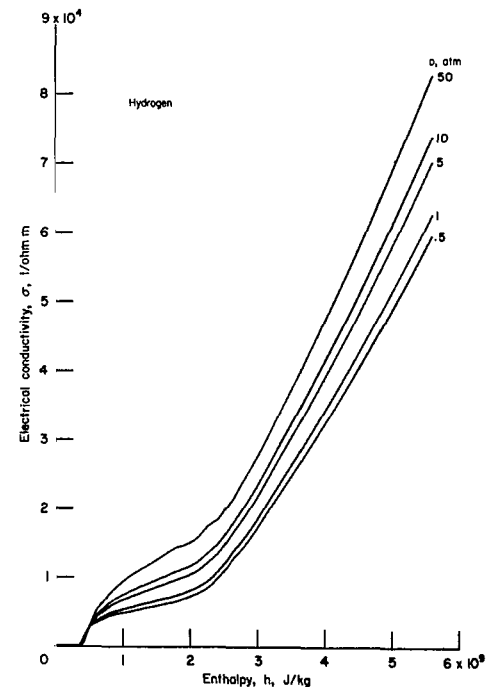




(a) Hydrogen, temperature.

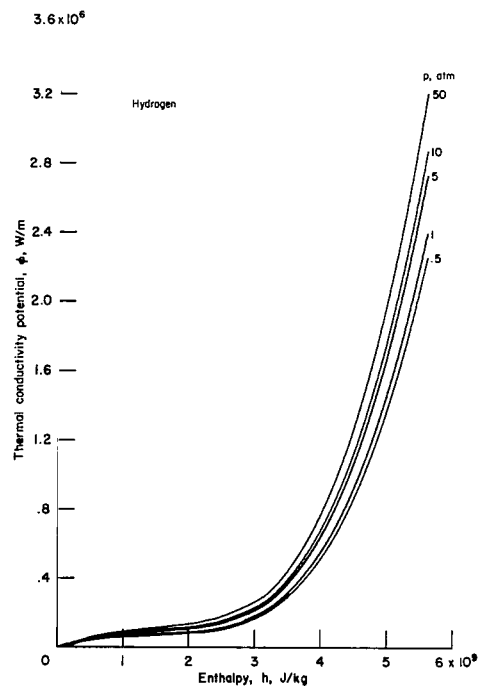


(b) Hydrogen, pressure/density.

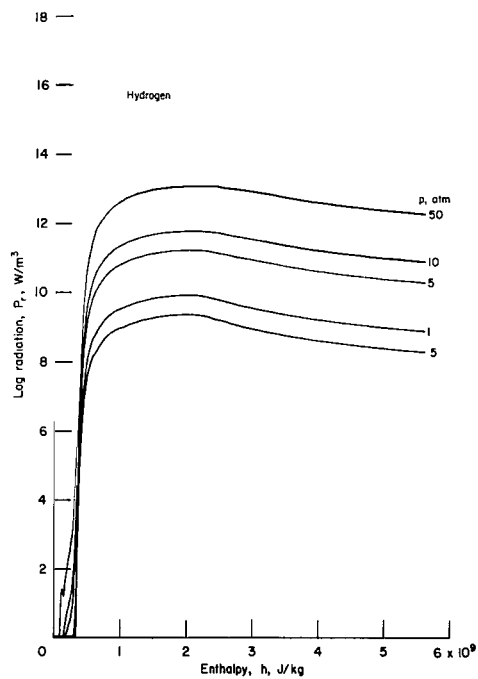


(c) Hydrogen, electrical conductivity.

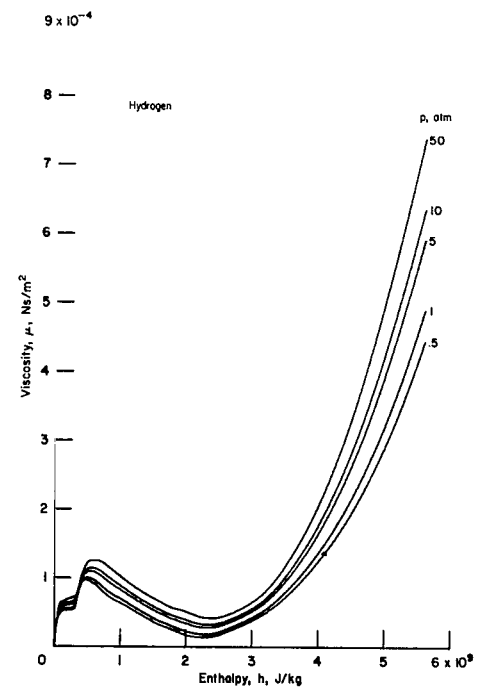
Figure 3.- Values of gas properties generated from the prepared tapes by the machine programs for the numerical calculations.



(d) Hydrogen, thermal conductivity.

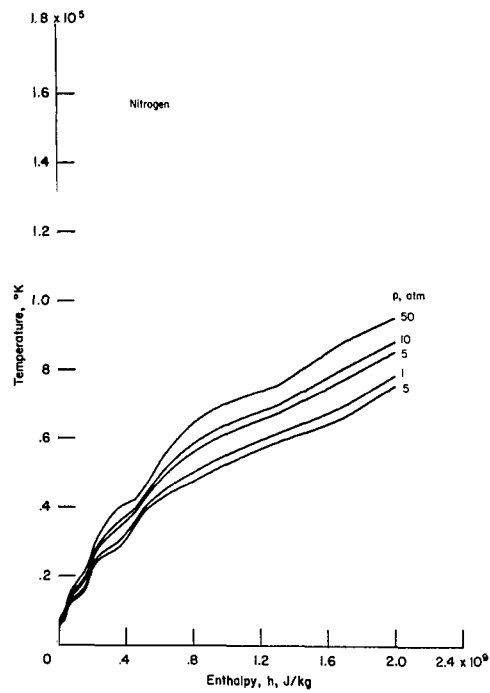


(e) Hydrogen, radiation.

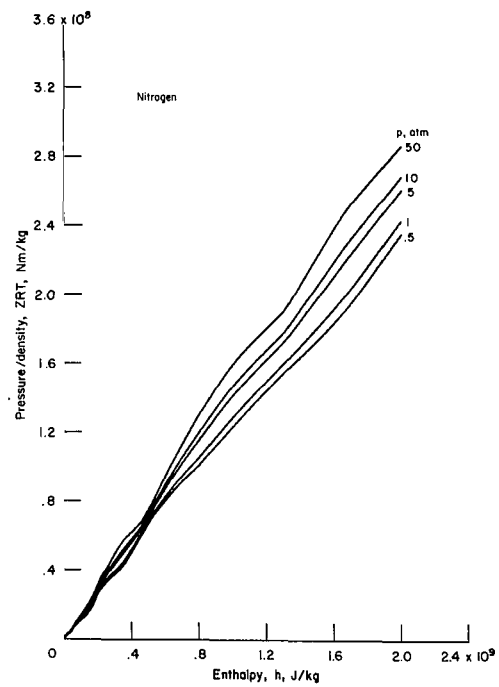


(f) Hydrogen, viscosity.

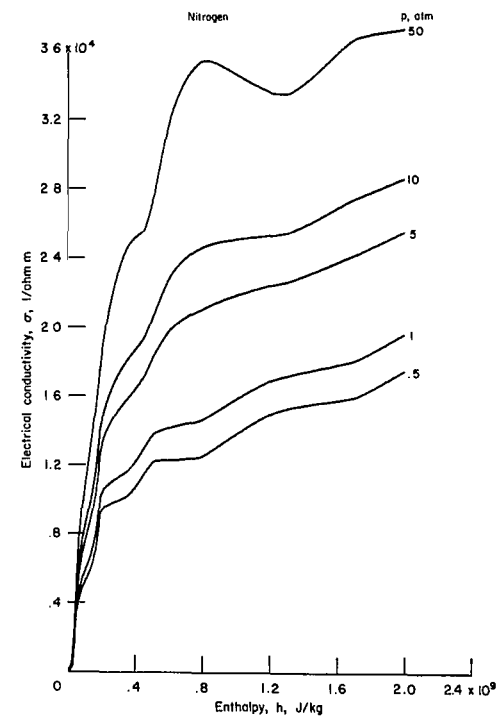
Figure 3.- Continued.



(g) Nitrogen, temperature.

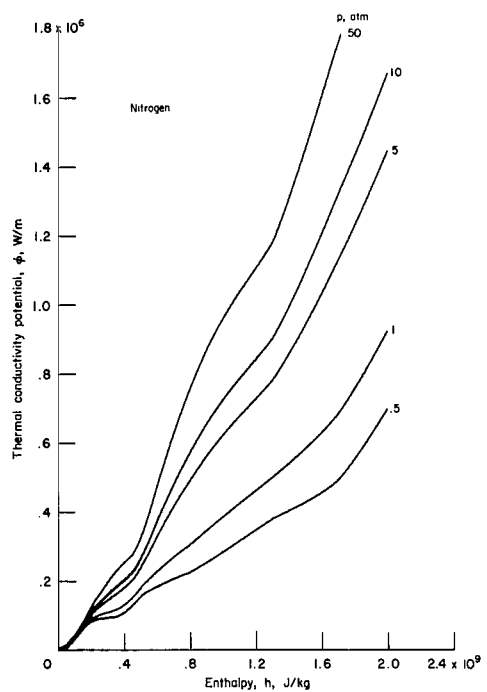


(h) Nitrogen, pressure/density.

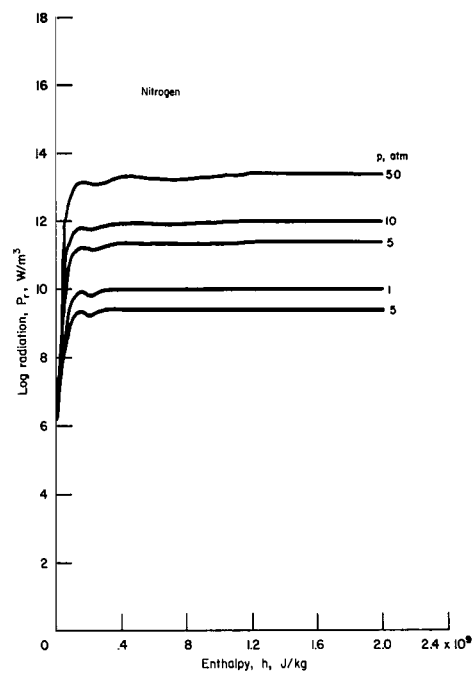


(i) Nitrogen, electrical conductivity.

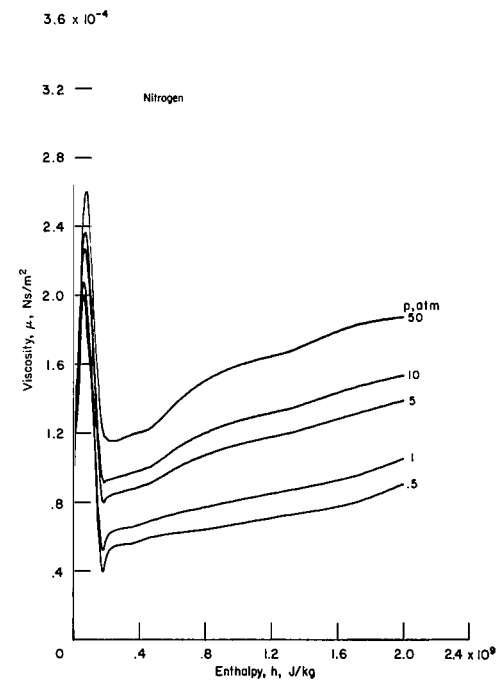
Figure 3.- Continued.



(j) Nitrogen, thermal conductivity.

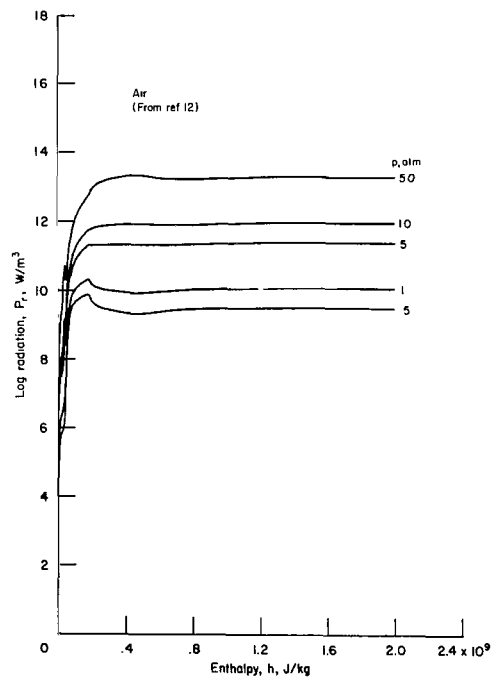


(k) Nitrogen, radiation.



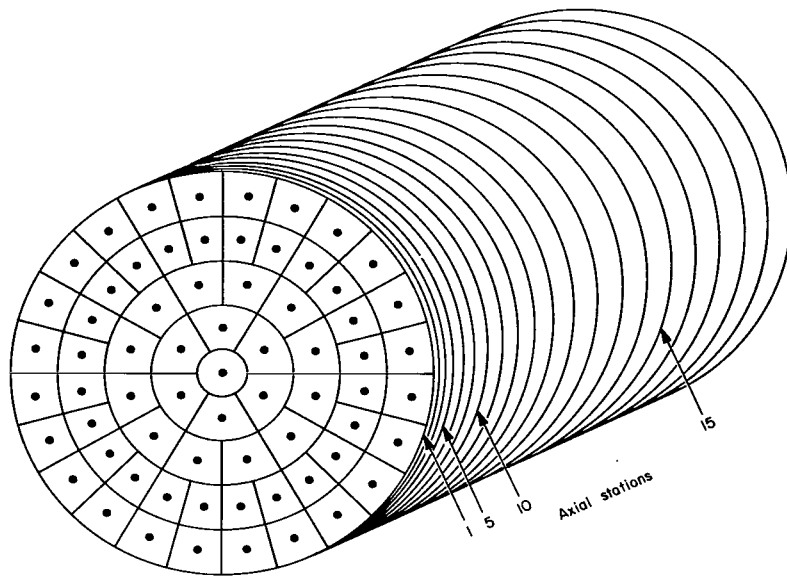
(l) Nitrogen, viscosity.

Figure 3.- Continued.

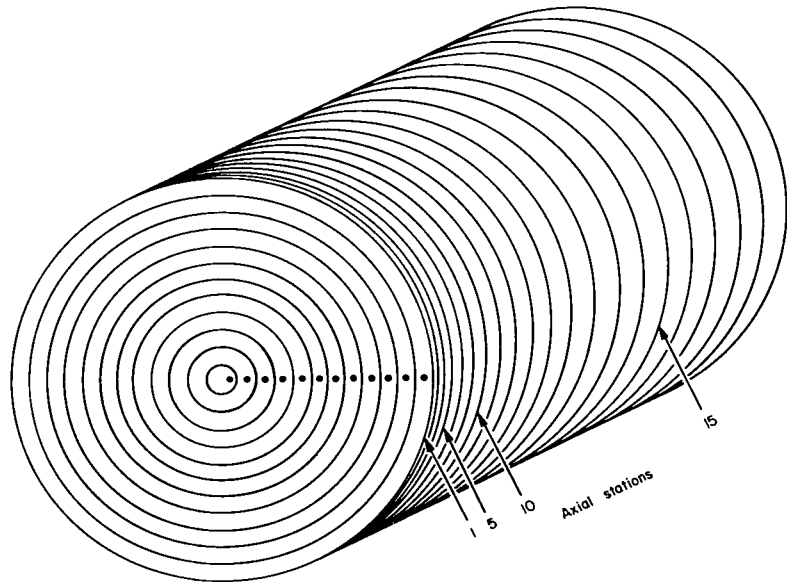


(m) Air, radiation.

Figure 3.- Concluded.

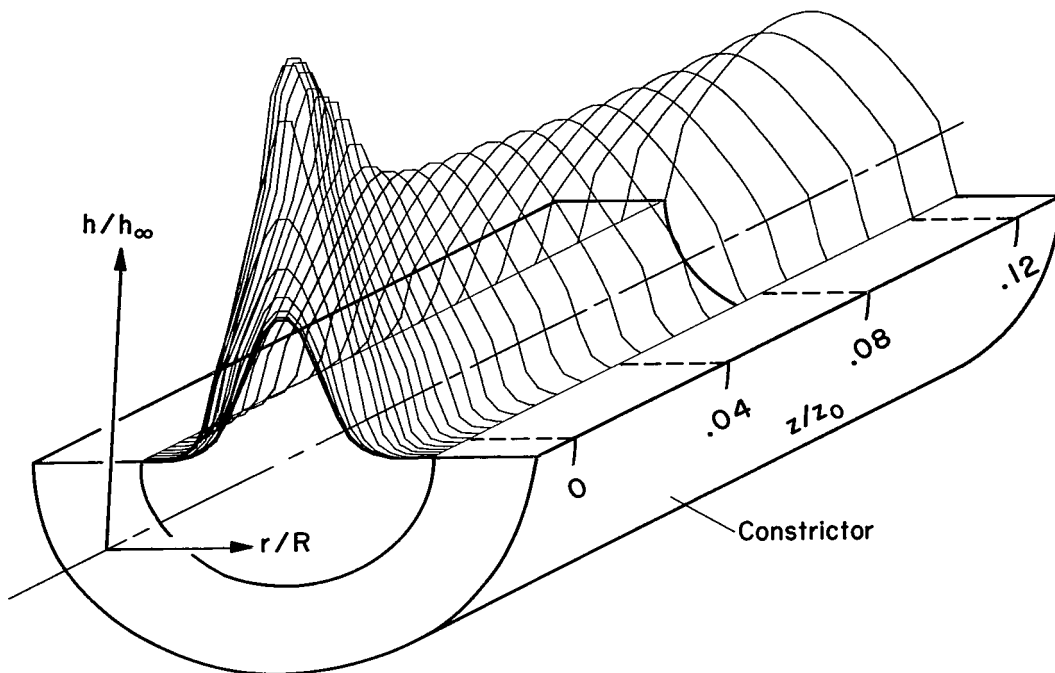


(a) Asymmetric constricted arc.

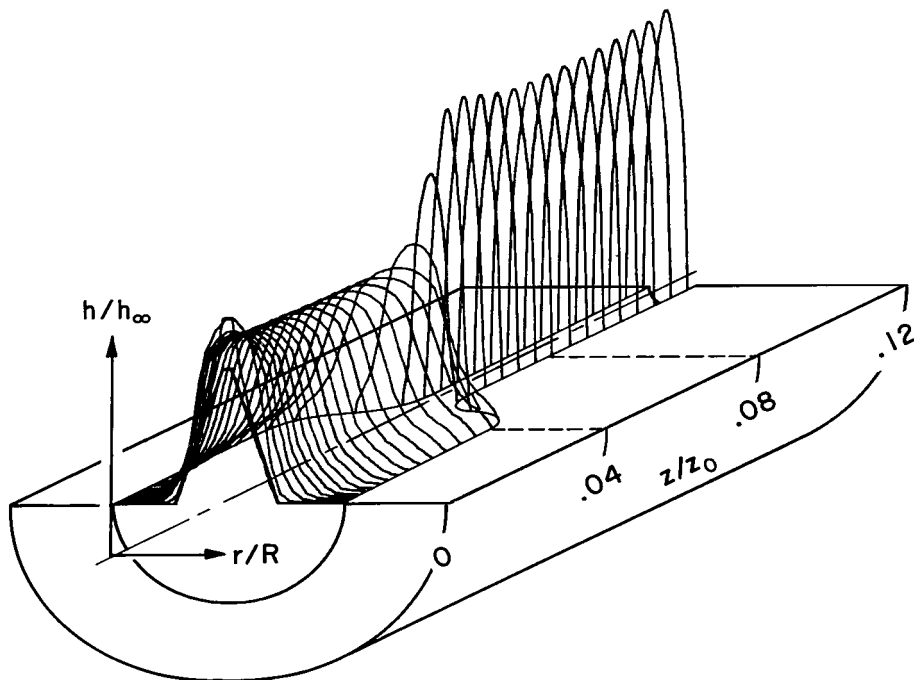


(b) Symmetric constricted arc.

Figure 4.- Mesh configuration for finite difference representation.

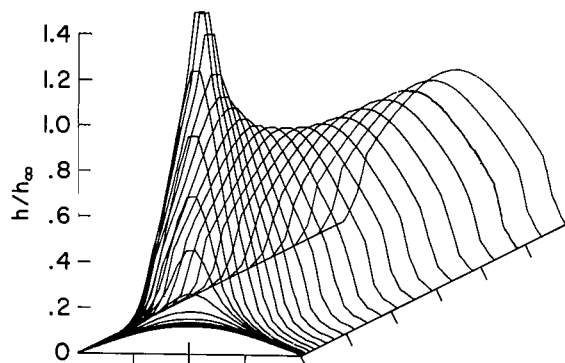


(a) Constant area constricter.

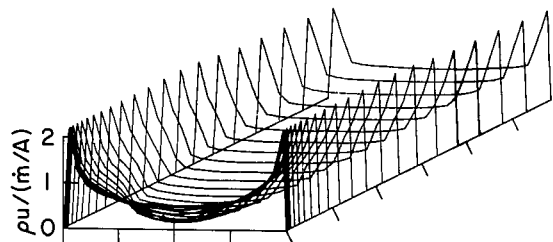


(b) Flared inlet constricter.

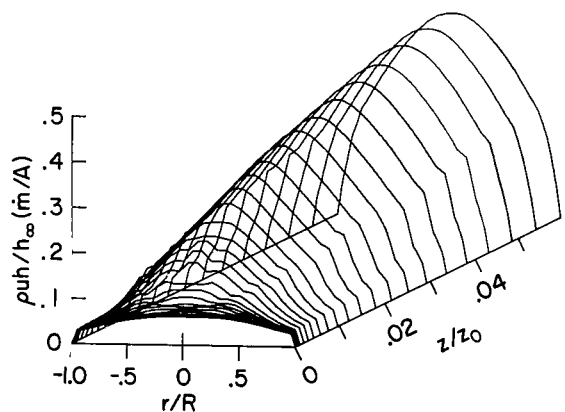
Figure 5.- Pictorial representation of the numerical solutions for the symmetric constricted arc.



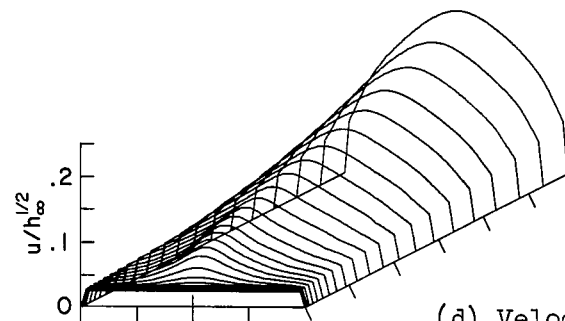
(a) Enthalpy.



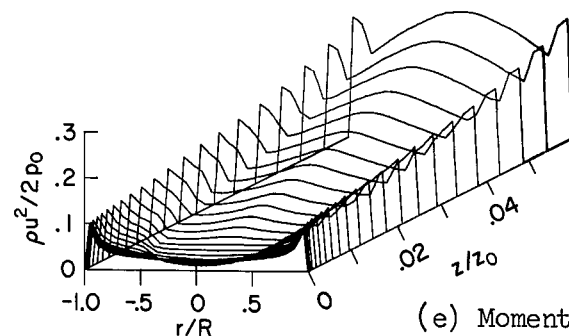
(b) Mass flow.



(c) Energy flux density.



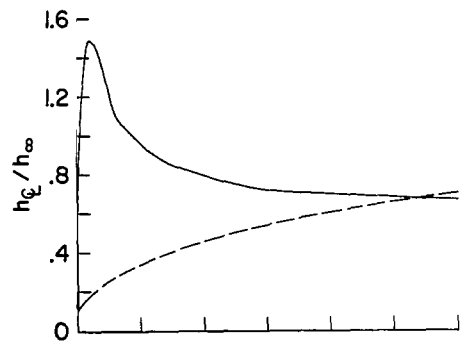
(d) Velocity.



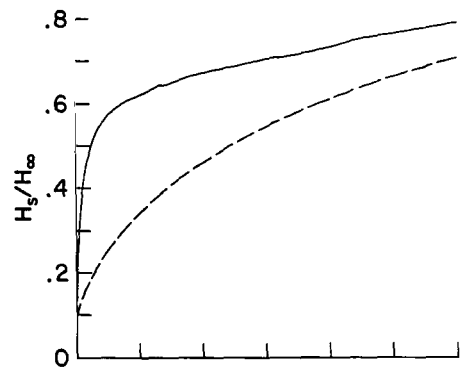
(e) Momentum flux.

$I = 580$	A	$h_\infty = 1.89 \times 10^8$	J/kg
$\dot{m} = .00353$	kg/s	$\dot{m}/A = 27.8$	kg/sm ²
$R = .00635$	m	$h_\infty \dot{m}/A = 5.29 \times 10^9$	W/m ²
$z_0 = 3.50$	m	$\sqrt{h_\infty} = 1.37 \times 10^4$	m/s
		$p_0 = 1.17 \times 10^5$	N/m ² (1.16 atm)
		$H_\infty = 8.17 \times 10^7$	J/kg
		$E_\infty = 819$	V/m
		$q_\infty = 1.19 \times 10^7$	W/m ²

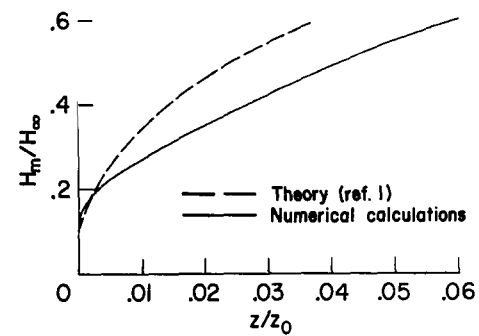
Figure 6.- Parabolic enthalpy and uniform velocity inlet distributions.



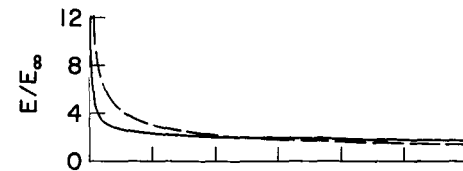
(f) Center-line enthalpy.



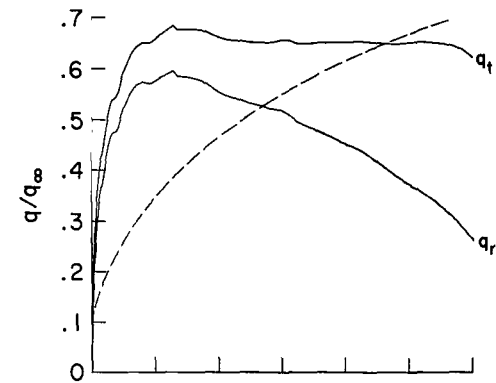
(g) Space-average enthalpy.



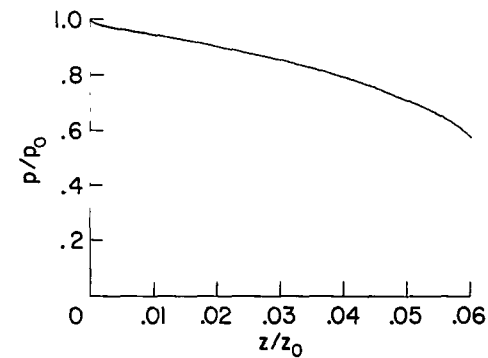
(h) Mass-average enthalpy.



(i) Voltage gradient.

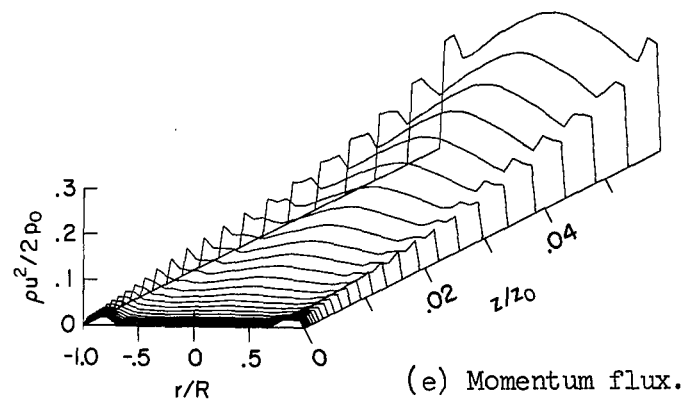
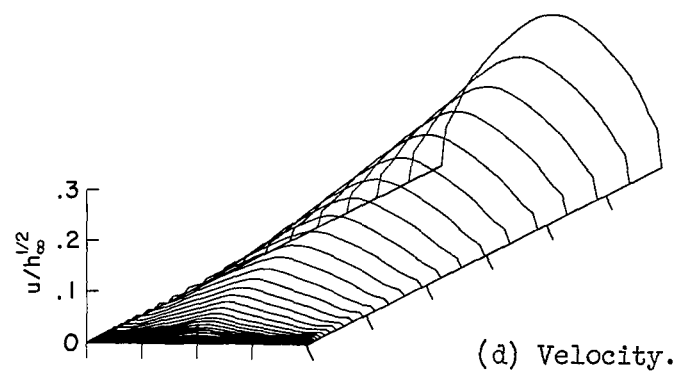
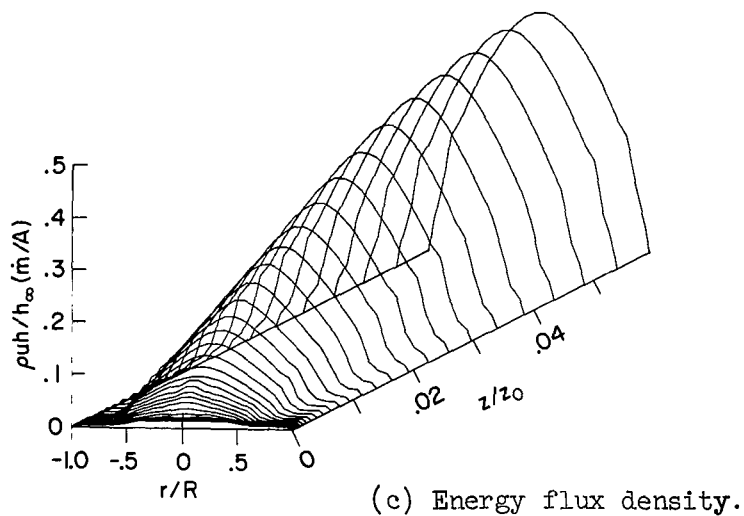
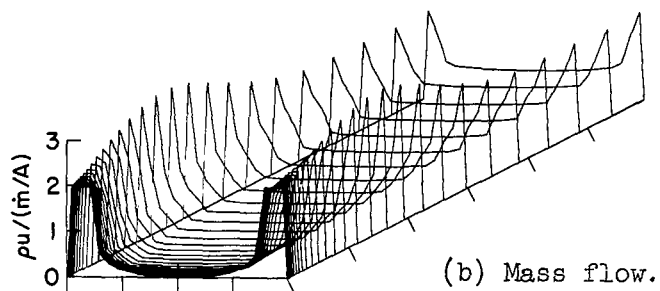
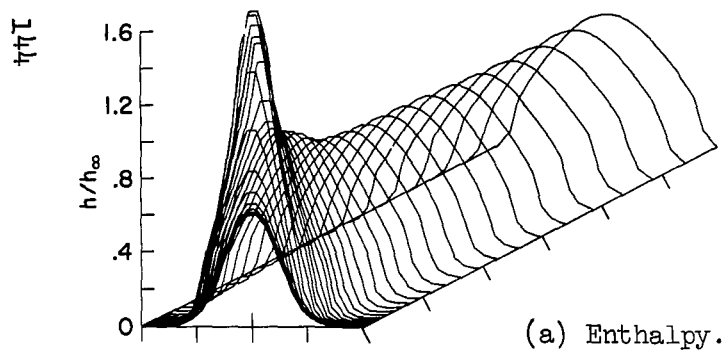


(j) Local heat transfer rate.



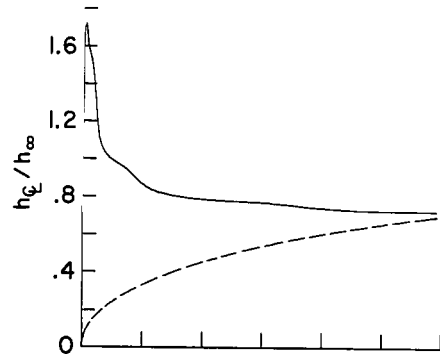
(k) Pressure.

Figure 6.- Concluded.

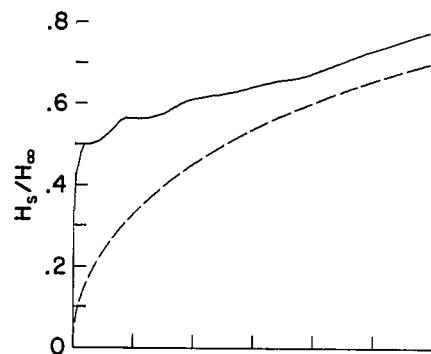


$I = 580$	A	$h_\infty = 1.89 \times 10^8$	J/kg
$\dot{m} = .00353$	kg/s	$\dot{m}/A = 27.8$	kg/sm ²
$R = .00635$	m	$h_\infty \dot{m}/A = 5.29 \times 10^9$	W/m ²
$z_0 = 3.50$	m	$\sqrt{h_\infty} = 1.37 \times 10^4$	m/s
		$p_0 = 1.17 \times 10^5$	N/m ² (1.16 atm)
		$H_\infty = 8.17 \times 10^7$	J/kg
		$E_\infty = 819$	V/m
		$q_\infty = 1.19 \times 10^7$	W/m ²

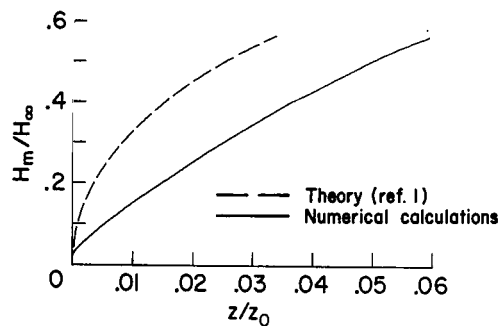
Figure 7.- Peaked enthalpy and uniform velocity inlet distributions.



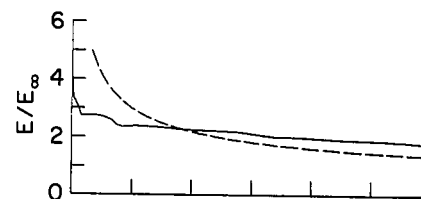
(f) Center-line enthalpy.



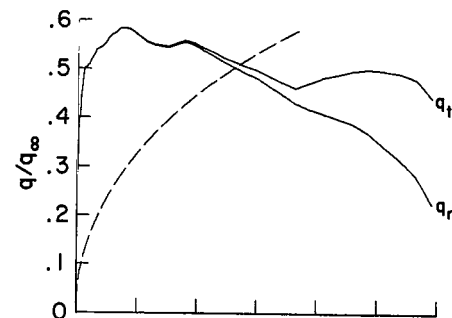
(g) Space-average enthalpy.



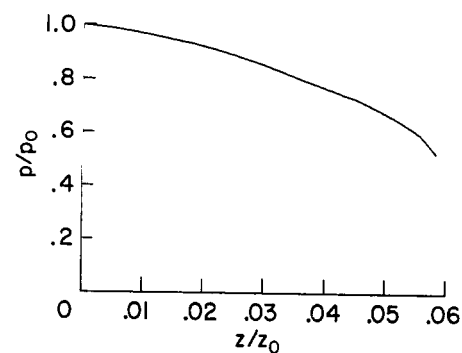
(h) Mass-average enthalpy.



(i) Voltage gradient.

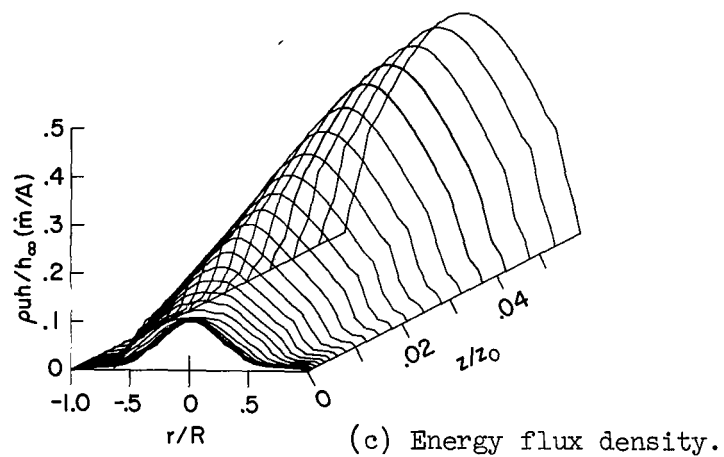
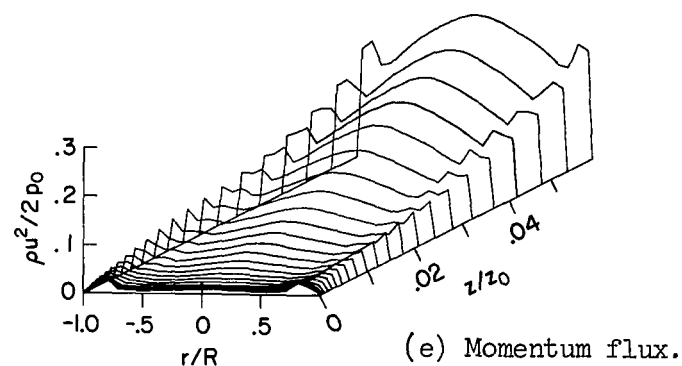
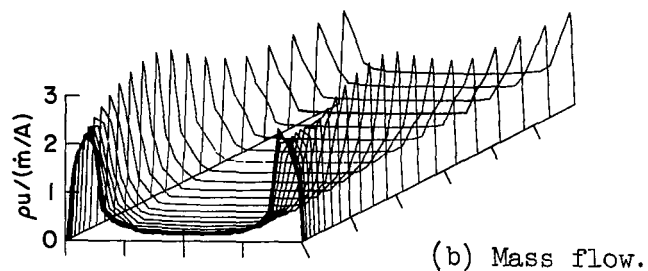
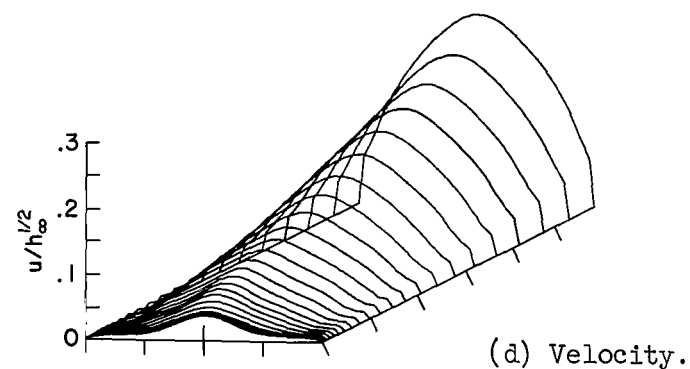
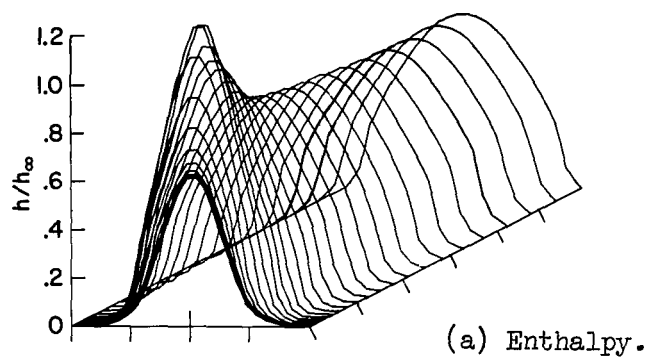


(j) Local heat transfer rate.



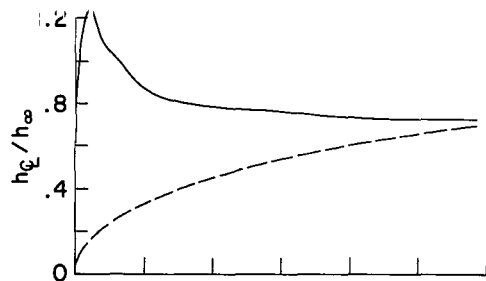
(k) Pressure.

Figure 7.- Concluded.

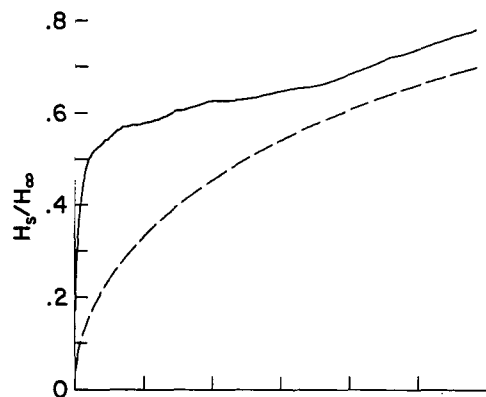


$I = 580$	A	$h_\infty = 1.89 \times 10^8$	J/kg
$\dot{m} = .00353$	kg/s	$\dot{m}/A = 27.8$	kg/sm ²
$R = .00635$	m	$h_\infty \dot{m}/A = 5.29 \times 10^9$	W/m ²
$z_0 = 3.50$	m	$\sqrt{h_\infty} = 1.37 \times 10^4$	m/s
		$p_0 = 1.17 \times 10^5$	N/m ² (1.16 atm)
		$H_\infty = 8.17 \times 10^7$	J/kg
		$E_\infty = 819$	V/m
		$q_\infty = 1.19 \times 10^7$	W/m ²

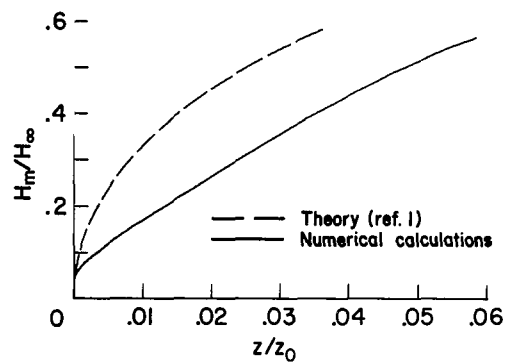
Figure 8.- Peaked enthalpy and velocity inlet distributions.



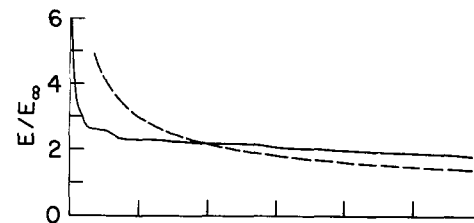
(f) Center-line enthalpy.



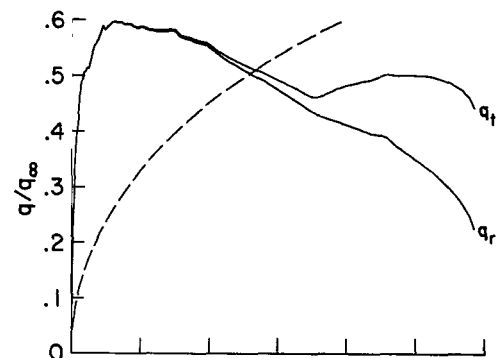
(g) Space-average enthalpy.



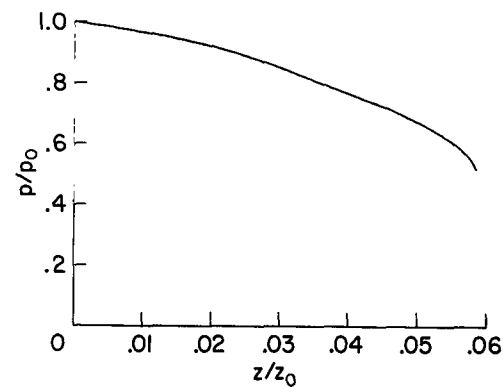
(h) Mass-average enthalpy.



(i) Voltage gradient.

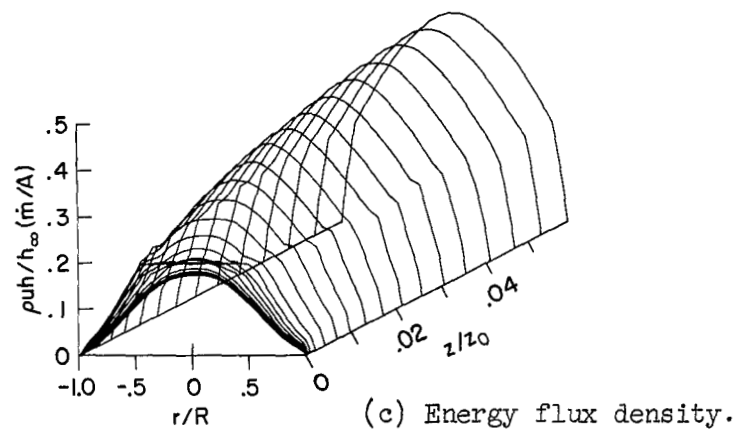
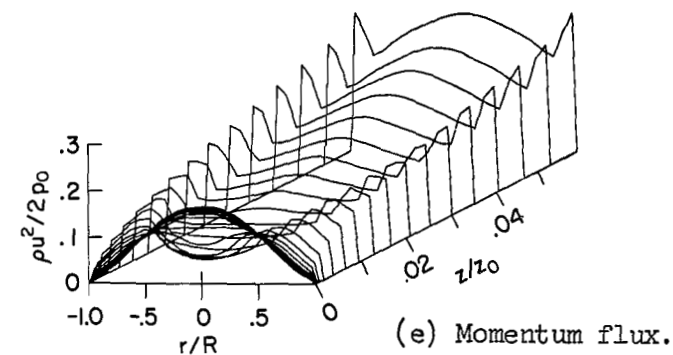
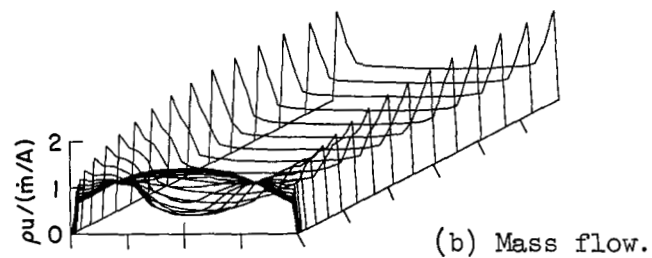
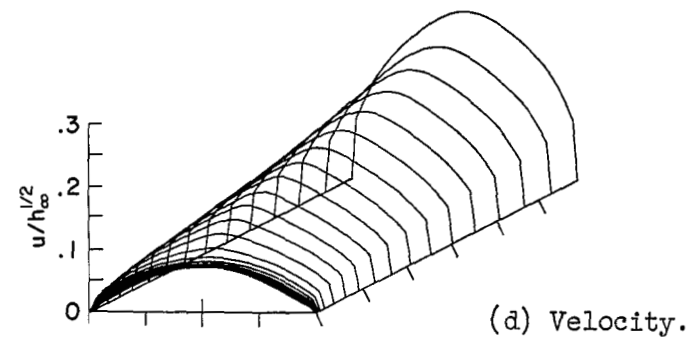
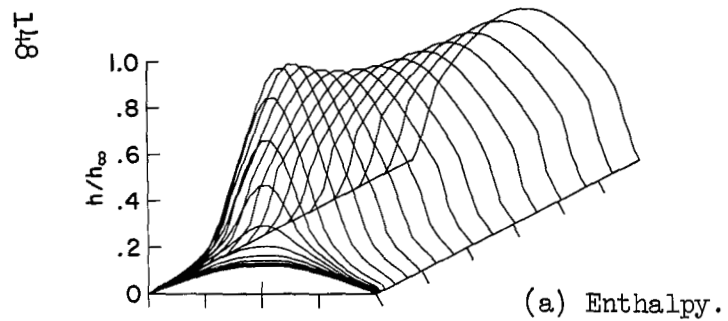


(j) Local heat transfer rate.



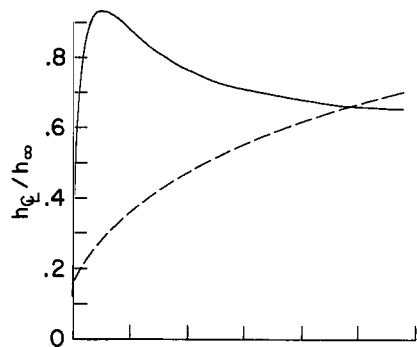
(k) Pressure.

Figure 8.- Concluded.

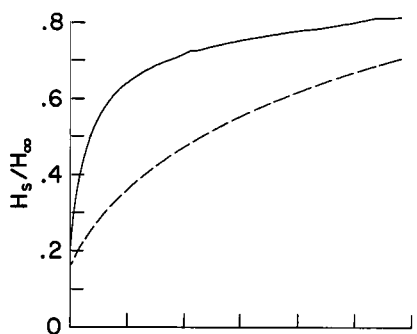


$I = 580$	A	$h_{\infty} = 1.89 \times 10^8$	J/kg
$\dot{m} = .00353$	kg/s	$\dot{m}/A = 27.8$	kg/sm ²
$R = .00635$	m	$h_{\infty} \dot{m}/A = 5.29 \times 10^9$	W/m ²
$z_0 = 3.50$	m	$\sqrt{h_{\infty}} = 1.37 \times 10^4$	m/s
		$p_0 = 1.17 \times 10^5$	N/m ² (1.16 atm)
		$H_{\infty} = 8.17 \times 10^7$	J/kg
		$E_{\infty} = 819$	V/m
		$q_{\infty} = 1.19 \times 10^7$	W/m ²

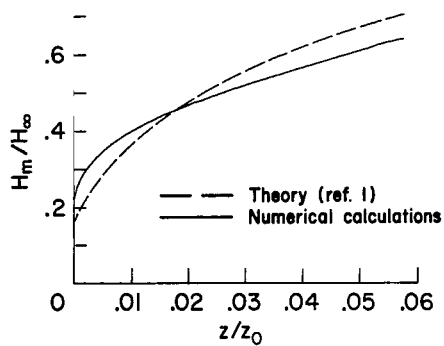
Figure 9.- Parabolic enthalpy and velocity inlet distributions.



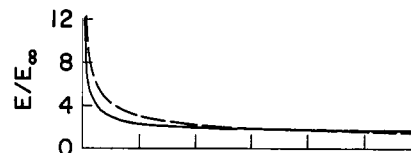
(f) Center-line enthalpy.



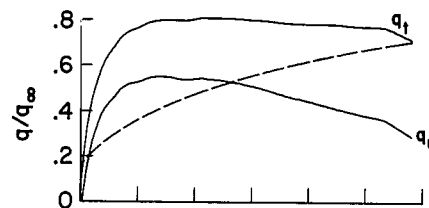
(g) Space-average enthalpy.



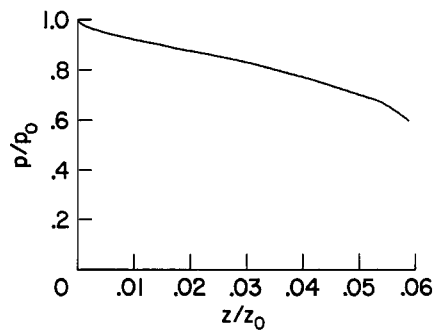
(h) Mass-average enthalpy.



(i) Voltage gradient.

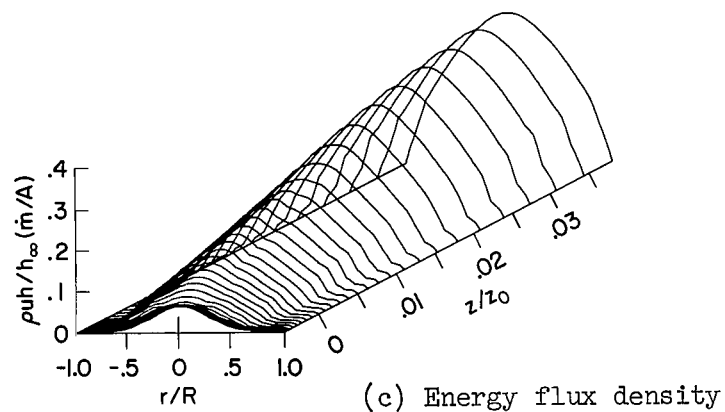
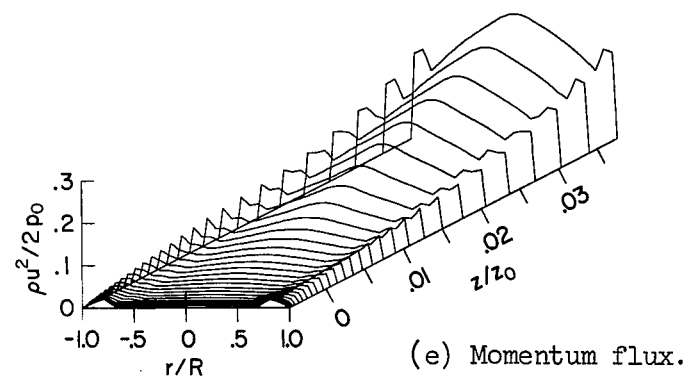
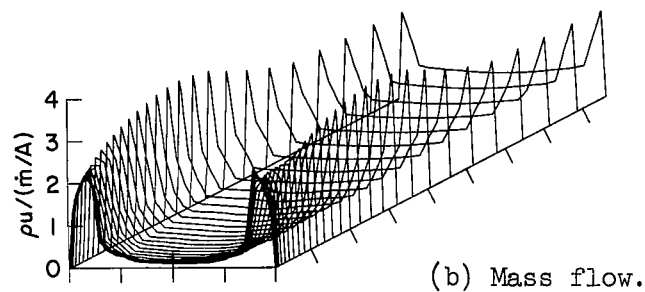
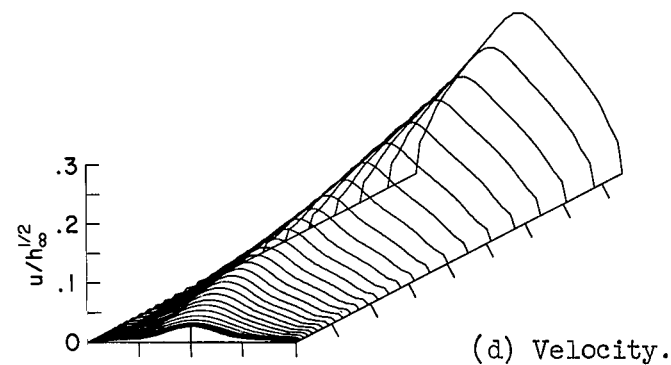
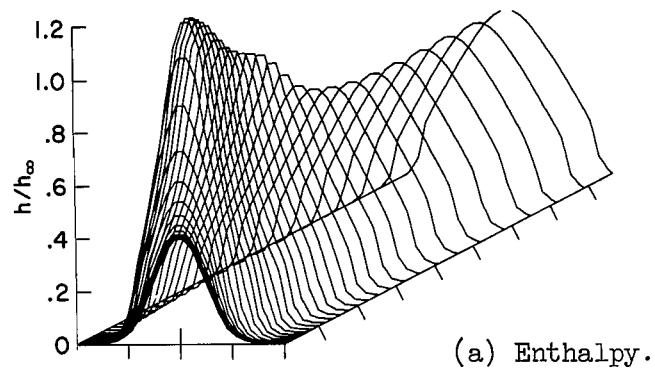


(j) Local heat transfer rate.



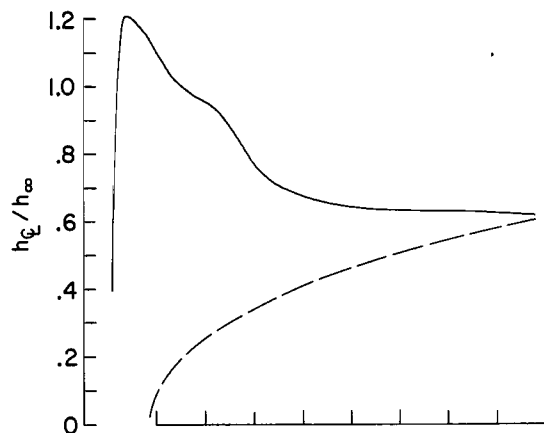
(k) Pressure.

Figure 9.- Concluded.

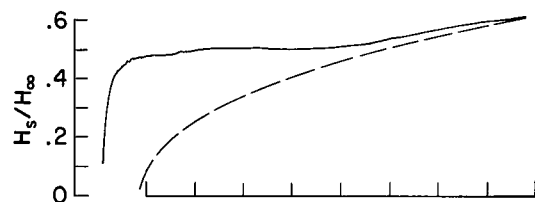


$I = 896$	A	$h_\infty = 2.91 \times 10^8$	J/kg
$\dot{m} = .00480$	kg/s	$\dot{m}/A = 37.9$	kg/sm ²
$R = .00635$	m	$h_\infty \dot{m}/A = 1.10 \times 10^{10}$	W/m ²
$z_0 = 4.76$	m	$\sqrt{h_\infty} = 1.71 \times 10^4$	m/s
		$p_0 = 1.72 \times 10^5$	N/m ² (1.70 atm)
		$H_\infty = 1.26 \times 10^8$	J/kg
		$E_\infty = 819$	V/m
		$q_\infty = 1.84 \times 10^7$	W/m ²

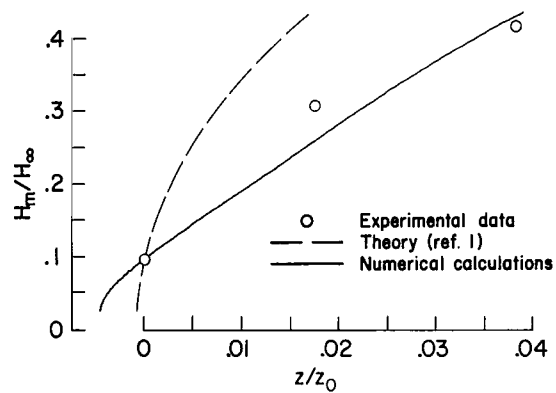
Figure 10.- Comparison of numerical solutions with experimental measurements; 1.27-cm-diameter constrictor; $I = 896$ A, $\dot{m} = 4.80$ g/s.



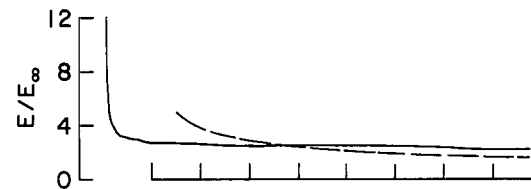
(f) Center-line enthalpy.



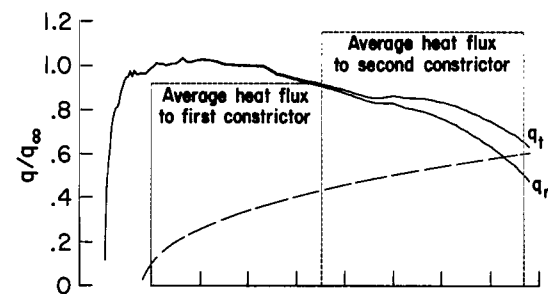
(g) Space-average enthalpy.



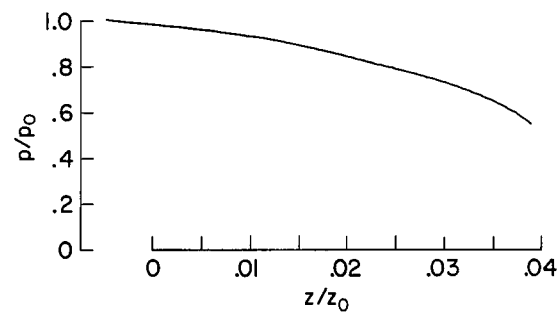
(h) Mass-average enthalpy.



(i) Voltage gradient.

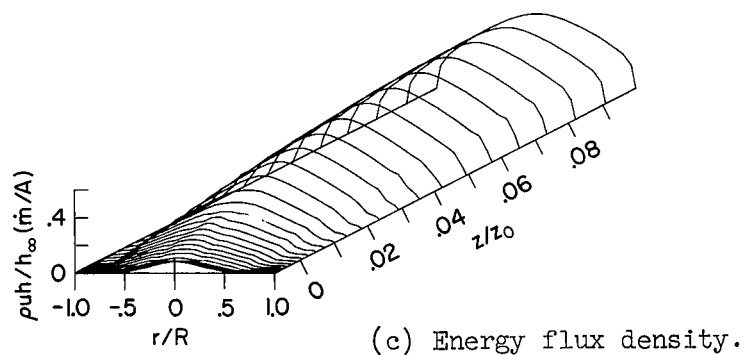
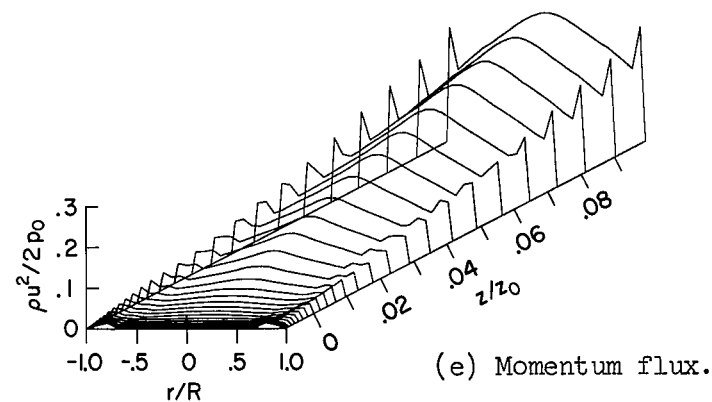
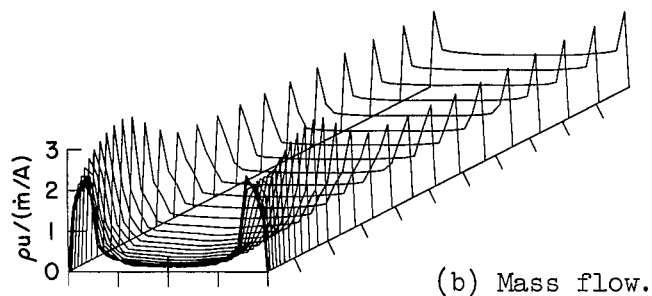
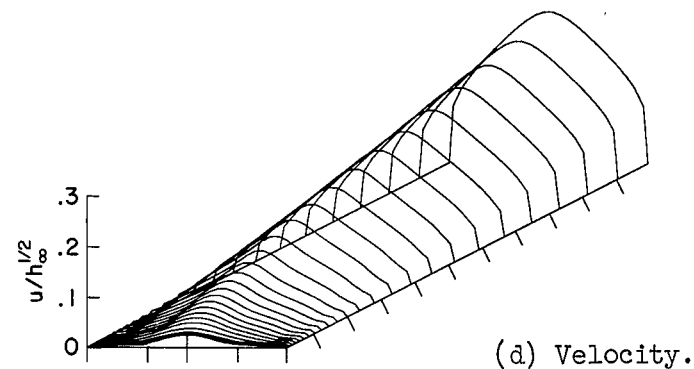
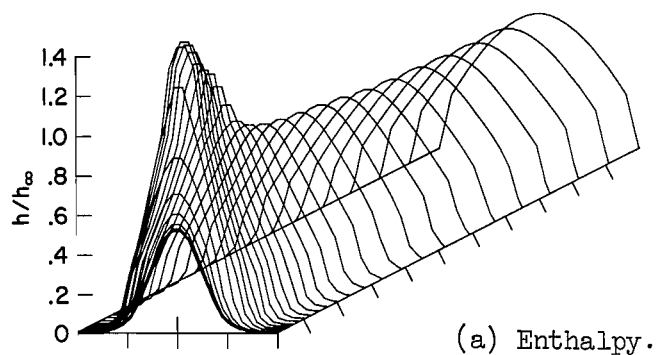


(j) Local heat transfer rate



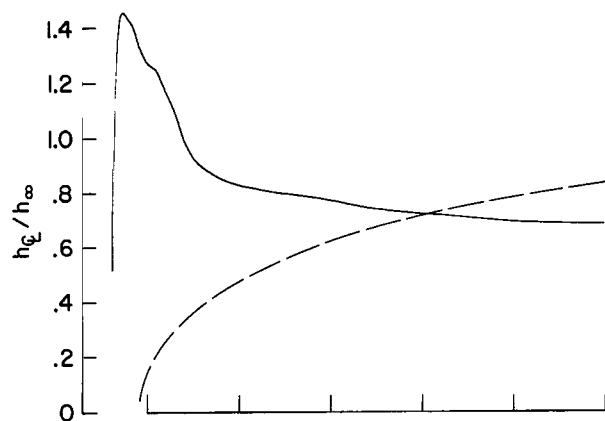
(k) Pressure.

Figure 10.- Concluded.

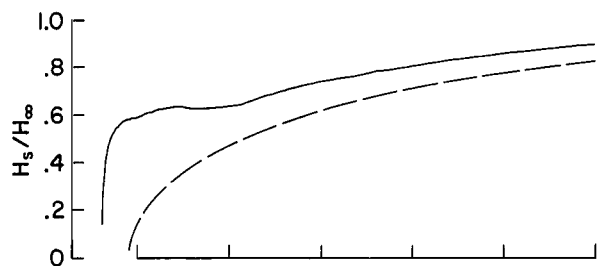


$I = 693$	A	$h_\infty = 2.25 \times 10^8$	J/kg
$\dot{m} = .00216$	kg/s	$\dot{m}/A = 17.1$	kg/sm ²
$R = .00635$	m	$h_\infty \dot{m}/A = 3.85 \times 10^9$	W/m ²
$z_0 = 2.14$	m	$\sqrt{h_\infty} = 1.50 \times 10^4$	m/s
		$p_0 = 9.65 \times 10^4$	N/m ² (.952 atm)
		$H_\infty = 9.76 \times 10^7$	J/kg
		$E_\infty = 819$	V/m
		$q_\infty = 1.42 \times 10^7$	W/m ²

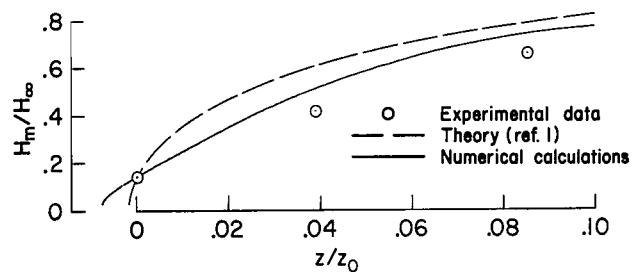
Figure 11.- Comparison of the numerical solutions with experimental measurements; 1.27-cm-diameter constrictor; $I = 693$ A, $\dot{m} = 2.16$ g/s.



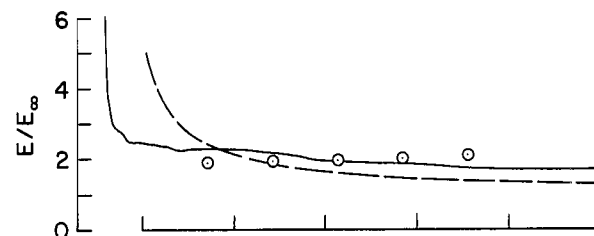
(f) Center-line enthalpy.



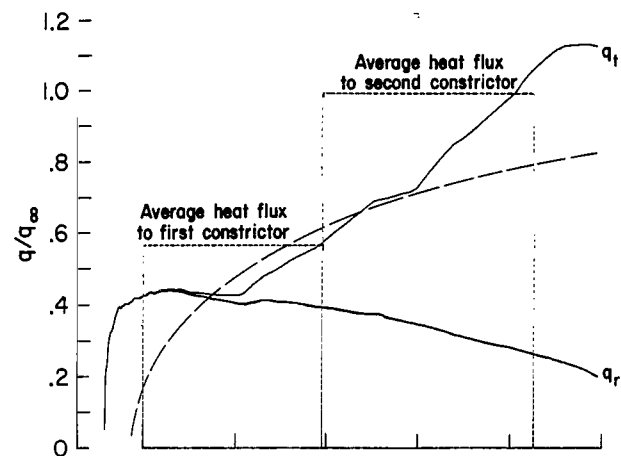
(g) Space-average enthalpy.



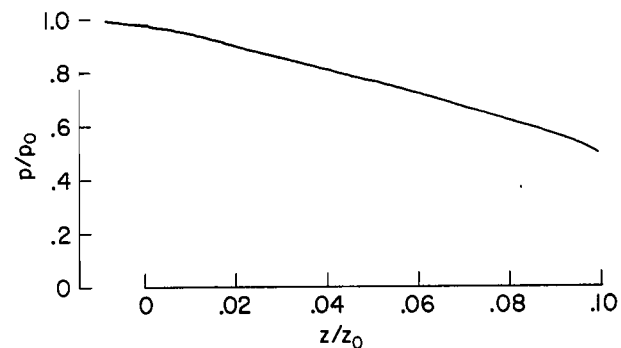
(h) Mass-average enthalpy.



(i) Voltage gradient.

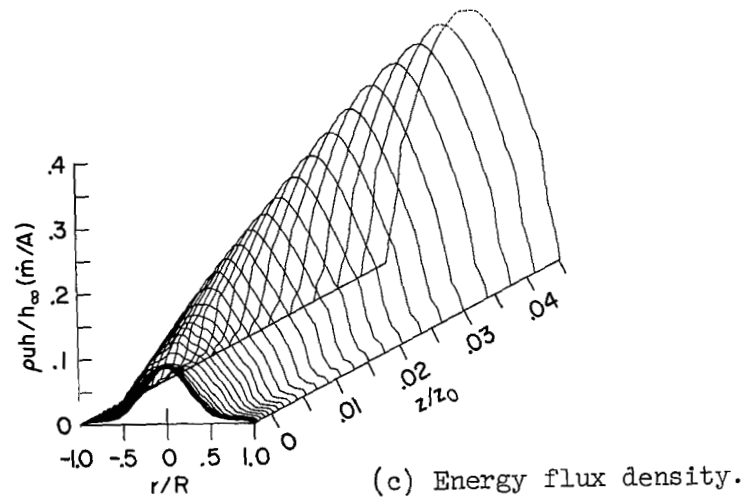
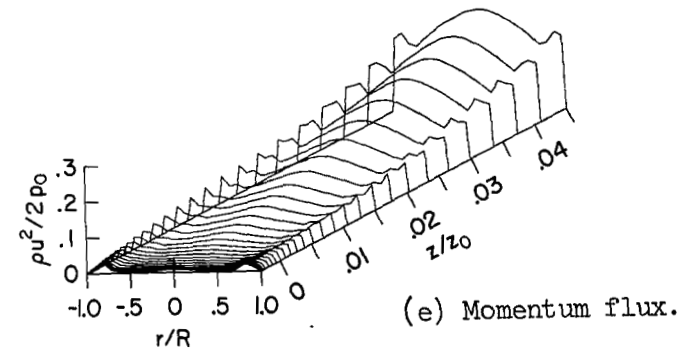
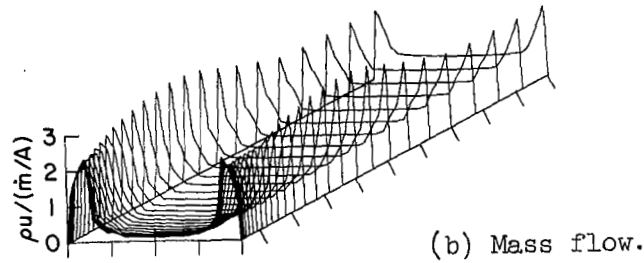
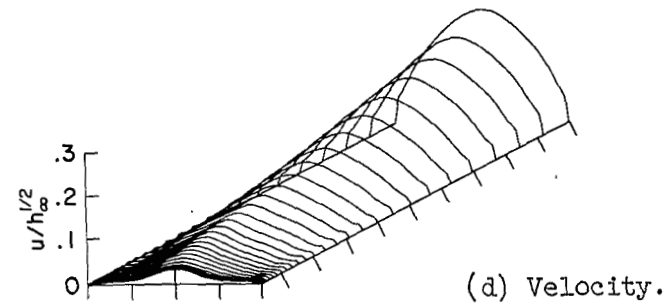
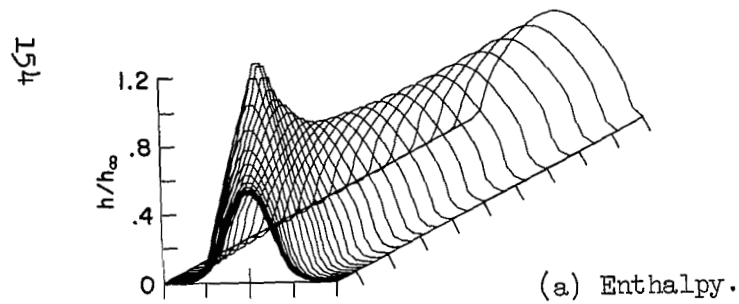


(j) Local heat transfer rate.



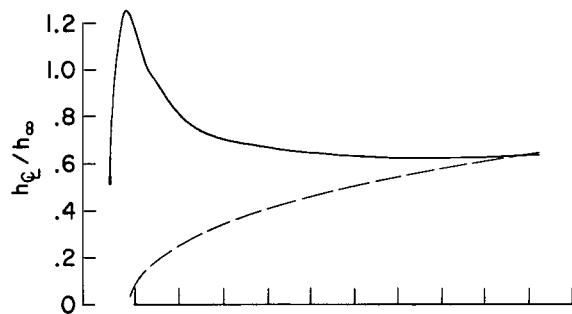
(k) Pressure.

Figure 11.- Concluded.

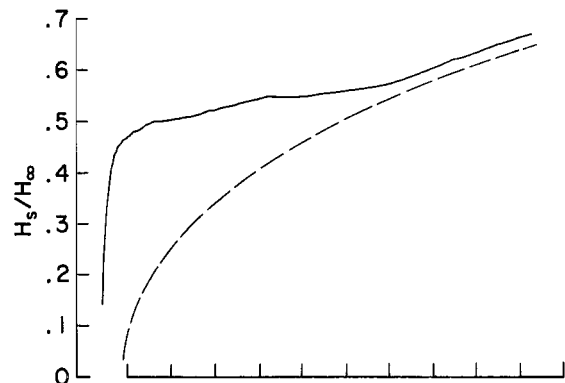


$I = 686$	A	$h_{\infty} = 2.23 \times 10^8$	J/kg
$\dot{m} = .00476$	kg/s	$\dot{m}/A = 37.7$	kg/sm ²
$R = .00635$	m	$h_{\infty} \dot{m}/A = 8.41 \times 10^9$	W/m ²
$z_0 = 4.73$	m	$\sqrt{h_{\infty}} = 1.50 \times 10^4$	m/s
		$p_0 = 1.56 \times 10^5$	N/m ² (1.54 atm)
		$H_{\infty} = 9.66 \times 10^7$	J/kg
		$E_{\infty} = 819$	V/m
		$q_{\infty} = 1.41 \times 10^7$	W/m ²

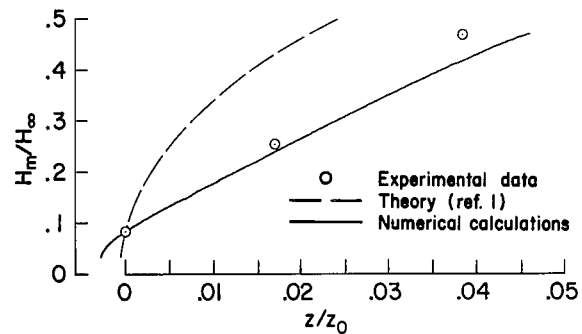
Figure 12.- Comparison of the numerical solutions with experimental measurements; 1.27-cm-diameter constrictor; $I = 686$ A, $\dot{m} = 4.76$ g/s.



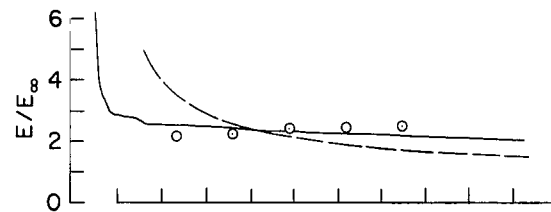
(f) Center-line enthalpy.



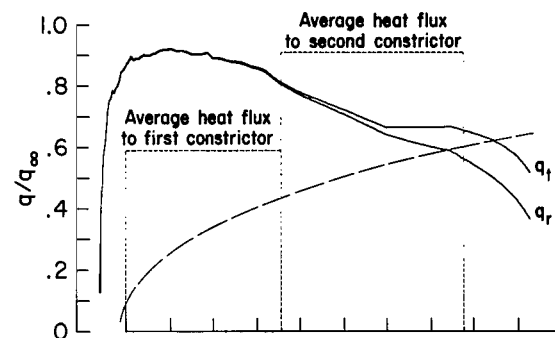
(g) Space-average enthalpy.



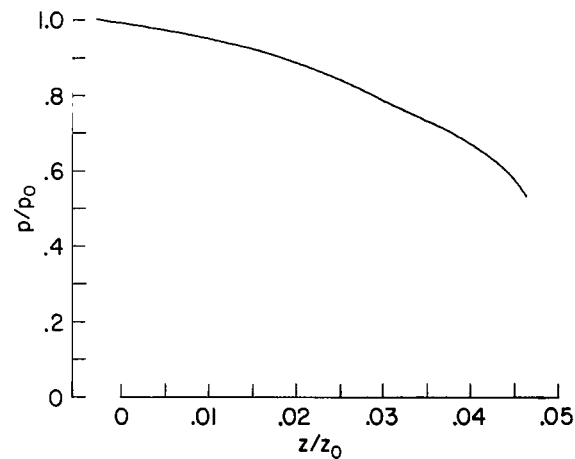
(h) Mass-average enthalpy.



(i) Voltage gradient.

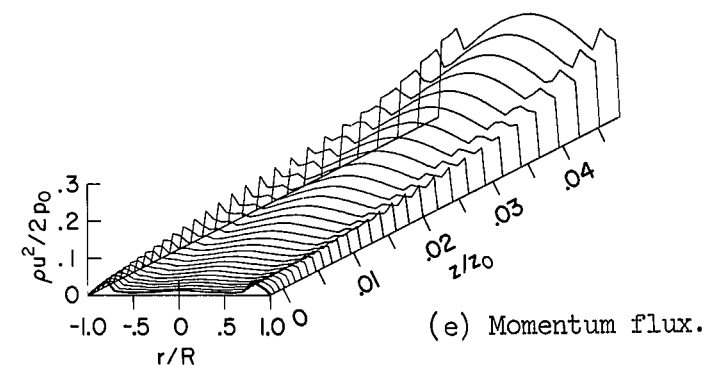
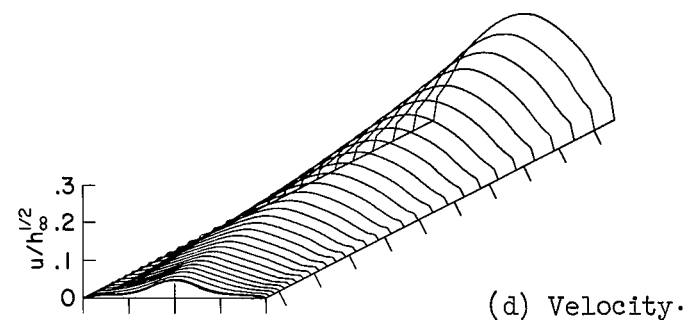
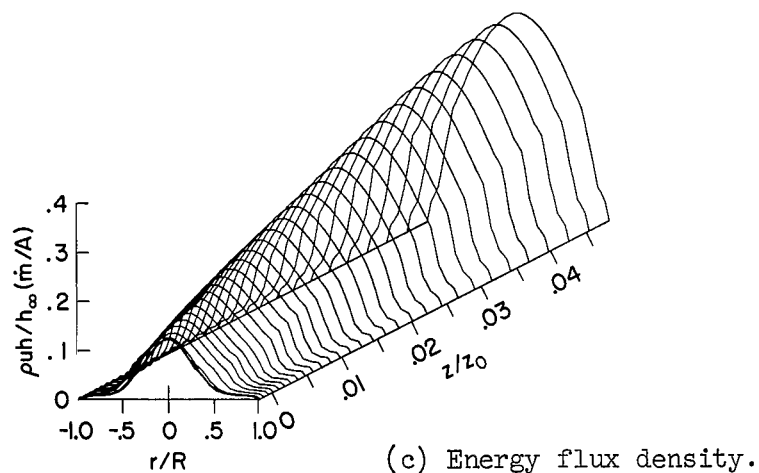
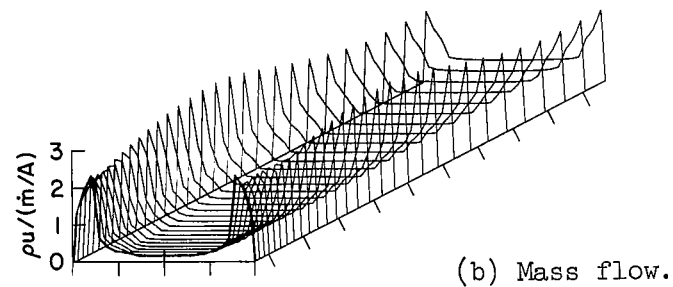
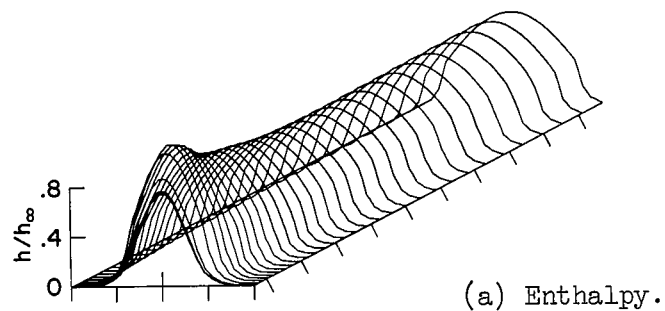


(j) Local heat transfer rate.



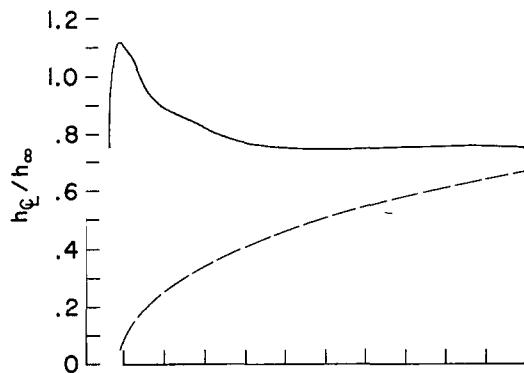
(k) Pressure.

Figure 12.- Concluded.

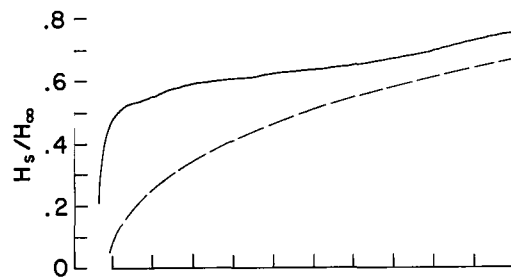


$I = 473$	A	$h_{\infty} = 1.54 \times 10^8$	J/kg
$\dot{m} = .00485$	kg/s	$\dot{m}/A = 38.8$	kg/sm ²
$R = .00635$	m	$h_{\infty} \dot{m}/A = 5.98 \times 10^9$	W/m ²
$z_0 = 4.81$	m	$\sqrt{h_{\infty}} = 1.24 \times 10^4$	m/s
		$p_0 = 1.36 \times 10^5$	N/m ² (1.35 atm)
		$H_{\infty} = 6.67 \times 10^7$	J/kg
		$E_{\infty} = 819$	V/m
		$q_{\infty} = 9.73 \times 10^6$	W/m ²

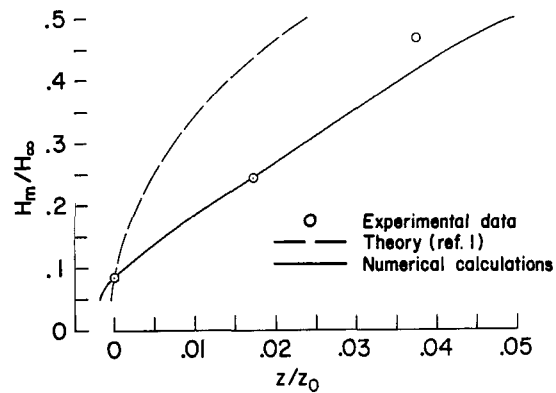
Figure 13.- Comparison of the numerical solutions with experimental measurements; 1.27-cm-diameter constrictor; $I = 473$ A, $\dot{m} = 4.85$ g/s.



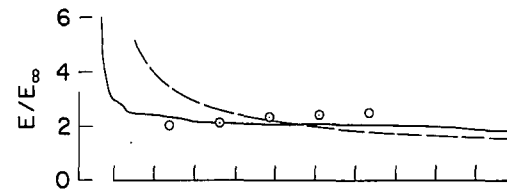
(f) Center-line enthalpy.



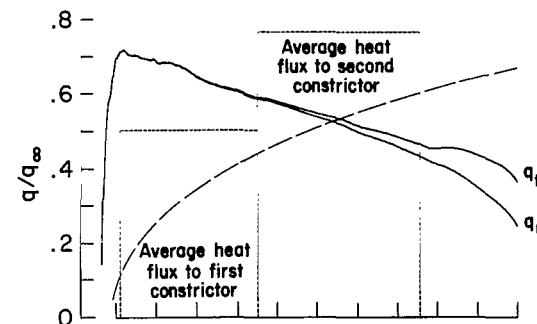
(g) Space-average enthalpy.



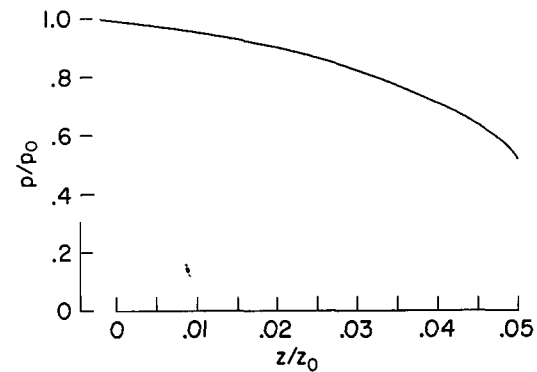
(h) Mass-average enthalpy.



(i) Voltage gradient.

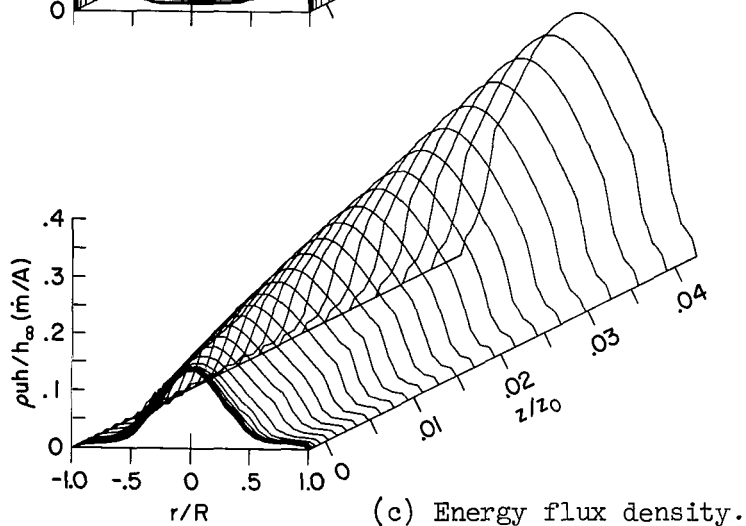
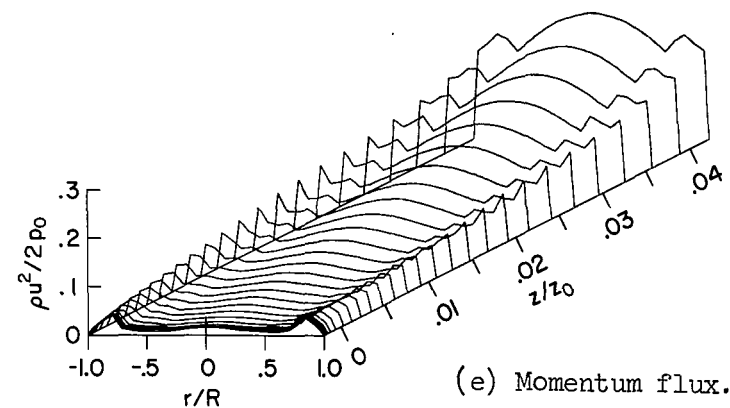
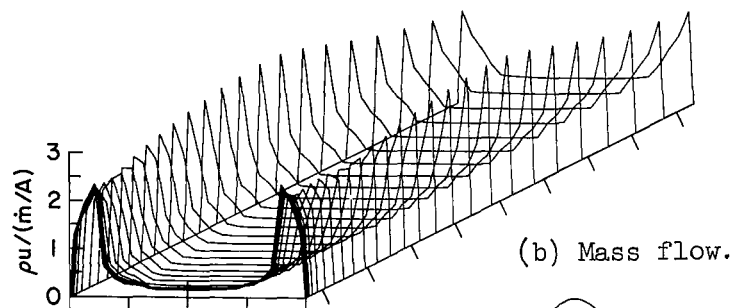
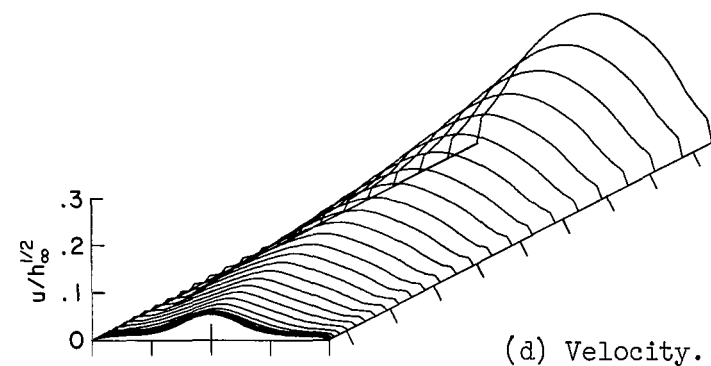
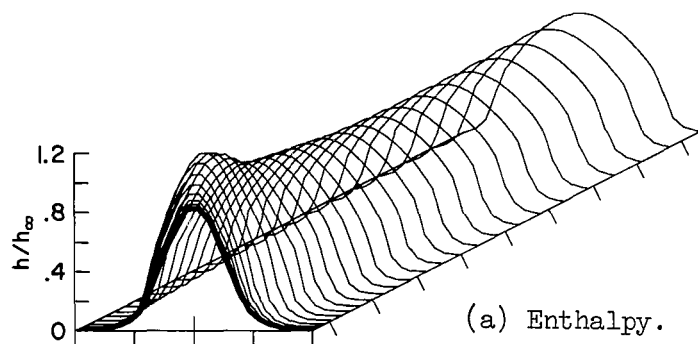


(j) Local heat transfer rate.



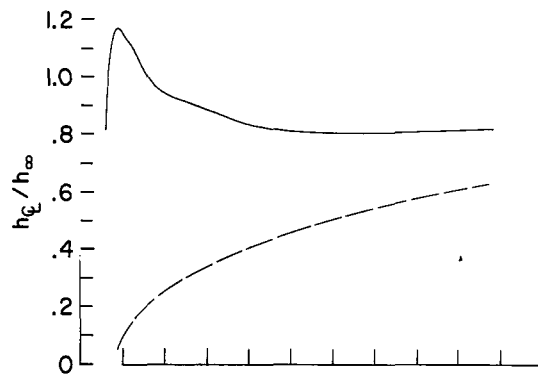
(k) Pressure.

Figure 13. - Concluded.

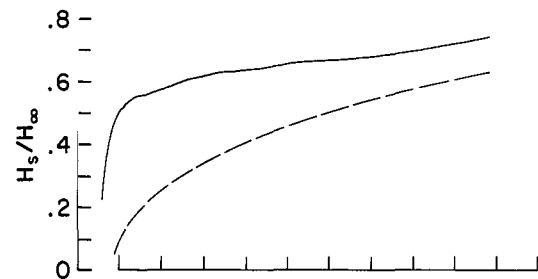


$I = 437$	A	$h_\infty = 1.42 \times 10^8$	J/kg
$\dot{m} = .00479$	kg/s	$\dot{m}/A = 37.8$	kg/sm ²
$R = .00635$	m	$h_\infty \dot{m}/A = 5.37 \times 10^9$	W/m ²
$z_0 = 4.75$	m	$\sqrt{h_\infty} = 1.19 \times 10^4$	m/s
		$p_0 = 1.23 \times 10^5$	N/m ² (1.21 atm)
		$H_\infty = 6.15 \times 10^7$	J/kg
		$E_\infty = 819$	V/m
		$q_\infty = 8.98 \times 10^6$	W/m ²

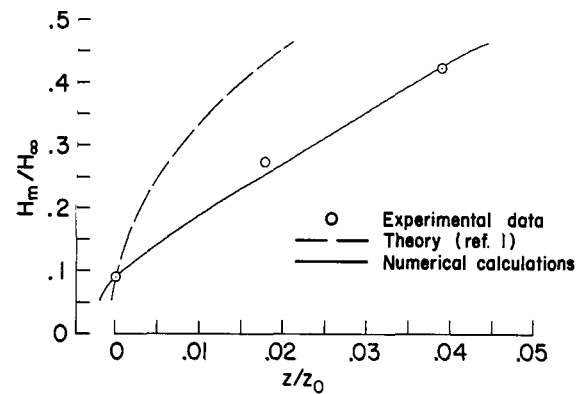
Figure 14.- Comparison of the numerical solutions with experimental measurements; 1.27-cm-diameter constrictor; $I = 436$ A, $\dot{m} = 4.78$ g/s.



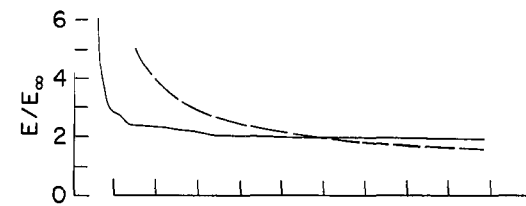
(f) Center-line enthalpy.



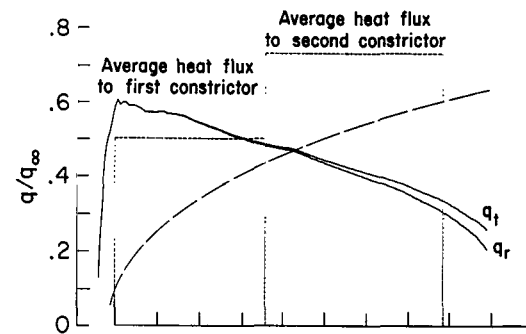
(g) Space-average enthalpy.



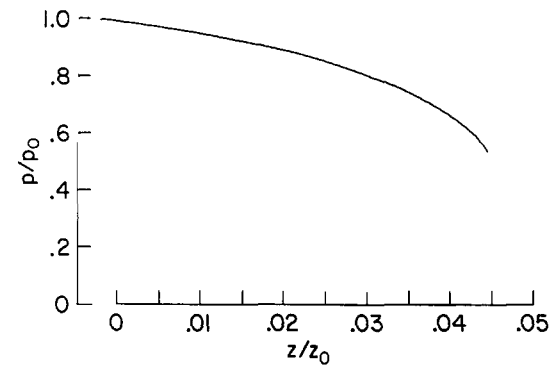
(h) Mass-average enthalpy.



(i) Voltage gradient.

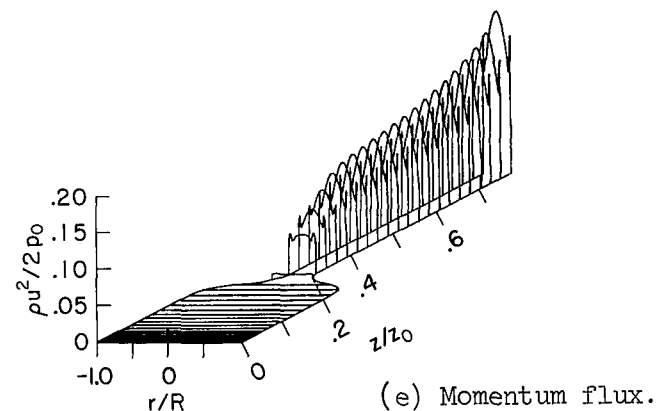
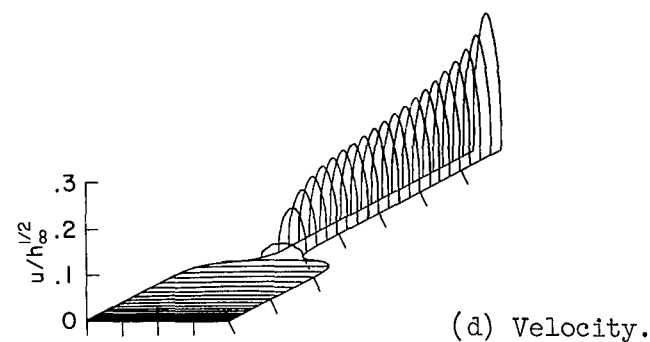
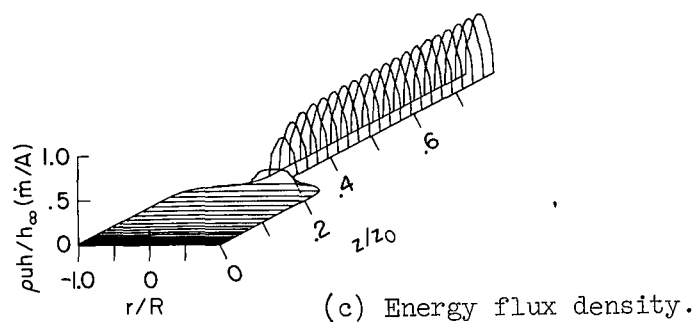
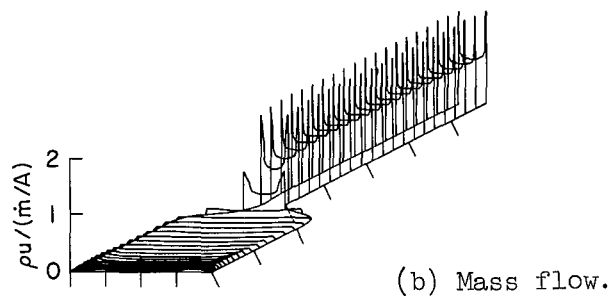
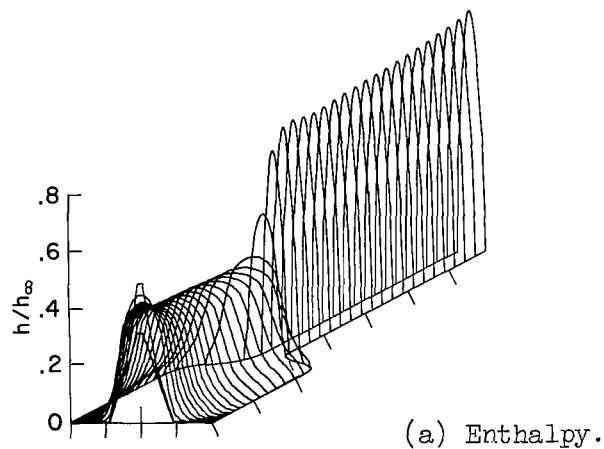


(j) Local heat transfer rate.



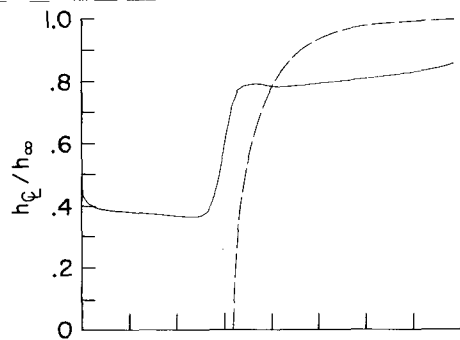
(k) Pressure.

Figure 14.- Concluded.

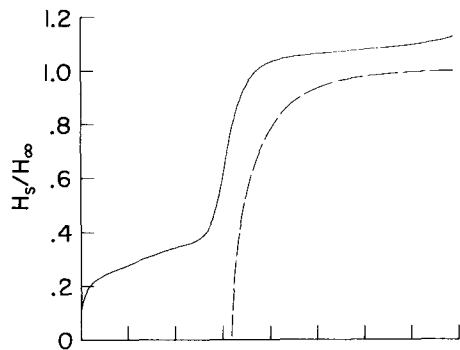


$I = 240$	A	$h_\infty = 1.56 \times 10^8$	J/kg
$\dot{m} = .000240$	kg/s	$\dot{m}/A = 7.58$	kg/sm ²
$R = .00318$	m	$h_\infty \dot{m}/A = 1.18 \times 10^9$	W/m ²
$z_0 = .238$	m	$\sqrt{h_\infty} = 1.25 \times 10^4$	m/s
		$p_0 = 5.11 \times 10^4$	N/m ² (.504 atm)
		$H_\infty = 6.77 \times 10^7$	J/kg
		$E_\infty = 1636$	V/m
		$q_\infty = 1.97 \times 10^7$	W/m ²

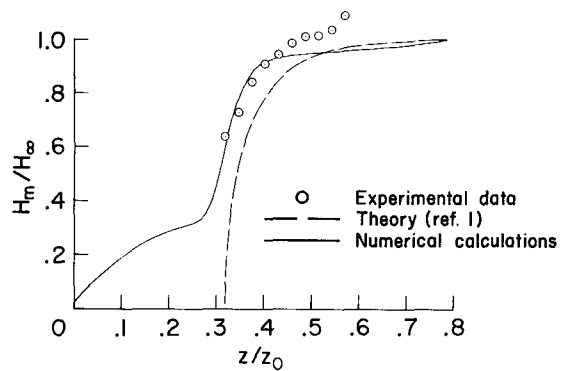
Figure 15.- Comparison of the numerical solutions with experimental measurements; 0.635-cm-diameter constrictor; $I = 240$ A, $\dot{m} = 0.24$ g/s.



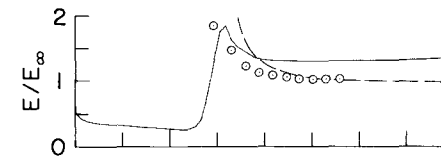
(f) Center-line enthalpy.



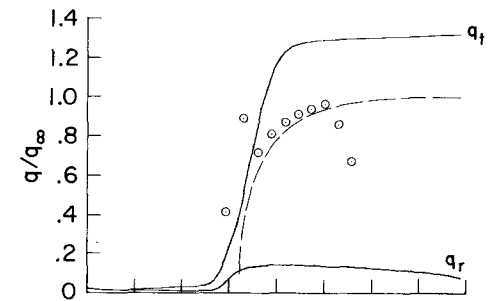
(g) Space-average enthalpy.



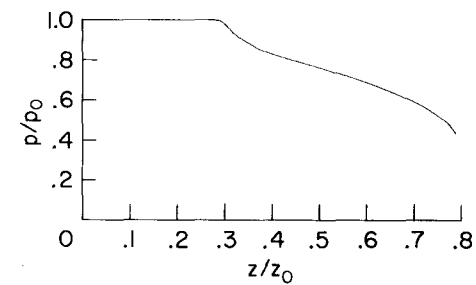
(h) Mass-average enthalpy.



(i) Voltage gradient.

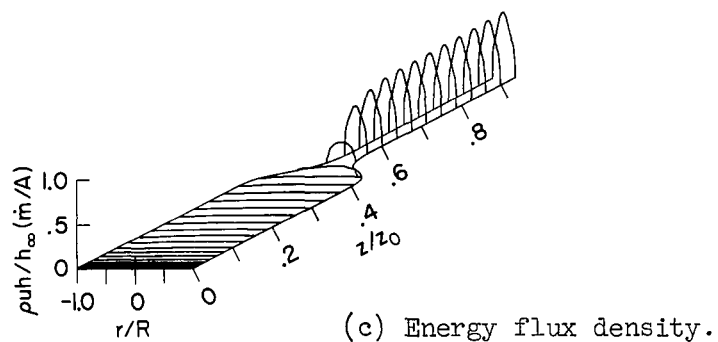
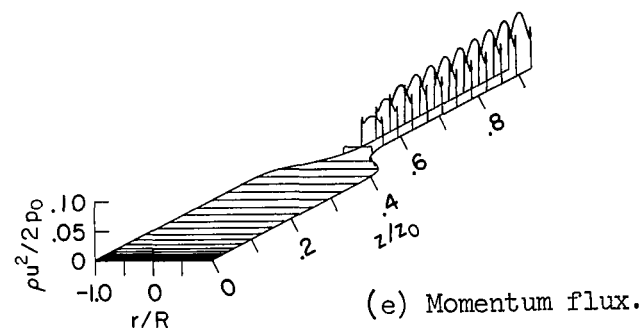
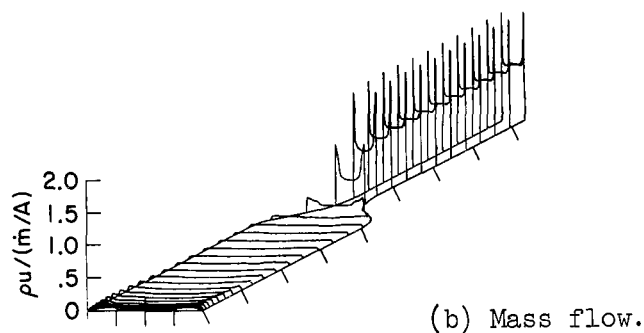
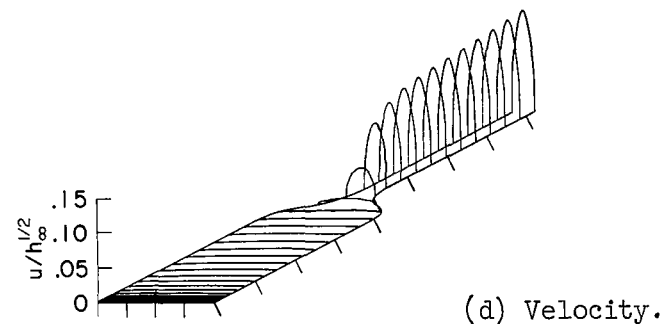
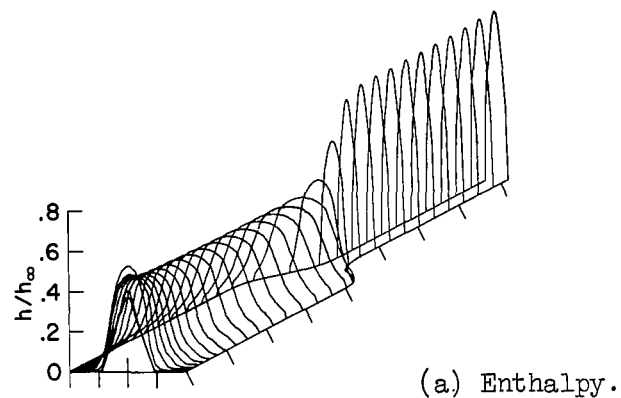


(j) Local heat transfer rate.



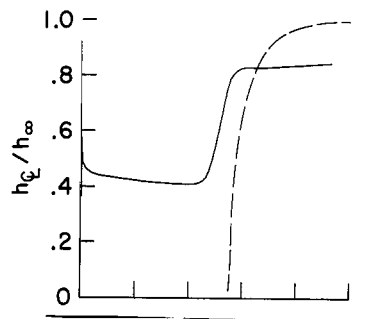
(k) Pressure.

Figure 15.- Concluded.

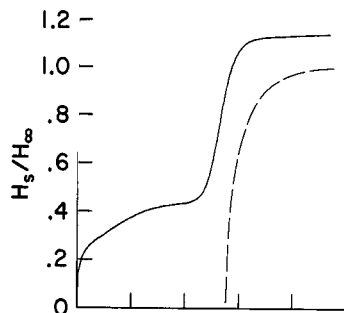


$I = 210$	A	$h_\infty = 1.37 \times 10^8$	J/kg
$\dot{m} = .000139$	kg/s	$\dot{m}/A = 4.39$	kg/sm ²
$R = .00318$	m	$h_\infty \dot{m}/A = 6.00 \times 10^8$	W/m ²
$z_0 = .138$	m	$\sqrt{h_\infty} = 1.17 \times 10^4$	m/s
		$p_0 = 3.41 \times 10^4$	N/m ² (.337 atm)
		$H_\infty = 5.92 \times 10^7$	J/kg
		$E_\infty = 1636$	V/m
		$q_\infty = 1.73 \times 10^7$	W/m ²

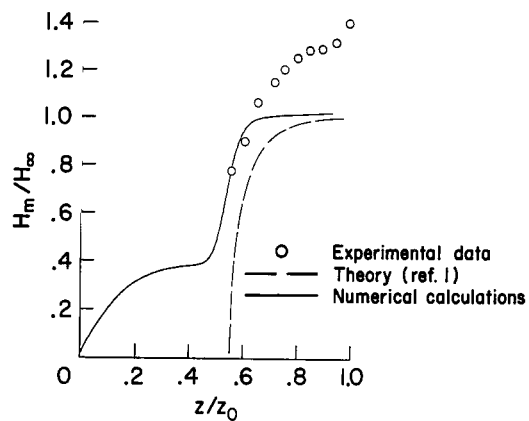
Figure 16.- Comparison of the numerical solutions with experimental measurements; 0.635-cm-diameter constrictor; $I = 210$ A, $\dot{m} = 0.14$ g/s.



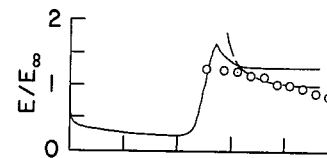
(f) Center-line enthalpy.



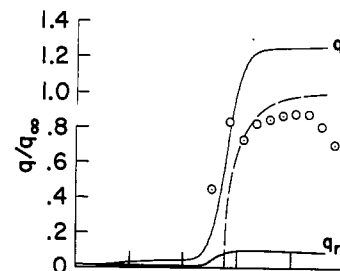
(g) Space-average enthalpy.



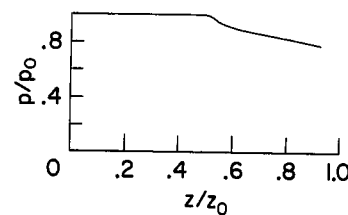
(h) Mass-average enthalpy.



(i) Voltage gradient.

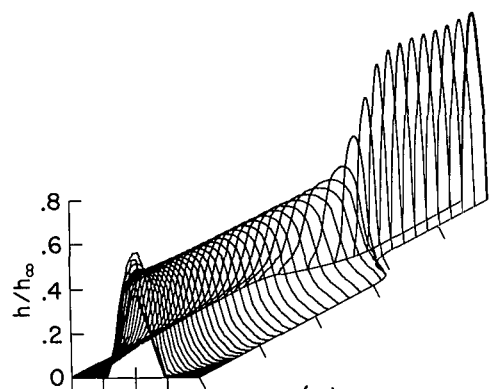


(j) Local heat transfer rate.

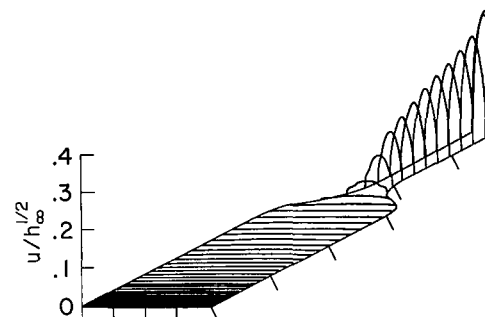


(k) Pressure.

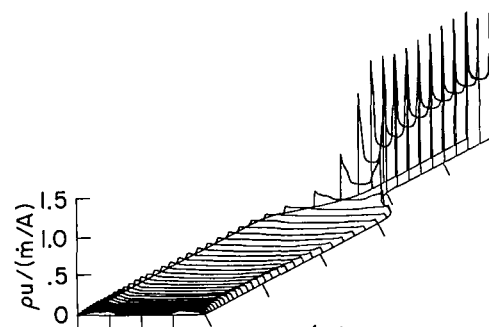
Figure 16.- Concluded.



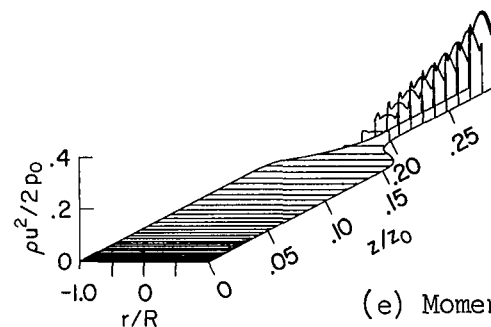
(a) Enthalpy.



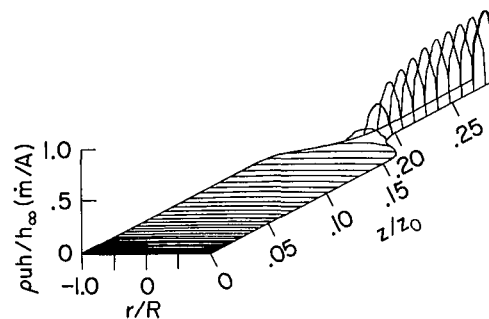
(d) Velocity.



(b) Mass flow.



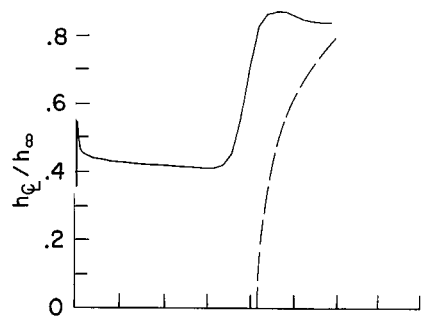
(e) Momentum flux.



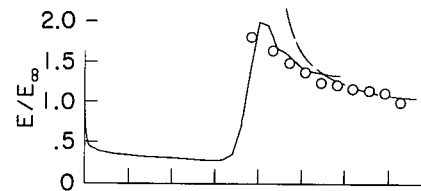
(c) Energy flux density.

$I = 210$	A	$h_{\infty} = 1.37 \times 10^8$	J/kg
$\dot{m} = .000369$	kg/s	$\dot{m}/A = 11.7$	kg/sm ²
$R = .00318$	m	$h_{\infty} \dot{m}/A = 1.59 \times 10^9$	W/m ²
$z_0 = .365$	m	$\sqrt{h_{\infty}} = 1.17 \times 10^4$	m/s
		$p_0 = 5.72 \times 10^4$	N/m ² (565 atm)
		$H_{\infty} = 5.92 \times 10^7$	J/kg
		$E_{\infty} = 1636$	V/m
		$q_{\infty} = 1.73 \times 10^7$	W/m ²

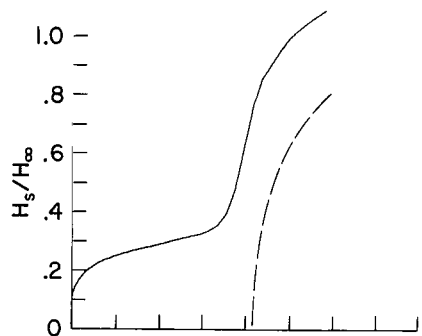
Figure 17.- Comparison of the numerical solutions with experimental measurements; 0.635-cm-diameter constrictor; $I = 210$ A, $\dot{m} = 0.37$ g/s.



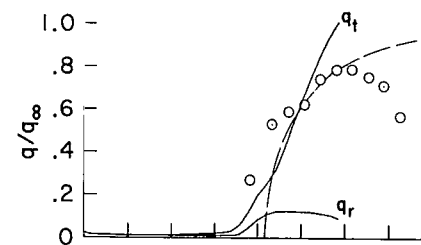
(f) Center-line enthalpy.



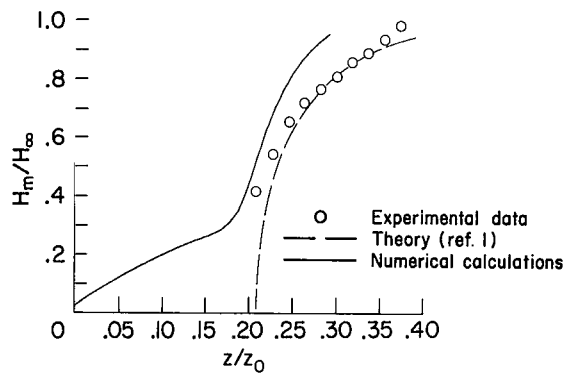
(i) Voltage gradient.



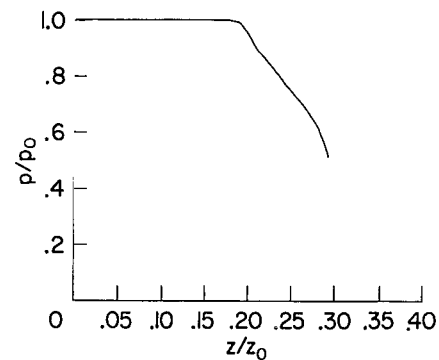
(g) Space-average enthalpy.



(j) Local heat transfer rate.

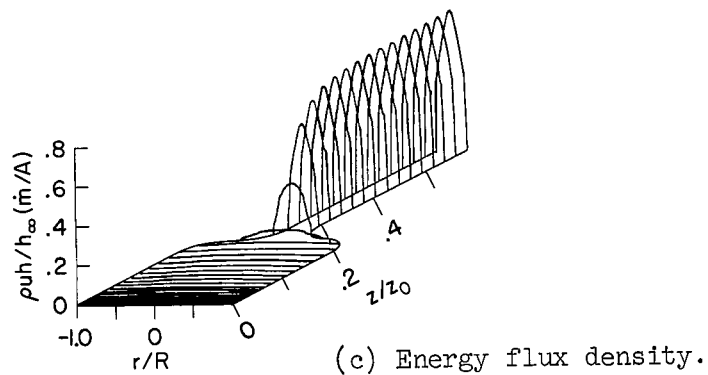
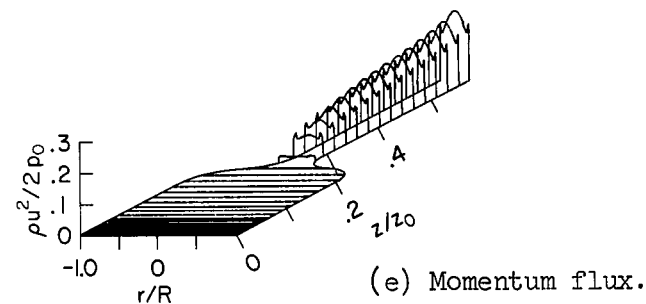
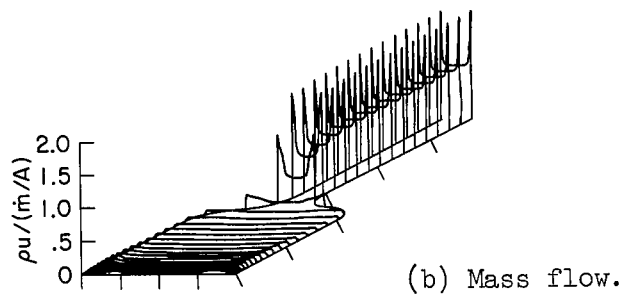
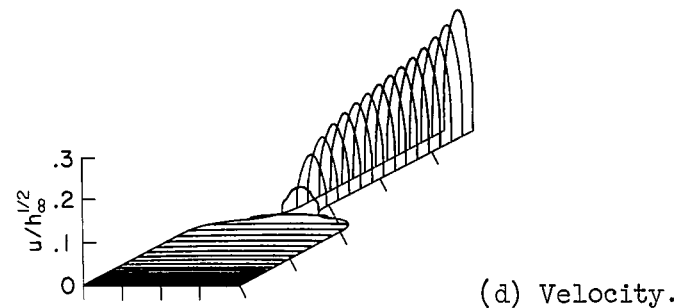
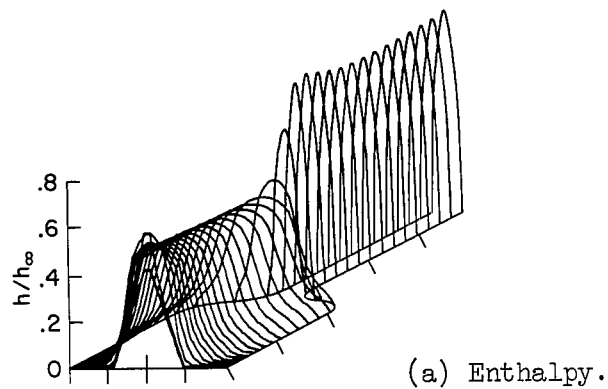


(h) Mass-average enthalpy.



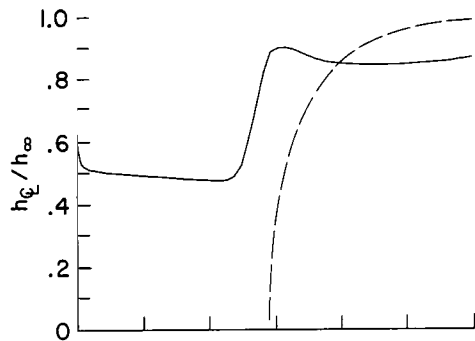
(k) Pressure.

Figure 17.- Concluded.

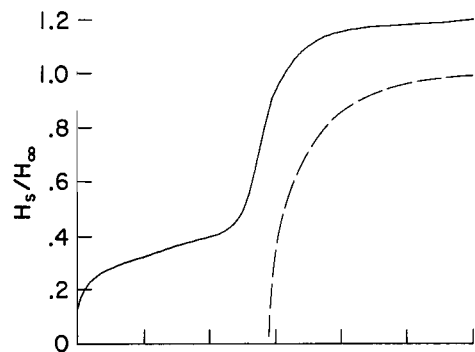


$I = 183$	A	$h_\infty = 1.19 \times 10^8$	J/kg
$\dot{m} = .000265$	kg/s	$\dot{m}/A = 8.37$	kg/sm ²
$R = .00318$	m	$h_\infty \dot{m}/A = 9.97 \times 10^8$	W/m ²
$z_0 = .262$	m	$\sqrt{h_\infty} = 1.09 \times 10^4$	m/s
		$p_0 = 4.76 \times 10^4$	N/m ² (.470 atm)
		$H_\infty = 5.16 \times 10^7$	J/kg
		$E_\infty = 1636$	V/m
		$q_\infty = 1.51 \times 10^7$	W/m ²

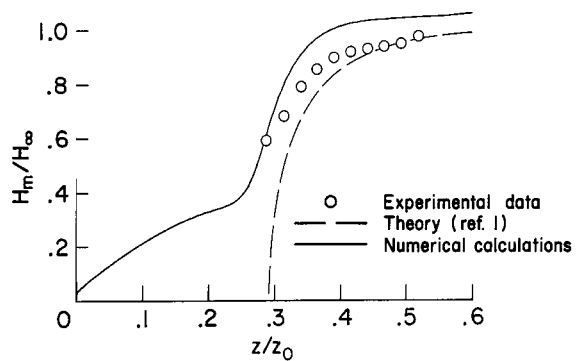
Figure 18.- Comparison of the numerical solutions with experimental measurements; 0.635-cm-diameter constrictor; $I = 183$ A, $\dot{m} = 0.27$ g/s.



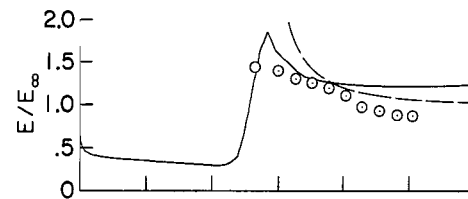
(f) Center-line enthalpy.



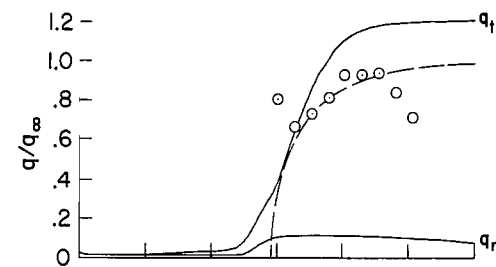
(g) Space-average enthalpy.



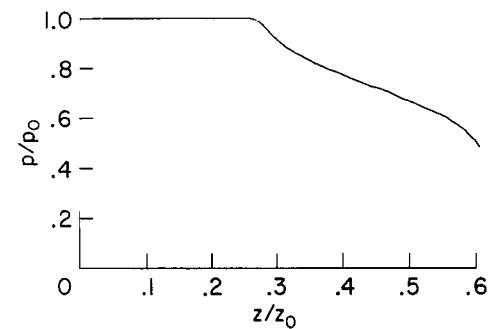
(h) Mass-average enthalpy.



(i) Voltage gradient.

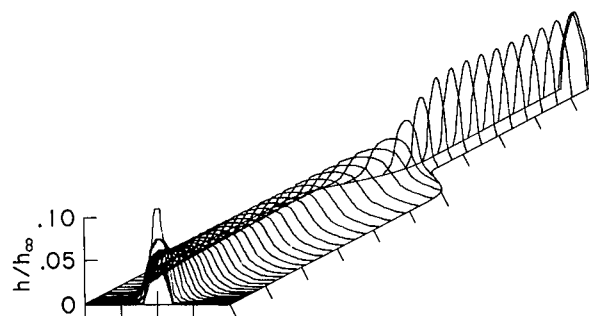


(j) Local heat transfer rate.

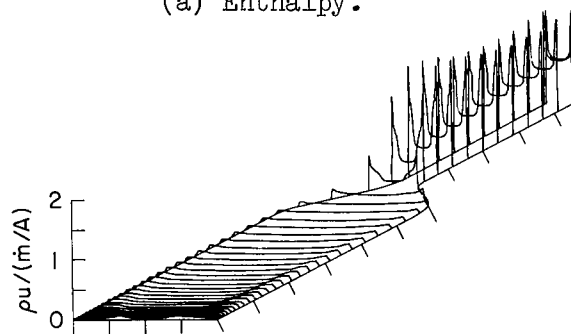


(k) Pressure.

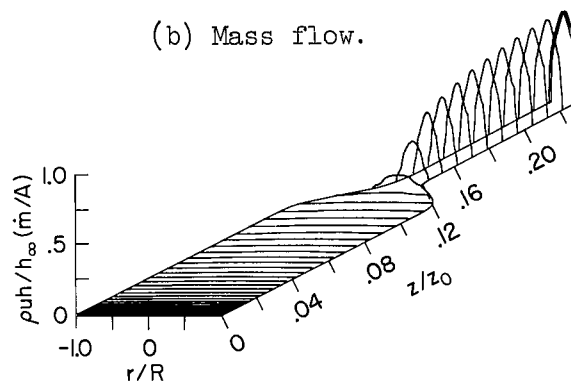
Figure 18.- Concluded.



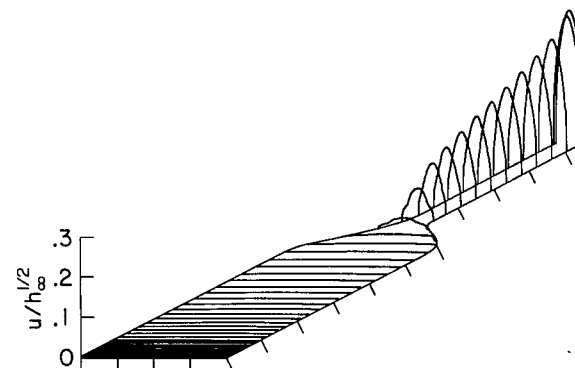
(a) Enthalpy.



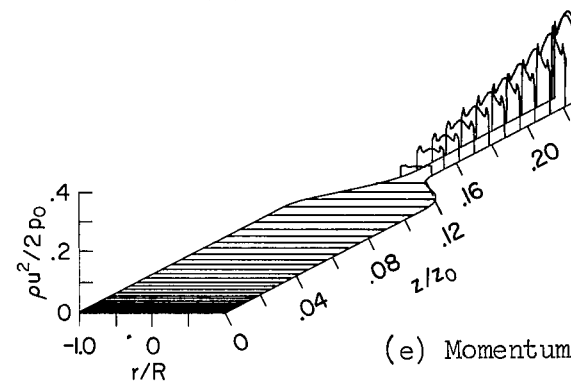
(b) Mass flow.



(c) Energy flux density.



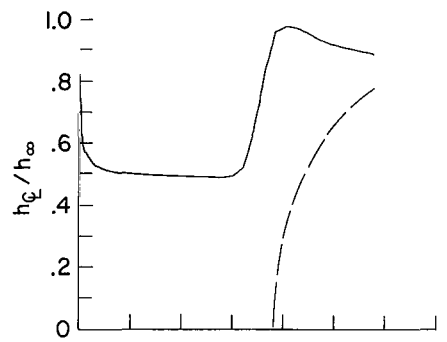
(d) Velocity.



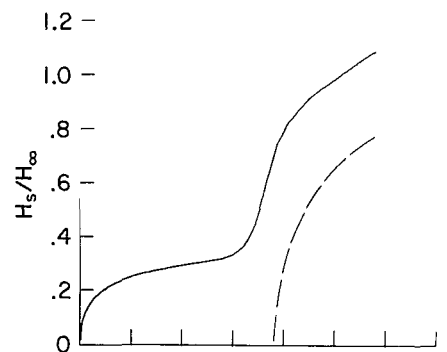
(e) Momentum flux.

$I = 180$	A	$h_{\infty} = 1.17 \times 10^8$	J/kg
$\dot{m} = .000503$	kg/s	$\dot{m}/A = 15.9$	kg/sm ²
$R = .00318$	m	$h_{\infty} \dot{m}/A = 1.87 \times 10^9$	W/m ²
$z_0 = .499$	m	$\sqrt{h_{\infty}} = 1.08 \times 10^4$	m/s
		$p_0 = 7.19 \times 10^4$	N/m ² (.710 atm)
		$H_{\infty} = 5.08 \times 10^7$	J/kg
		$E_{\infty} = 1636$	V/m
		$q_{\infty} = 1.48 \times 10^7$	W/m ²

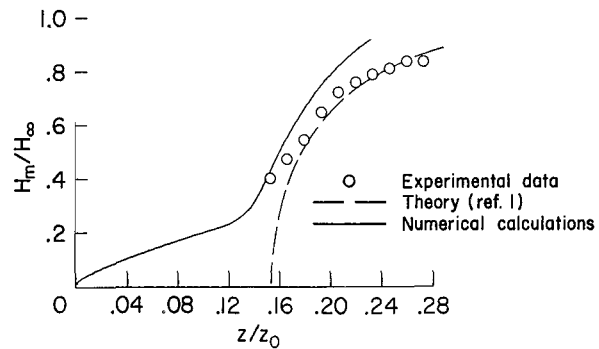
Figure 19.- Comparison of the numerical solutions with experimental measurements; 0.635-cm-diameter constrictor; $I = 180$ A, $\dot{m} = 0.50$ g/s.



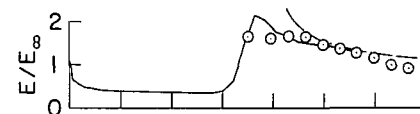
(f) Center-line enthalpy.



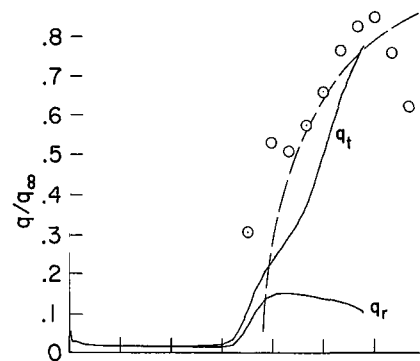
(g) Space-average enthalpy.



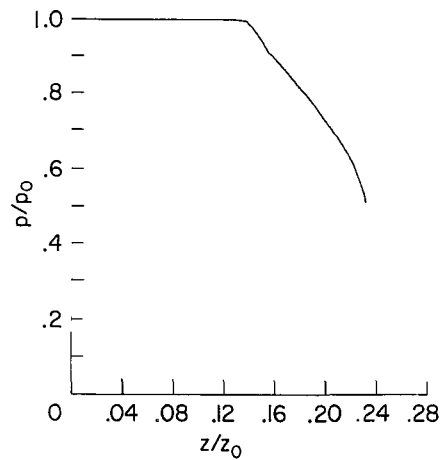
(h) Mass-average enthalpy.



(i) Voltage gradient.

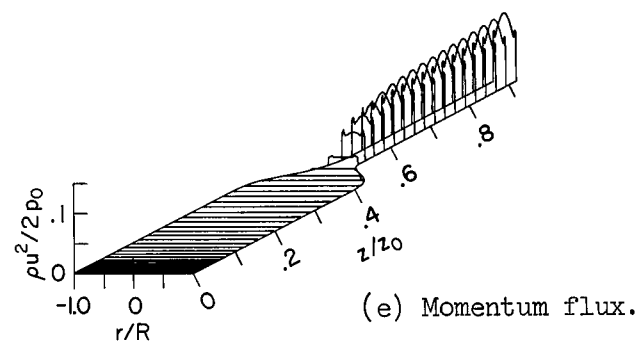
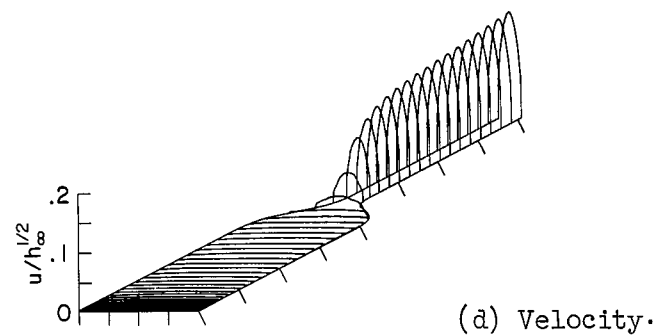
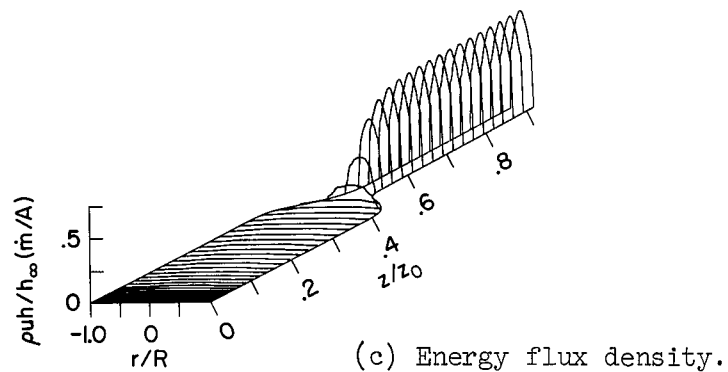
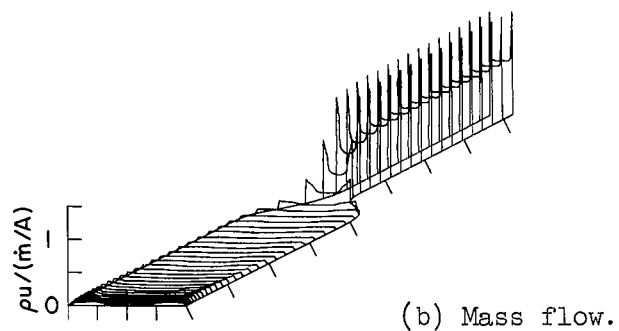
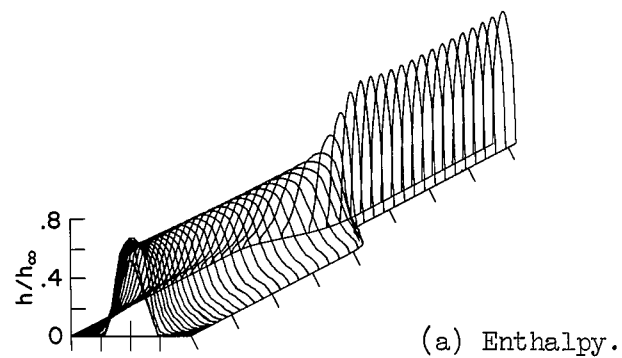


(j) Local heat transfer rate.



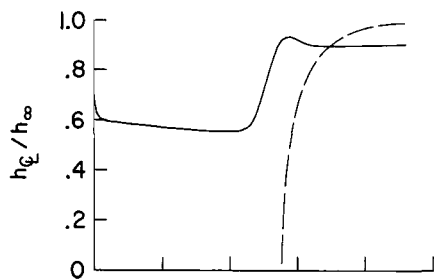
(k) Pressure.

Figure 19.- Concluded.

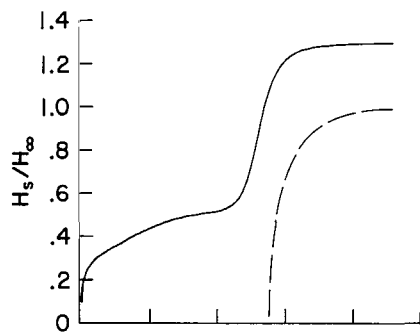


$I = 150$	A	$h_{\infty} = 9.77 \times 10^7$	J/kg
$\dot{m} = .000139$	kg/s	$\dot{m}/A = 4.39$	kg/sm ²
$R = .00318$	m	$h_{\infty} \dot{m}/A = 4.29 \times 10^8$	W/m ²
$z_0 = .138$	m	$\sqrt{h_{\infty}} = 9.88 \times 10^3$	m/s
		$p_0 = 2.82 \times 10^4$	N/m ² (.278 atm)
		$H_{\infty} = 4.23 \times 10^7$	J/kg
		$E_{\infty} = 1636$	V/m
		$q_{\infty} = 1.23 \times 10^7$	W/m ²

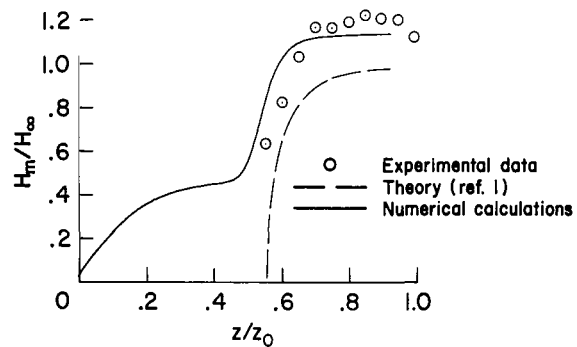
Figure 20.- Comparison of the numerical solutions with experimental measurements; 0.635-cm-diameter constrictor; $I = 150$ A, $\dot{m} = 0.14$ g/s.



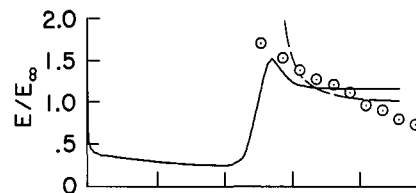
(f) Center-line enthalpy.



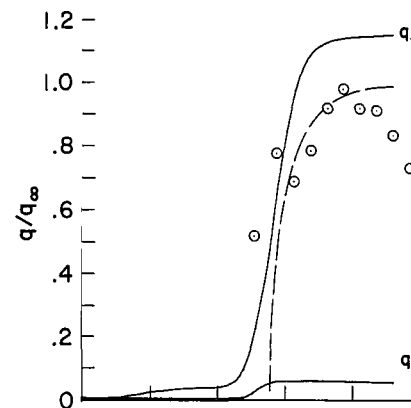
(g) Space-average enthalpy.



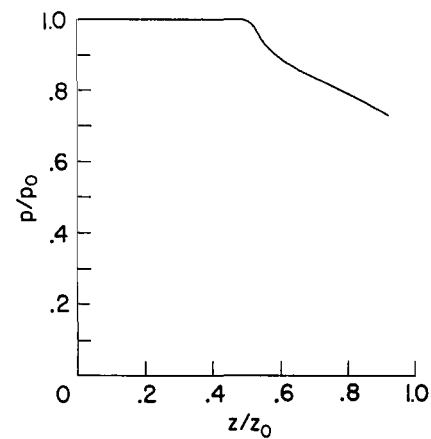
(h) Mass-average enthalpy.



(i) Voltage gradient.

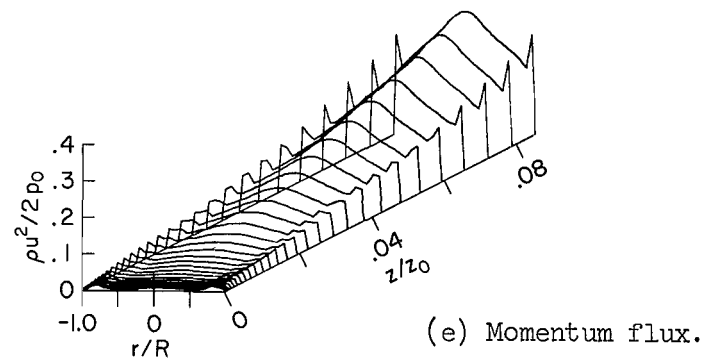
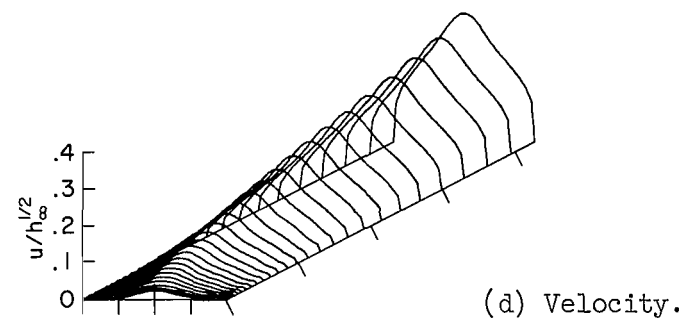
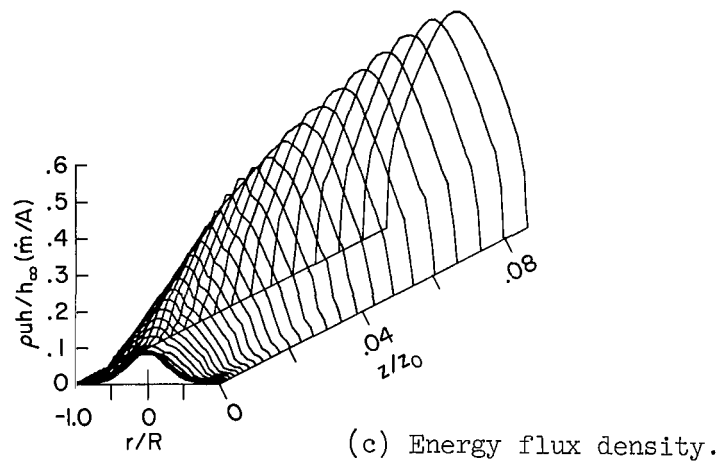
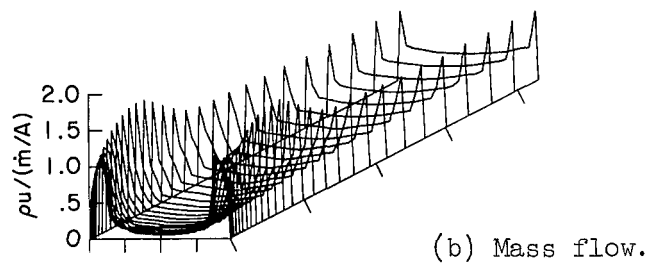
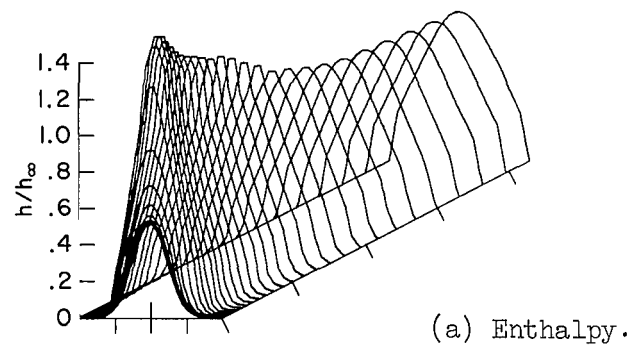


(j) Local heat transfer rate.



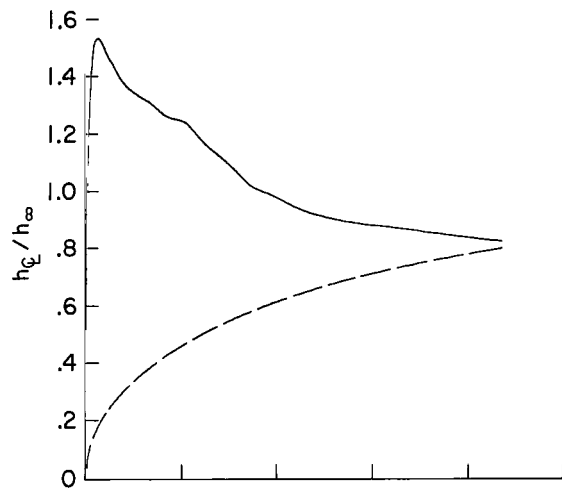
(k) Pressure.

Figure 20.- Concluded.

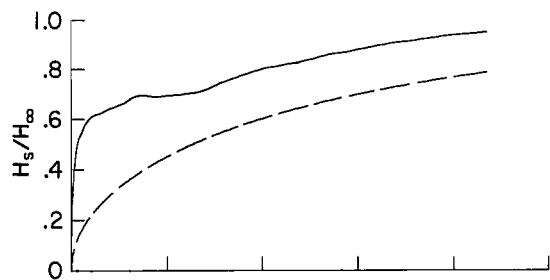


$I = 693$	A	$h_\infty = 2.25 \times 10^8$	J/kg
$\dot{m} = .00216$	kg/s	$\dot{m}/A = 17.1$	kg/sm ²
$R = .00635$	m	$h_\infty \dot{m}/A = 3.85 \times 10^9$	W/m ²
$z_0 = 2.14$	m	$\sqrt{h_\infty} = 1.50 \times 10^4$	m/s
		$p_0 = 9.65 \times 10^4$	N/m ² (952 atm)
		$H_\infty = 9.76 \times 10^7$	J/kg
		$E_\infty = 819$	V/m
		$q_\infty = 1.42 \times 10^7$	W/m ²

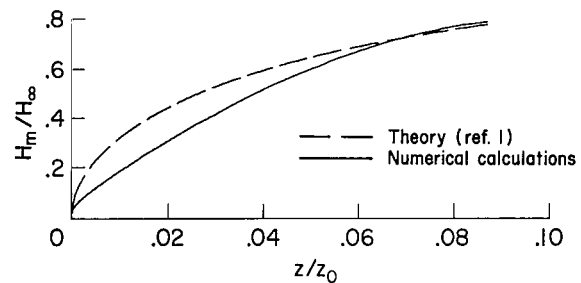
Figure 21.- The constricted arc with no radiation losses (radiance set equal to zero).



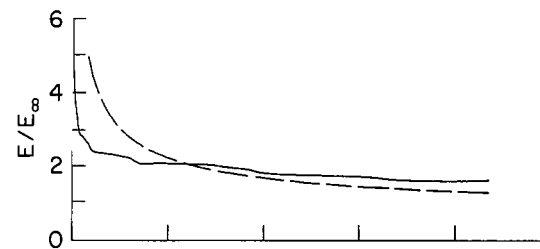
(f) Center-line enthalpy.



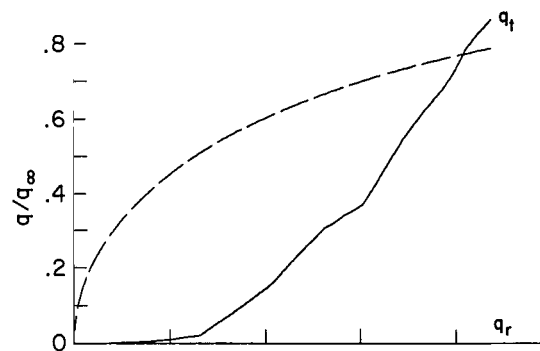
(g) Space-average enthalpy.



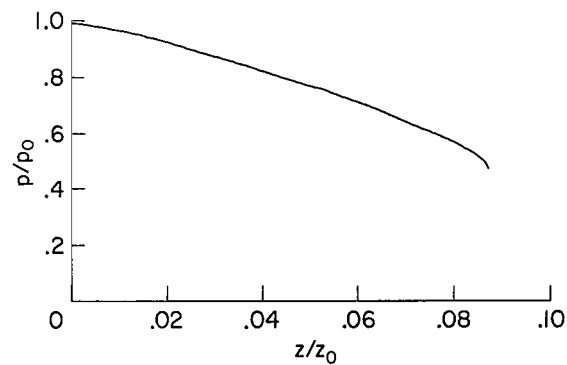
(h) Mass-average enthalpy.



(i) Voltage gradient.

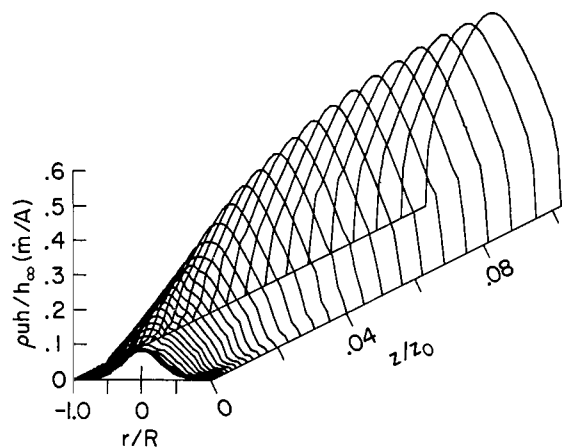
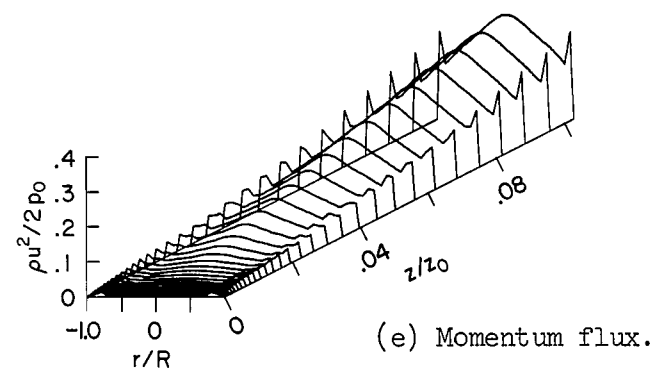
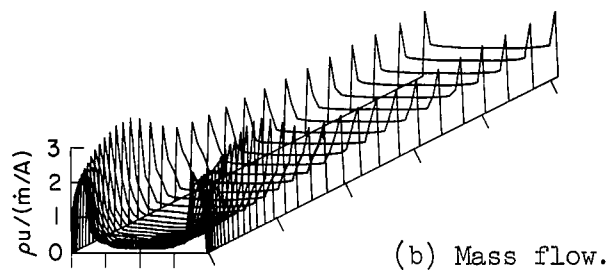
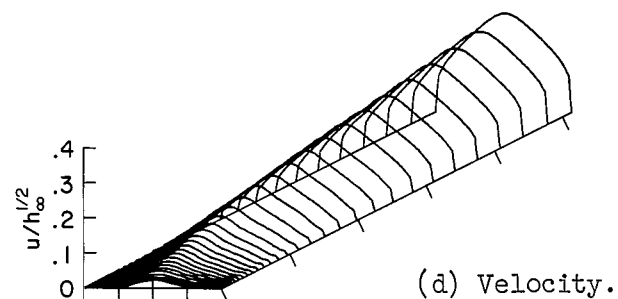
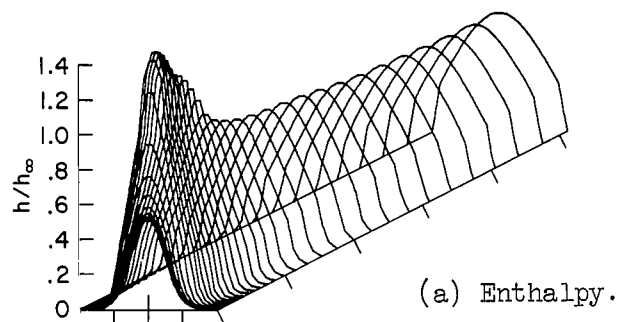


(j) Local heat transfer rate.



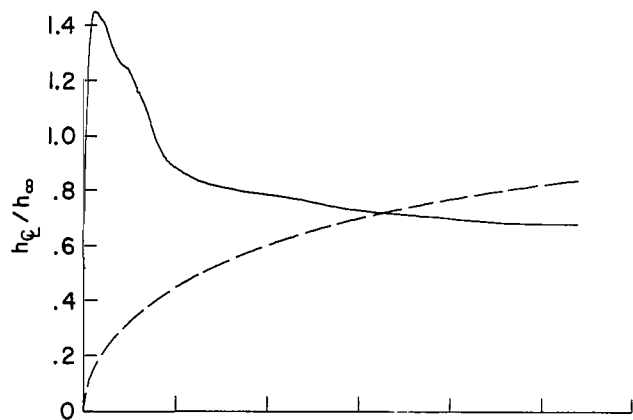
(k) Pressure.

Figure 21.- Concluded.

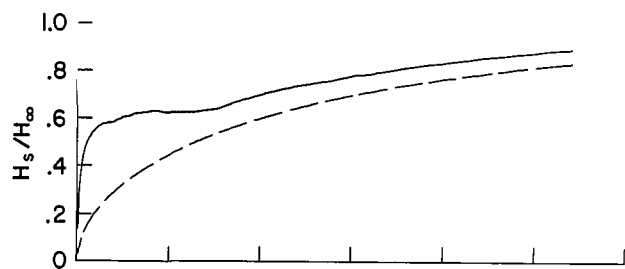


$I = 693$	A	$h_\infty = 2.25 \times 10^8$	J/kg
$\dot{m} = .00216$	kg/s	$\dot{m}/A = 17.1$	kg/sm ²
$R = .00635$	m	$h_\infty \dot{m}/A = 3.85 \times 10^9$	W/m ²
$z_0 = 2.14$	m	$\sqrt{h_\infty} = 1.50 \times 10^4$	m/s
		$p_0 = 9.65 \times 10^4$	N/m ² (.952 atm)
		$H_\infty = 9.76 \times 10^7$	J/kg
		$E_\infty = 819$	V/m
		$q_\infty = 1.42 \times 10^7$	W/m ²

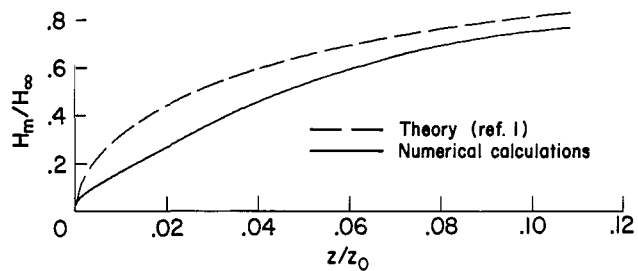
Figure 22.- The constricted arc with approximately equal radiation and conduction losses.



(f) Center-line enthalpy.



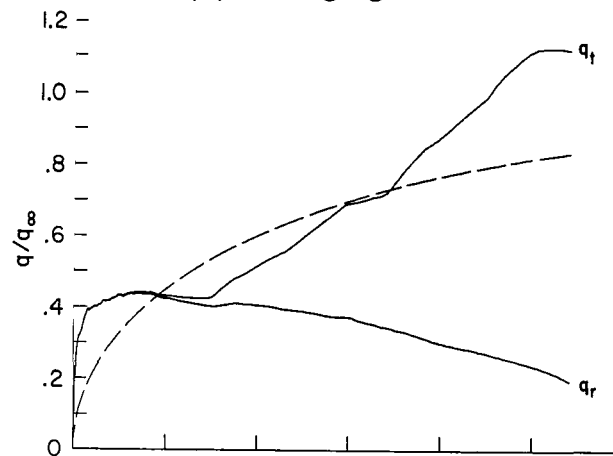
(g) Space-average enthalpy.



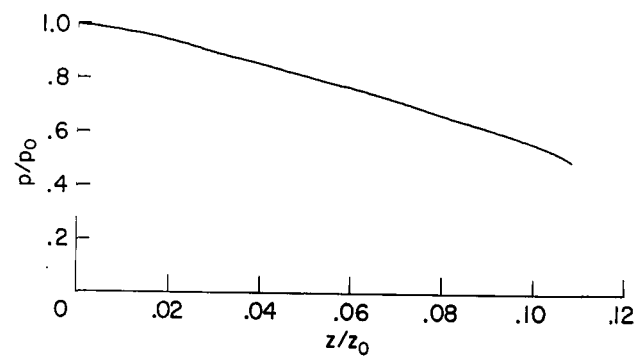
(h) Mass-average enthalpy.



(i) Voltage gradient.

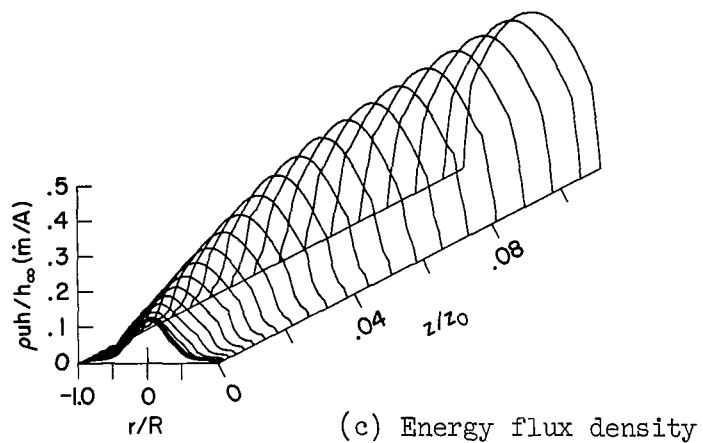
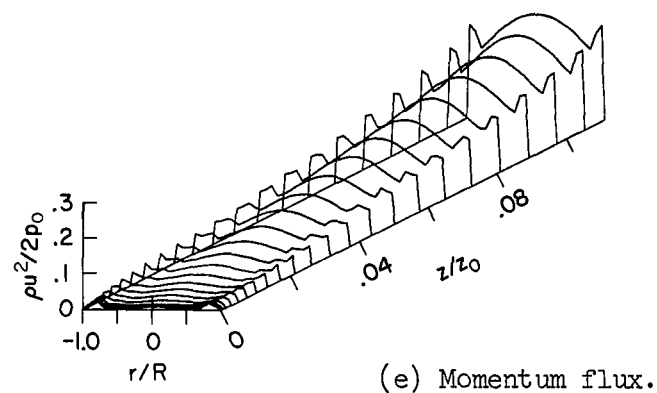
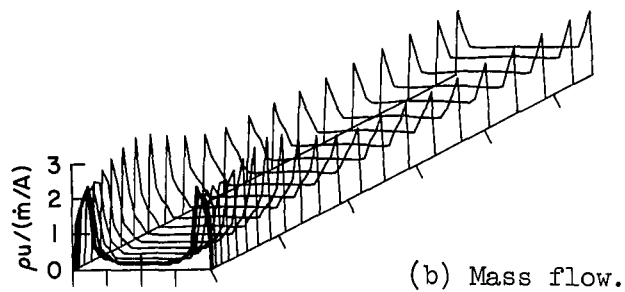
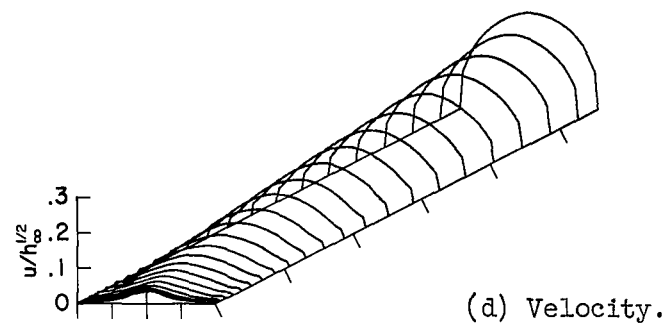
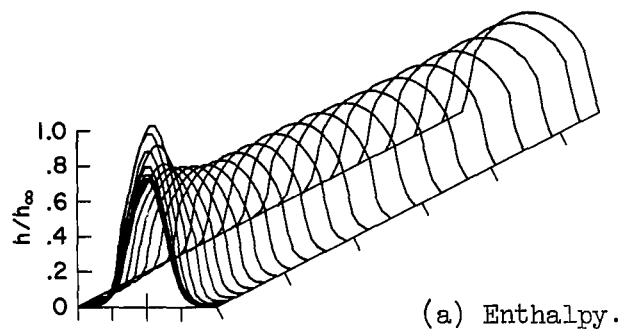


(j) Local heat transfer rate.



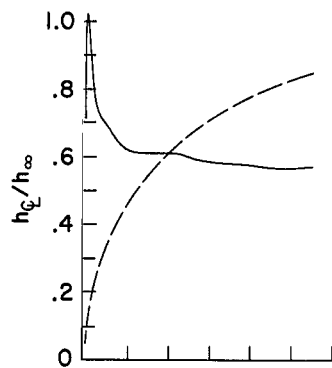
(k) Pressure.

Figure 22.- Concluded.

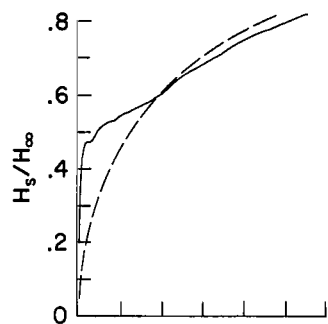


$I = 1000$	A	$h_\infty = 1.62 \times 10^8$	J/kg
$\dot{m} = .0113$	kg/s	$\dot{m}/A = 22.4$	kg/sm ²
$R = .0127$	m	$h_\infty \dot{m}/A = 3.63 \times 10^9$	W/m ²
$z_0 = 11.2$	m	$\sqrt{h_\infty} = 1.28 \times 10^4$	m/s
		$p_0 = 1.013 \times 10^5$	N/m ² (1.0 atm)
		$H_\infty = 7.04 \times 10^7$	J/kg
		$E_\infty = 409$	V/m
		$q_\infty = 5.14 \times 10^6$	W/m ²

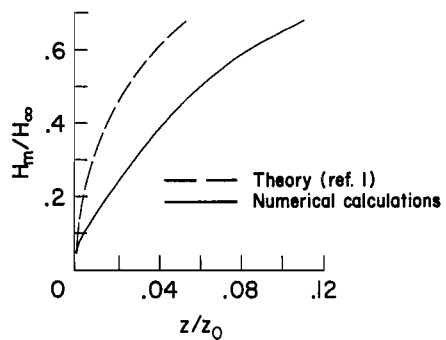
Figure 23.- The constricted arc with radiation losses much greater than conduction losses.



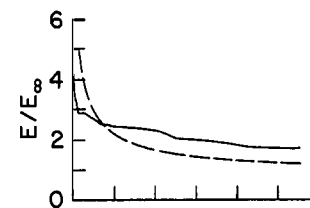
(f) Center-line enthalpy.



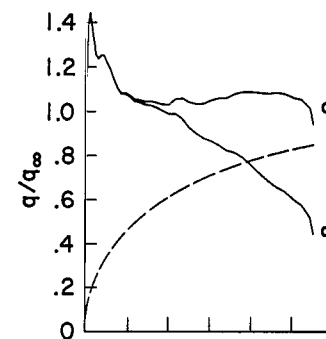
(g) Space-average enthalpy.



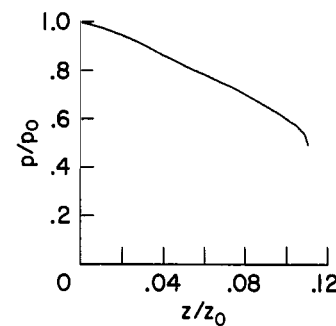
(h) Mass-average enthalpy.



(i) Voltage gradient.

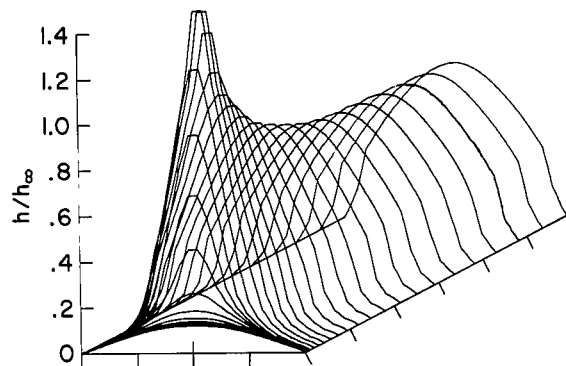


(j) Local heat transfer rate.

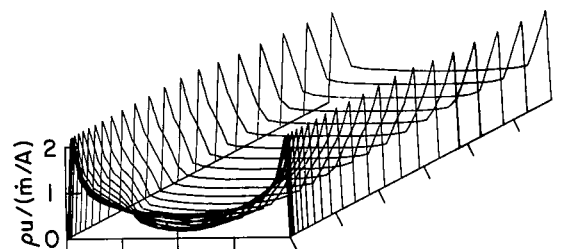


(k) Pressure.

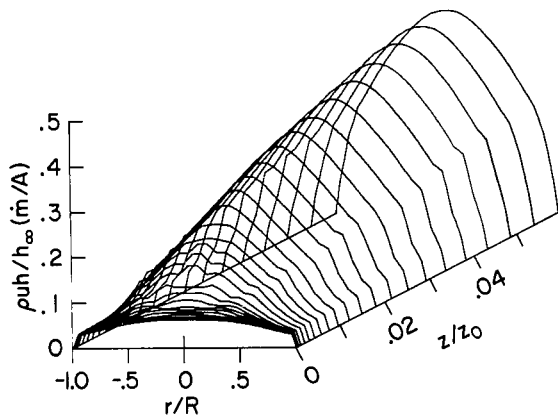
Figure 23.- Concluded.



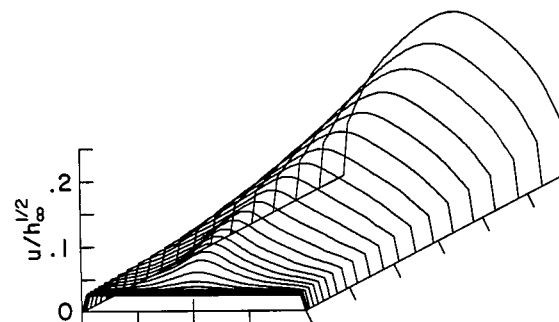
(a) Enthalpy.



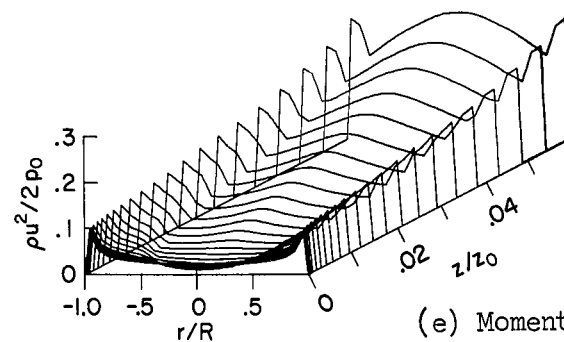
(b) Mass flow.



(c) Energy flux density



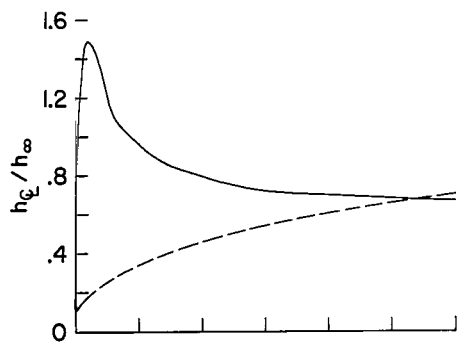
(d) Velocity.



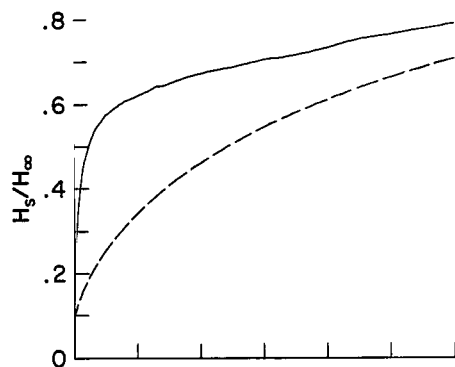
(e) Momentum flux.

$I = 580$	A	$h_{\infty} = 1.89 \times 10^8$	J/kg
$\dot{m} = .00353$	kg/s	$\dot{m}/A = 27.8$	kg/sm ²
$R = .00635$	m	$h_{\infty} \dot{m}/A = 5.29 \times 10^9$	W/m ²
$z_0 = 3.50$	m	$\sqrt{h_{\infty}} = 1.37 \times 10^4$	m/s
		$p_0 = 1.17 \times 10^5$	N/m ² (1.16 atm)
		$H_{\infty} = 8.17 \times 10^7$	J/kg
		$E_{\infty} = 819$	V/m
		$q_{\infty} = 1.19 \times 10^7$	W/m ²

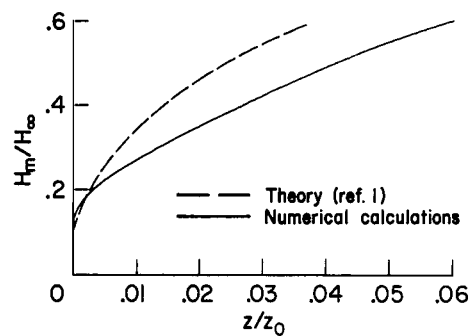
Figure 24.- The numerical solutions for a 1.27-cm constricted arc with viscous forces included.



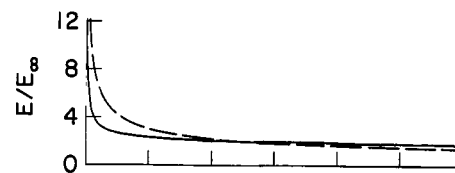
(f) Center-line enthalpy.



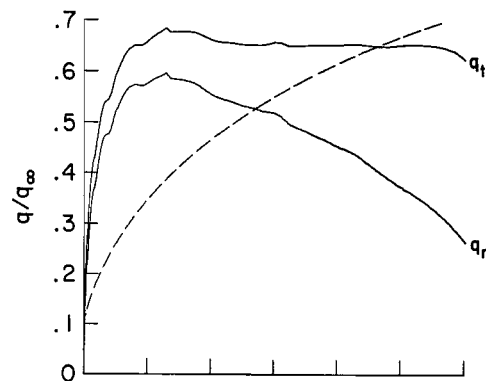
(g) Space-average enthalpy.



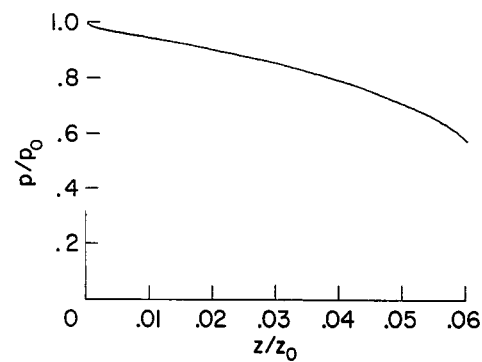
(h) Mass-average enthalpy.



(i) Voltage gradient.

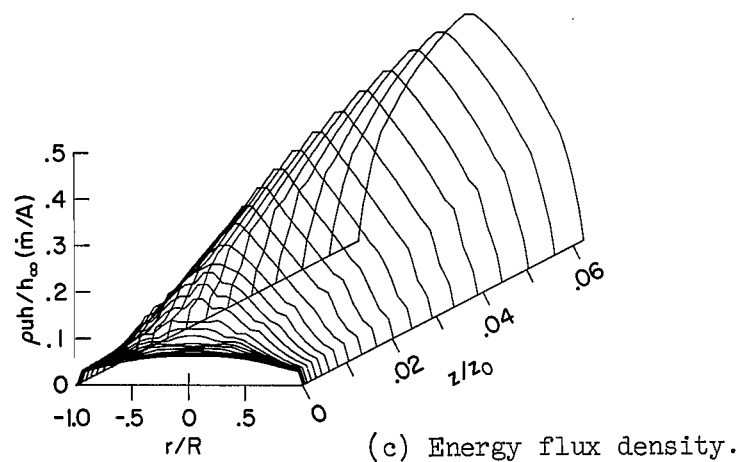
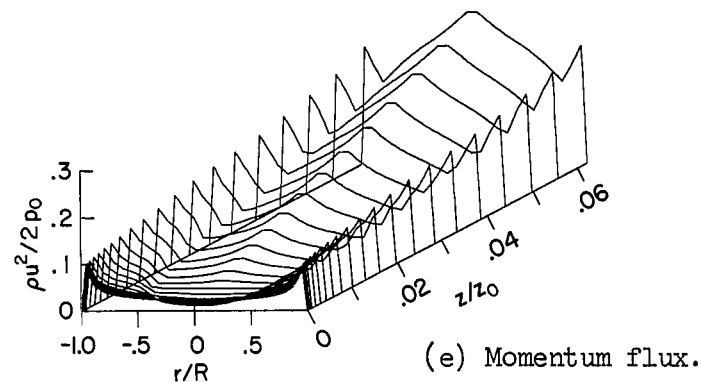
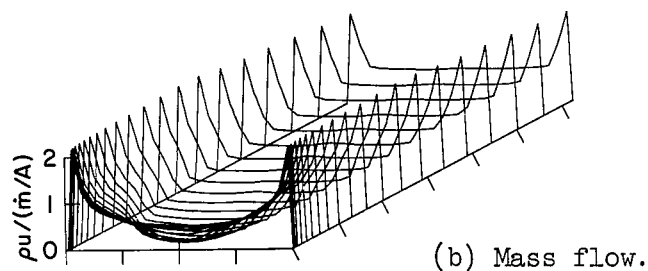
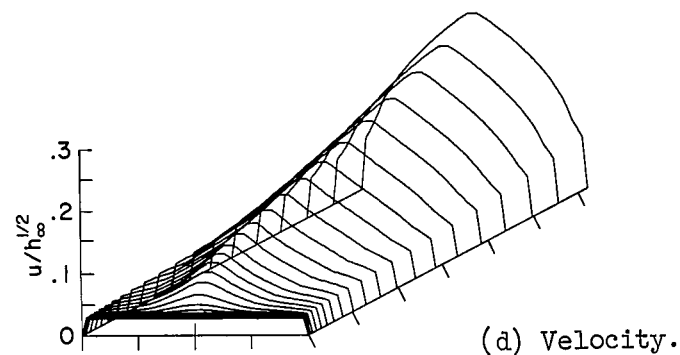
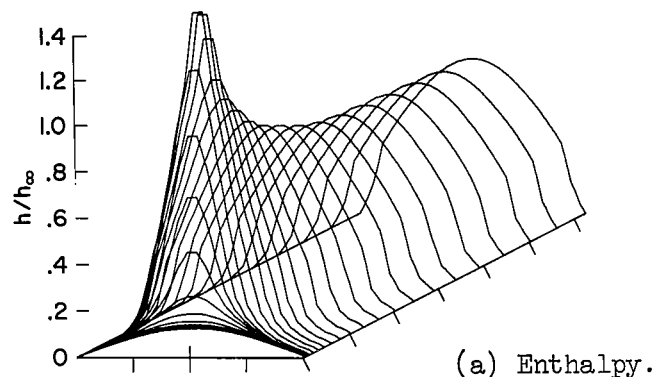


(j) Local heat transfer rate.



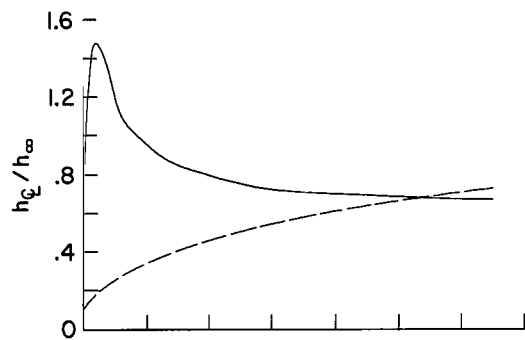
(k) Pressure.

Figure 24.- Concluded.

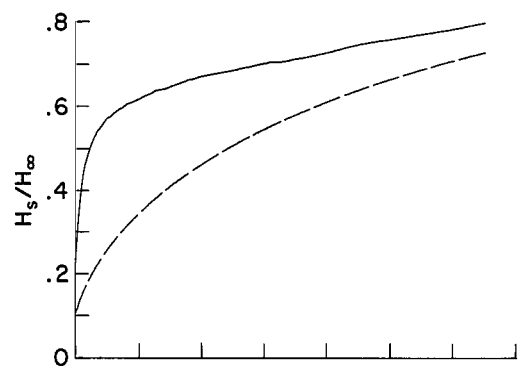


$I = 580$	A	$h_\infty = 1.89 \times 10^8$	J/kg
$\dot{m} = .00353$	kg/s	$\dot{m}/A = 27.8$	kg/sm ²
$R = .00635$	m	$h_\infty \dot{m}/A = 5.29 \times 10^9$	W/m ²
$z_0 = 3.50$	m	$\sqrt{h_\infty} = 1.37 \times 10^4$	m/s
		$p_0 = 1.17 \times 10^5$	N/m ² (1.16 atm)
		$H_\infty = 8.17 \times 10^7$	J/kg
		$E_\infty = 819$	V/m
		$q_\infty = 1.19 \times 10^7$	W/m ²

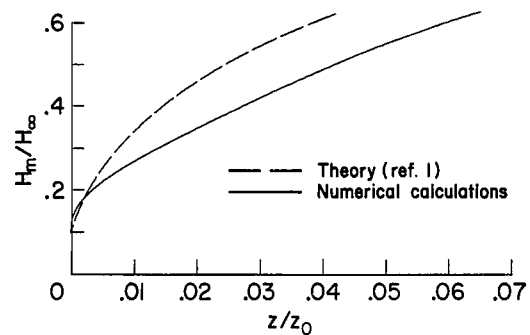
Figure 25.- The numerical solutions for a 1.27-cm constricted arc with viscosity set equal to zero.



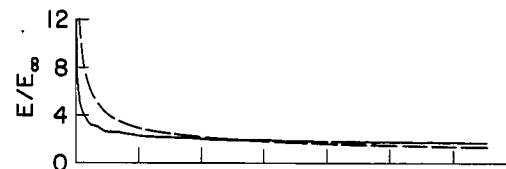
(f) Center-line enthalpy.



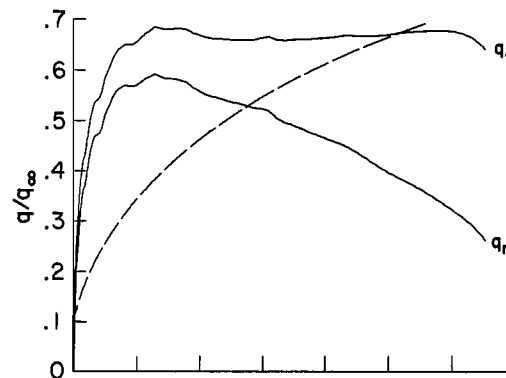
(g) Space-average enthalpy.



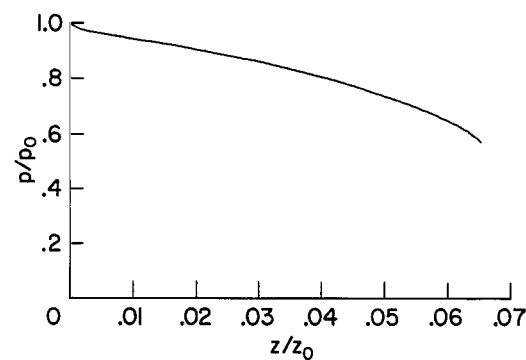
(h) Mass-average enthalpy.



(i) Voltage gradient.

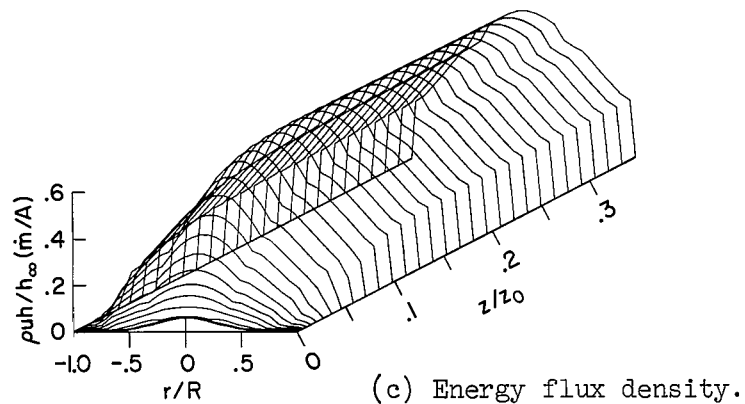
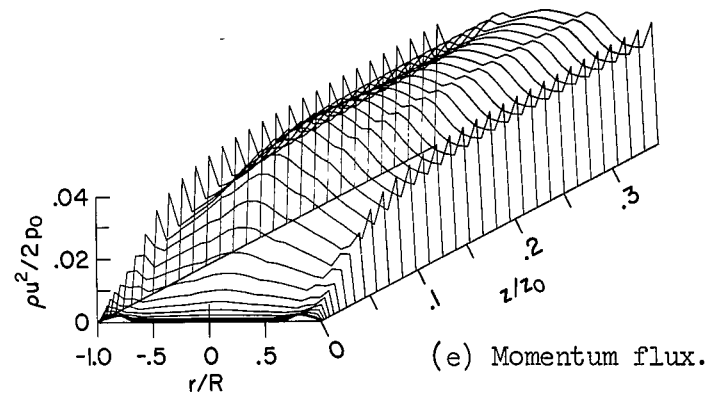
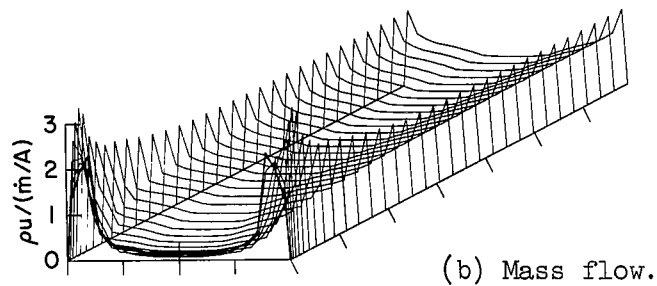
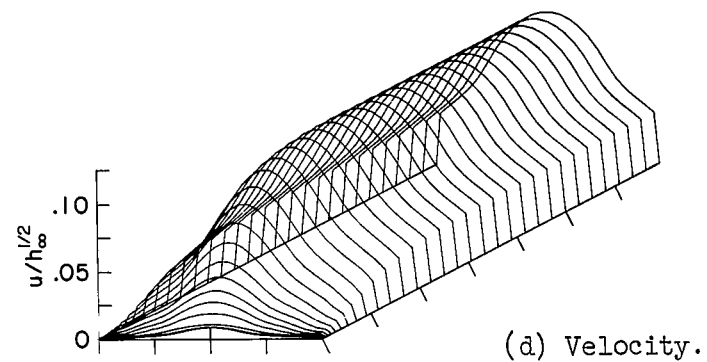
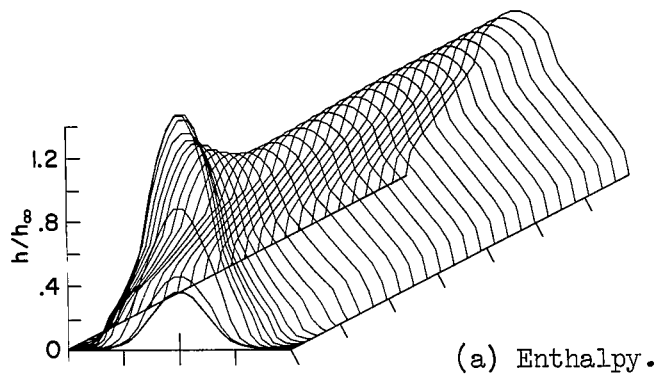


(j) Local heat transfer rate.



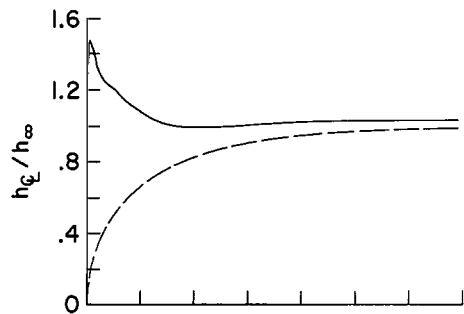
(k) Pressure.

Figure 25.- Concluded.

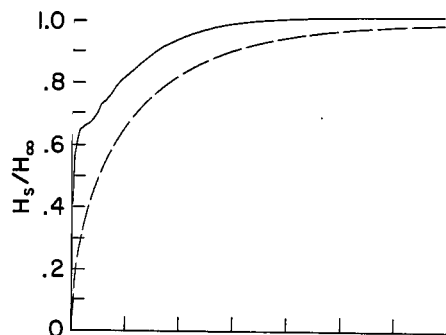


$I = 500$	A	$h_\infty = 3.25 \times 10^8$	J/kg
$\dot{m} = .000227$	kg/s	$\dot{m}/A = 7.16$	kg/sm ²
$R = .00318$	m	$h_\infty \dot{m}/A = 2.33 \times 10^9$	W/m ²
$z_0 = .225$	m	$\sqrt{h_\infty} = 1.80 \times 10^4$	m/s
		$p_0 = 1.013 \times 10^5$	N/m ² (1.0 atm)
		$H_\infty = 1.41 \times 10^8$	J/kg
		$E_\infty = 1638$	V/m
		$q_\infty = 4.11 \times 10^7$	W/m ²

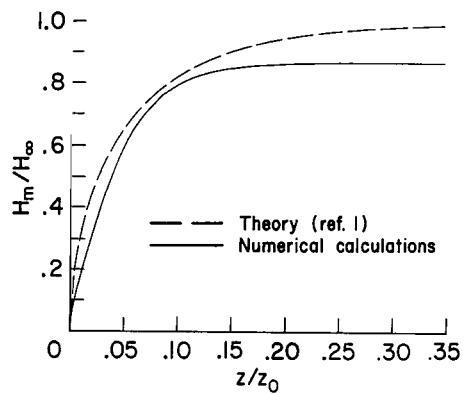
Figure 26.- The numerical solutions for a 0.635-cm constricted arc with viscous forces included.



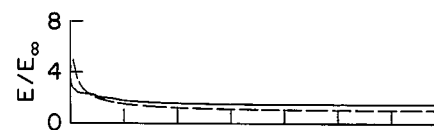
(f) Center-line enthalpy.



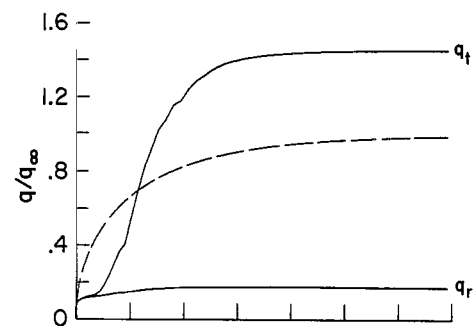
(g) Space-average enthalpy.



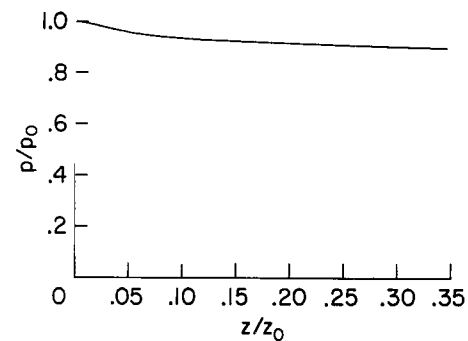
(h) Mass-average enthalpy.



(i) Voltage gradient.

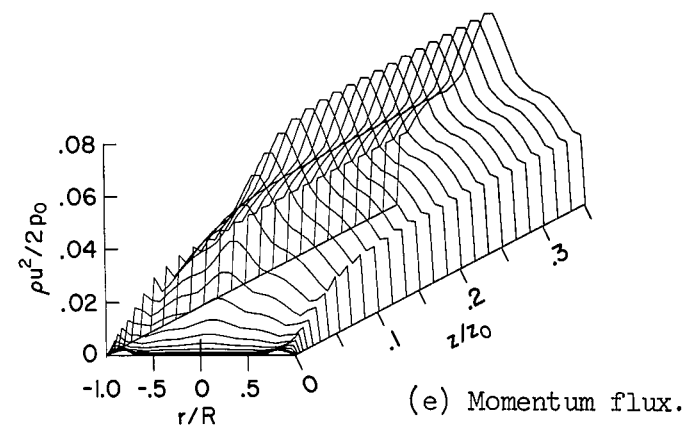
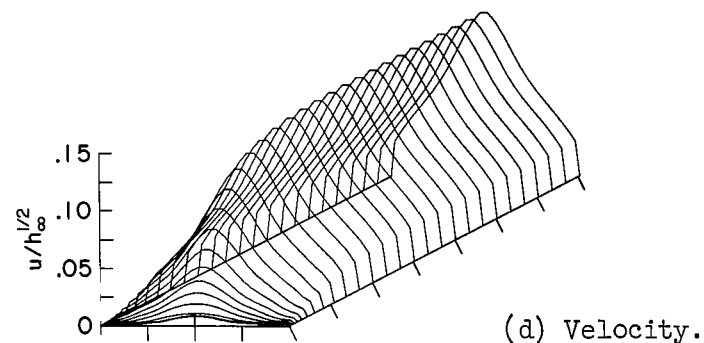
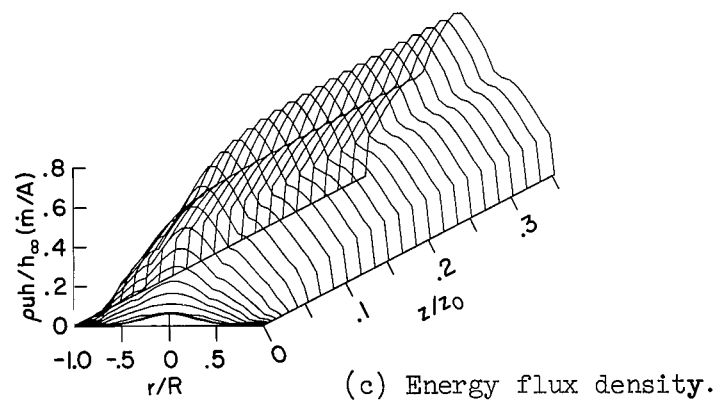
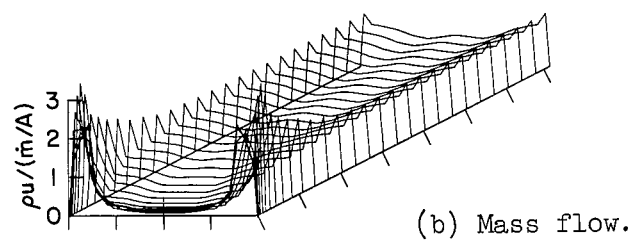
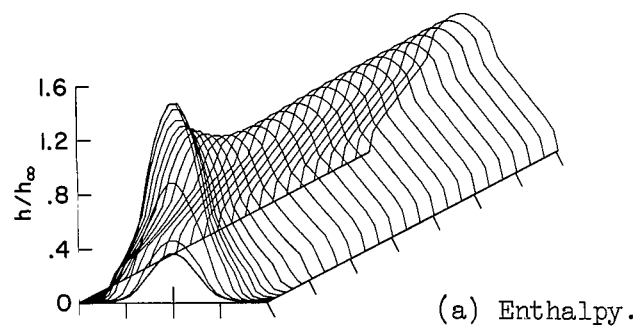


(j) Local heat transfer rate.



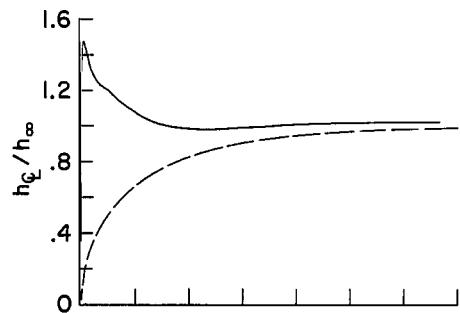
(k) Pressure.

Figure 26.- Concluded.

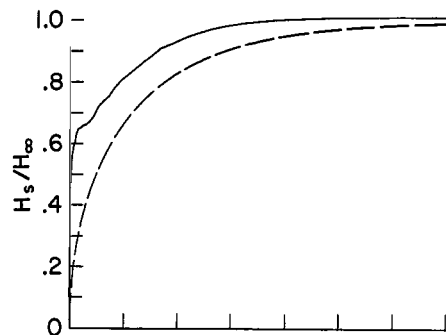


$I = 500$	A	$h_\infty = 3.25 \times 10^8$	J/kg
$\dot{m} = .000227$	kg/s	$\dot{m}/A = 7.16$	kg/sm ²
$R = .00318$	m	$h_\infty \dot{m}/A = 2.33 \times 10^9$	W/m ²
$z_0 = .225$	m	$\sqrt{h_\infty} = 1.80 \times 10^4$	m/s
		$p_0 = 1.013 \times 10^5$	N/m ² (1.0 atm)
		$H_\infty = 1.41 \times 10^8$	J/kg
		$E_\infty = 1638$	V/m
		$q_\infty = 4.11 \times 10^7$	W/m ²

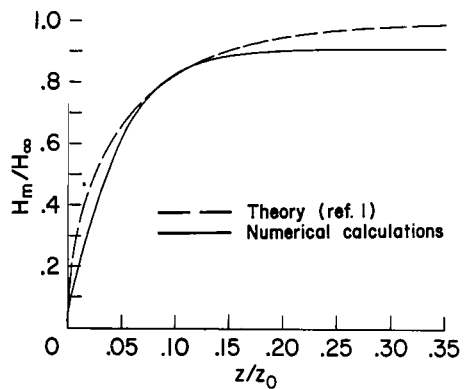
Figure 27.- The numerical solutions for a 0.635-cm constricted arc with viscosity set equal to zero.



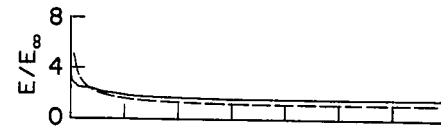
(f) Center-line enthalpy.



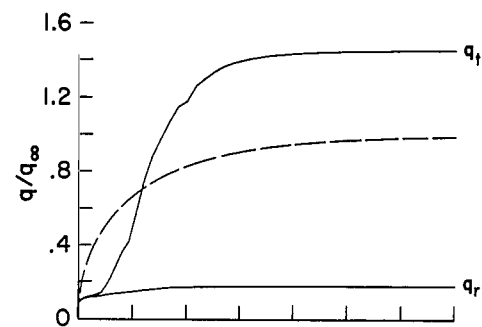
(g) Space-average enthalpy.



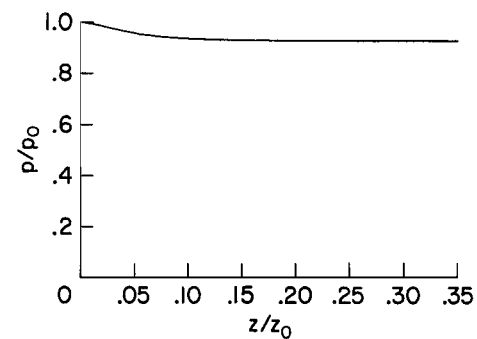
(h) Mass-average enthalpy.



(i) Voltage gradient.

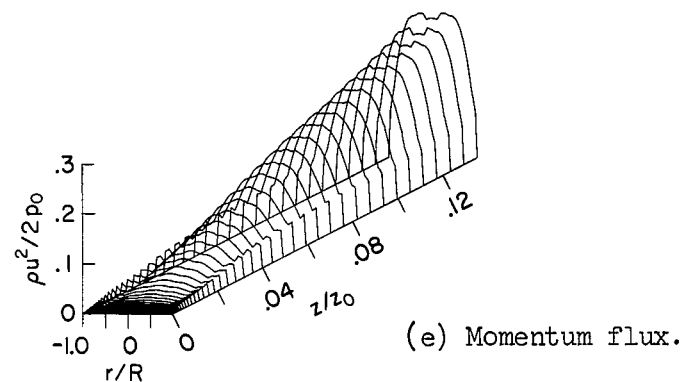
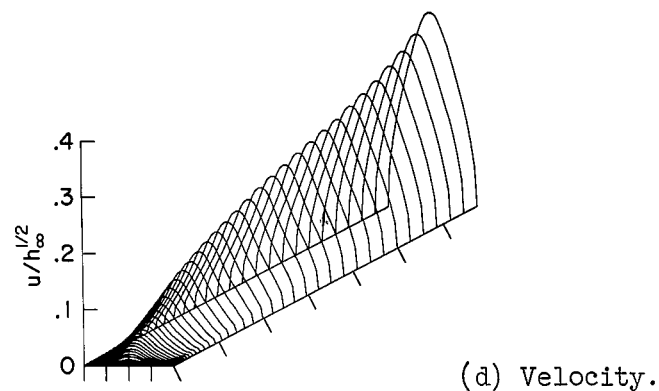
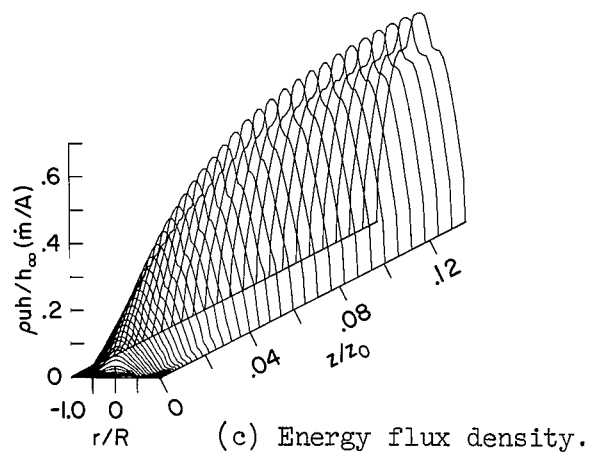
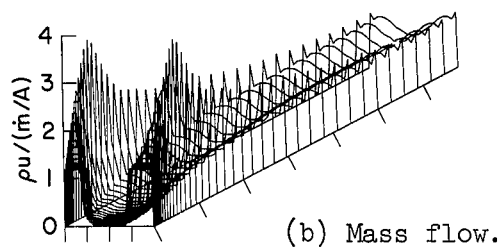
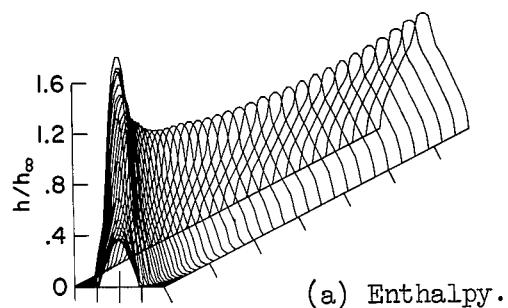


(j) Local heat transfer rate.



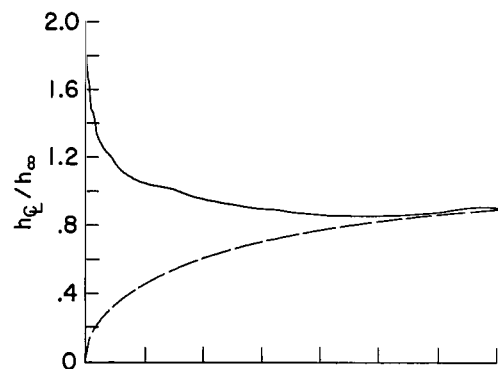
(k) Pressure.

Figure 27.- Concluded.

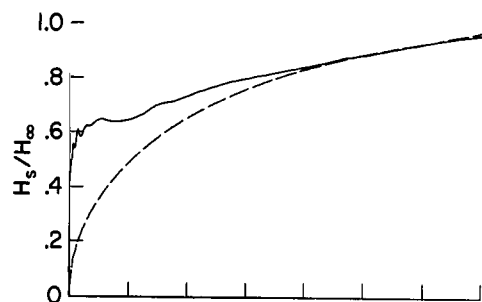


$I = 1000$	A	$h_{\infty} = 3.25 \times 10^8$	J/kg
$\dot{m} = .00162$	kg/s	$\dot{m}/A = 12.8$	kg/sm ²
$R = .00635$	m	$h_{\infty} \dot{m}/A = 4.15 \times 10^9$	W/m ²
$z_0 = 1.60$	m	$\sqrt{h_{\infty}} = 1.81 \times 10^4$	m/s
		$p_0 = 1.013 \times 10^5$	N/m ² (1.0 atm)
		$H_{\infty} = 1.41 \times 10^8$	J/kg
		$E_{\infty} = 819$	V/m
		$q_{\infty} = 2.05 \times 10^7$	W/m ²

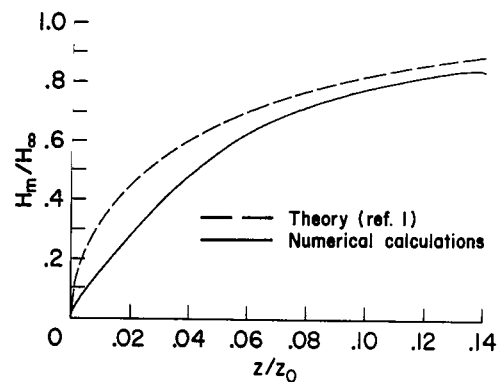
Figure 28.- The numerical solutions with the effects of radial convection included.



(f) Center-line enthalpy.



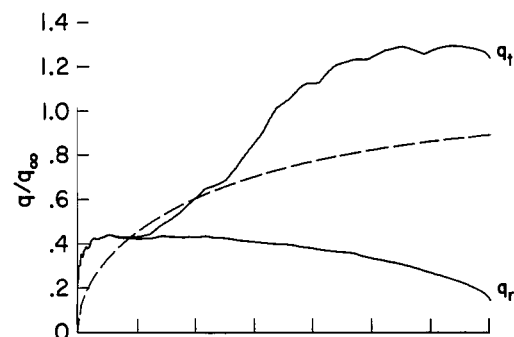
(g) Space-average enthalpy.



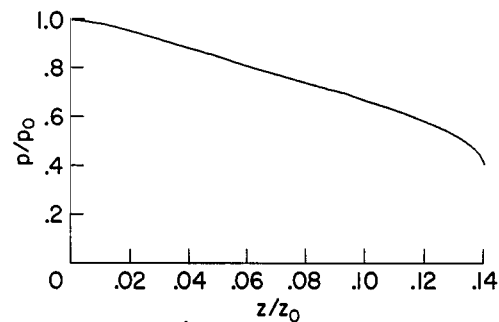
(h) Mass-average enthalpy.



(i) Voltage gradient.

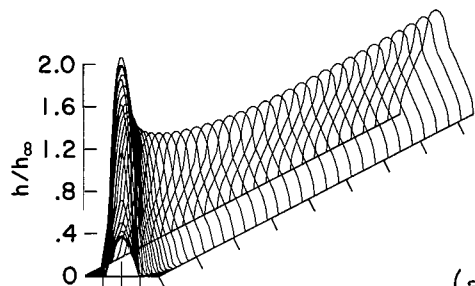


(j) Local heat transfer rate.

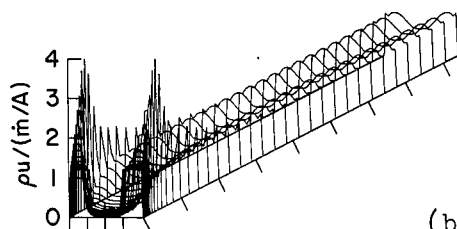


(k) Pressure.

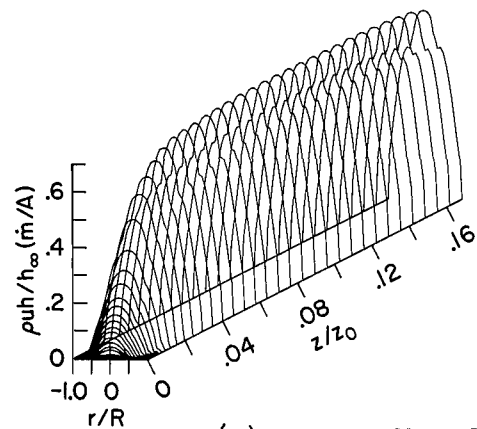
Figure 28. - Concluded.



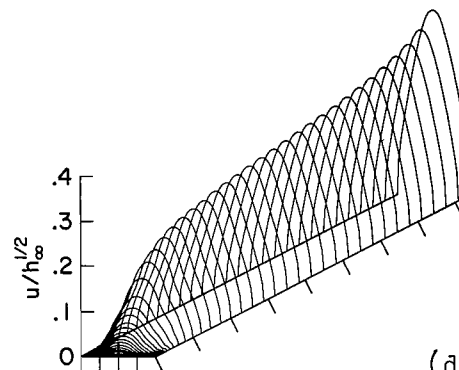
(a) Enthalpy.



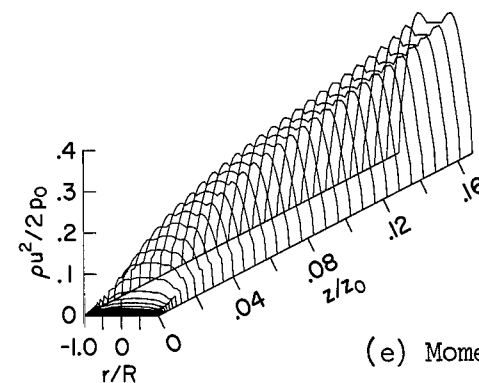
(b) Mass flow.



(c) Energy flux density.



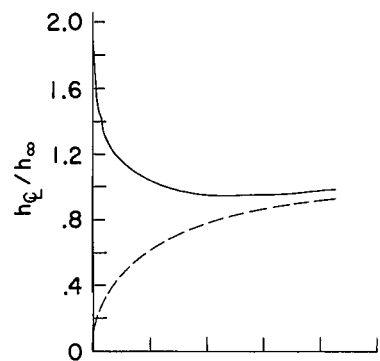
(d) Velocity.



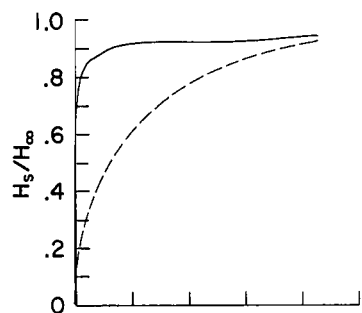
(e) Momentum flux.

$I = 1000$	A	$h_\infty = 3.25 \times 10^8$	J/kg
$\dot{m} = .00162$	kg/s	$\dot{m}/A = 12.8$	kg/sm ²
$R = .00635$	m	$h_\infty \dot{m}/A = 4.15 \times 10^9$	W/m ²
$z_0 = 1.60$	m	$\sqrt{h_\infty} = 1.81 \times 10^4$	m/s
		$p_0 = 1.013 \times 10^5$	N/m ² (1.0 atm)
		$H_\infty = 1.41 \times 10^8$	J/kg
		$E_\infty = 819$	V/m
		$q_\infty = 2.05 \times 10^7$	W/m ²

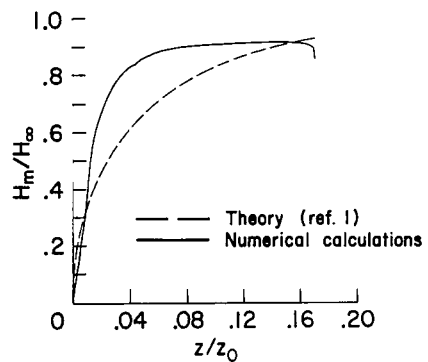
Figure 29.- The numerical solutions without radial convection of energy and momentum.



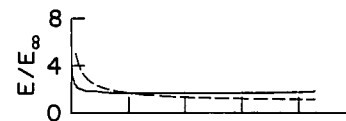
(f) Center-line enthalpy.



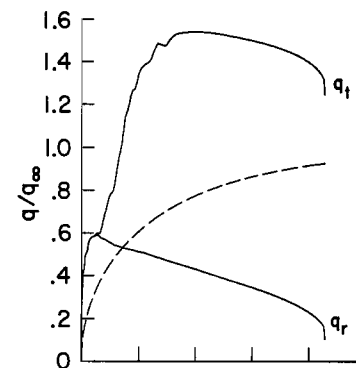
(g) Space-average enthalpy.



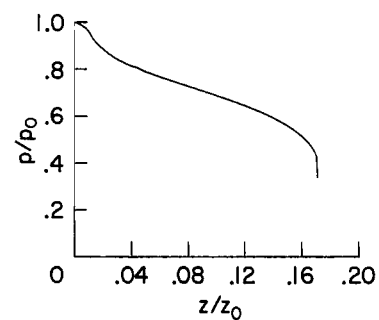
(h) Mass-average enthalpy.



(i) Voltage gradient.

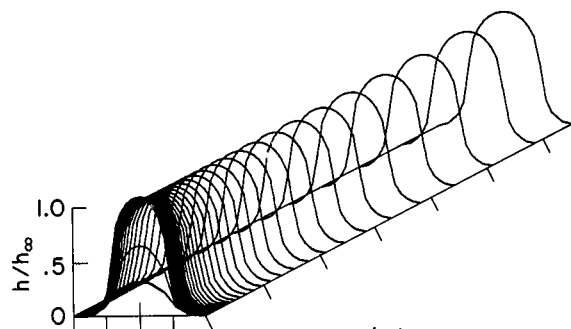


(j) Local heat transfer rate.

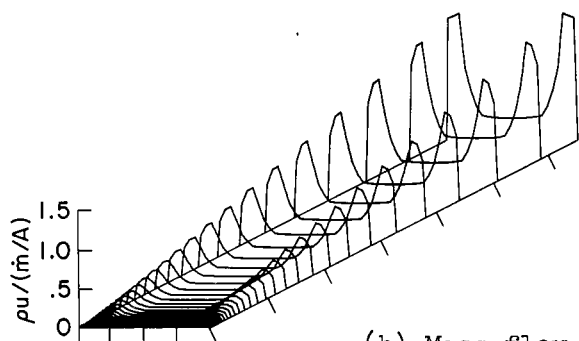


(k) Pressure.

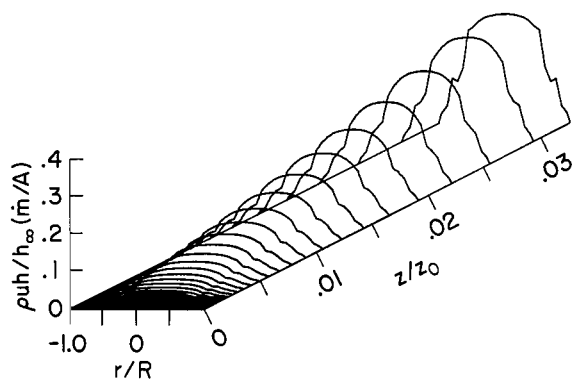
Figure 29.- Concluded.



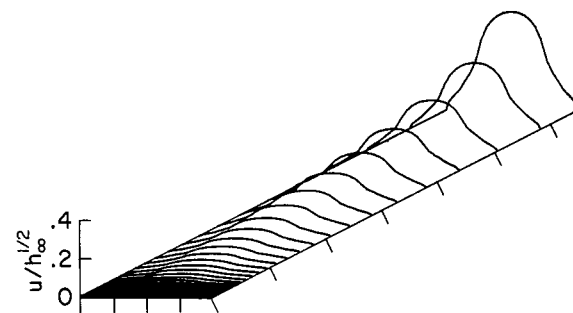
(a) Enthalpy.



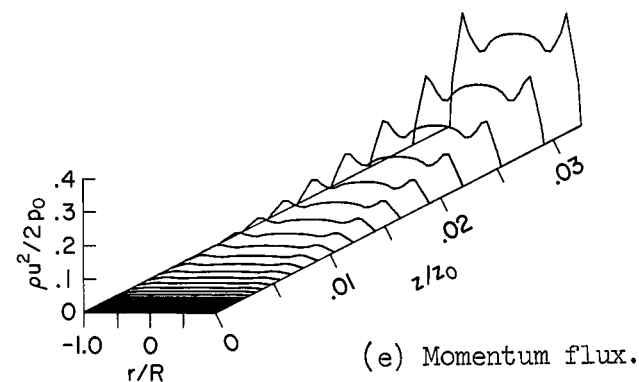
(b) Mass flow.



(c) Energy flux density.



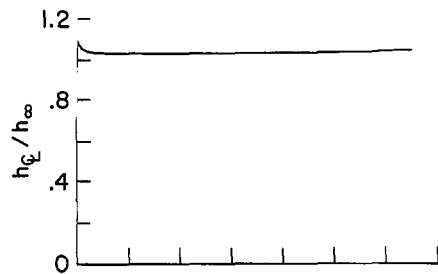
(d) Velocity.



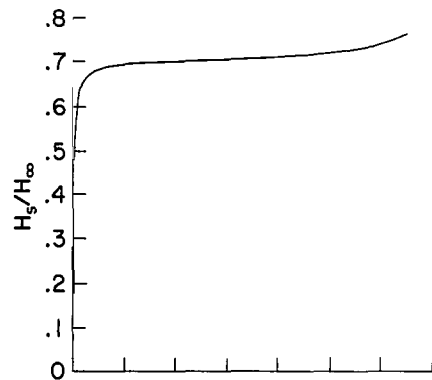
(e) Momentum flux.

$I = 1000$	A	$h_\infty = 3.28 \times 10^9$	J/kg
$\dot{m} = .0538$	kg/s	$\dot{m}/A = 6.85$	kg/sm ²
$R = .005$	m	$h_\infty \dot{m}/A = 2.25 \times 10^{10}$	W/m ²
$z_0 = 3.42$	m	$\sqrt{h_\infty} = 5.73 \times 10^4$	m/s
		$p_0 = 1.013 \times 10^5$	N/m ² (1.00 atm)
		$H_\infty = 1.42 \times 10^9$	J/kg
		$E_\infty = 1283$	V/m
		$q_\infty = 4.10 \times 10^7$	W/m ²

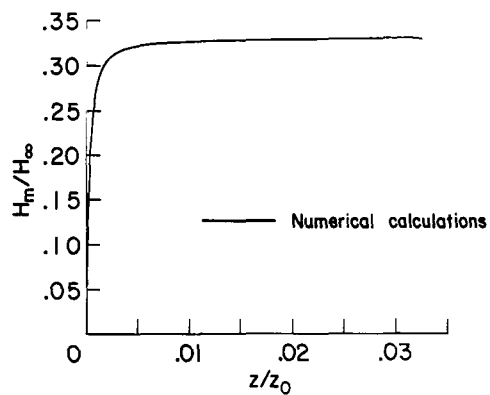
Figure 30.- The hydrogen arc with transpiration-cooled constrictor walls.



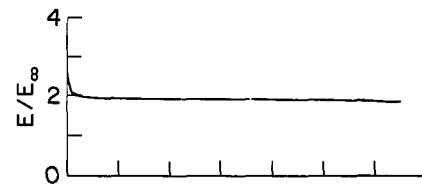
(f) Center-line enthalpy.



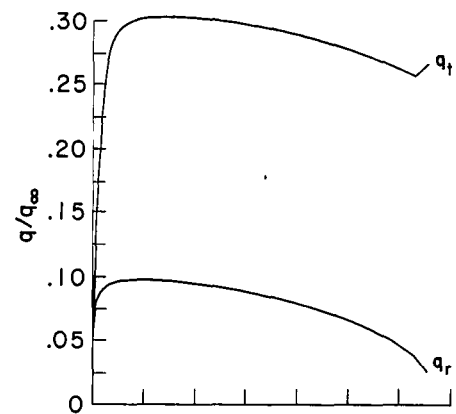
(g) Space-average enthalpy.



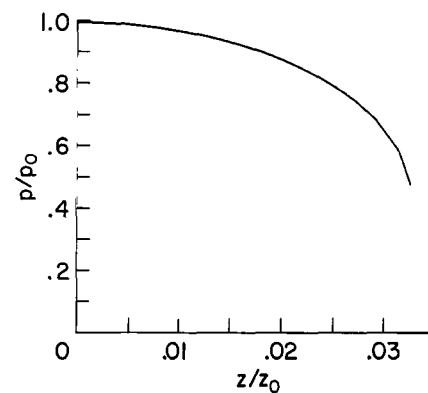
(h) Mass-average enthalpy.



(i) Voltage gradient.

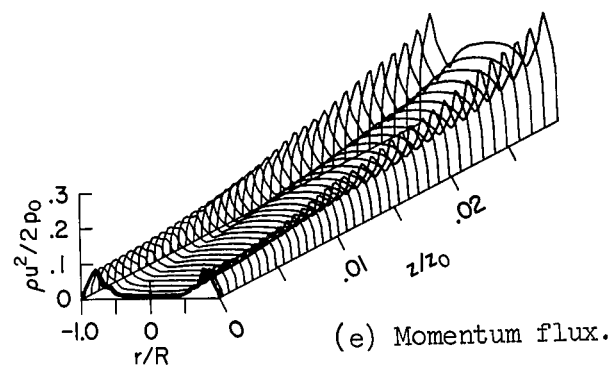
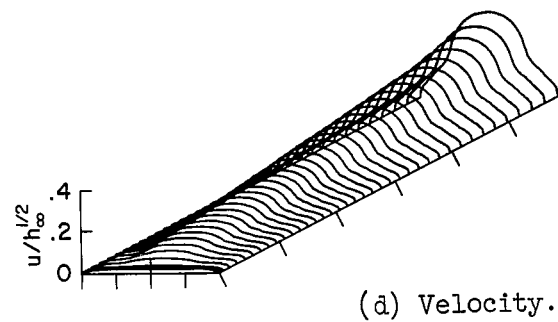
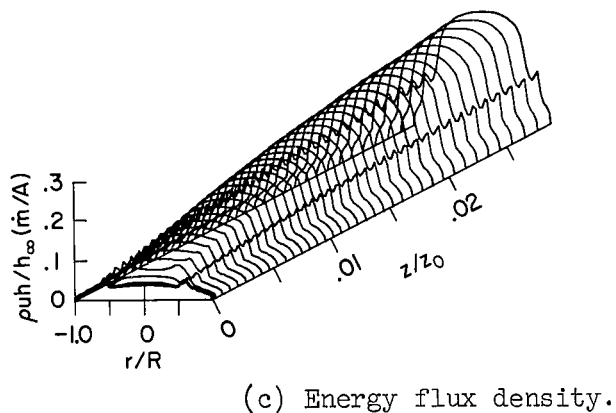
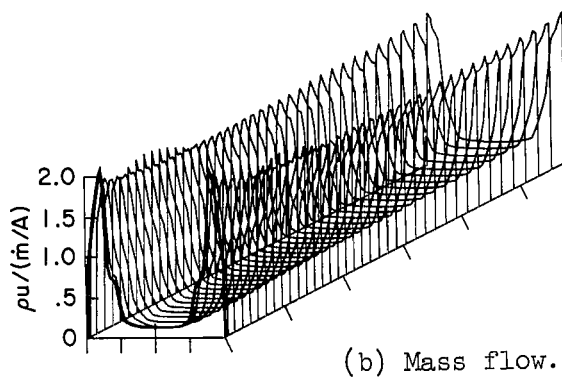
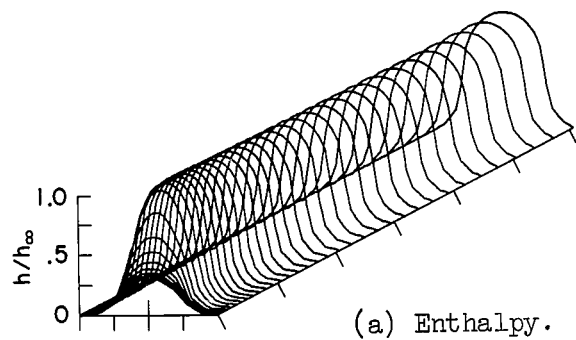


(j) Local heat transfer rate



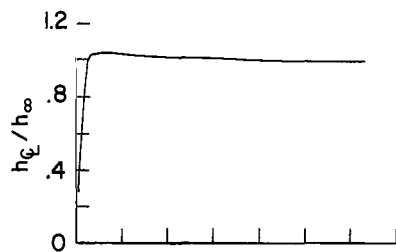
(k) Pressure.

Figure 30.- Concluded.

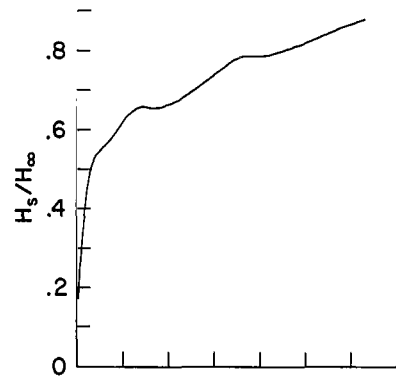


$I = 1000$	A	$h_\infty = 3.28 \times 10^9$	J/kg
$\dot{m} = .0538$	kg/s	$\dot{m}/A = 6.85$	kg/sm ²
$R = .005$	m	$h_\infty \dot{m}/A = 2.25 \times 10^{10}$	W/m ²
$z_0 = 3.42$	m	$\sqrt{h_\infty} = 5.73 \times 10^4$	m/s
		$p_0 = 1.013 \times 10^5$	N/m ² (1.0 atm)
		$H_\infty = 1.42 \times 10^9$	J/kg
		$E_\infty = 1283$	V/m
		$q_\infty = 4.10 \times 10^7$	W/m ²

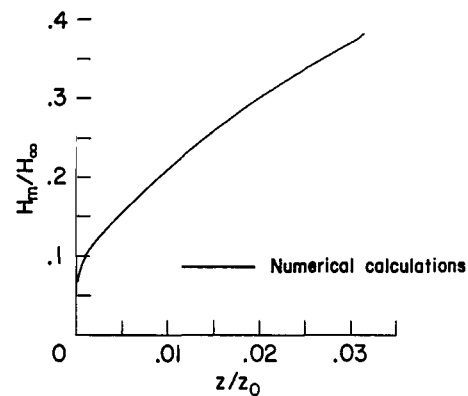
Figure 31.- The hydrogen arc with water-cooled constrictor walls.



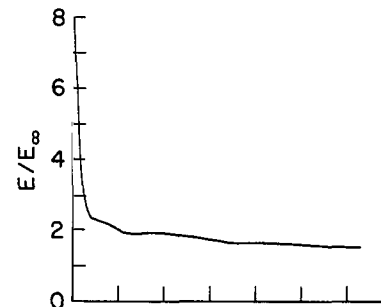
(f) Center-line enthalpy.



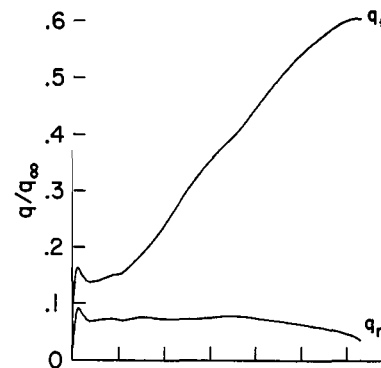
(g) Space-average enthalpy.



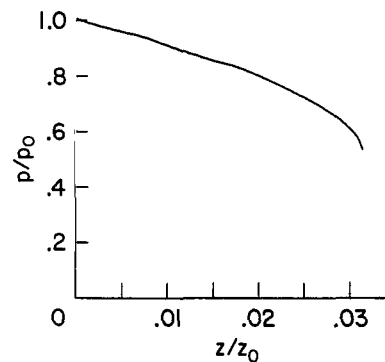
(h) Mass-average enthalpy.



(i) Voltage gradient.

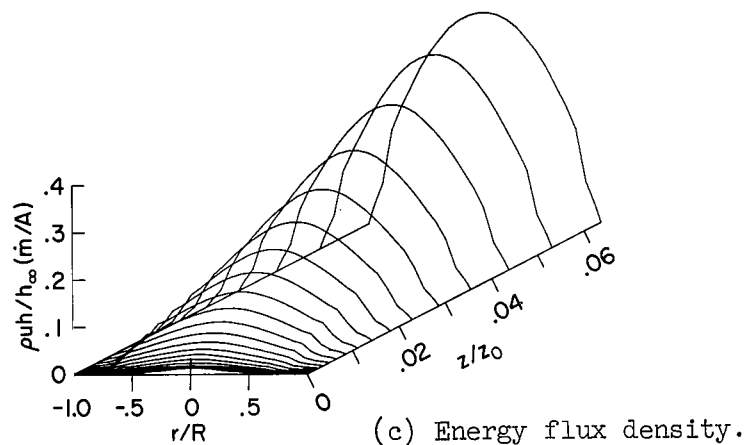
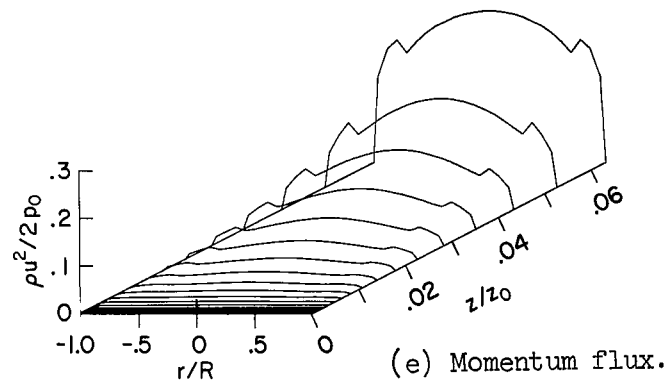
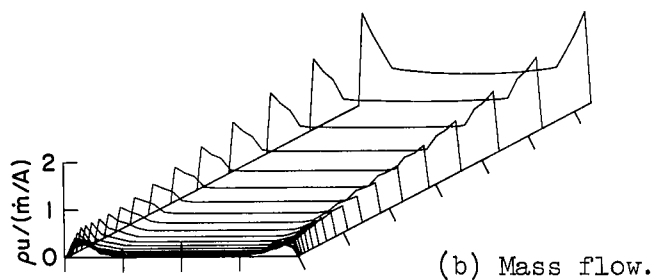
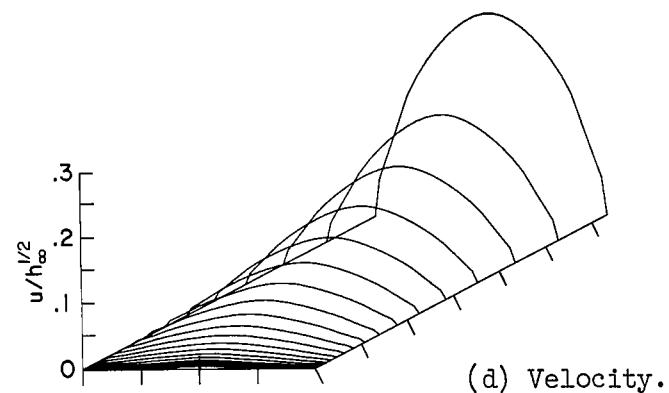
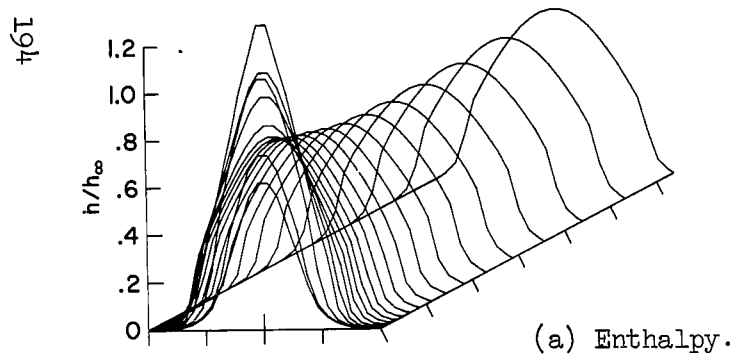


(j) Local heat transfer rate.



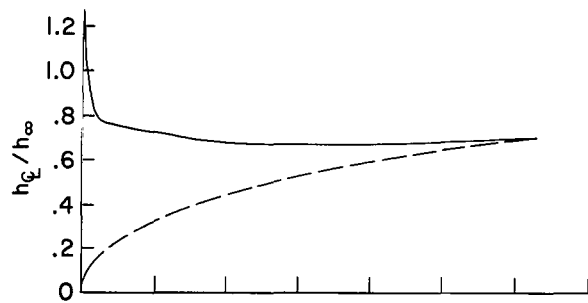
(k) Pressure.

Figure 31.- Concluded.

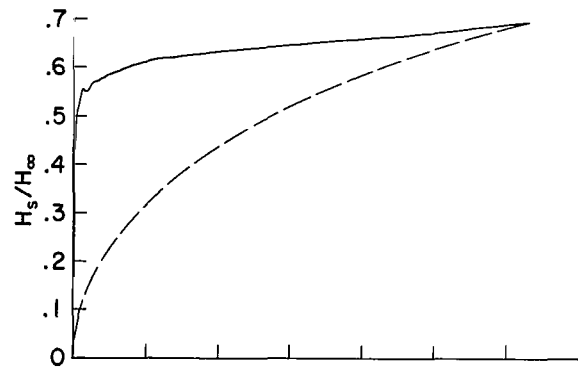


$I = 580$	A	$h_\infty = 1.89 \times 10^8$	J/kg
$\dot{m} = .00353$	kg/s	$\dot{m}/A = 27.8$	kg/sm ²
$R = .00635$	m	$h_\infty \dot{m}/A = 5.29 \times 10^9$	W/m ²
$z_0 = 3.50$	m	$\sqrt{h_\infty} = 1.37 \times 10^4$	m/s
		$p_0 = 1.17 \times 10^5$	N/m ² (1.16 atm)
		$H_\infty = 8.17 \times 10^7$	J/kg
		$E_\infty = 819$	V/m
		$q_\infty = 1.19 \times 10^7$	W/m ²

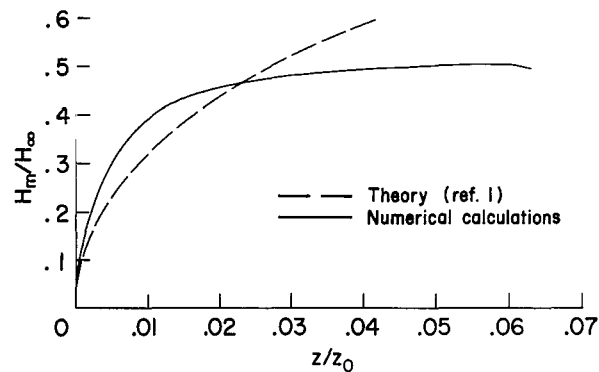
Figure 32.- The nitrogen arc with transpiration-cooled constrictor walls.



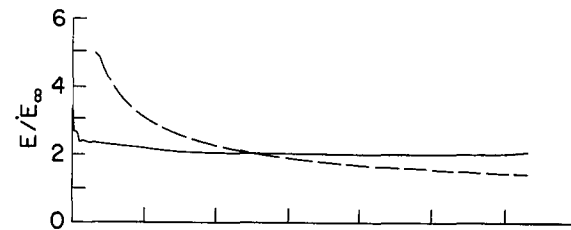
(f) Center-line enthalpy.



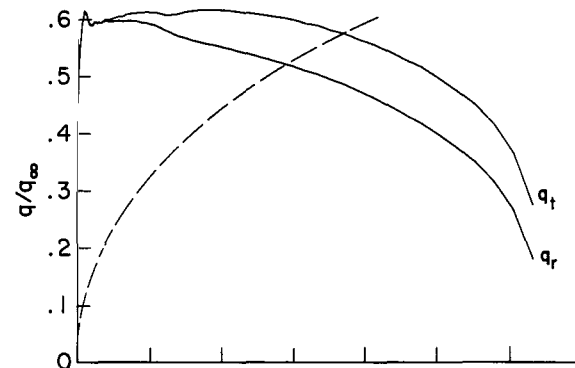
(g) Space-average enthalpy.



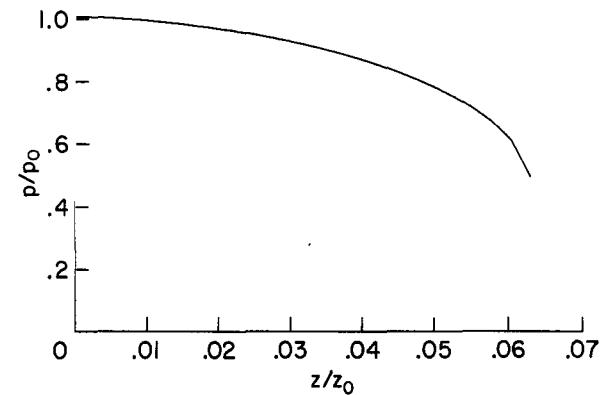
(h) Mass-average enthalpy.



(i) Voltage gradient.

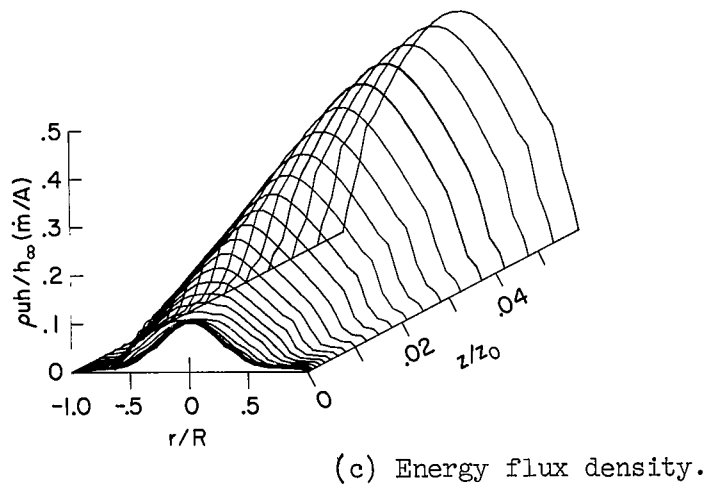
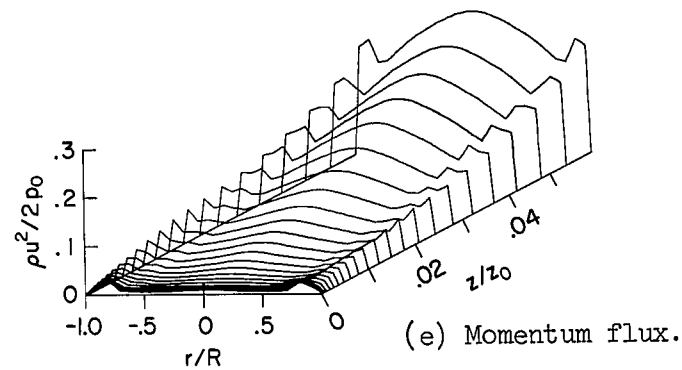
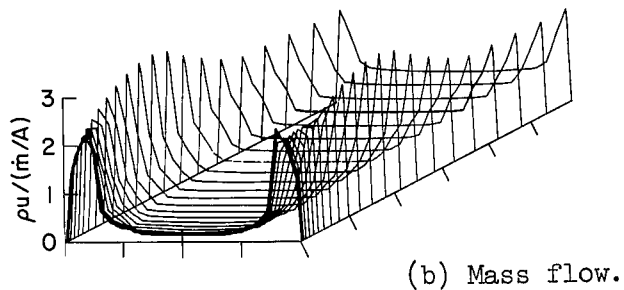
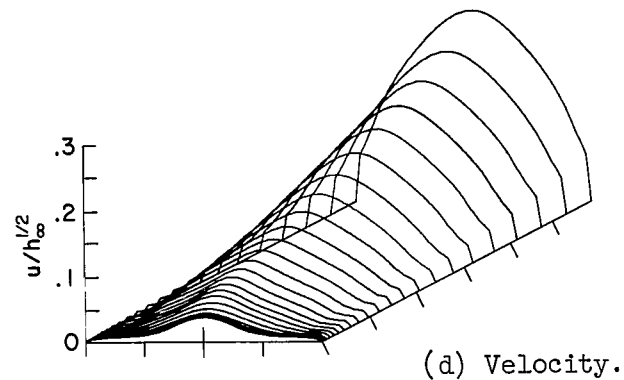
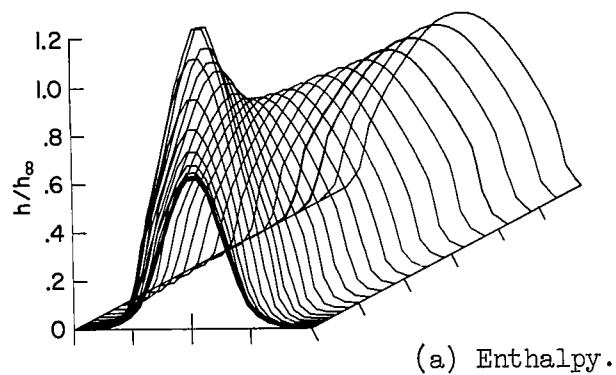


(j) Local heat transfer rate.



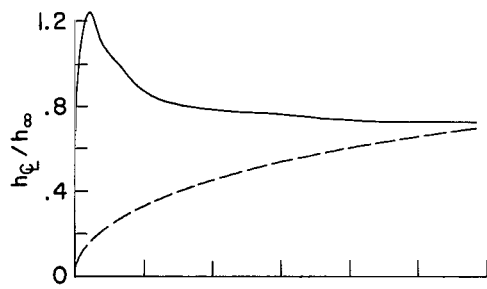
(k) Pressure.

Figure 32.- Concluded.

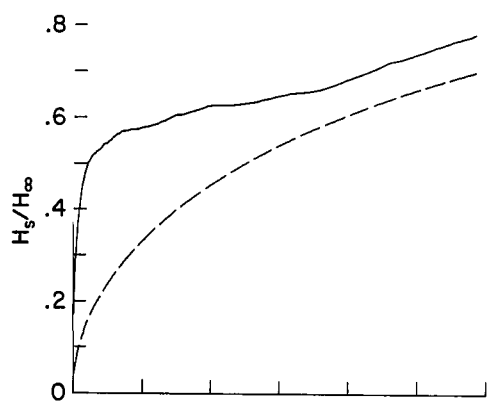


$I = 580$	A	$h_{\infty} = 1.89 \times 10^8$	J/kg
$\dot{m} = .00353$	kg/s	$\dot{m}/A = 27.8$	kg/sm ²
$R = .00635$	m	$h_{\infty} \dot{m}/A = 5.29 \times 10^9$	W/m ²
$z_0 = 3.50$	m	$\sqrt{h_{\infty}} = 1.37 \times 10^4$	m/s
		$p_0 = 1.17 \times 10^5$	N/m ² (1.16 atm)
		$H_{\infty} = 8.17 \times 10^7$	J/kg
		$E_{\infty} = 819$	V/m
		$q_{\infty} = 1.19 \times 10^7$	W/m ²

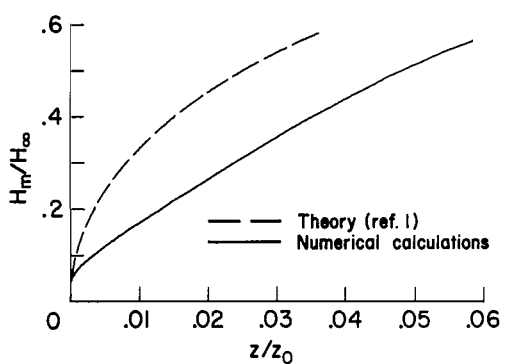
Figure 33.- The nitrogen arc with water-cooled constrictor walls.



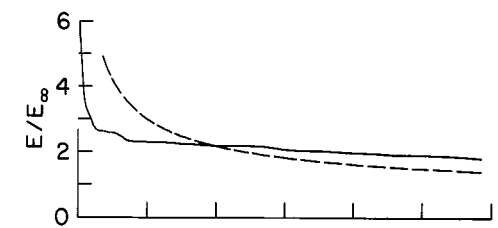
(f) Center-line enthalpy.



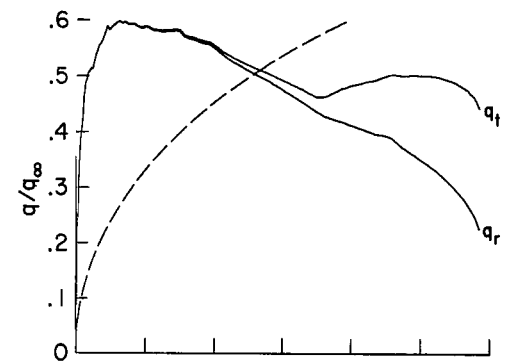
(g) Space-average enthalpy.



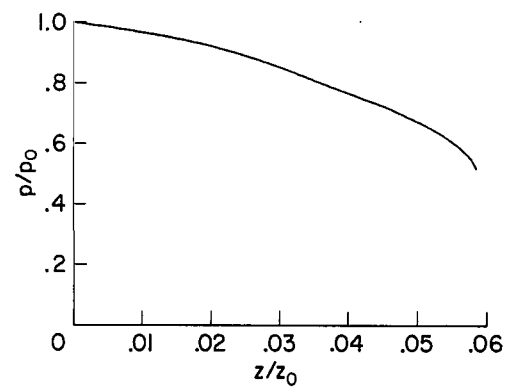
(h) Mass-average enthalpy.



(i) Voltage gradient.

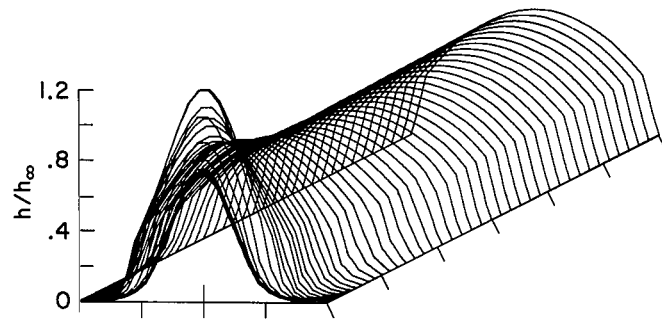


(j) Local heat transfer rate.

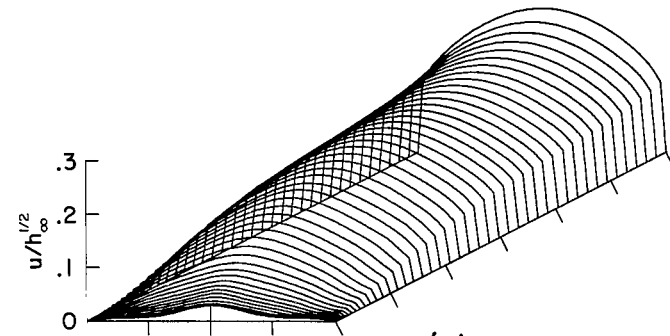


(k) Pressure.

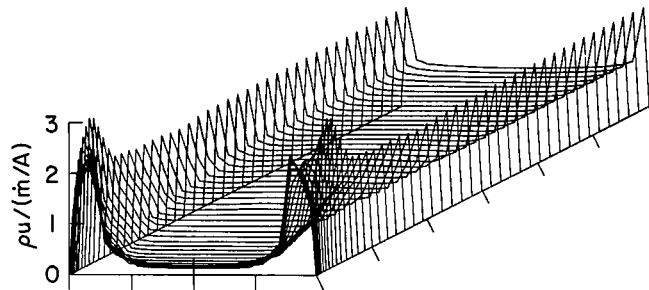
Figure 33.- Concluded.



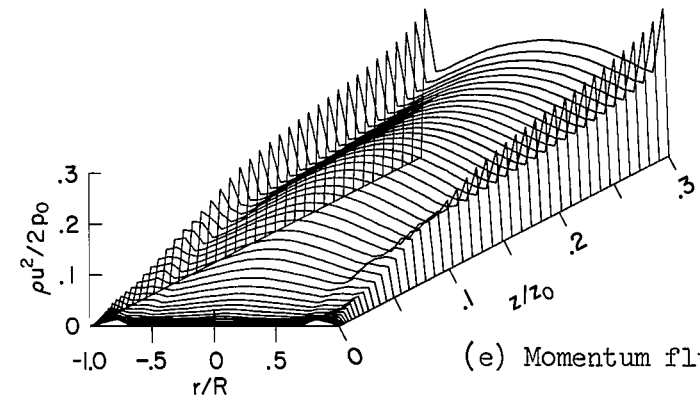
(a) Enthalpy.



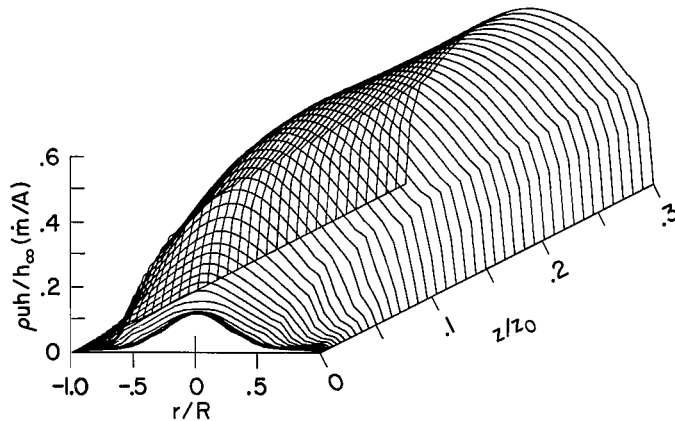
(d) Velocity.



(b) Mass flow.



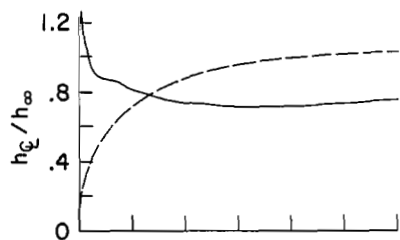
(e) Momentum flux.



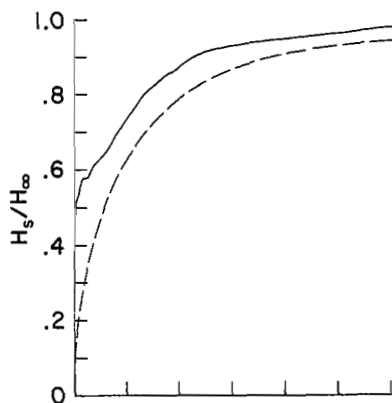
(c) Energy flux density.

$I = 500$	A	$h_{\infty} = 1.63 \times 10^8$	J/kg
$\dot{m} = .00227$	kg/s	$\dot{m}/A = 17.9$	kg/sm ²
$R = .00635$	m	$h_{\infty} \dot{m}/A = 2.92 \times 10^9$	W/m ²
$z_0 = 2.25$	m	$\sqrt{h_{\infty}} = 1.28 \times 10^4$	m/s
		$p_0 = 1.013 \times 10^5$	N/m ² (1.0 atm)
		$H_{\infty} = 7.05 \times 10^7$	J/kg
		$E_{\infty} = 819$	V/m
		$q_{\infty} = 1.02 \times 10^7$	W/m ²

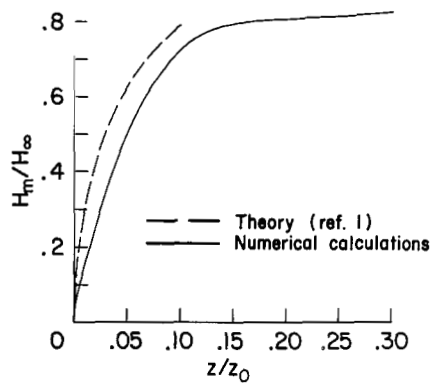
Figure 34.- Behavior of the constricted arc at large dimensionless length.



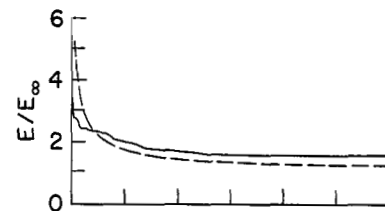
(f) Center-line enthalpy.



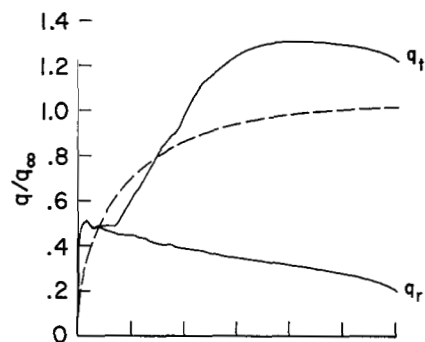
(g) Space-average enthalpy.



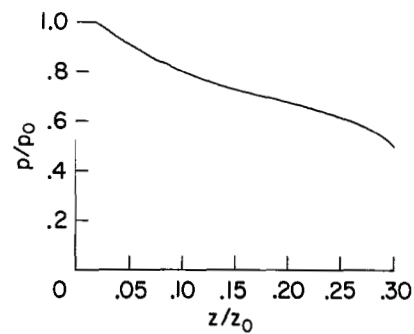
(h) Mass-average enthalpy.



(i) Voltage gradient.



(j) Local heat transfer rate.

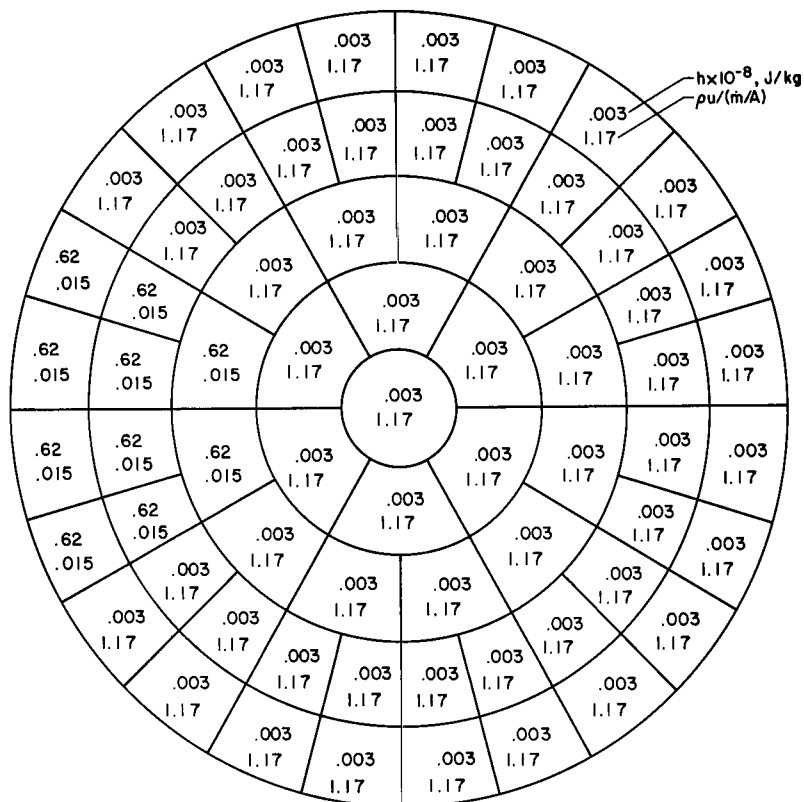
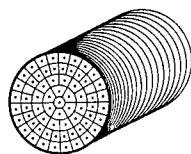


(k) Pressure.

Figure 34.- Concluded.

Axial station no. 1

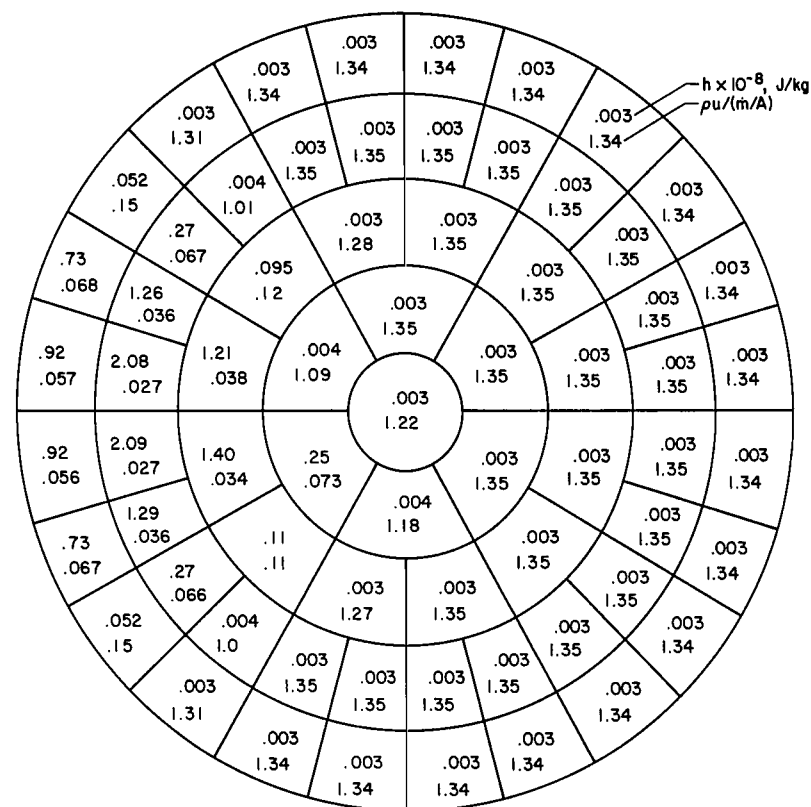
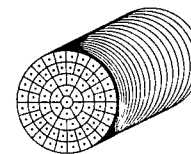
$z = 0$ m
 $H_m = 8.363 \times 10^5$ J/kg
 $E = 5020$ V/m
 $q_{\max} = 6.594 \times 10^7$ W/m²
 $p = 1.16$ atm



(a) Constrictor inlet.

Axial station no. 13

$z = 0.0029$ m
 $H_m = 2.239 \times 10^6$ J/kg
 $E = 2943$ V/m
 $q_{\max} = 1.074 \times 10^8$ W/m²
 $p = 1.15$ atm

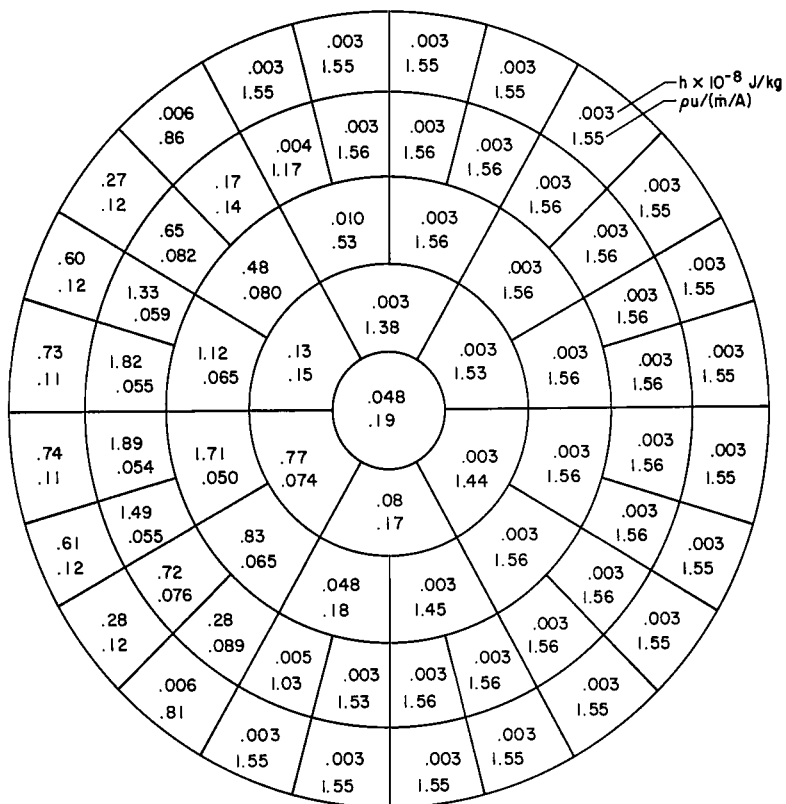
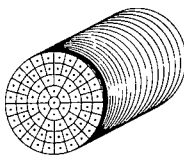


(b) 0.0029 m from the constriction inlet.

Figure 35.- The asymmetrical constricted arc with an axial flow of gas; enthalpy and mass flux as functions of radius and azimuthal position; $I = 580$ A; $\dot{m} = 0.00353$ kg/s; $R = 0.00635$ m; $z_0 = 3.50$ m; $h_\infty = 1.89 \times 10^8$ J/kg; $\dot{m}/A = 27.8$ kg/sm²; $p_0 = 1.17 \times 10^5$ N/m² (1.16 atm).

Axial station no. 17

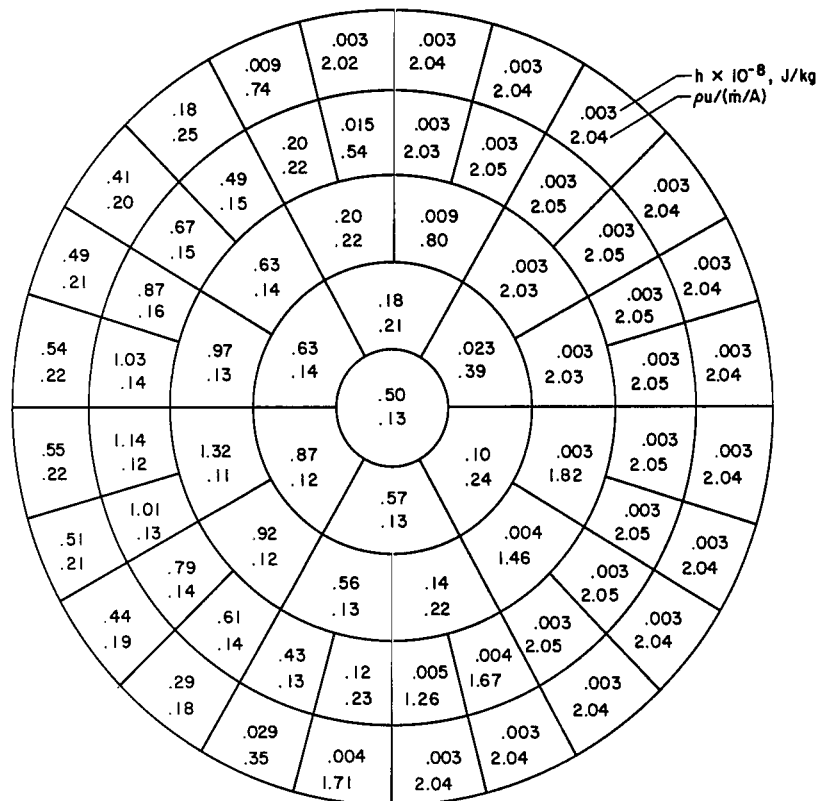
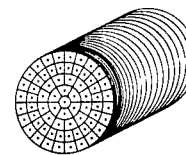
$z = .00836$ m
 $H_m = 4.063 \times 10^6$ J/kg
 $E = 2244$ V/m
 $q_{max} = 8.263 \times 10^7$ W/m²
 $p = 1.15$ atm



(c) 0.00836 m from the constrictor inlet.

Axial station no. 24

$z = .0257$ m
 $H_m = 8.412 \times 10^6$ J/kg
 $E = 1827$ V/m
 $q_{max} = 5.868 \times 10^7$ W/m²
 $p = 1.14$ atm

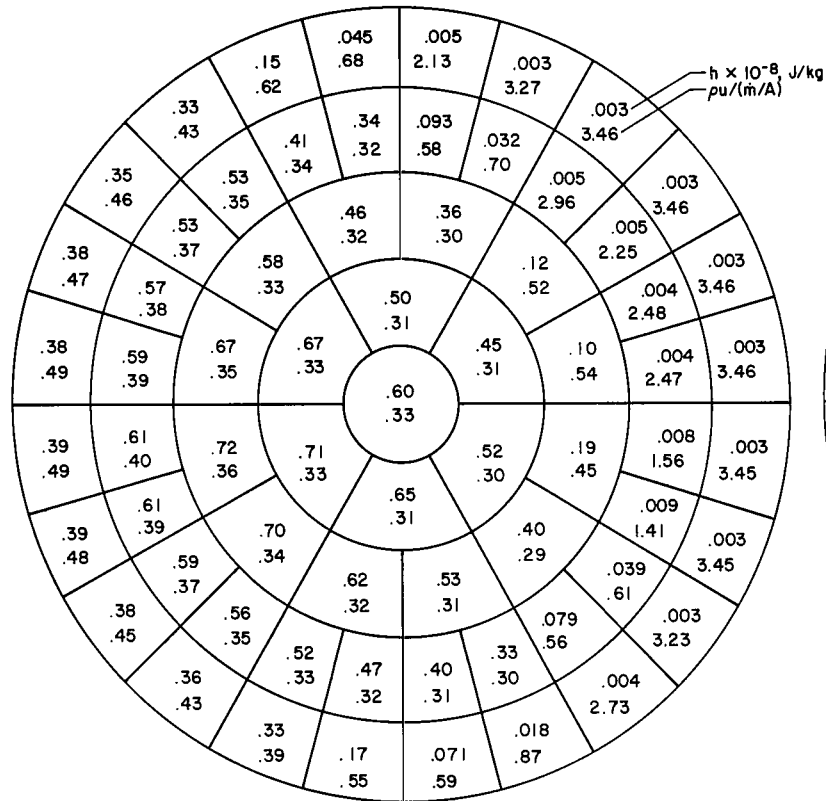
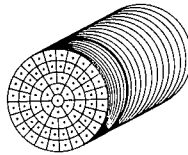


(d) 0.0257 m from the constrictor inlet.

Figure 35.- Continued.

Axial station no. 34

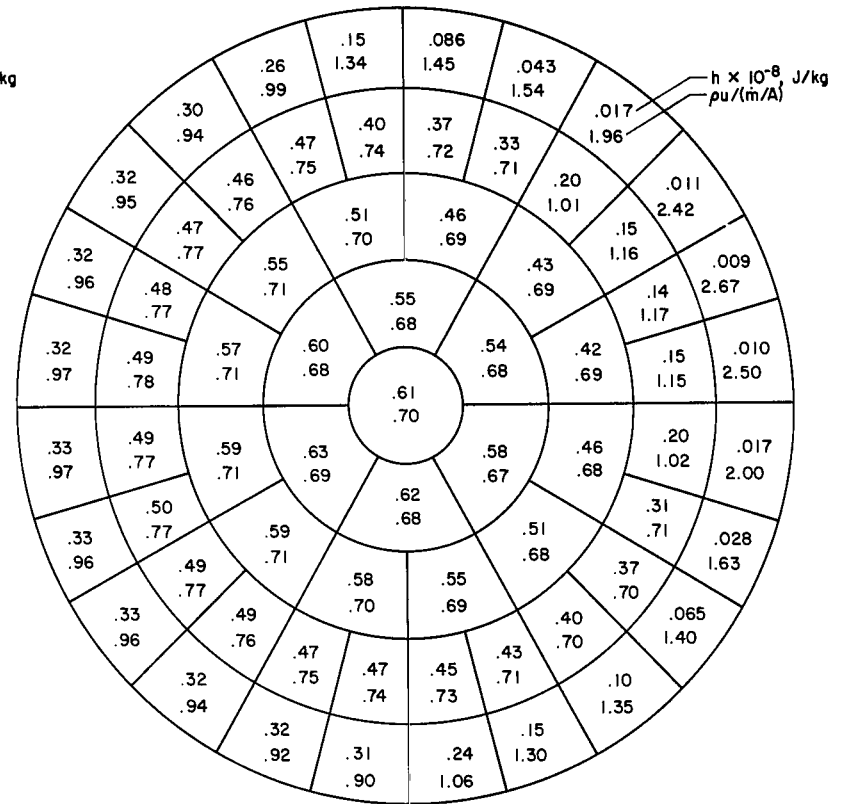
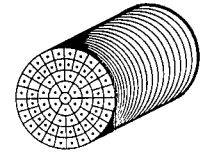
$z = .0864$ m
 $H_m = 2.178 \times 10^7$ J/kg
 $E = 1486$ V/m
 $q_{\max} = 3.257 \times 10^7$ W/m²
 $p = 1.09$ atm



(e) 0.0864 m from the constrictor inlet.

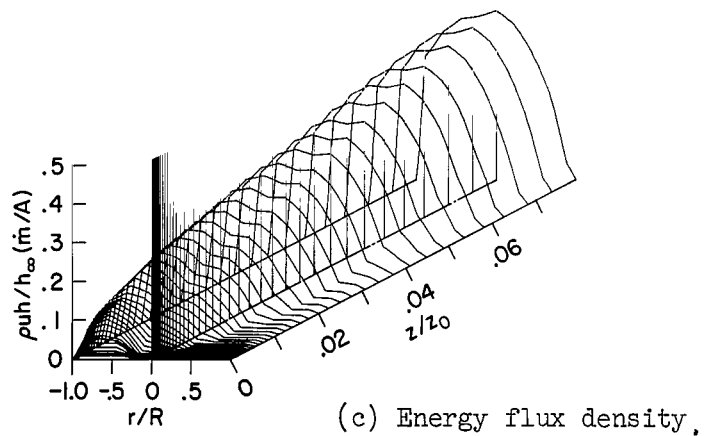
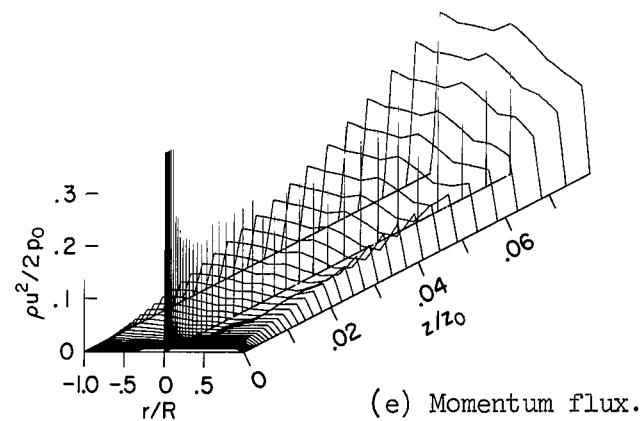
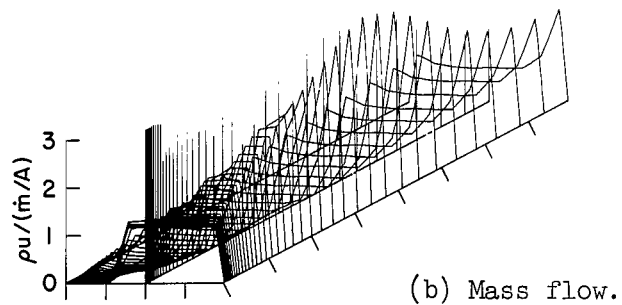
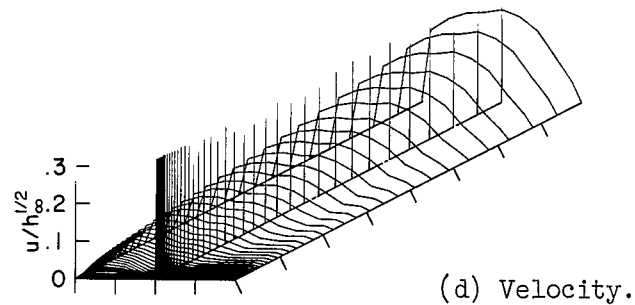
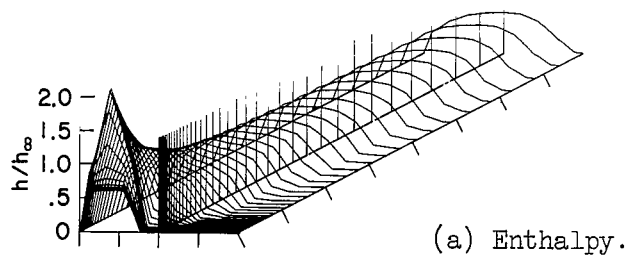
Axial station no. 46

$z = .254$ m
 $H_m = 5.25 \times 10^7$ J/kg
 $E = 1339$ V/m
 $q_{\max} = 0$ W/m²
 $p = .786$ atm



(f) 0.254 m from the constrictor inlet.

Figure 35.- Concluded.



$I = 580$	A	$h_{\infty} = 1.89 \times 10^8$	J/kg
$\dot{m} = .00353$	kg/s	$\dot{m}/A = 27.8$	kg/sm ²
$R = .00635$	m	$h_{\infty} \dot{m}/A = 5.29 \times 10^9$	W/m ²
$z_0 = 3.50$	m	$\sqrt{h_{\infty}} = 1.37 \times 10^4$	m/s
		$p_0 = 1.17 \times 10^5$	N/m ² (1.6 atm)
		$H_{\infty} = 8.17 \times 10^7$	J/kg
		$E_{\infty} = 819$	V/m
		$q_{\infty} = 1.19 \times 10^7$	W/m ²

Figure 36.- The asymmetrical constricted arc with an axial flow of gas; gas properties.

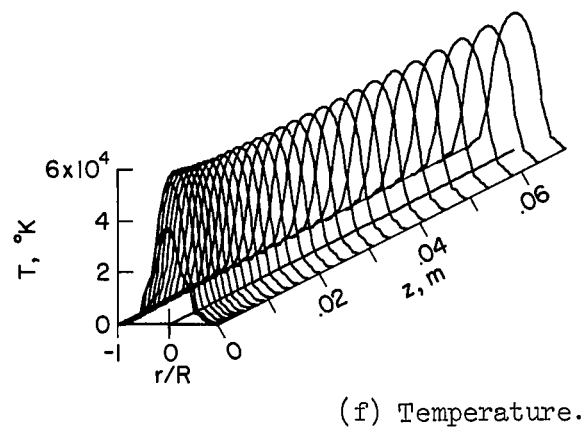
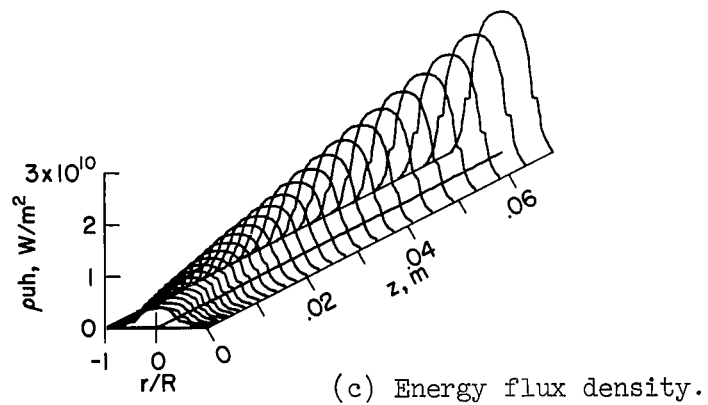
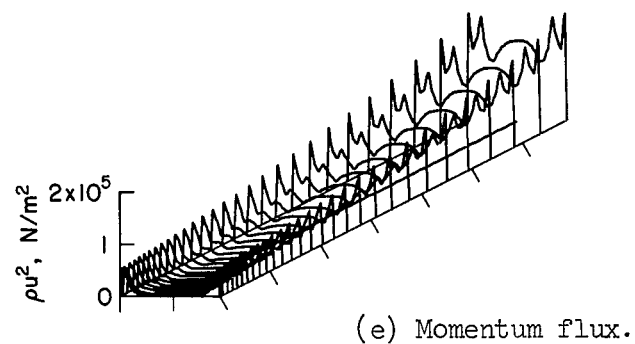
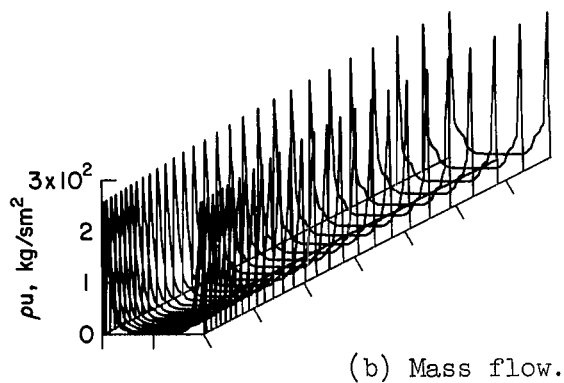
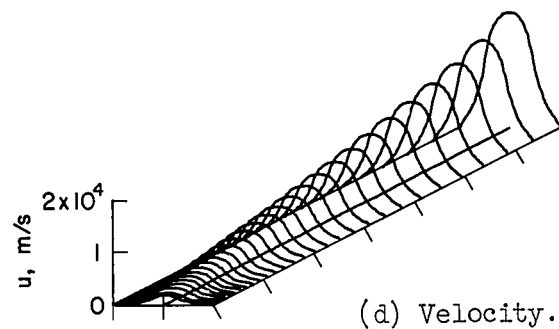
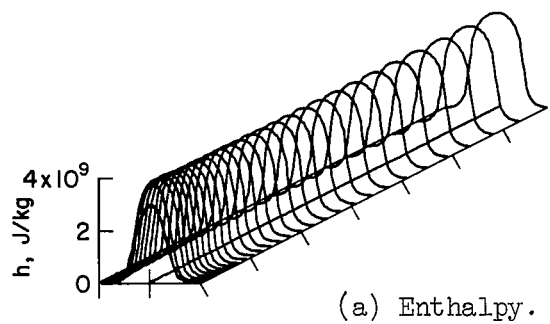
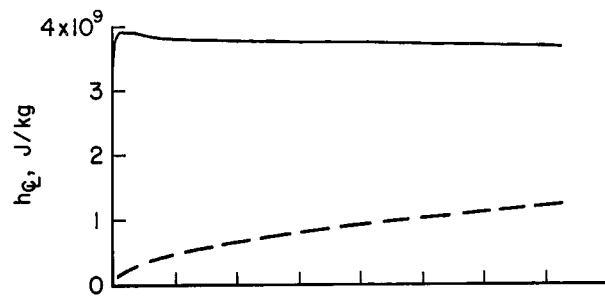
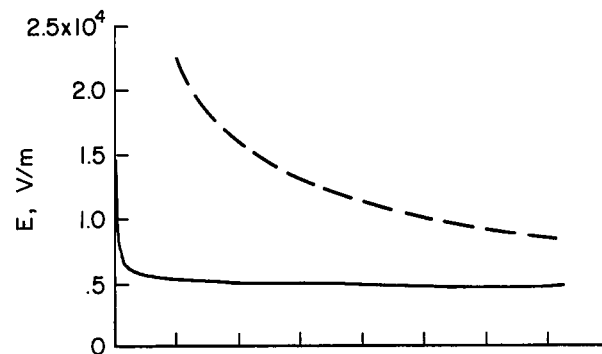


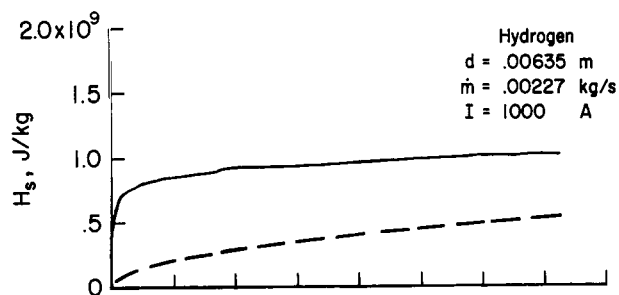
Figure 37.- Example of the high energy flux density that may be obtainable with a small diameter hydrogen arc.



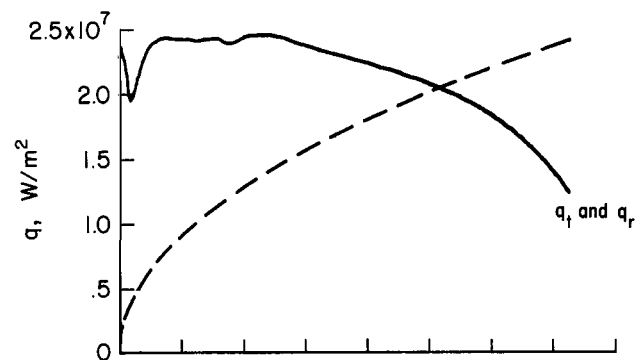
(g) Center-line enthalpy.



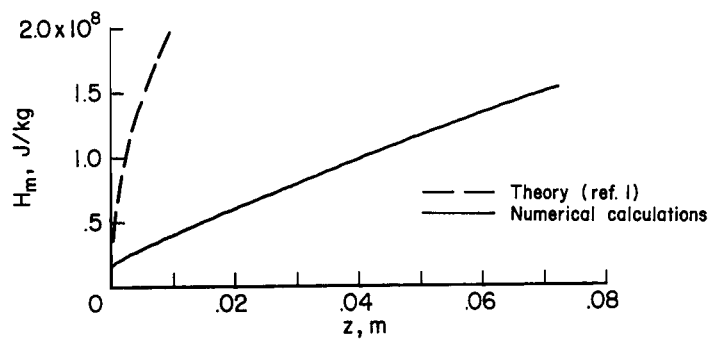
(j) Voltage gradient.



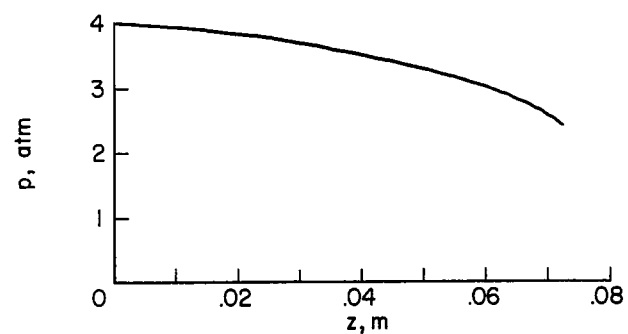
(h) Space-average enthalpy.



(k) Local heat transfer rate.

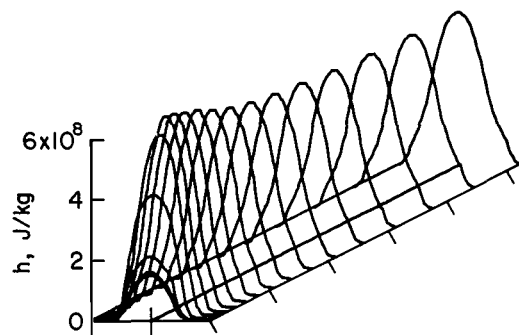


(i) Mass-average enthalpy.

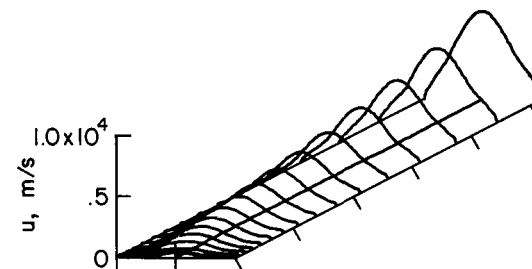


(l) Pressure.

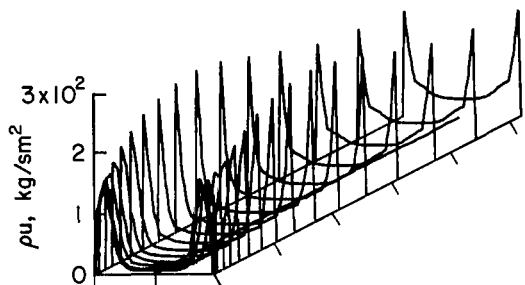
Figure 37.- Concluded.



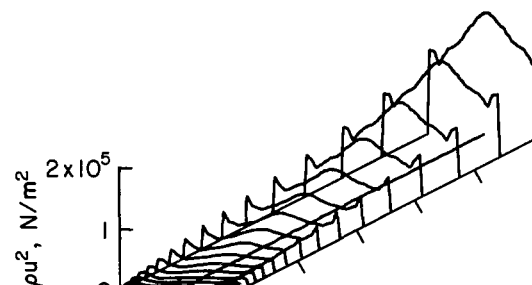
(a) Enthalpy.



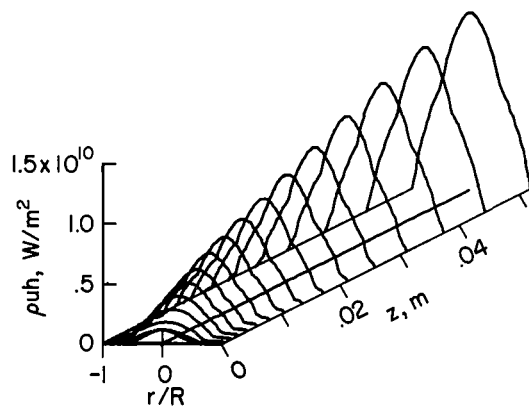
(d) Velocity.



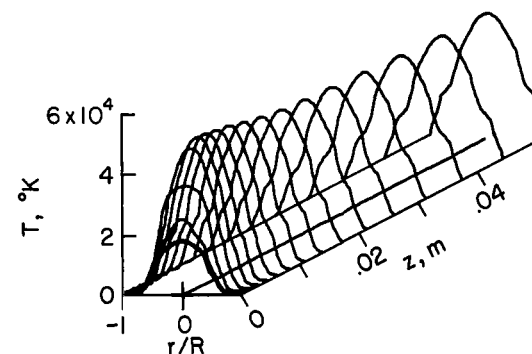
(b) Mass flow.



(e) Momentum flux.

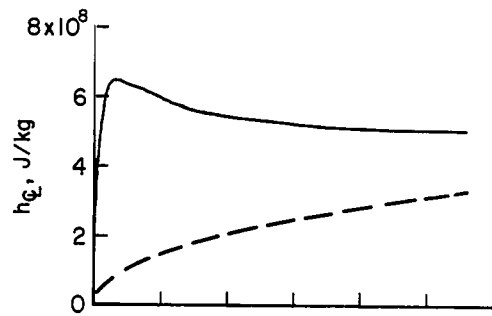


(c) Energy flux density.

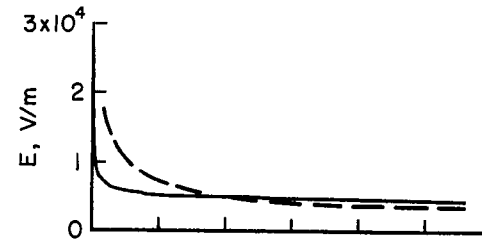


(f) Temperature.

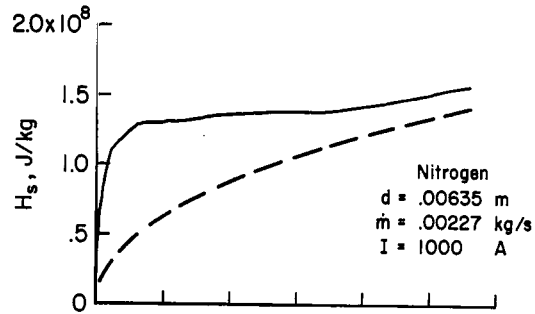
Figure 38.- Example of the high energy flux density that may be obtainable with a small diameter nitrogen arc.



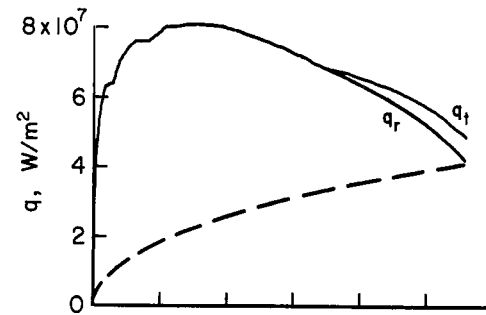
(g) Center-line enthalpy.



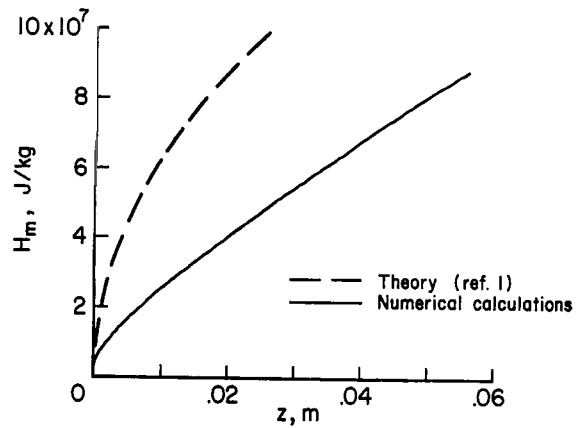
(j) Voltage gradient.



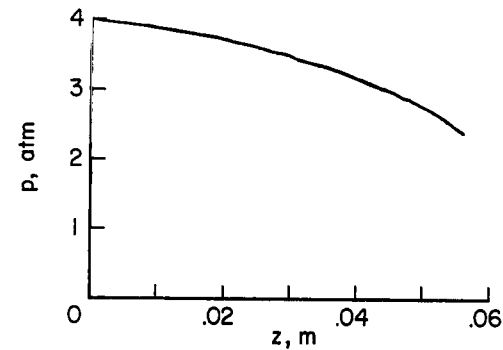
(h) Space-average enthalpy.



(k) Local heat transfer rate.



(i) Mass-average enthalpy.



(l) Pressure.

Figure 38.- Concluded.

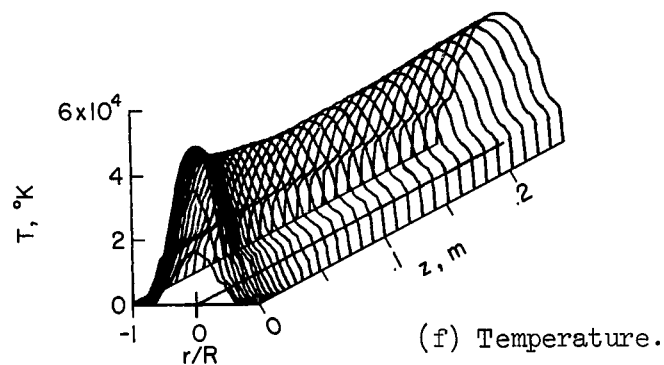
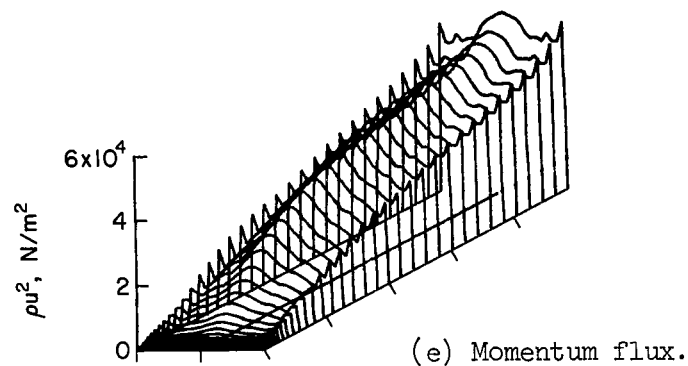
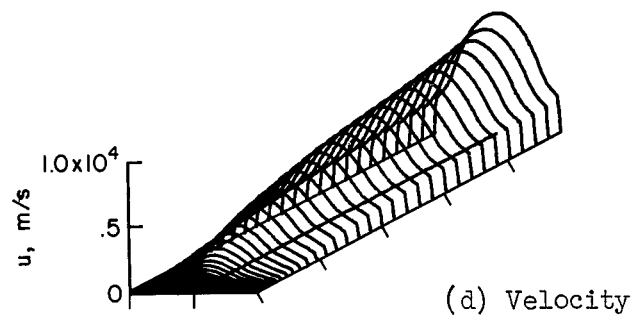
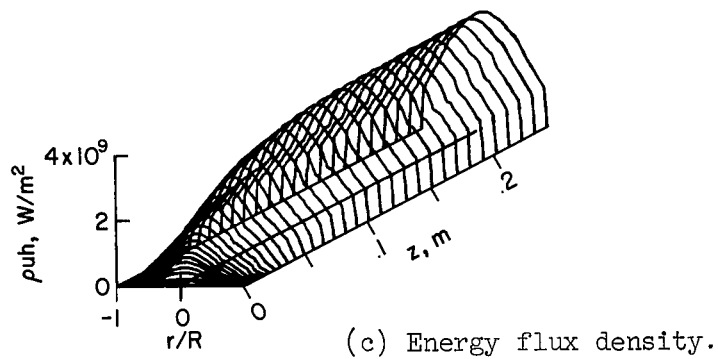
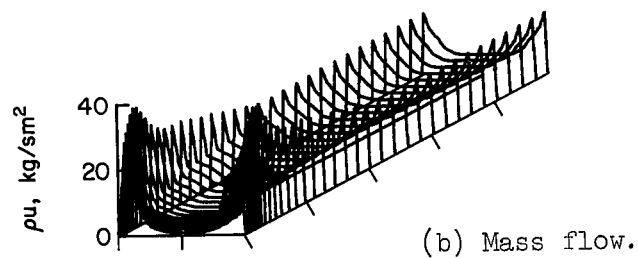
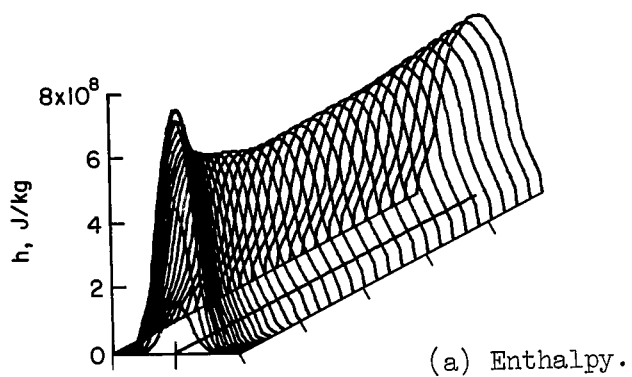
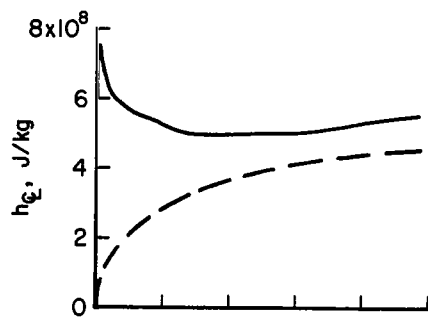
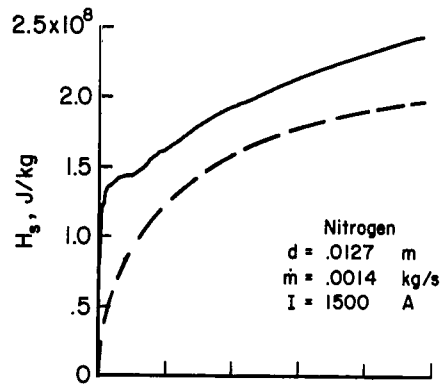


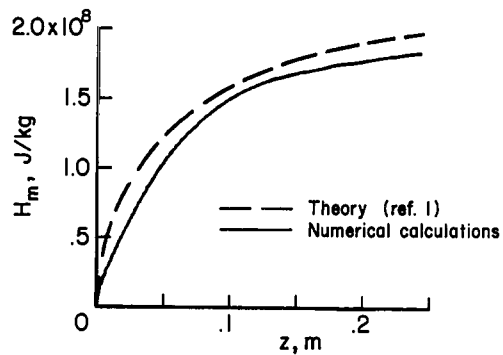
Figure 39.- Example of the high gas velocity that may be obtainable with a nitrogen arc.



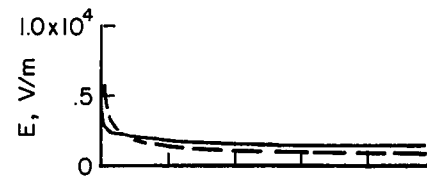
(g) Center-line enthalpy.



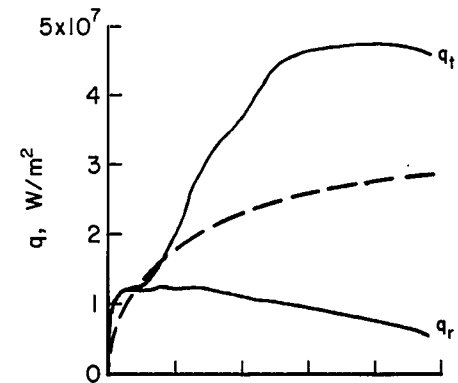
(h) Space-average enthalpy.



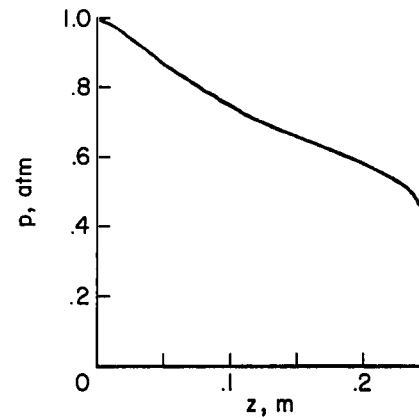
(i) Mass-average enthalpy.



(j) Voltage gradient.



(k) Local heat transfer rate.



(l) Pressure.

Figure 39.- Concluded.

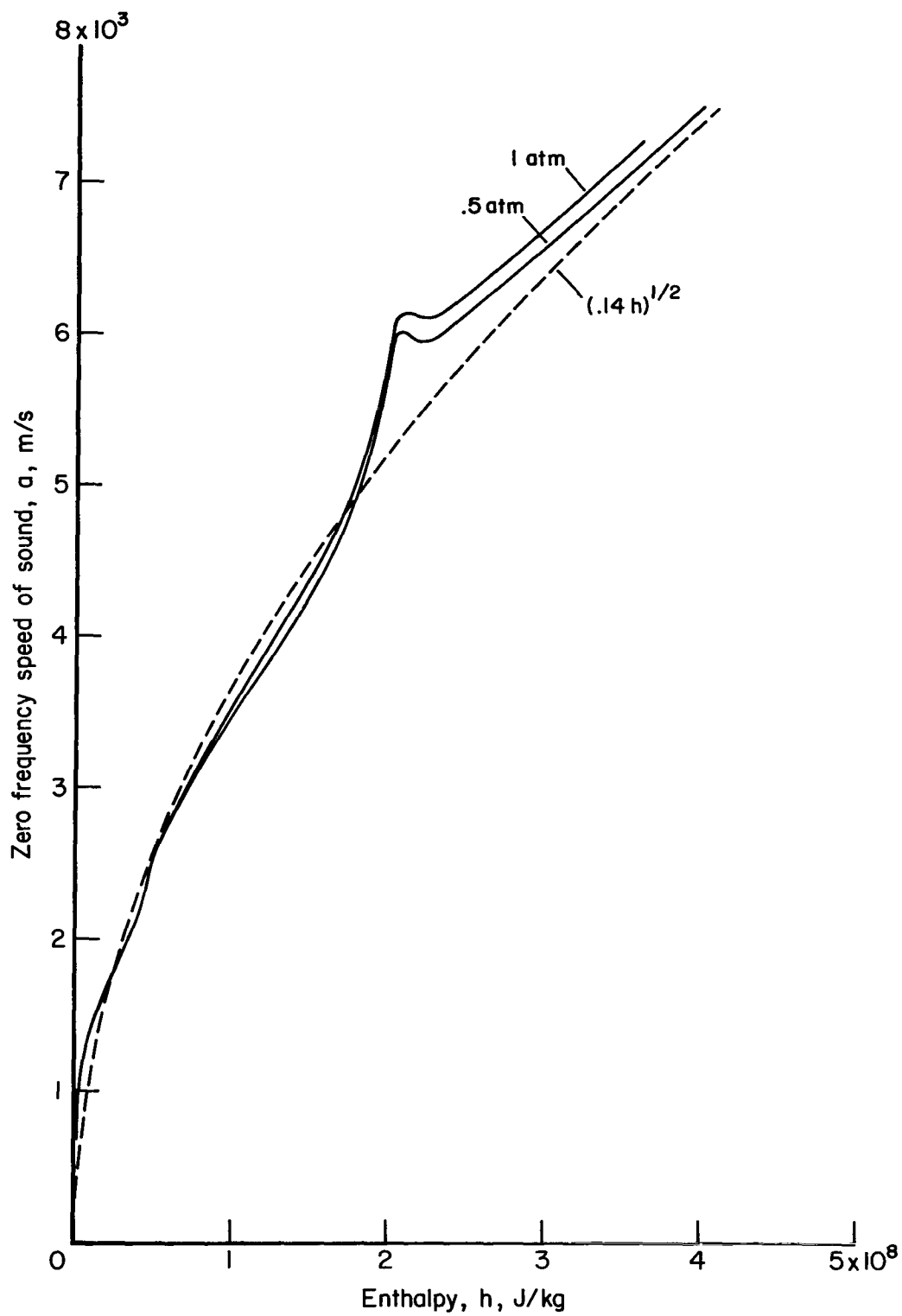


Figure 40.- Zero frequency speed of sound for nitrogen.

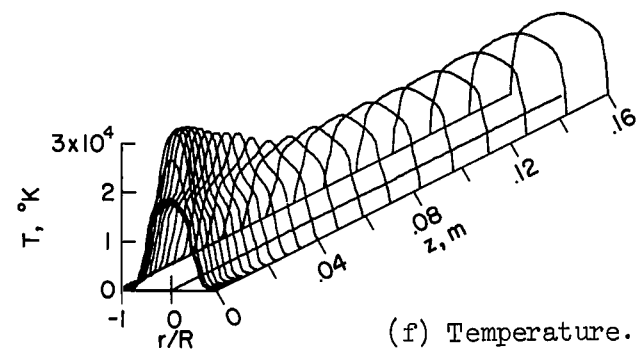
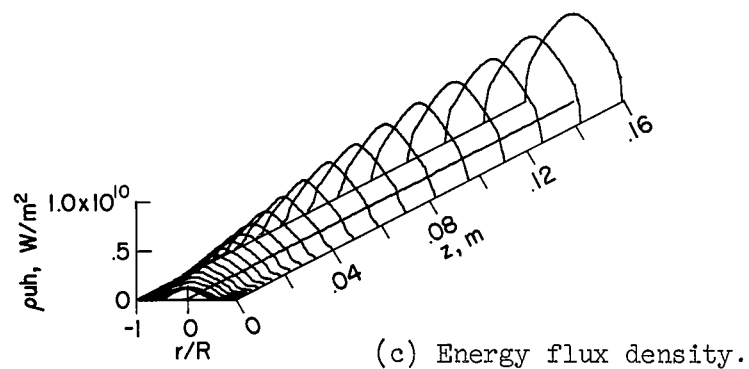
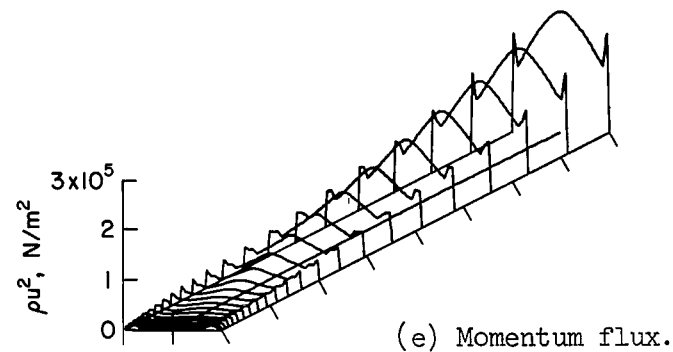
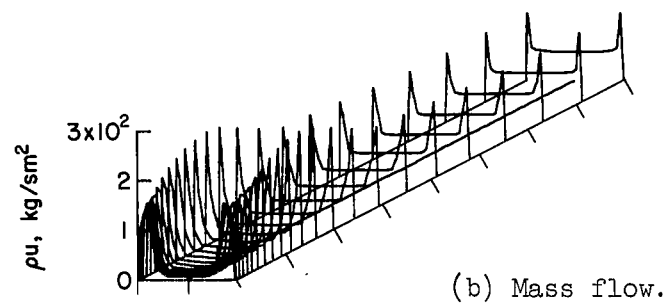
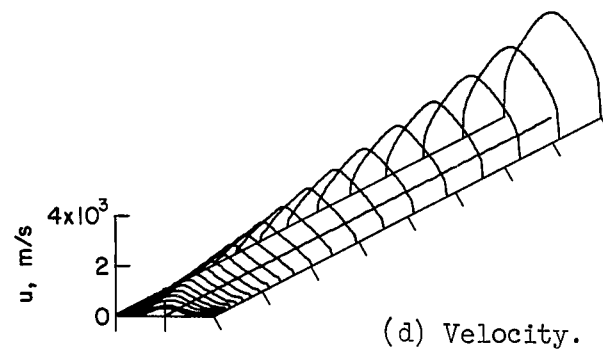
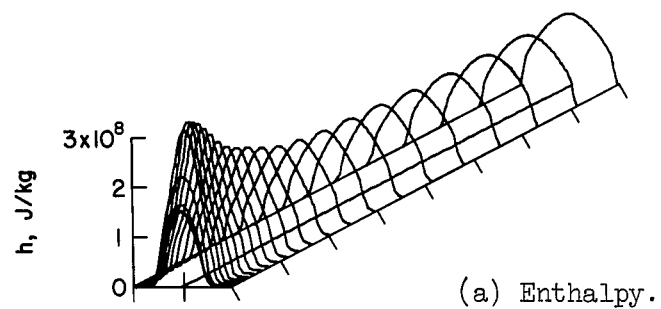
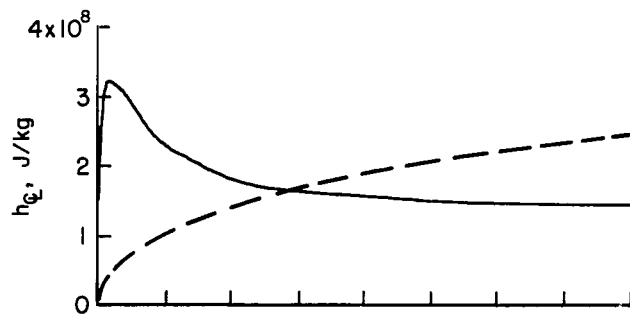
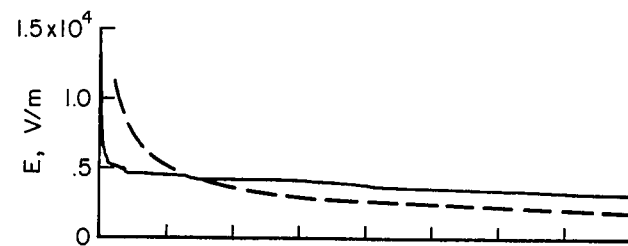


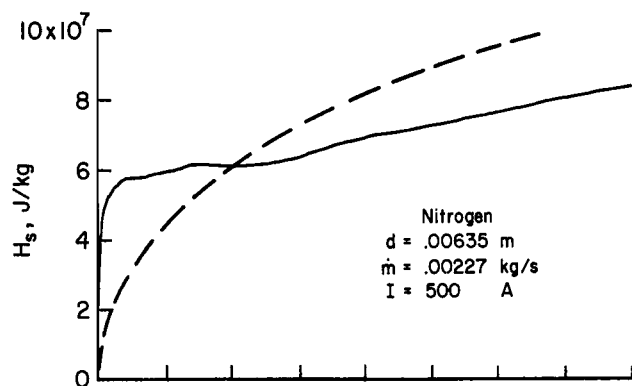
Figure 41.- Numerical solution used for the theoretical estimates of plasma generator performance given in table III.



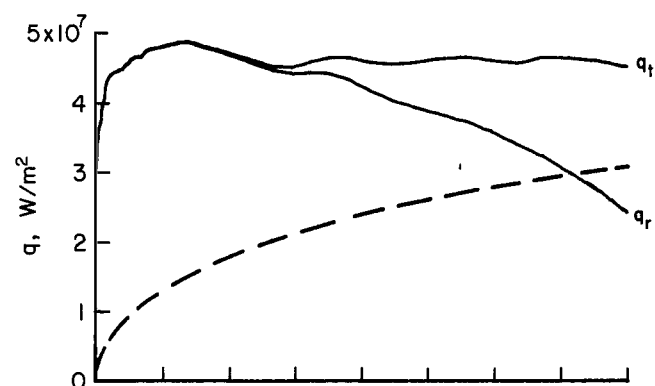
(g) Center-line enthalpy.



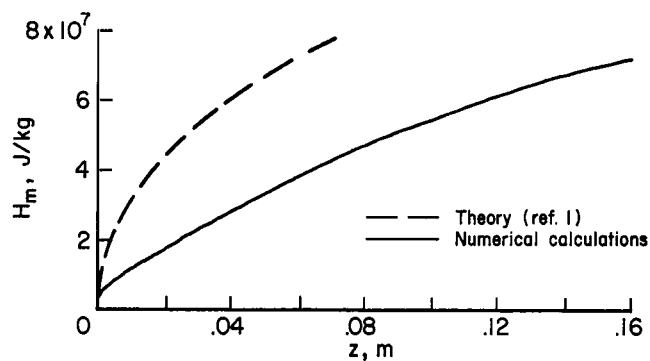
(j) Voltage gradient.



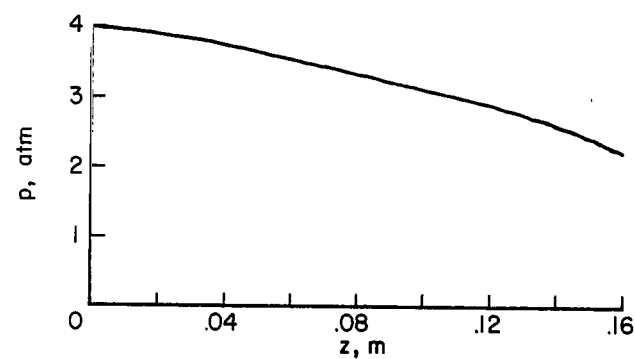
(h) Space-average enthalpy.



(k) Local heat transfer rate.



(i) Mass-average enthalpy.



(l) Pressure.

Figure 41.- Concluded.

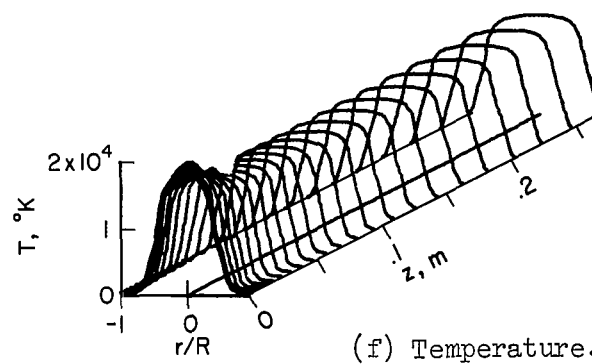
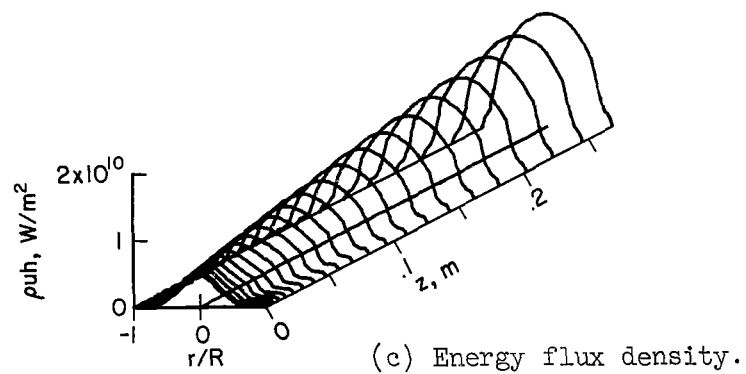
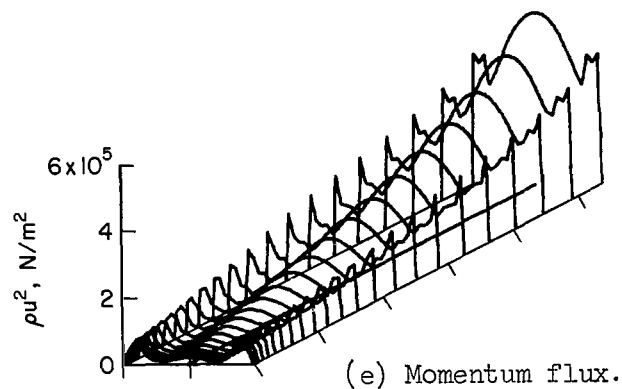
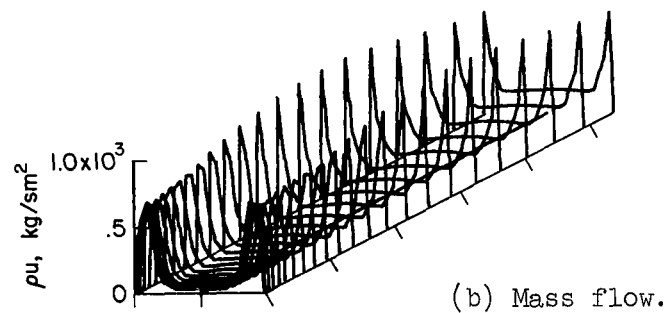
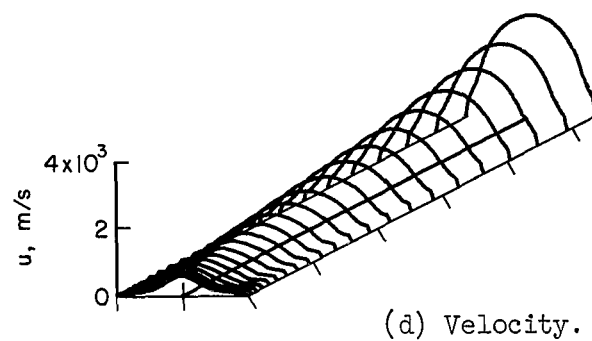
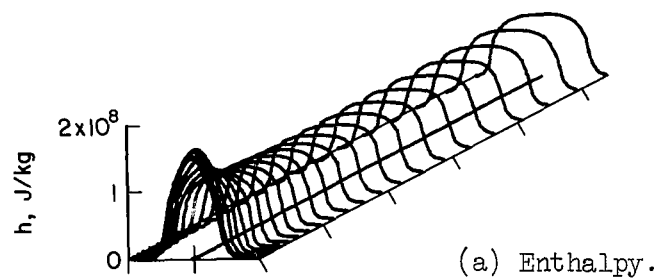
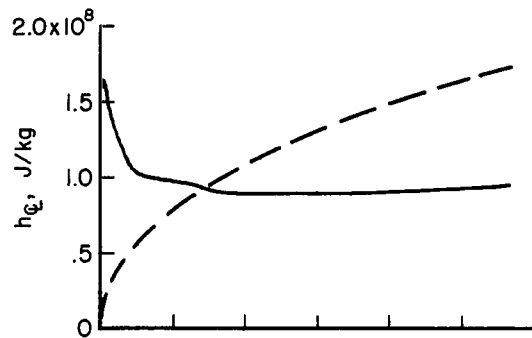
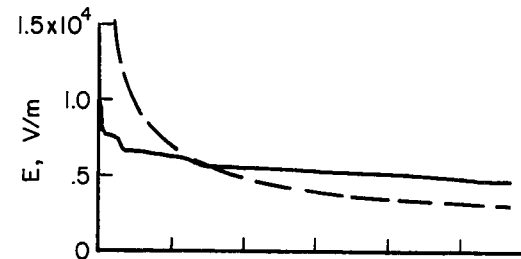


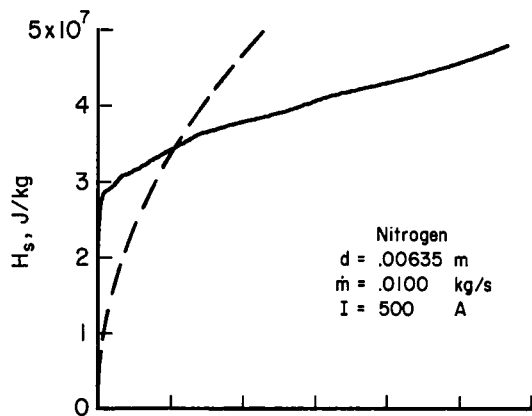
Figure 42.- Investigation of the effect of constrictor length on efficiency for a fixed exit mass average enthalpy - intermediate constrictor length.



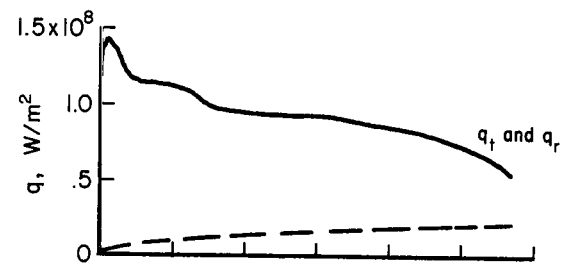
(g) Center-line enthalpy.



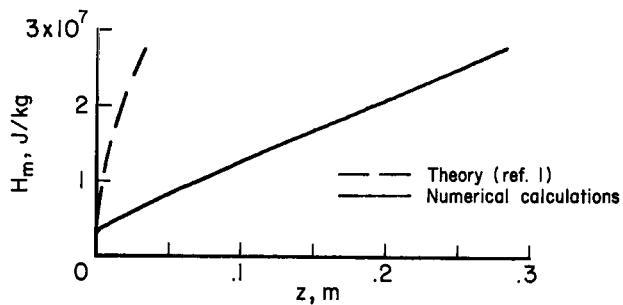
(j) Voltage gradient.



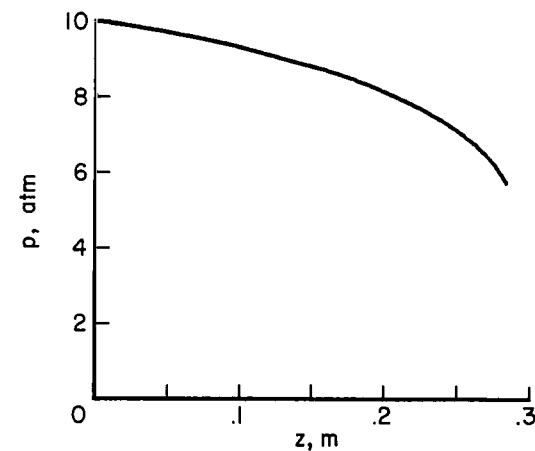
(h) Space-average enthalpy.



(k) Local heat transfer rate.



(i) Mass-average enthalpy.



(l) Pressure.

Figure 42.- Concluded.

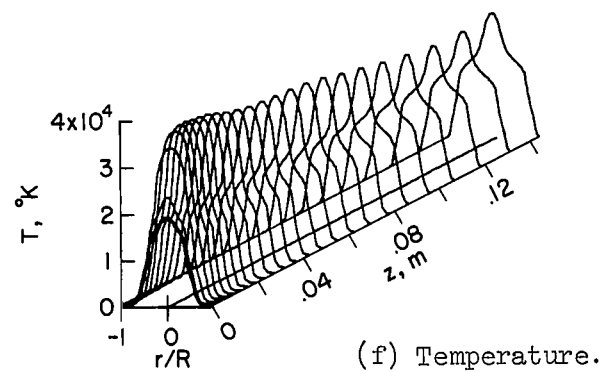
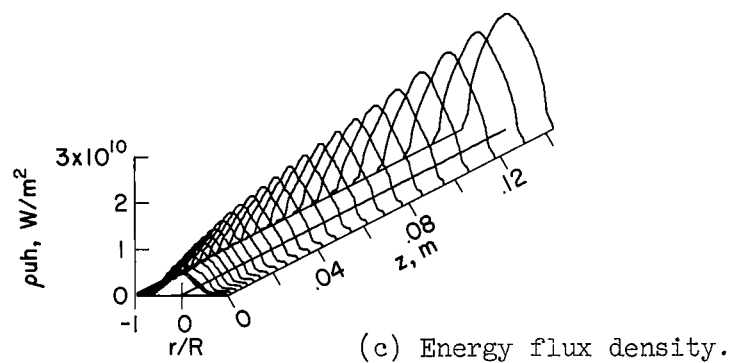
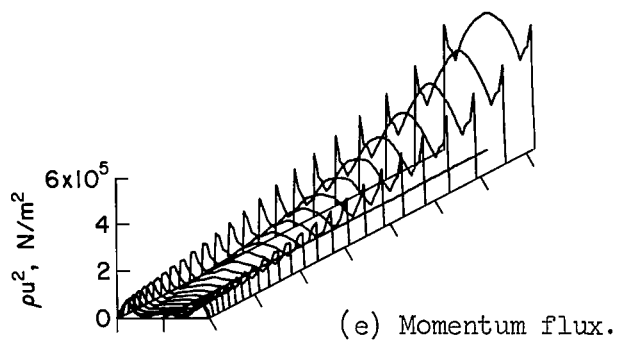
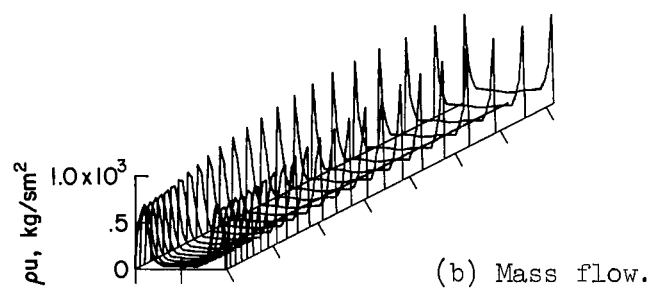
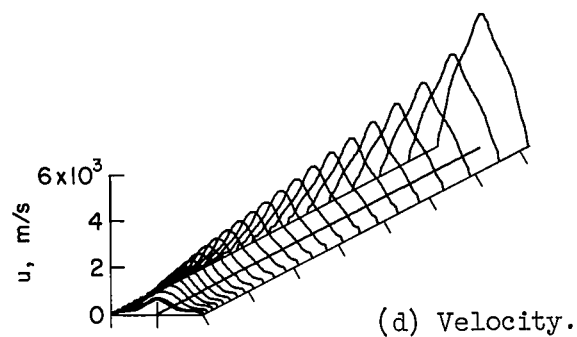
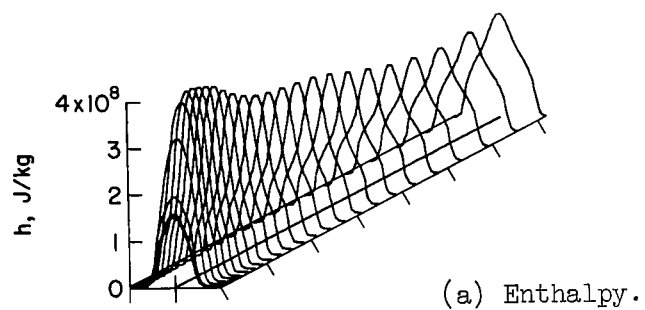
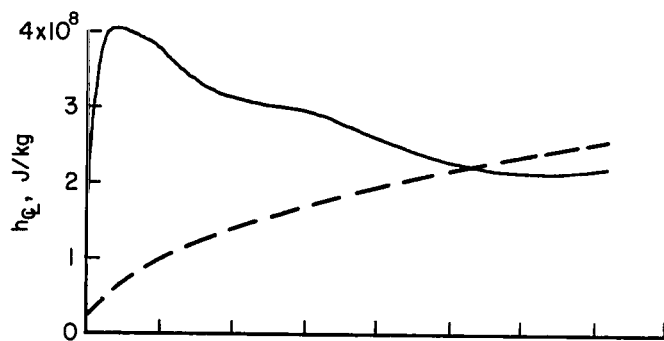
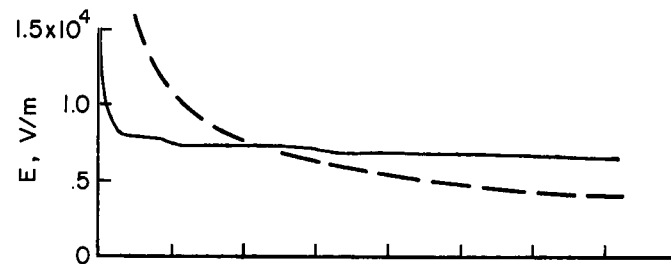


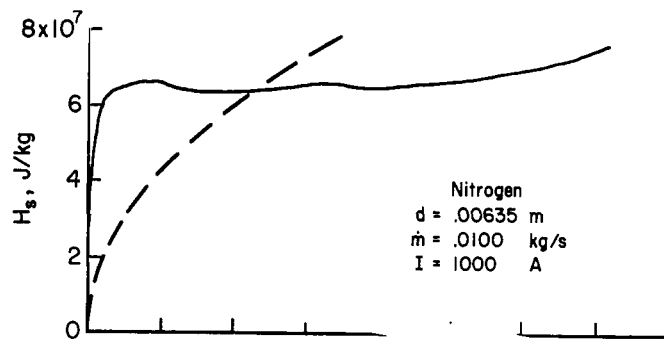
Figure 43.- Investigation of the effect of constrictor length on efficiency for a fixed exit mass average enthalpy - shorter constrictor length.



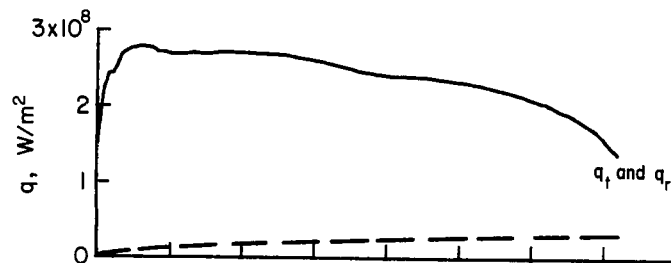
(g) Center-line enthalpy.



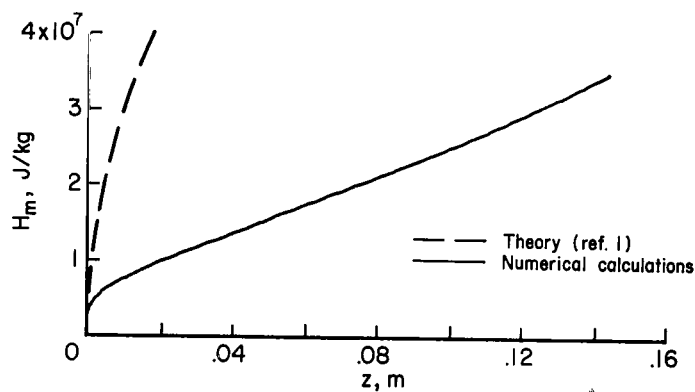
(j) Voltage gradient.



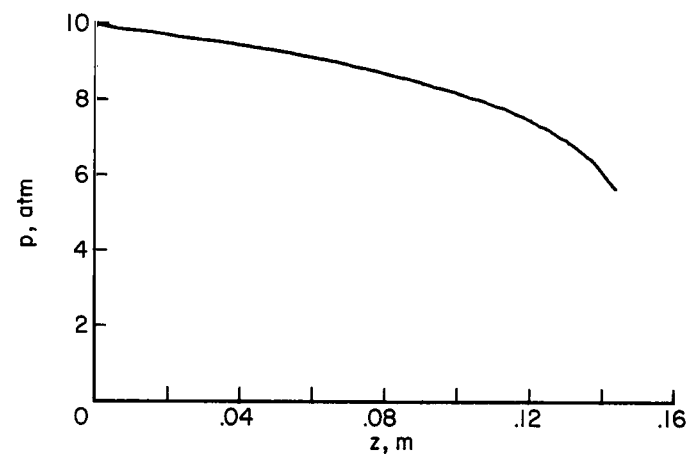
(h) Space-average enthalpy.



(k) Local heat transfer rate.



(i) Mass-average enthalpy.



(l) Pressure.

Figure 43.- Concluded.

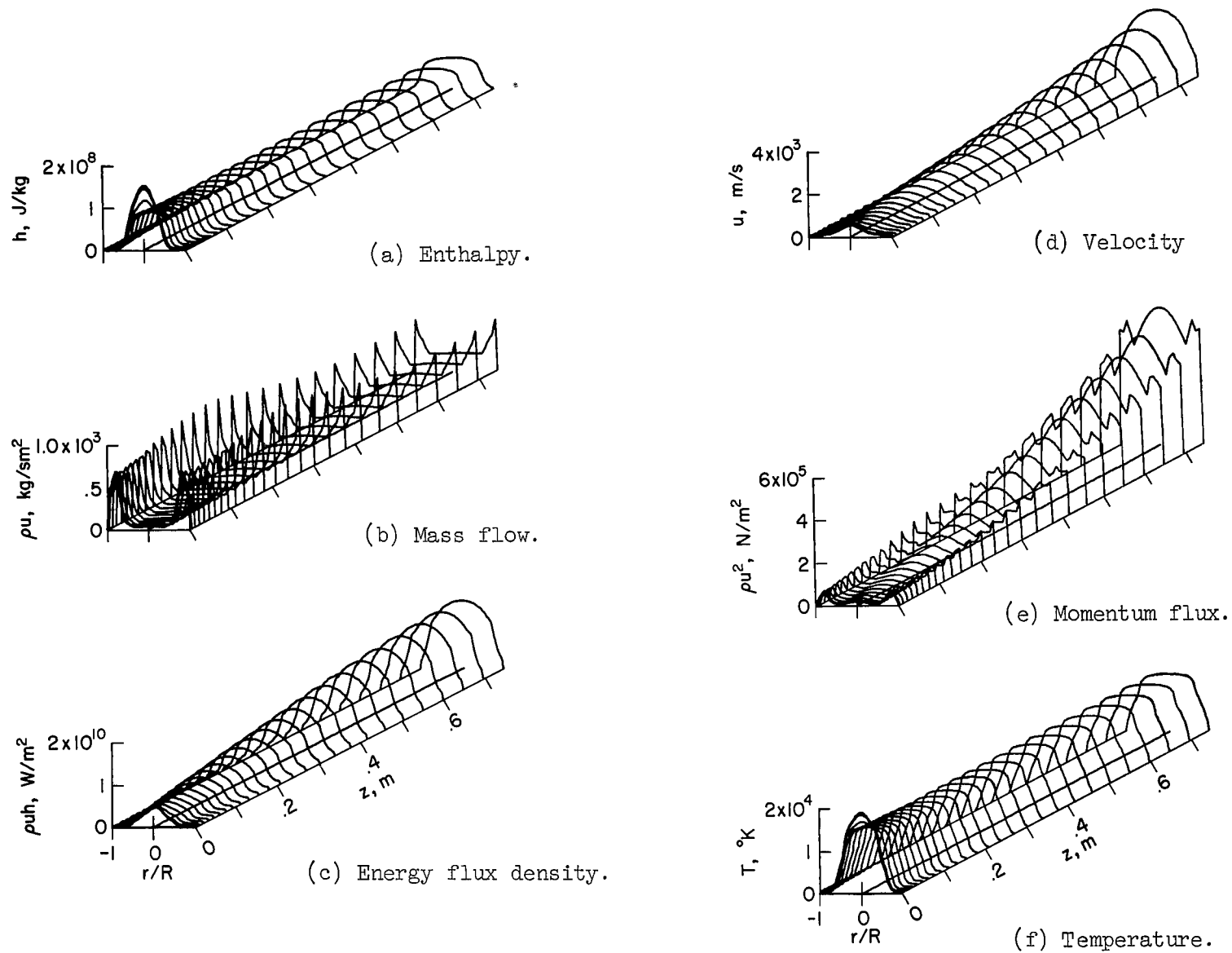
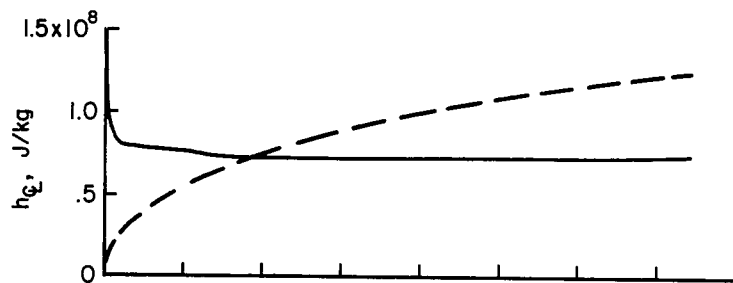
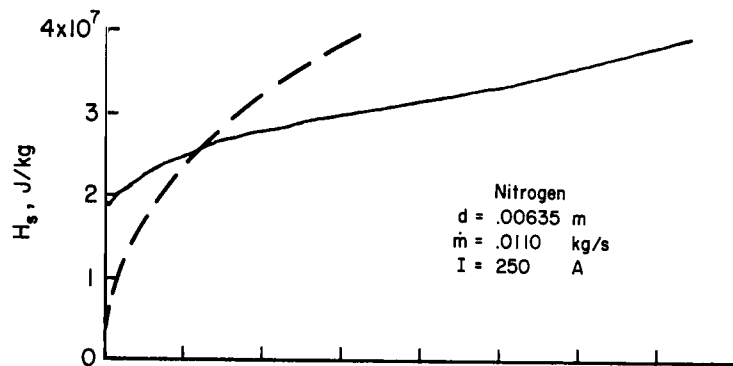


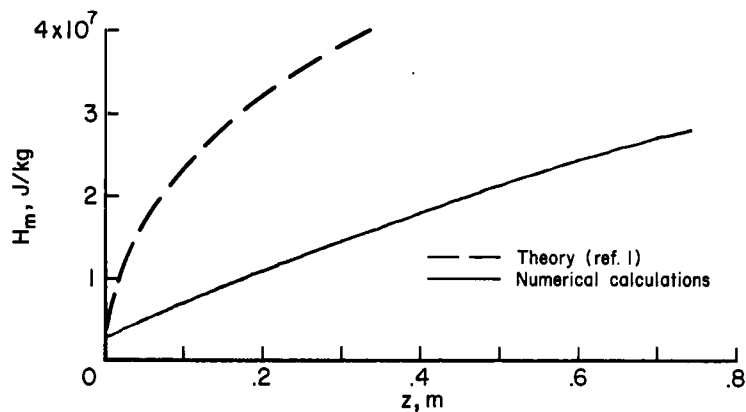
Figure 44.- Investigation of the effect of constrictor length on efficiency for a fixed exit mass average enthalpy - longer constrictor length.



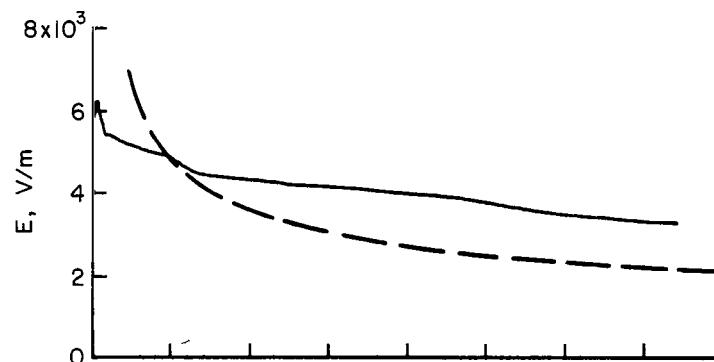
(g) Center-line enthalpy.



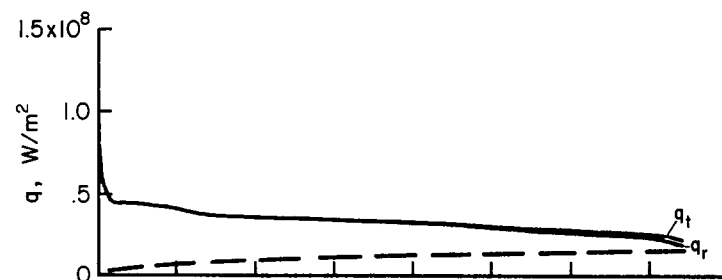
(h) Space-average enthalpy.



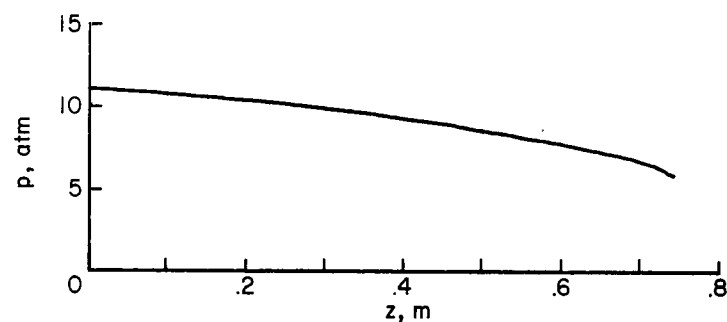
(i) Mass-average enthalpy.



(j) Voltage gradient.



(k) Local heat transfer rate.



(l) Pressure.

Figure 44.- Concluded.

"The aeronautical and space activities of the United States shall be conducted so as to contribute . . . to the expansion of human knowledge of phenomena in the atmosphere and space. The Administration shall provide for the widest practicable and appropriate dissemination of information concerning its activities and the results thereof."

—NATIONAL AERONAUTICS AND SPACE ACT OF 1958

NASA SCIENTIFIC AND TECHNICAL PUBLICATIONS

TECHNICAL REPORTS: Scientific and technical information considered important, complete, and a lasting contribution to existing knowledge.

TECHNICAL NOTES: Information less broad in scope but nevertheless of importance as a contribution to existing knowledge.

TECHNICAL MEMORANDUMS: Information receiving limited distribution because of preliminary data, security classification, or other reasons.

CONTRACTOR REPORTS: Scientific and technical information generated under a NASA contract or grant and considered an important contribution to existing knowledge.

TECHNICAL TRANSLATIONS: Information published in a foreign language considered to merit NASA distribution in English.

SPECIAL PUBLICATIONS: Information derived from or of value to NASA activities. Publications include conference proceedings, monographs, data compilations, handbooks, sourcebooks, and special bibliographies.

TECHNOLOGY UTILIZATION PUBLICATIONS: Information on technology used by NASA that may be of particular interest in commercial and other non-aerospace applications. Publications include Tech Briefs, Technology Utilization Reports and Notes, and Technology Surveys.

Details on the availability of these publications may be obtained from:

SCIENTIFIC AND TECHNICAL INFORMATION DIVISION
NATIONAL AERONAUTICS AND SPACE ADMINISTRATION

Washington, D.C. 20546